Optimisation of a chimeric antigen receptor targeting anaplastic lymphoma kinase for immunotherapy for childhood solid cancers

Emma Halliwell

University College London

A dissertation submitted to University College London in candidature for the degree of Doctor of Philosophy

2021

I, Emma Halliwell, confirm that the work presented in this thesis is my own. Where information has been derived from other sources, I can confirm that this has been indicated in the thesis.

_____

Emma Halliwell

Abstract

Cancer immunotherapy with chimeric antigen receptor (CAR) engineered T cells has shown great promise in the treatment of haematological malignancies. Paediatric neuroblastoma is one of the most common solid extracranial tumours found in children and currently accounts for ~15% of deaths from childhood cancers. Despite multimodal chemotherapy and immunotherapeutic strategies, high-risk patients suffer relapse and treatment related morbidities. This project aims to optimise a novel CAR, targeting the neuroblastoma associated antigen, anaplastic lymphoma kinase (ALK) and we hypothesised that ALK will represent a suitable target this therapy. A panel of second generation anti-ALK CAR T cells was investigated containing multiple anti-ALK single chain variable fragments (scFvs) and stalk regions combined with CD28 and CD3ζ signalling endodomains. *In vitro* investigations demonstrated effective functional activity at high target antigen densities, which significantly diminishes at lower antigen expression levels. ALK8-CD8-28ζ demonstrated antigen dependent and ALK restricted cytotoxic activity, cytokine production and proliferation and was therefore identified as the 'lead' CAR. Interestingly, when the same anti-ALK binder was combined with an Fc spacer of differing origin and length, there was an indication of antigen independent proliferation, indicative of tonic signalling. Despite this differing activity, there were minimal differences found between the ALK-CAR T cells' activation, exhaustion and memory immunophenotypes. ALK8-CD8-28ζ was compared to another panel of ALK-CAR T cells combining a previously published anti-ALK scFv with various stalk and transmembrane regions, however ALK8-CD8-28ζ demonstrated superior activity in cytokine and proliferation assays. Finally, ALK was combined into a dual-targeting CAR T cell

system with another neuroblastoma associated antigen, GD2, in an attempt to increase *in vitro* activity at low target antigen densities. Despite evidence of background single endodomain CAR activity, the engagement of the double targeting CAR T cell demonstrated increased levels of antigen specific proliferation, proinflammatory cytokine release, activation and degranulation.

Impact Statement

Neuroblastoma is a disease that still has an unmet clinical need, with high risk patients still suffering relapse and treatment related long term implications. CAR T cell therapy is currently of huge medical interest with hopes that moving into the solid tumour field can one day yield the same results as seen with haematological malignancies. Beyond identifying potential clinical applications for ALK-CAR T cells as a therapy for neuroblastoma, this thesis has further contributed to understanding more generic principles around CAR T cell therapy in the solid tumour setting, for example the issues surrounding CAR architecture and design, and low target antigen density on tumour cells. Hopefully, this research will contribute to the huge effort committed to improving CAR T cell therapies for the future treatment of cancers.

Acknowledgements

This thesis would not have been possible without the unwavering support I have from so many people. Firstly to my supervisor John Anderson, who has consistently remained so supportive and positive throughout times where I have struggled to see how to move forward. His enthusiasm and passion for science and true drive to find better therapies for patients is quite inspirational. Secondly, I would like to thank my second supervisor Tessa Crompton for her support and guidance throughout the thesis project. Next, I would like to thank the Anderson and Straathof lab groups who have become so much more than work colleagues. Without you, this experience would have not been possible. Despite the PhD lows, we have had some of the best times together and you have provided me with support, both scientifically and personally, through every step of the way. I have laughed more times than I have cried – and that must count for something! I will remember my three years with the fondest of memories, and that is because of all of you.

At this point I would like to thank the two best post docs I could have been graced with, Artemis Gavriil and Alice Piapi. Artemis, you are the reason I am here in the first place! You have helped me through so much, and I could not be more grateful for the friendship that has formed which I have no doubt that will be here for many years to come. Alice, equally, the support have you have given me has been more than I could have ever wished for and I am truly grateful for everything you have done for me (including the constant supply of tea bags). You both believed in me from the start and that has always counted for so much.

To my friends outside of the lab that I have collected along the years, again without whom this thesis would not have been possible. I could not be more

grateful for every 1Rebel class attended, rosé drank and PhD related rant of mine that was listened to, it would not have been possible without all of you.

Last, but certainly not least, to my parents, brother and family. It is not an understatement to say that everything I have achieved is because of you.

Contents

List of Figures

List of Tables

Abbreviations

ACK	Ammonium-chloride-potassium
ACT	Adoptive cell therapy
AICD	Activation induced cell death
ALCL	Anaplastic large cell lymphoma
ALK	Anaplastic Lymphoma Kinase
ANOVA	Analysis of variance
APC	Antigen presenting cell
CAFs	Cancer associated fibroblasts
CAR	Chimeric Antigen Receptor
CCR	Chimeric Costimulatory receptor
CDR	Complementary determining regions
CRS	Cytokine release syndrome
CS	Co-stimulatory domain
cSMAC	Central supramolecular activation clusters
cTEC	Cortical thymic epithelial cells
DAG	Diacyglycerol
DAMP	Damage-associated molecular patterns
DC	Dendritic cells
DN	Double negative
DP	Double positive
dSMAC	Distal supramolecular activation clusters
ECD	Extracellular domain
EFS	Event free survival
ELISA	Enzyme-linked immunoabsorbent assay
ER	Endoplasmic reticulum
ETP	Early thymocyte progenitor
FAP	Fibroblast activation protein
FBS	Foetal bovine serum
FcγR	Fc gamma receptor
FDA	Food and Drug Administration
GOF	Gain of function
GR	Glycine rich

GWAS	Genome wide association study
H/TM	Hinge/transmembrane region
HER2	Human epidermal growth factor 2
ICB	Immune checkpoint blockade
IFNγ	Interferon Gamma
IL(-2)	Interleukin(-2)
IP3	Inositol 1,4,5-triphosphate
IS	Immune synapse
ITAM	Immunoreceptor tyrosine-based activation motif
ITK	Interleukin-2-inducibile kinase
KD	Kinase domain
L1-CAM	L1 cell adhesion molecule
LAMP	Lysosomal associated membrane glycoproteins
LAT	Linker for activation of T cells
LDL	Low density lipoprotein receptor class A
LTR	Long terminal repeats
mAbs	Monoclonal antibodies
MAM	Meprin, A-5 protein, and receptor protein-tyrosine phosphatase mu domain
MAS	Macrophage activation syndrome
MDSCs	Myeloid derived suppressor cells
MFI	Median fluorescence intensity
MHC	Major histocompatibility complex
MoMLV	Moloney murine leukaemia virus
MRD	Minimal residual disease
mTEC	Medullary thymic epithelial cells
MYCN	V-Myc proto-oncogene protein
NCAM	Neural cell adhesion molecule
NFAT	Nuclear factors of activated T cells
NK	Natural killer
NPM	Nuclear phosphoprotein
NSCLC	Non small cell lung cancer
ORF	Open reading frame

PAMP	Pathogen-associated molecular patterns
PBMC	Peripheral blood mononuclear cells
PBS	Phosphate-buffered saline
PCR	Polymerase chain reaction
PI3K	Phosphoinositide 3-kinase
PIP2	Phosphatidylinositol triphosphate
PKC	Protein kinase C
PLCγ-1	Phospholipase C gamma 1
pMHC	Peptide-Major Histocompatibility Complex
PRR	Pattern recognition receptors
pSMAC	Peripheral supramolecular activation clusters
ROS	Reactive oxygen species
RPM	Revolutions Per Minute
RTK	Receptor tyrosine kinase
scFv	Single chain variable fragment
SMAC	Supramolecular activation clusters
SNP	Single nucleotide polymorphisms
SNS	Sympathetic Nervous System
SOC	Super Optimal broth with Catabolite repression
SP	Single positive
JAK/STAT	Janus kinase/Signal transducer and activator of transcription
STR	Short tandem repeat
T2A	Thosea asigna 2A
TAA	Tumour-associated antigen
TAMs	Tumour associated macrophages
TCM	Central memory T cell
TCR	T cell receptor
TEM	Effector memory T cell
TEMRA	Terminally differentiated effector T cells
Tfh	Follicular helper T cells
TGFβ	Transforming growth factor beta
TIL	Tumour infiltrating lymphocytes
TKI	Tyrosine kinase inhibitor

TM	Transmembrane
TMD	Transmembrane domain
TME	Tumour microenvironment
TN	Naïve T cell
TNFα	Tumour necrosis factor alpha
TRAIL	TNF-related apoptosis inducing ligand
Treg	Regulatory T cells
TRUCK	T cells redirected for antigen-unrestricted cytokine-initiated killing (also known as 4th generation)
TSA	Tumour-specific antigen
TSCM	Memory stem T cell
UT	Untransduced
VEGF	Vascular endothelial growth factor
Vh	Heavy chain
Vl	Light chain
WT	Wild type
Zap-70	Zeta-chain-associated protein kinase 70
ΔMFI	Delta MFI

1 Introduction

1.1 Neuroblastoma

Neuroblastoma is one of the most common solid extracranial tumours in children, most commonly diagnosed in infants below the age of one year (Heck et al., 2009). The disease arises due to defects in neural crest progenitor cells during the development of the sympathetic nervous system (SNS) (Whittle et al., 2017). Neuroblastoma tumours typically arise from the adrenal glands and follow the distribution of the sympathetic ganglia along the paraspinal areas from the neck to the pelvis. Based on this, the most common sites for tumour development include the adrenal medulla (35%), the extra-adrenal paraspinal ganglia (30-35%) and the mediastinum (20%). It accounts for ~10% of paediatric cancers, but is responsible for ~15% of cancer related deaths in children due to high rate of relapse after therapy (Trigg and Turner, 2018).

1.1.1 Genetics

The vast majority of neuroblastoma cases present sporadically, while ~1-2% of cases are familial, inherited in an autosomal dominant manner (Whittle et al., 2017, Mosse et al., 2008). A number of germline mutations which are associated with neuroblastoma predisposition have been identified. The majority of them are found in the following genes: Paired-Like Homeobox 2B (*PHOX2B)* which regulates autonomic nervous system development, Anaplastic Lymphoma Kinase *(ALK)* also believed to be involved in nervous system development; and Kinesin Family Member 1B (*KIF1Bβ),* which is a proposed tumour suppressor

gene thought to play a role in the pathogenesis of neural crest tumours (Barr and Applebaum, 2018).

Within sporadic cases of the disease, it is thought that several common germline variations, each with low relative risk, act in combination to increase chances of the disease occurring (Trigg and Turner, 2018). A recent genome wide association study (GWAS) looking at 720 cases of neuroblastoma identified loss or gain of function single nucleotide polymorphisms (SNPs) in a number different genes, including *BARD1, DUSP12* and *TP53* (Trigg and Turner, 2018). *ALK* is also one of the most commonly somatically mutated genes in sporadic neuroblastoma, with ~14% of tumours having missense alterations or gene amplification events (Bosse and Maris, 2016).

The genetic aberration which is classically and consistently associated with poorer outcomes in neuroblastoma is genomic amplification of the V-Myc Avian Myelocytomatosis Viral Oncogene Neuroblastoma Derived Homolog (*MYCN)* oncogene, located on the short arm of chromosome 2 (2p24). It is present in 20% of all neuroblastoma cases, and is found in 50% of those diagnosed with high-risk disease (Bosse and Maris, 2016, Huang and Weiss, 2013). It encodes a transcription factor which ultimately influences many biological processes leading to aggressive disease including migration and metastases, cell survival, apoptosis, proliferation, blocking of cell cycle arrest and angiogenesis (Huang and Weiss, 2013). Overexpression of MYCN in neural crest progenitor cells of transgenic mice and zebrafish is sufficient to induce neuroblastoma development, and amplification in tumours is associated with shorter progression free survival and treatment failure (Trigg and Turner, 2018, Bosse and Maris, 2016, Dzieran et al., 2018, Seeger et al., 1985). Other recurrent genomic alterations include,

gain of chromosome 17q and deletions of chromosome arms 1p, 3p, 4p and 11q (Bosse and Maris, 2016).

1.1.2 Disease staging and treatment

Neuroblastoma is a highly heterogeneous disease which accounts for its diverse clinical presentation, treatment response and overall prognosis in patients (Bosse and Maris, 2016). Based on a combination of multiple factors, including; *MYCN* status (amplified vs nonamplified), age at diagnosis, disease stage and tumour histology, patients can be categorised into risk groups consisting of low-, intermediate- and high-risk disease (Papaioannou and McHugh, 2005, Sokol and Desai, 2019). A patient's treatment regimen is determined by their disease risk category and therefore it is important to appropriately stratify cases so the suitable treatment is given.

Low and intermediate risk disease

Patients who present with low- or intermediate-risk cases are often diagnosed at a younger age with more localised tumours and subsequently have higher survival rates of approximately 90%. Moreover, they commonly have more favourable biological features, such as nonamplified *MYCN* and minimal rates of metastases. Children with low-risk neuroblastoma can be observed or undergo surgery to remove the lesion (Sokol and Desai, 2019). In some cases, tumours spontaneously regress with no treatment needed (Matthay et al., 2016). Patients who are diagnosed with intermediate-risk disease may receive chemotherapy or surgical removal of the tumour (Sokol and Desai, 2019).

High risk disease

Approximately 50% of patients will be diagnosed with high-risk neuroblastoma. In most cases this is metastatic disease with unfavourable features, such as *MYCN* amplification (Matthay et al., 2016). These patients usually receive multimodal therapy which can be separated into three main phases: induction, consolidation and maintenance. The induction phase involves chemotherapy with the aim to shrink the tumour before surgical removal. The consolidation phase has a goal of eliminating the remaining minimal residual disease (MRD), followed by an autologous stem cell transplant to re-instate a patient's immune system (Matthay et al., 2016). During maintenance therapy patients may receive radiation and immunotherapies. FDA-approved therapeutic monoclonal antibodies against GD2 (a disialoganglioside expressed in neuroblastoma), namely Dinituximab, are incorporated in high risk patient treatment regimens. A phase III study in 2010 showed an increase in 2 year event free survival (EFS) from 46-66% and overall survival from 75-86% for patients who received anti-GD2 monoclonal antibody with IL-2, GM-CSF and retinoic acid compared to patients who received retinoic acid alone (Yu et al., 2010, Sokol and Desai, 2019, Smith and Foster, 2018).

Despite this intensive treatment, ~50% of patients will inevitably relapse with poor outcomes. For those who do survive, many are left with long term comorbidities such as hearing loss, growth retardation and secondary malignancies (Richards et al., 2018). Further attempts have been made to identify an 'ultra-high-risk' subpopulation of children who have particularly poor outcomes in order to tailor treatment strategies more carefully (Morgenstern et al., 2019).

1.2 Anaplastic Lymphoma Kinase

Anaplastic Lymphoma Kinase (ALK), or CD246, is a receptor tyrosine kinase (RTK) that belongs to the insulin receptor (IR) superfamily (Zhao et al., 2015). It was originally identified as a fusion partner in the t(2;5)(p23;q35) chromosomal rearrangement in anaplastic large cell lymphoma (ALCL). This mutation results in a fusion of the cytoplasmic domain of ALK to the N-terminal portion of the nucleolar phosphoprotein, NPM (Morris et al., 1994). ALK was then further identified to be rearranged, mutated or amplified in a series of other tumour types including lymphoma, neuroblastoma and non-small cell lung cancer (NSCLC) (Soda et al., 2007).

1.2.1 Structure

Human ALK exists as a 220 kDa full length receptor that can be cleaved into a truncated 140 kDa isoform. The full structure of the RTK was not fully elucidated until 1997, but it is believed to be made up of an extracellular domain (ECD), a transmembrane (TM) and a cytoplasmic intracellular kinase domain (KD) (Figure 1.1) (Hallberg and Palmer, 2016). Structurally, the ECD is made up of a low-density lipoprotein receptor class A (LDL) domain which is surrounded by two meprin, A-5 protein and receptor protein-tyrosine phosphatase mu (MAM) domains. This extracellular structure is unique to the RTK family and is thought to be involved in cell-cell interaction, ligand binding and dimerisation resulting in conformational changes that initiate the activation of the intracellular kinase domain (Hallberg and Palmer, 2016). The ECD also contains a glycine-rich region (GR), a region that contains stretches of up to six glycines in a row (Lorén et al., 2003). Artificial mutations in this region showed the crucial importance of the

glycine-rich region in *Drosophila* ALK function, however the specific function of the glycine-rich region is not completely clear (Lorén et al., 2003). Despite this, monoclonal antibodies (mAbs) which inhibit the glycine-rich region of ALK results in an inhibition of ALK activation (Guan et al., 2015).

The intracellular kinase domain of ALK contains the tyrosine kinase domain and the transmembrane region. This kinase domain contains an amino-terminal lobe and a carboxy-terminal lobe; the catalytic activity of ALK occurs in this domain (Huang, 2018). Furthermore, it contains an "Y*XXX*YY" motif in the activation loop, as per other members of the IR kinase subfamily (Tartari et al., 2008). *In vitro* mutations in this Y*XXX*YY motif have been demonstrated to affect the conformation of this kinase domain. For example, the absence of all three tyrosine residues in the activation loop appears to cause destabilisation of the inactive confirmation leading to partial activation which doesn't require phosphorylation of the first tyrosine, activity that is required to activate ALK under normal conditions (Tartari et al., 2008).

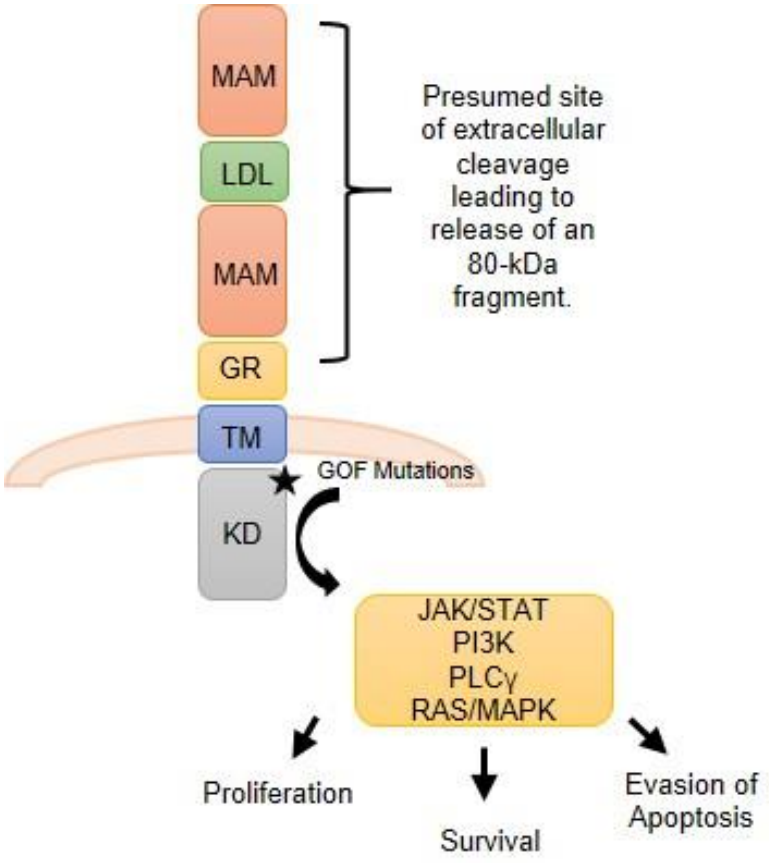

Figure 1.1 Schematic representation of full length ALK

The receptor is made up of an extracellular portion containing an LDL domain flanked by two MAM domains, and a glycine rich region (GR). The intracellular kinase domain (KD) is the location of multiple gain of function (GOF) mutations associated with neuroblastoma, resulting in constitutively active downstream signalling pathways contributing to neuroblastoma disease progression.

1.2.2 ALK function

The physiological role of full length wild-type (WT) ALK is not entirely clear. Studies in mice have shown ALK mRNA is detectable throughout the nervous system during embryogenesis and its expression is restricted to discrete tissues of the developing central and peripheral nervous system (Vernersson et al., 2006, Trigg and Turner, 2018). Furthermore, knockout of the *ALK* gene has shown effects on mouse brain function (Huang, 2018). Similarly, in humans ALK is more highly expressed in the neonatal brain and in the developing sympatho-adrenal

lineage of the neural crest; its expression is then downregulated in children and remains low through adulthood, therefore believed to be implicated in neural development (Passoni et al., 2009, Iwahara et al., 1997). Along with brain regions, human ALK expression has also been noted in the small intestine, testis, prostate and the colon (Della Corte et al., 2018).

Until relatively recently no activating ligands of ALK were known, rendering it an orphan receptor. Family with sequence similarity 150, member A or FAM150A (AUGβ) and Family with sequence similarity 150, member B or FAM150B (AUGα), both known as activating ligands of another closely related RTK, which bind the ECD of the protein have now been reported to also strongly activate ALK (Guan et al., 2015). Interestingly, FAM150B is found to be highly expressed in the human adrenal gland (Zhang et al., 2014). One study also reported the proteins midkine and pleiotropin to be activating ligands for ALK, but this is yet to be independently confirmed (Zhao et al., 2015). Upon ligand binding, homo-dimerisation of ALK and phosphorylation is induced, which is inactivated through de-phosphorylation when there is no stimulation by a ligand (Bossi et al., 2010). ALK activates multiple signalling pathways, including phospholipase Cγ (PLCγ), janus kinase (JAK)- signal transducer and activator of transcription (STAT) and phosphoinositide 3-kinase (PI3K) which affect proliferation, differentiation, transformation and anti-apoptotic signalling (Mosse et al., 2009, Palmer et al., 2009, Chiarle et al., 2008, Hallberg and Palmer, 2013).

1.2.3 ALK in disease

Mutated or aberrant expression of ALK is implicated in a number of malignant tumours. Indeed, ALK receptor signalling has been best characterised in

malignancies where ALK plays a role, including ALCL and NSCLC, where the receptor is activated as a result of translocation events (Bosse and Maris, 2016). Lymphoma cells that express the NPM-ALK fusion oncoprotein result in constitutive kinase activity arising from self-dimerisation of ALK leading to auto- and transphosphorylation (Trigg and Turner, 2018). In ALK-positive ALCL, NPM-ALK results in constitutive signalling from the ALK kinase domain and activation of downstream pathways, including *MYCN* transcription, leading to cell cycle progression, migration and evasion of apoptosis (Trigg and Turner, 2018).

Consistent with other tumours of neural origin, most neuroblastoma tumours express full-length ALK (Lamant et al., 2000). The receptor is implicated in a number of different ways in both neuroblastoma development and its subsequent progression. Most commonly found are gain-of-function activating mutations within the intracellular kinase domain, found in ~8-10% of sporadic and ~50% of familial cases, in which the mutation is also found in the germline (Matthay et al., 2016, Mosse et al., 2008, Janoueix-Lerosey et al., 2008, Schleiermacher et al., 2014). These single-base missense mutations result in ligand-independent phosphorylation and signalling by disruption of the auto-inhibited conformation of the kinase domain. Furthermore, it has been demonstrated that ALK activating ligands, such as FAM150A and FAM150B, can ‘superactivate’ already active ALK mutants found within neuroblastoma, resulting in increased downstream signalling (Guan et al., 2015). One study looking at 1,596 diagnostic neuroblastoma samples showed that ALK mutations were associated with about 14% of high-risk cases (Bresler et al., 2014). Moreover, ALK cooperates with MYCN to drive malignancy, as activation of ALK results in increased expression of MYCN by elevating activity of its promoter and stabilising protein expression,

likely via activation of AKT and ERK (Huang and Weiss, 2013). The co-expression of ALK and MYCN is associated with poorer disease outcome (Figure 1.2).

The 3 main mutation hot spots found in the ALK kinase domain and identified within neuroblastoma are: R1275 (mutated to Q or L), F1174 (mutated to L, S, I, C or V) and F1245 (mutated to L, I, V or C) which account for 85% of ALK mutations, distributed with even frequency amongst clinical stages (Javanmardi et al., 2019). R1275Q is the most common mutation, found in both 33% of sporadic cases and 45% of familial cases (Zhu et al., 2012). On the other hand, the F1174 and F1245 mutations are typically found in sporadic cases of neuroblastoma, 30% and 12%, respectively and are rarely germline (Barr and Applebaum, 2018).

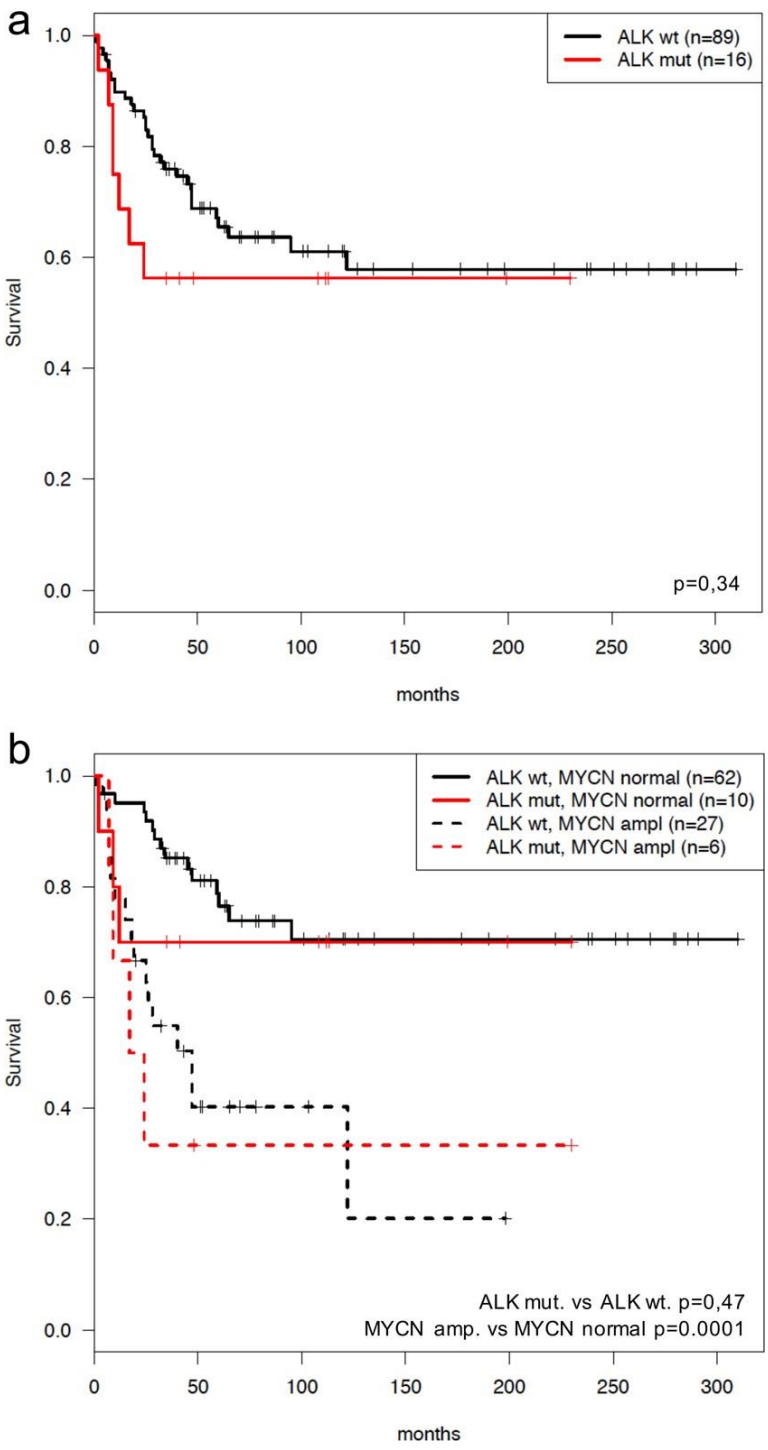

Figure 1.2 Survival Curves of neuroblastoma cases

Kaplan-Meier survival curve comparing overall survival in 105 cases of neuroblastoma with (a) ALK mutations vs WT (non-mutated) ALK and (b) ALK mutation status with and without MYCN amplification. Graph taken from (Javanmardi et al., 2019).

In 2-3% of neuroblastoma cases ALK is amplified resulting in an increased ALK protein expression, and a consequential increase in kinase activity (Trigg and

Turner, 2018). This genomic amplification of ALK is almost exclusively co-amplified alongside MYCN, as the genes are located in close proximity on the 2p arm (2p23-24), and together they are associated with poorer disease outcome (Bresler et al., 2014, Matthay et al., 2016). Interestingly, oncogenic signalling through ALK has also been observed in the absence of activating mutations or gene amplification. It is postulated that WT ALK expressed above a critical level can become constitutively active and contribute to oncoprogression of the disease (Trigg and Turner, 2018). Other more rare mechanisms of ligand-independent ALK signalling found in other diseases include chromosomal translocations and large deletions resulting in truncation of the extracellular region, or aberrant forms or isoforms of ALK that can transmit signalling of downstream pathways (Palmer et al., 2009, Huang, 2018). Furthermore, it has recently been shown that ALK mutations were enriched at relapse and correlated with unresponsiveness to therapy in 54 paired diagnosis-relapse neuroblastoma samples (Zhu et al., 2012, Javanmardi et al., 2019).

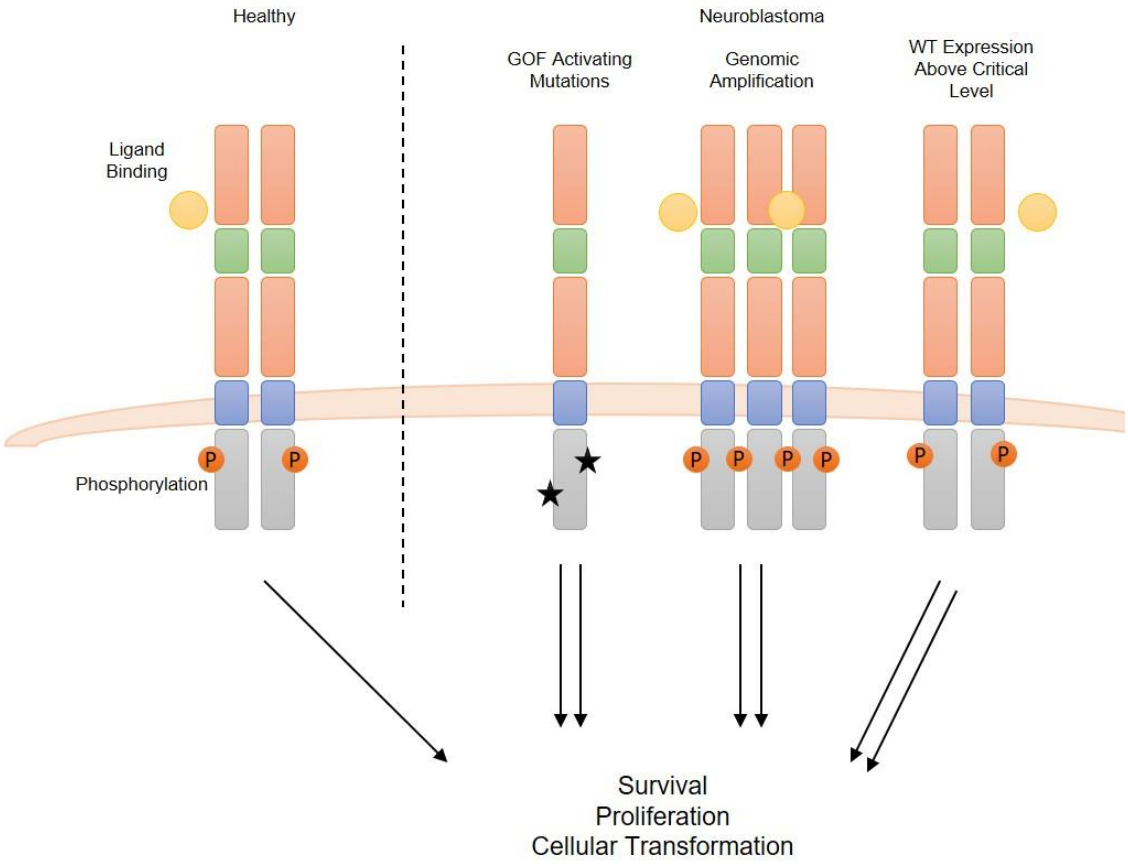

Figure 1.3 Signalling through ALK in healthy tissue and in neuroblastoma

Under healthy conditions, ligand binding results in ALK receptor dimerisation and phosphorylation of the intracellular kinase domain, resulting in activation of signalling pathways. This downstream signalling stops when there is no activating ligand present. In neuroblastoma, gain of function mutations, genomic amplification and ALK expression above a critical level can all result in constitutively active downstream signalling, regardless of the presence of an activating ligand. The over-activation of these downstream signalling pathways contributes to the disease progression of neuroblastoma.

1.2.4 Treatments targeting ALK

The presence of ALK fusion proteins and constitutive ALK tyrosine kinase activity represent a therapeutic target in all malignancies with ALK rearrangement (Della Corte et al., 2018). Previous approaches have included small-molecules tyrosine kinase inhibitors (TKIs), which have led to increases in survival and time to progression in multiple cancers with ALK translocations. Single drug treatment with the small molecule ALK/MET inhibitor, Crizotinib, has shown promising

results in adult NSCLC and ALCL which harbour ALK translocations. However inhibition of ALK mutations in the context of the full length receptor is more complex, and Crizotinib has proved less effective in cases of neuroblastoma (Javanmardi et al., 2019).

ALK may represent a potential target for immunotherapy for neuroblastoma. Multiple studies have highlighted the role of ALK in both sporadic and familial cases of neuroblastoma, irrespective of disease stage. It is not widely expressed on the surface of healthy tissue, with the exception of the developing nervous system and immune privileged sites, and therefore few toxic side effects might be expressed from treatment aimed at blocking ALK function (Della Corte et al., 2018, Lamant et al., 2000).

1.3 T cell mediated immunity: the adaptive immune system

The immune system can be split into two branches; the innate and adaptive arms of defence. The innate immune system represents the first response; it is quicker and of broader specificity, made up of macrophages, neutrophils and NK cells amongst other immune cells. T and B cells form the adaptive immune response, which is mounted when innate immune cells are insufficient to deal with a pathogen. This response is slower, but highly specific and creates a lasting immunological memory. The focus of this thesis is on T cells, specifically the use of alpha-beta (αβ) T cells and how they can be manipulated for immunotherapeutic treatments.

1.3.1 T cell development

1.3.1.1 T cell development in the thymus

During the production of T cells, multipotent precursor cells, or early thymocyte progenitors (ETP), originate in the bone marrow and travel to the thymus where they will differentiate to form either αβ (~95% of the population) or gamma-delta (γδ) T cells. The thymus consists of multiple lobules, through which ETPs migrate and differentiate from CD4-CD8- double negative (DN) into CD4+CD8+ double positive (DP) thymocytes (Figure 1.4). During this process, ETPs go through four separate populations based on their expression of CD44 and CD25 (DN1-4) (Joachims et al., 2006).

Following genetic recombination to generate a functioning T cell receptor (TCR) (described in the following section), thymocytes go through positive and negative selections based on the interaction with major histocompatibility complex (MHC)

molecules expressed by cortical thymic epithelial cells (cTECs), medullary thymic epithelial cells (mTECs) or dendritic cells (DCs) (Takaba and Takayanagi, 2017). This process allows the removal of thymocytes through apoptosis which express TCRs with high affinity for self-peptides (negative selection) while thymocytes with low affinity TCRs for self-peptides are rescued (positive selection) (Spits, 2002). Failure of these selections results in the release of T cells unable to recognise ‘self’ or T cells that are ‘self-reactive’ into the periphery (Takaba and Takayanagi, 2017).

Finally, T cells become single positive (SP) for CD4+ or CD8+, after which they migrate out of the thymus, as naïve T cells. In the peripheral circulation, weak TCR signals are required for the maintenance of T cells, while strong signals generate an immune response (Kannan et al., 2012).

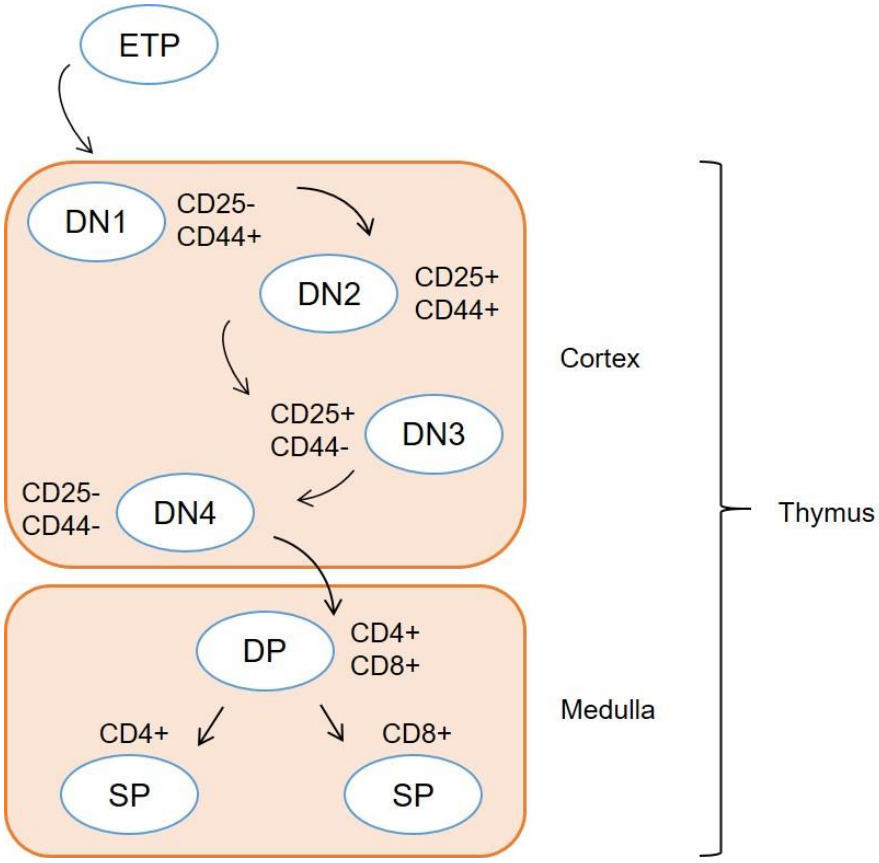

Figure 1.4 T cell development through the thymus

Early thymocyte progenitors (ETPs) produced in the bone marrow, migrate to the thymus for their development into single positive T cells. ETPs move through the cortex where their expression of CD25 and CD44 changes, until they finally become single positive for CD4 or CD8 in the medulla, before entering the peripheral circulation.

1.3.1.2 The T cell receptor

The ability of T cells to detect abnormalities is primarily achieved through the presentation and detection of peptide antigens recognised by the TCR, which is also developed within the thymus. This receptor, present on the surface of all T cells, also determines the specificity of the T cell. The TCR is a heterodimeric structure that has been described as the most intricate receptor structure of the mammalian system (Clambey et al., 2014). It is composed of an alpha (α) and a beta (β) chain which are linked by disulphide bonds. Within these chains there are constant and variable regions. The variable regions, made up of

complementary determining regions (CDRs), determines which antigen is recognised by a T cell. The huge diversity of these receptors is created through somatic recombination; a process in which the variable (V), joining (J) and, in the β and δ chains, diversity (D) gene segments are rearranged to generate CDRs with random and unique specificity. Of the three CDRs, CDR1 and CDR2 bind MHC, while CDR3 contains the site for antigen binding and is the most variable. The CDR1 and CDR2 loops are encoded within the V gene segment portion of the variable-region gene, whereas CDR3 is encoded by the region spanning the V and J, or the V, D and J junctions (Hughes et al., 2003). Therefore, CDR3 has significantly higher levels of diversity due to the addition or loss of nucleotides during the joining process (Hughes et al., 2003). The ultimate goal of this recombination process is to create diversity within CDR3. Whilst in B cells, additional antibody diversity is generated by somatic hypermutation, this phenomenon is not described in human TCR genes. Nevertheless V(D)J recombination, along with addition or deletion of nucleotides at the junctions between gene segments at CDR3 helps to generate an astounding amount of TCR diversity, exceeding 10^{15} distinct TCR specificities per individual (Nikolich-Zugich et al., 2004).

1.3.1.3 TCR CD3 complex

The TCR lacks any signalling domain and subsequent signalling is dependent on the association with the CD3 complex. Moreover, TCR expression on the cell surface can only occur in a complex with the CD3 co-receptor. The CD3 complex consists of 1 gamma (γ), 1 delta (δ), 2 epsilon (ε) and 2 zeta (ζ) chains. They are essential for trafficking to, and the stability of the αβ subunits at, the plasma

membrane, and they also transmit signals across the plasma membrane (Cantrell, 2015). These form three dimers: gamma epsilon (γε), delta epsilon (δε); heterodimers, and two zetas (ζζ); a homodimer. CD3γ, -δ and -ε each contain single immunoreceptor tyrosine-based activation motif (ITAM) in their cytoplasmic tail whereas CD3ζ contains three ITAMs. These ITAMs are responsible for propagating the TCR signal through the cell. Signalling solely through the TCR is not sufficient for T cell activation, and can result in the induction of an anergic state in the thymus, in which T cells fail to respond to antigen stimulation and cannot be further restimulated, or activation induced cell death (AICD) due to lack of further survival signals (Smith-Garvin et al., 2009).

1.3.2 T cell activation

T cell activation is triggered by TCR engagement with its cognate peptide. For sufficient activation and the subsequent signalling cascade to occur, it requires multiple components including; the TCR to be in complex with CD3, the engagement of co-receptors and co-stimulatory molecules, and the formation of a functional immune synapse (IS). These components are discussed below.

1.3.2.1 Antigen processing and presentation

The differentiation of naïve T cells into armed effector T cells is triggered by TCR engagement with its peptide antigen, presented via an MHC (Pennock et al., 2013). Classical antigen presenting cells (APCs), such as dendritic cells (DCs) and B cells, can process and present such antigens to circulating T cells. They express surface receptors, including pattern recognition receptors (PRRs) which detect pathogen-associated molecular patterns (PAMPs) produced by microbes, and damage-associated molecular patterns (DAMPs) which are produced by

damaged or mutated host cells (Gaudino and Kumar, 2019). After binding their appropriate DAMP or PAMP, APCs internalise their target by initiating phagocytosis, pinocytosis or clathrin-mediated endocytosis; the pathway by which the molecules are endocytosed determines how they will be degraded and then displayed by MHC for T cell recognition (Gaudino and Kumar, 2019). MHC I receptors are expressed by all nucleated cells and display endogenous antigens which are recognised by CD8 expressing T cells. Only APCs express MHC II receptors which display exogenous antigens and are recognised by CD4 expressing T cells (Gaudino and Kumar, 2019).

1.3.2.2 The immune synapse

An immune synapse (IS) is formed between T cells and APCs. The matured IS is a highly ordered structure characterised by the segregation of receptors and signalling molecules into distinct concentric rings known as supramolecular activation clusters (SMACs) (Griffiths et al., 2010, Watanabe et al., 2018). The accumulation of the TCR and the associated signalling proteins in the centre of the synapse is termed the cSMAC, while the adhesion molecules, such as integrins, which surround the outside on the periphery is known as the pSMAC (Cantrell, 2015). Larger molecules, such as CD43 and CD45, make up the distal SMAC (dSMAC) (Alarcón et al., 2011). Here, the TCR bound to its cognate peptide, initiates ‘signal 1’ in the process of T cell activation and further stabilises the interaction between the T cell and the APC (Pennock et al., 2013).

1.3.2.3 Accessory Molecules

For complete activation, resulting in transcriptional changes, IL-2 production and ultimately T cell proliferation, ‘signal 2’ of T cell activation is required. Signalling

solely through the TCR results in a non-responsive state in which T cells fail to respond and are then refractory to restimulation (Smith-Garvin et al., 2009). There are many cell surface receptors that can fulfil this role, but CD28 on T cells does so more robustly than other co-stimulatory molecules, and binds CD80/86 on APCs (Smith-Garvin et al., 2009). This co-stimulation can also be provided by other co-stimulatory molecules, such as those from the TNF receptor superfamily (CD27, OX-40 and 4-1BB) when interacting with their appropriate ligand on APCs (CD70, OX-40L and 41BBL, respectively) to promote the survival of proliferating cells and differentiation (Pennock et al., 2013, Gaudino and Kumar, 2019). The co-receptors aforementioned are positive co-regulators of T cell activation, however negative co-regulators also exist. For example, PD-1 and CTLA-4 expressed on T cells, which bind PD-L1 and CD80/86, respectively, result in exhaustion and apoptosis of T cells, as opposed to activation (Cantrell, 2015). These negative co-regulators are critical for limiting T cell function during immunity and tolerance, limiting the expansion of effector cells during an immune response, such as the pathology associated with effector CD8+ T cell mediated actions (Cantrell, 2015, Pennock et al., 2013).

The CD4 and CD8 co-receptors also play a role in the immune synapse. Along with determining which class of MHC is recognised and bound by TCR, the CD4 and CD8 accessory molecules are responsible for stabilising the interaction between the TCR and the pMHC (peptideMHC) by binding invariant regions of the MHC molecule (Artyomov et al., 2010, Miceli and Parnes, 1991). Moreover, the co-receptors also bring kinase molecules into the complex, attached to their cytoplasmic tails, which are required for the initiation of T cell signalling (Artyomov et al., 2010). Increasing evidence suggests that the primary function of the co-

receptors is to form a complex with the TCR for the recognition of antigen-bound MHC (Miceli and Parnes, 1991). Indeed, the co-receptor that is bound in complex with the TCR by the pMHC within the thymus determines the subsequent effector function of the T cell, becoming a CD4+ helper T cell, or a CD8+ cytotoxic T cell.

1.3.3 T cell signalling

Once the formation of the IS occurs, TCR signalling is initiated (Figure 1.5). ITAMs in the cytoplasmic tails of the CD3ζ chains are phosphorylated by tyrosine kinases of the Src-family, such as Lck. Lck is bound to the cytoplasmic tails of the CD4 and the CD8 co-receptors, brought into proximity of the TCR/CD3ζ during IS formation (Goyette et al., 2019). The ITAMs can then be bound by zeta-chain-associated protein kinase 70 (Zap-70) (Kannan et al., 2012). The binding of Zap-70 to ITAMs results in its activation which is proposed to release Zap-70 from an auto inhibited conformation and expose regulatory tyrosine residues for phosphorylation by Src-kinases (Cantrell, 2015). Zap-70 further phosphorylates linker for activation of T cells (LAT), leading to the creation of the LAT signalosome which is responsible for further downstream signalling (Pennock et al., 2013).

LAT is responsible for recruiting a second molecular scaffold, SH2 domain-containing leukocyte phosphoprotein of 76kDa (Slp-76), which is also phosphorylated by Zap-70, producing the LAT-Slp-76 complex, acting as a further scaffold for the recruitment of signalling effector molecules (Smith-Garvin et al., 2009, Pennock et al., 2013). Interleukin-2 inducible kinase (ITK) then interacts with LAT-Slp-76 complex and becomes activated by autophosphorylation which promotes the phosphorylation of the effector molecule

phospholipase C gamma 1 (PLC-γ1) (Cantrell, 2015). PLC-γ1 transduces signals by cleaving phosphatidylinositol triphosphate (PIP_2) in the plasma membrane to generate the second messengers, diacylglycerol (DAG) and inositol 1,4,5-triphosphate (IP_3) (Cantrell, 2015).

DAG activates a number of downstream proteins, including various isoforms of protein kinase C (PKC) and RasGRP which both in turn activate the NF-κB pathway and the MAPK pathway, respectively. IP_3 is responsible for the efflux of calcium ions from the endoplasmic reticulum (ER) to the cytoplasm and from extracellular fluid through plasma membrane channels. This increase in intracellular calcium levels results in the activation of calmodulin and calreticulin which further induces the de-phosphorylation and activation of the T cell transcription factor nuclear factors of activated T cells (NFAT). NFAT then migrates to the nucleus to join other transcription factors inducing the transcription of specific genes, such as IL-2, IL-4, TNFα and IFNγ (Cantrell, 2015).

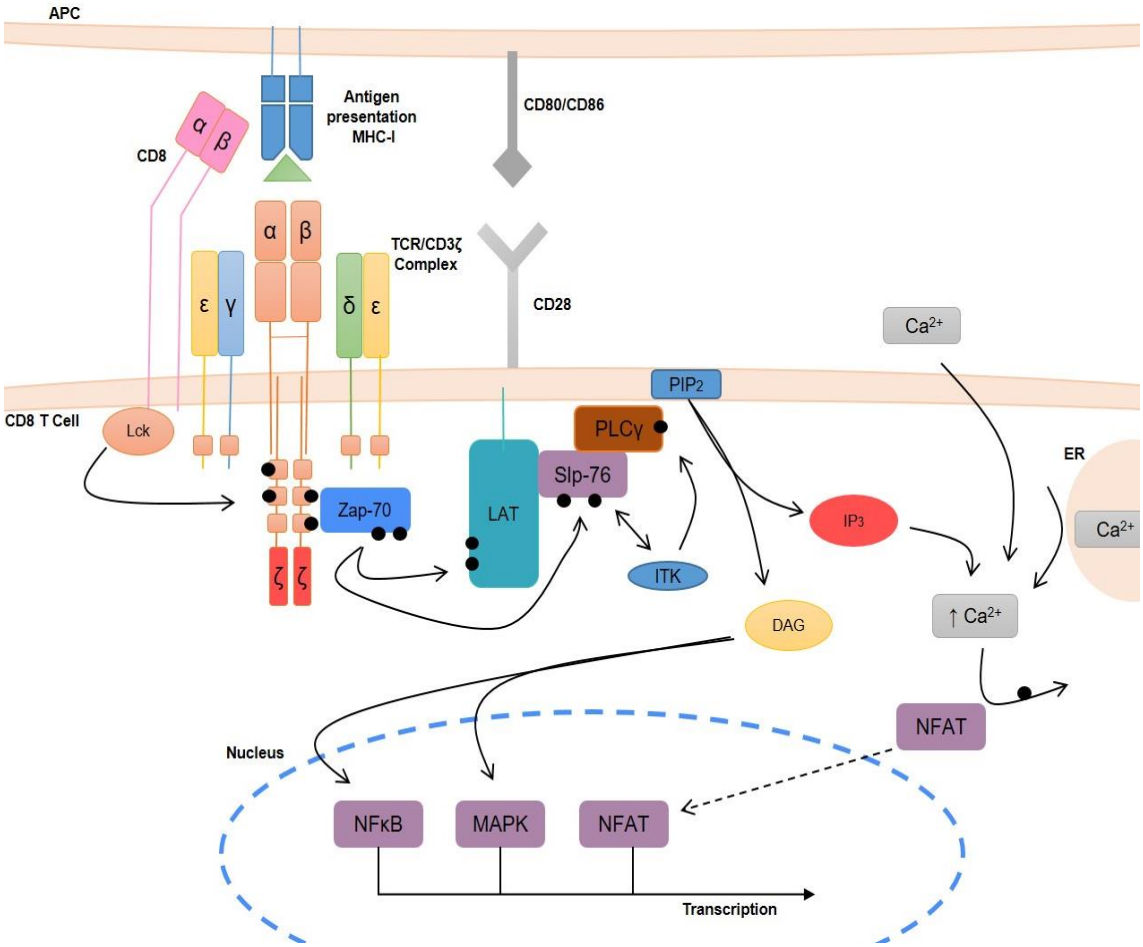

Figure 1.5 TCR signalling through CD8+ T cell on recognition of MHC I

The immune synapse is created through the detection of a peptide antigen on a MHC presented by an APC, which is bound by the αβ TCR and the CD8 co-receptor. The binding of CD28 co-stimulatory molecule to its relevant ligand on an APC, in this case CD80 or CD86, is also required. The downstream signalling is initiated through Lck, which phosphorylates ITAMs in the tails of CD3ζ which further phosphorylates Zap-70. Zap-70 subsequently phosphorylates LAT, creating the LAT-Zap-70 complex. This complex interacts with ITK, which promotes the phosphorylation of PLCγ which generates the secondary messenger molecules, IP_3 and DAG by cleaving membrane bound PIP_2. In turn, downstream pathways such as NFκB, MAPK and NFAT in the nucleus induce the transcription of genes such as IL-2 and IFNγ resulting in T cell effector functions. Adapted from (Schwartzberg et al., 2005).

1.3.3.1 Effector functions

Antigen stimulation of T cells results in clonal expansion of CD4+ T cells and CD8+ T cells, resulting in a pool of memory T cells that possess phenotypes and functions tailored to respond to reinfection (Pennock et al., 2013). CD4+ T cells, or T helper cells, support the immune system through the production of cytokines

and chemokines which recruit new immune cells to the site of infection. They mediate control of further T cell and B cell differentiation and/or direct the activity of macrophages and neutrophils (Pennock et al., 2013, Cantrell, 2015). At least five different major subpopulations of these mature CD4+ T helper cells exist, with distinct functions, that are tailored towards different pathogens (Cantrell, 2015). Th1 cells produce IFNγ; Th2 cell produce interleukin (IL)-4 and IL-13; Th17 cells produce proinflammatory cytokines such as IL-17 and IL-22; regulatory (Treg) T cells function to restrain autoimmunity and strong inflammatory responses; and follicular helper (Tfh) T cells regulate the development of antigen-specific B cell immunity (Cantrell, 2015, Gaudino and Kumar, 2019).

CD8+ T cells, or cytotoxic T cells, have an ability to detect and kill virus- or bacteria- infected and/or transformed neoplastic cells (Gaudino and Kumar, 2019, Cantrell, 2015). They play a pivotal role in providing effective antigen-specific immunity against tumours, through the presentation of tumour-derived antigens presented on MHC class I molecules (Menares et al., 2019). They elicit their cytotoxic activity through the release of granzyme and perforin granules, and the induction of FasL-mediated apoptosis of target cells (Menares et al., 2019, Pennock et al., 2013). It is important to note that while these are canonical functions of CD4+ and CD8+ T cells, numerous exceptions to these rules have been documented, and, in any setting, the potential of cytokine-producing helper CD8+ T cells and/or cytotoxic CD4+ T cells must be considered (Pennock et al., 2013).

1.3.4 Cancer and the Immune System

Cancer immune surveillance, or immunosurveillance, was first hypothesised by Burnet and Thomas in 1957, which explained that genetic changes must be common in somatic cells and a proportion of these changes will represent a step toward malignancy. It is therefore an evolutionary necessity that there should be some mechanism for eliminating or inactivating such mutant cells (Burnet, 1957). There is now a wealth of evidence supporting a dual role for the immune system in cancer. Research over the past two decades has demonstrated an ability of the immune system to constrain tumour development by destroying malignant cells and preventing their outgrowth, while simultaneously promoting tumour progression by selecting for more 'fit' tumour cells which have a higher chance of survival, and establishing a microenvironment which can promote this outgrowth (Schreiber et al., 2011, Vesely and Schreiber, 2013, O'Donnell et al., 2019). This is explained in the 'cancer immunoediting' hypothesis, which is described in three main phases: elimination, equilibrium and escape.

Elimination

During the elimination phase, also known as immunosurveillance, the innate and the adaptive immune system work together to detect the presence of malignant cells and attempt to destroy them before they are established and become clinically apparent (Vesely and Schreiber, 2013, Vesely et al., 2011). There are multiple ways the immune system can do this; through protection against viruses and subsequent suppression of virus-induced tumours, through the resolution of inflammatory environments that are conducive of tumourigenesis by the elimination of pathogens and finally, elimination of malignant cells through

lymphocyte detection of tumour antigens and subsequent destruction (Schreiber et al., 2011, Vesely et al., 2011). Intrinsic tumour-suppressor mechanisms exist, such as the ability of cells to repair genetic mutations and trigger senescence or apoptosis through cell death pathways, including TNF-related apoptosis inducing ligand (TRAIL) and FasL mediated pathways (Vesely et al., 2011). The type, location and density of immune cells, such as tumour-infiltrating lymphocytes (TILs), present in the tumour microenvironment of a patient is now recognised to be a prognostic predictor of a patient's overall survival duration and predictive of their response to treatment, demonstrating the protective role the immune system can play (O'Donnell et al., 2019). Furthermore, there is much evidence supporting the association of higher IFNγ producing CD4+ and CD8+ T cells and improved patient prognosis in many different cancer types (Schreiber et al., 2011). Despite this, some tumour cells evade the immune system and remain.

Equilibrium

Rare tumour subclones that are capable of surviving elimination by the host immune system enter a dynamic equilibrium. During this phase, which is often the longest, lymphocytes and IFNγ exert potent selection pressure on tumour cells which is enough to contain them, but not completely extinguish them (Dunn et al., 2002). This constant pressure from the adaptive immune system, coupled with genetic instability of tumour cells can select for subclones that have reduced immunogenicity and can therefore evade immune recognition and destruction (O'Donnell et al., 2019). These immunoedited tumours can then enter into the escape phase, in which their growth is unrestrained and disease becomes clinically apparent (O'Donnell et al., 2019).

Escape

There are multiple mechanisms by which tumour cells can escape this equilibrium phase. Changes to the tumour cell population itself can occur due to an active immunoediting process, such as the occurrence of new mutations which may confer increase resistance from an immune attack (Vesely et al., 2011, Dunn et al., 2002). For example, induction of anti-apoptotic mechanisms through activation of pro-oncogenic transcription factors such as STAT3, and downstream expression of anti-apoptotic effector molecules such as BCL-2 (Schreiber et al., 2011). Moreover, the loss of antigen presentation by malignant cells through MHC downregulation and genetic instability creates antigen loss variants that are no longer detectable by antigen specific CD8+ T cells (Chen and Mellman, 2013, Vesely et al., 2011). Tumour cells or surrounding immunosuppressive cells can have increased presentation of immune checkpoint inhibitors, such as PD-1 which can deactivate T cells (O'Donnell et al., 2019, Chen and Mellman, 2013). Furthermore, tumour cells can develop a decreased ability to respond to IFNγ through mutations or epigenetic silencing of genes encoding the IFNγ receptor signalling components (Vesely et al., 2011).

Alternatively, or simultaneously, changes to the host immune system can occur, such as cancer-induced immunosuppression or natural aging of the immune system which can allow these tumour cells to progress unhindered (Vesely et al., 2011). The establishment of an immunosuppressive tumour microenvironment (TME), promoted by suppressive cytokines secreted by tumour cells, or the presence of immunosuppressive immune cells, promotes the outgrowth of malignant cells (Schreiber et al., 2011).

Furthermore, tumour cells can evade detection due to the induction of central or peripheral tolerance. Central tolerance is the process of self-reactive T cells being eliminated or converted to a regulatory phenotype in the thymus. In this case, tumours that lack neoantigens will not be detected by the adaptive immune system and are free to grow unhindered (Vesely et al., 2011). Peripheral tolerance is an important process whereby T cells reactive with self-antigens not expressed in the thymus are deleted or rendered nonresponsive in the periphery. In this case, some level of anti-tumour immune response may be initiated transiently before tolerance is induced, leading to tumour progression (Vesely et al., 2011).

1.3.5 Cancer immunotherapy

For decades the standards for treating cancers included surgery, chemotherapy and radiotherapy. More recently, the manipulation of the immune system in order to reactivate its inherent anti-tumour response, or to overcome the pathways leading to escape, has gained much precedent (Kennedy and Salama, 2020). To be effective, immunotherapies must increase the quality or quantity of immune effector cells, reveal additional protective tumour antigens and/or eliminate cancer induced immunosuppressive mechanisms (Schreiber et al., 2011). Multiple mechanisms have been investigated, including; (a) vaccination approaches to elicit strong specific immune responses against tumour antigens, (b) immune checkpoint blockade (ICB) through inhibition of molecular and cellular mediators of cancer-induced suppression, such as CTLA-4 or PD-1, (c) administration of monoclonal antibodies (mAbs) against tumour antigens and (d) adoptive cell therapy (ACT) involving the transfer of expanded naturally arising or genetically engineered lymphocytes (Schreiber et al., 2011). Of the

aforementioned, a and b are considered to be active immunotherapy, while c and d are considered passive. Effective immunotherapy that can drive tumours back to the elimination phase, would be reflected in a complete response by a patient (O'Donnell et al., 2019).

1.4 Adoptive Cell Therapy

Harnessing the adaptive immune system, namely T cells, has multiple benefits. T cell responses are specific and can allow for the discrimination between malignant and non-malignant cells. On activation, T cell responses are robust and they have the ability to traffic to the site of infection or malignancy. Finally, T cells can form an immunological memory after initial response (Pennock et al., 2013). ACT has emerged as a new therapeutic pillar within oncology, aiming to overcome tumour-induced immunosuppression and to boost the immune system's ability to recognise tumour cells, thus enabling immune-mediated tumour clearance (O'Donnell et al., 2019). This can include the use of tumour-infiltrating lymphocytes (TIL), or T cells engineered to express a TCR or a chimeric antigen receptor (CAR) (Rohaan et al., 2019).

1.4.1 Chimeric Antigen Receptors

The concept of CAR T cell therapy was originally developed by Eshhar et al., who created fusion molecules which utilised the specificity of monoclonal antibodies directed against surface antigens expressed on tumour cells. These were combined with the cytotoxic activity of T cells resulting in the destruction of said tumour cells without the requirement of antigen presentation through MHC (Eshhar and Gross, 1990). In this way CAR T cells employ natural T cell activation pathways as TCR expressing cells, but bypass the need for peptide presentation (Lim and June, 2017, Rohaan et al., 2019). The use of CAR T cells targeting CD19 has been revolutionary in the treatment of haematological malignancies; yielding up to 90% complete remission in refractory B cell leukaemia (Labanieh et al., 2018).

These engineered molecules are generally comprised of three modular regions; an extracellular binding domain, a spacer and transmembrane domain followed by intracellular signalling domain(s) (Figure 1.6). The generation of CAR is dependent on how many co-stimulatory domains are present (Gacerez et al., 2016). It is still not completely understood how the complete CAR structure determines its function or the complexity of CAR intracellular signalling as well the web of interactions between CAR T cells and other protagonist cells within the tumour microenvironment (TME) of a cancer *in vivo* (Ajina and Maher, 2018). Table 1.1 documents the pros and cons comparing first, second and third generation CAR T cells.

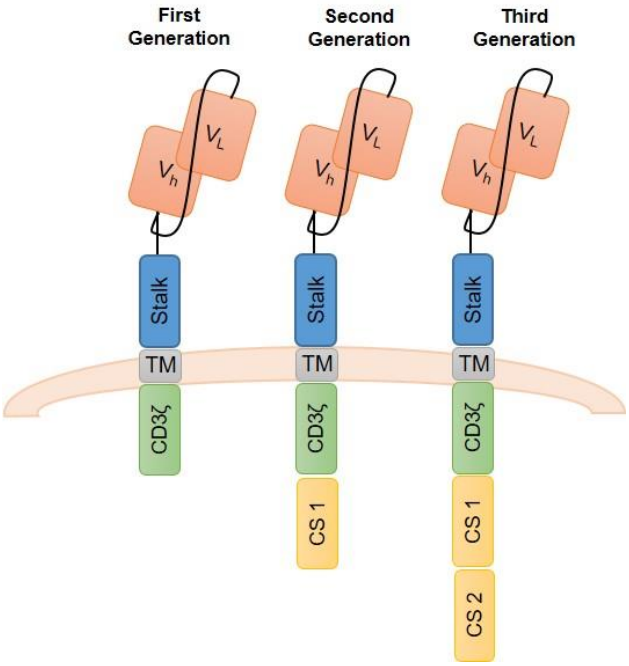

Figure 1.6 Schematic showing the generations of CAR T cell therapies

CAR T cell constructs comprise of an single chain variable fragment (scFv) domain made up of heavy (V_h) and light (V_l) chains derived from monoclonal antibodies, joined by a linker. They also contain a spacer region, transmembrane domain (TM) and a CD3ζ domain. The inclusion of one or more co-stimulatory domains (CS) determines which generation the CAR construct is classified as; first generation CARs contain CD3ζ only, second generation CARs contain the addition one co-stimulatory domain and third generation contain the addition of two co-stimulatory domains.

Table 1.1 Pros and cons for three CAR T cell generations

CAR Generation	Pros	Cons
First generation	Less prone to exhaustion or side effects	Lacks potency and proliferation with no costimulatory domain
Second generation	Increased potency and efficacy with inclusion of one co-stimulatory domain	Increased chance of side effects with inclusion of one co-stimulatory domain
Third generation	Higher potency with two co-stimulatory domains, can mix and match co-stimulatory domains of different phenotypes	Higher potency increases rick of side effects and exhaustion

1.4.1.1 CAR binding domain

The antigen recognition and binding domain of the CAR construct is the extracellular portion that re-directs the specificity of the T cell. Most commonly, this is a single-chain variable fragment (scFv) composed of variable heavy (V_H) and light (V_L) chains derived from monoclonal antibodies. These are often joined with a glycine-serine flexible linker; the commonly used $(Gly_4Ser)_3$ peptide results in a flexible and soluble linker that results in proper scFv folding (Dwivedi et al., 2019).

Since the scFv is derived from an antibody, the receptor is able to bind antigens without the need for these to be presented by MHC molecules, thus enabling MHC-independent activation (Rafiq et al., 2020). Usually, a CAR is targeted against an antigen which is expressed on tumour cells. Ideally this antigen would be restricted to, and universally expressed on malignant cells alone, such as a tumour-specific antigen (TSA) or a neoantigen. However the identification of truly cancer specific antigens is rare and expression of TSAs can be highly heterogeneous, both within the same patient and amongst different patients suffering from the same malignancy (Liu et al., 2019). Therefore, CAR T cells are

most commonly redirected against tumour-associated antigens (TAAs). These antigens are overexpressed on malignant cells but are still present on non-malignant cells, albeit at much lower densities (Watanabe et al., 2018). Targeting of these TAAs, however, carries the risk of on-target off-tumour toxicity through the destruction of otherwise healthy tissue that express the antigen of interest. Discovering targets that provide sufficient discrimination between malignant and healthy tissue is challenging and the majority of clinical trials investigating CAR T cells so far demonstrate evidence of some cross-reactivity toward non-malignant cells (Lim and June, 2017). In some cases, CAR T cells are directed against alternative targets, for example, inhibitory cells or soluble ligands that are present in the TME. Transforming growth factor beta (TGF_{β}) is an example of a cytokine which plays a suppressive role in the microenvironment of many cancer types. Targeting of this cytokine by CAR T cells can silence it, preventing its inhibition of T cells and transforming the TME from a suppressive to an immune supporting environment (Chang et al., 2018).

The scFv can affect the characteristics of the CAR beyond solely recognising and binding the target antigen. The affinity and avidity of an scFv are important considerations. The affinity is defined as the strength of the binding interaction between a single antigen and the binding region of an scFv, while the avidity is the accumulated strength of multiple affinities, from multiple binding interactions, and therefore depends on the number of receptor ligand pairs and target antigen density (Rudnick and Adams, 2009). The affinity can be affected by the interaction of the CDRs in the light and heavy chains of the scFv (Chailyan et al., 2011). Equally, the avidity of an scFv is required to be high enough to effectively recognise tumour cells and induce CAR signalling and T cell activation; however,

exclusively high affinity scFvs can lead to activation-induced cell death (AICD) of the CAR expressing cell, antigen-independent tonic signalling and potential toxicities (Watanabe et al., 2014). Drent *et al*., demonstrated that a reduced affinity scFv combined in a CAR directed against CD38, showed optimal proliferation, production of cytokines and cytotoxic activity against CD38 expressing multiple myeloma cells, but spared CD38+ healthy hematopoietic cells *in vitro* and *in vivo* (Drent et al., 2017). This demonstrates the importance of the balance between target antigen expression levels on malignant and healthy tissues to achieve discrimination between reactivity against these respective tissues. There is seemingly a 'therapeutic window' that can be exploited, by which healthy antigens overexpressed on malignant cells, can be targeted with affinity tuned CAR T cells which won't be activated in the presence of low target antigen; on healthy tissue for example (Hudecek et al., 2013, Caruso et al., 2015, Majzner et al., 2020).

It further highlights that the binding affinity of a CAR is related to both safety and efficacy, and that higher affinity is not necessarily better (Martinez and Moon, 2019). For example, an *in vivo* study found that CAR T cells targeting ICAM-1, a marker associated with many solid tumours but also on normal tissue, were safer and more effective when bearing CARs with micromolar affinity than those with higher, nanomolar affinity (Park et al., 2017). Furthermore, it was demonstrated that the CAR with lower affinity showed less exhaustion and enhanced proliferation *in vivo* (Ghorashian et al., 2019). Low affinity of a TCR and its cancer associated pMHC can result in failed antigen recognition, however high affinity can be accompanied by autoimmune responses, which can lead to adverse effects of those treated with ACT (Zhong et al., 2013). CAR T cell function is

governed by CAR density as well as target antigen density, where low expression of either can result in limited functionality and sensitivity of CAR T cells (Watanabe et al., 2018). On the other hand, continuous signalling of the CAR, or tonic signalling, due to the CAR structure, or high CAR density, can result in inferior anti-tumour effects, increased T cell differentiation, exhaustion and activation induced cell death (AICD) (Long et al., 2015).

1.4.1.2 Transmembrane and spacer region

The transmembrane domain (TMD) and spacer region (also referred to as 'hinge' or 'stalk' depending on the length) connect the extracellular scFv of the CAR to the intracellular signalling domains. While the TMD anchors the structure to the cell membrane, the spacer projects the scFv into the extracellular cytoplasmic space and should provide both sufficient flexibility to mediate an immune synapse, and length to facilitate access to the target antigen (Rafiq et al., 2020, Chailyan et al., 2011). The TMD is usually derived from type I proteins such as CD3ζ, CD28, CD4 and CD8α chain (van der Stegen et al., 2015). It has been shown that the domain used can influence the stability and function of the CAR. For example, CAR T cells containing the CD28 TMD are thought to be more stable than those harbouring the TMD of CD3ζ (Dotti et al., 2014).

The importance of including a spacer region was originally documented by Moritz and Groner (1995) who demonstrated it was crucial for the function of an anti-ErbB2 CD3ζ first generation CAR (Moritz and Groner, 1995). Amino acid sequences from CD8, CD28 and IgG-derived peptides such as IgG1 or IgG4, have all been utilised as CAR spacer regions (Gacerez et al., 2016). Along with projection into the extracellular space and flexibility, the spacer allows for

dimerisation between scFvs which can further improve CAR stability (Guedan et al., 2018a, Gacerez et al., 2016). The optimal length of each CAR spacer should be determined on a case by case basis, as it represents an important domain of the receptor. Of course, this can be influenced by multiple factors; including the architecture of the target antigen and the position of the binding epitope on the target antigen that the scFv is recognising. Factors such as these will determine the size of the immune synapse, and therefore the distance that is required between the effector and target cell to obtain optimal T cell activation. A longer and/or more flexible spacer might provide extra flexibility to allow for a CAR to have better access to binding epitopes that are proximal to the target cell membrane (Guedan et al., 2018a). An example of this is the Fc IgG derived 'CH2CH3 spacer', composed of the constant heavy chain domains, CH2 and CH3, from either IgG1 or IgG4 (Gacerez et al., 2016).

Two of the most frequently used spacer regions are the CD8 and Fc spacers, which are used in this project. The CD8 spacer is shorter, made up of 45 amino acids, while Fc spacers are longer depending on which immunoglobulin they are derived from; IgG1 CH2CH3 made up 234 amino acids, and IgG4 CH2CH3 made up of 228 (Schäfer et al., 2020). The use of Ig-derived spacers is particularly attractive as it provides the opportunity to modulate the spacer length, by removing parts of the CH2CH3 domain, while still retaining the nature of the parent protein (Schäfer et al., 2020). Another common reason for the use of Fc spacers, is the ability to quantify and purify Fc CAR expressing cells from T cell populations, using anti-Fc antibodies (Jayaraman et al., 2020). Saying this, the use of Fc spacers has been heavily linked to off-target activity (Watanabe et al., 2016). Typically, the CD8 spacer is used instead of a CD28 derived spacer, which

has been shown to have increased dimerisation, greater cytokine release and subsequently AICD (Jayaraman et al., 2020). Modulation of the CD8 spacer, through the addition of residues or truncation, dramatically altered *in vitro* and *in vitro* responses, demonstrating the importance in considerations in the spacer region used within CAR T cell structures (Ying et al., 2019). It is important to remember that the choice of spacer should reflect the immune synapse, and the location of the binding epitope.

1.4.1.3 Signalling domains

In order to generate a productive T cell response upon scFv engagement, a CAR must contain intracellular signalling domains. Initial experiments using a single CD3ζ domain first generation CAR showed low cytotoxicity and proliferation due to lack of co-stimulation and lack of cytokine production (Eshhar and Gross, 1990, Eshhar et al., 1993). The addition of co-stimulatory domains gave more optimal T cell function, comprising of increased T cell persistence, cytokine production and proliferation, especially on repeated antigen exposure (Maher et al., 2002). Co-stimulatory domains including CD27, OX40, ICOS and signalling modules from the innate immune system such as MyD88 and CD40 have all shown to induce different CAR T cell properties (Lim and June, 2017).

Probably the most widely investigated co-stimulatory domains are CD28 and 4-1BB (CD137), which when incorporated into CAR design, have been shown to increase levels of IL-2 secretion, increase T cell proliferation and mediate greater tumour rejection in patients (Lim and June, 2017). However, perhaps not surprisingly, functionally these two domains endow a CAR T cell with different functional characteristics (Maher et al., 2002). The use of the CD28 domain has been shown to induce remission more quickly in patients with more rapid T cell

activity and differentiation into effector memory cells (Kawalekar et al., 2016), which subsequently results in CAR T cell exhaustion (Lim and June, 2017). This higher level of initial CAR activation could also contribute to side effects such as cytokine release syndrome (CRS) in patients, which can be fatal.

Conversely, CAR T cells expressing 4-1BB has been associated with lower peak levels of T cell expansions, leading to increased T cell endurance, persistence and a lower risk of side effects including cytokine-mediated toxicities (Maher et al., 2002, Lim and June, 2017, Kawalekar et al., 2016). Furthermore, they tend to differentiate more frequently into central memory cells (Kawalekar et al., 2016). Different malignancies might benefit from CAR T cells incorporating different co-stimulatory domains. For example, patients with high disease burden and/or tumours with a high target antigen density, the inclusion of the 4-1BB endodomain may be sufficient and result in less toxicities (Long et al., 2015). On the other hand, where low target antigen density is present or an scFv has low affinity for its target, the CD28 endodomain may be required to reach the threshold required for T cell activation (Maher et al., 2002).

1.4.2 CAR T cell therapy in neuroblastoma

As discussed earlier, treatments for neuroblastoma have developed, however high relapse rates for high-risk disease cases and unacceptable side effects from treatments shows the need for new innovative treatments. While low- and intermediate-risk forms of neuroblastoma are highly curable, over half of patients with high-risk disease suffer relapse and five year survival is 40-50% (Trigg et al., 2019). Novel therapies that can offer long-term disease remission, without long lasting side effects are required. Naturally with the success of Dinutiximab, the

anti-GD2 mAb, GD2 targeted CAR T cell therapies have been investigated. While these GD2 targeting CAR T cells have shown success in neuroblastoma mouse models, they have also demonstrated lethal CNS toxicity due to CAR T cell infiltration and proliferation within brain regions (Richman et al., 2018, Long et al., 2015, Long et al., 2016). Furthermore, several clinical trials have shown partial responses to GD2 CAR T cell therapy, these results have not been as robust and prolonged as seen with those in haematological malignancies (Pule et al., 2008, Louis et al., 2011, Park et al., 2007, Yang et al., 2017, Straathof et al., 2020).

Preclinical mouse model investigations have sought to identify other CAR T cell therapies for neuroblastoma. CAR T cells developed against Glypican-2 (GPC2), a cell surface heparan sulfate proteoglycan important for neuronal cell adhesion and neurite outgrowth, was investigated in a disseminated neuroblastoma mouse model. This model had tumour metastasis to multiple clinically relevant sites, in which a GPC2 CAR T cell significantly suppressed the growth of metastatic neuroblastoma cells in mice (Li et al., 2017). Furthermore, CAR T cells targeting B7-H3 have been utilised in neuroblastoma xenograft models. B7-H3 belongs to the B7 immune co-stimulatory and co-inhibitory family and is aberrantly expressed in neuroblastoma, along with other malignancies. B7-H3 targeting CAR T cells have also shown antitumour effects in neuroblastoma xenograft models (Du et al., 2019). An alternative ALK CAR T cell was also investigated in a xenograft mouse model of neuroblastoma. Walker *et al.,*demonstrated limited efficacy *in vivo* with this anti-ALK CAR (Walker et al., 2017). However, as with CAR T cells in all solid tumours, there remains challenges in the design of these therapies for neuroblastoma; including suboptimal T cell persistence and

potency, lack of target antigen choice and the immunosuppressive microenvironment (Richards et al., 2018, Lim and June, 2017).

1.4.3 Challenges for solid tumours

There are multiple reasons why translating CAR T cells from haematological malignancies to solid tumours is difficult. These include; finding the tumour, access into the tumour, and surviving in the tumour, which are discussed below.

Antigen selection

The first step to a successful ACT is selection of an optimal antigen for CAR targeting. One major limitation in solid tumours is antigen heterogeneity; the variability in the expression of the antigen on the cells within a given tumour (Newick et al., 2017). Solid tumours rarely express one tumour specific antigen, most likely expressing multiple TAAs which are enriched on the tumour but also present at low levels of normal tissue, in most cases the organ of tumour origin (Martinez and Moon, 2019, Richards et al., 2018). Of course, this raises safety concerns - for example in one case, fatal cytokine release syndrome (CRS) was reported from the targeting of human epidermal growth factor 2 (HER2) with CAR T cells for metastatic colon cancer, due to the recognition of low-levels of HER2 expressed in healthy lung epithelium (Morgan et al., 2010).

Even in a setting of a uniformly expressed TAA, there is a possibility of antigen loss or antigen escape in which the target antigen disappears from the surviving tumour. Both heterogeneity of target antigen expression and evolution of antigen-loss variants under selection pressure from CAR T cells represent a major limitation of CAR therapy, which normally has been restricted to one or two tumour antigens (Brown et al., 2019). Immunoediting can occur with the

subsequent removal of the most immunogenic epitopes which can lead to tumour escape; this has previously been shown with CD19 negative escape variants in leukaemia (Restifo et al., 2012).

Overcoming physical barriers

In the case of solid tumours, it is necessary that CAR T cells should traffic and infiltrate the tumour site (Brown et al., 2019). Access of CAR T cells to their target is, in part, dictated by the surrounding TME. Tumour cells establish a complex, immunosuppressive niche made up of multiple components which contribute to physical, chemical and metabolic barriers to infiltrating immune cells. The tumours are surrounded by dense extracellular matrix, tumour stroma and abnormal vasculature, which physically impede CAR T cell entry (Watanabe et al., 2018, Martinez and Moon, 2019). Compared to healthy vasculature, tumour vasculature is disorganised resulting in impaired circulation and resultant hypoxia with increased interstitial pressure (Galluzzi et al., 2018, Richards et al., 2018). The TME contains multiple suppressive cell types, both from the tumour and the immune system, namely; cancer associated fibroblasts (CAFs), tumour associated macrophages (TAMs), myeloid-derived suppressor cells (MDSCs) and Tregs. These cells, along with tumour cells, secrete factors such as TGF_{β}, reactive oxygen species (ROS) and lactate which contribute towards abnormal vasculature production and further render the microenvironment toxic and suppressive (Martinez and Moon, 2019). A mismatch between the chemokines released by the tumour or tumour stroma and the chemokine receptors expressed on T cells can also impede lymphocyte homing to the tumour site (Martinez and Moon, 2019, Vignali and Kallikourdis, 2017).

Surviving the tumour microenvironment

The expression of CD19 on healthy B cells, as well as on malignant B cells, might be one of the many reasons the anti-CD19 CAR T cell therapy can persist and proliferate *in vivo*. Furthermore, this works in a patient scenario because the loss of CD19+ healthy B cells, also known as B cell aplasia, is considered a tolerable side effect which can be treated. This is most likely not the case with solid tumour antigen expression on healthy tissues, and on-target off-tumour toxicity would be mostly intolerable.

Tumours overexpress immunosuppressive cytokines, including vascular endothelial growth factor (VEGF) and TGF_{β} which further promotes the expression of co-inhibitory receptors, such as PD-1 and CTLA-4 (O'Donnell et al., 2019). Moreover, suppressive immune cells such as Tregs, MDSCs and TAMs also express inhibitory ligands which drive tumour-infiltrating CD8+ T cells into exhaustion (Maher et al., 2002, Galluzzi et al., 2018, Chen and Mellman, 2013). The glycolytic metabolism of tumour cells produces soluble metabolites that render the TME hypoxic, acidic, low in nutrients and prone to oxidative stress; all of which contribute too reduced lymphocyte activation, diminished proliferation and reduction in effector activity (Martinez and Moon, 2019, O'Donnell et al., 2019).

Understanding how CAR T cells gain access to the solid tumour is an important and interesting question. Animal models of solid tumours where CAR T cells are effective show accumulation in the tumour site, but limited accumulation in other organs (Martinez and Moon, 2019). There are two broad hypothesis of this; the first being there is increased recruitment to the tumour site because of

inflammatory cues such as local cytokine and chemokine leading to enhanced extravasation. The second being that CAR T cells pass through all tissues including the tumour, but specifically remain in the tumour due to the formation of a synapse through antigen recognition, leading to local cytokine production to recruit more T cells leading to local accumulation (Benmebarek et al., 2019). This is known as antigen specific retention.

1.4.4 Mechanisms to overcome challenges in solid tumours

Given the challenges presented above with targeting solid tumours, there are multiple novel CAR engineering strategies to attempt to overcome these issues. The lack of cancer specific antigens which are present only on the surface of tumours can result in the destruction of healthy tissues also expressing these antigens. Dual-targeting CAR systems have been investigated by multiple groups in which signal 1 and signal 2 within the CAR are physically dissociated into two separate CAR T cells of differing antigen specificity. In this way, the CAR should only signal effectively on engagement with both cancer associated antigens, which in theory has a higher chance of being solely at the tumour site (Lanitis et al., 2013, Wilkie et al., 2012, Kloss et al., 2013). This system can also help overcome tumour heterogeneity and tumour escape due to loss of antigen expression.

Attempts to overcome the suppressive TME has included development of CAR T cells targeting elements of this microenvironment, for example, targeting fibroblast activation protein (FAP) have been investigated, a protease involved in extracellular matrix remodelling (Tran et al., 2013, Kakarla et al., 2013). Further attempts to enhance CAR T cell functionality involve boosting proliferation and

persistence. For example, engineering CD19 CAR T cells to constitutively express CD40 ligand (CD40L), a protein which binds to its cognate receptor CD40 expressed on multiple malignancies, but a pathway involved in multiple events such as T cell proliferation and cytokine secretion (Curran et al., 2015). Fourth generation CAR T cells, or ‘T cells redirected for antigen-unrestricted cytokine-initiated killing’ (TRUCKS), are designed to deliver a cytokine of choice to the targeted tissue on engagement of target antigen, driven by a promoter stimulated through CD3ζ-ZAP70 cascade (Chmielewski and Abken, 2020). Given the therapeutic success of CAR T cell therapies in haematological malignancies, there is much research into improving their use in the solid tumour field.

1.5 PhD research aims

This project was designed to investigate a potential CAR therapeutic targeting ALK. We hypothesised that ALK will represent a suitable target for CAR T cell therapy in neuroblastoma. Based on this, the individual results chapter aims were as follows:

1. Investigate the feasibility of ALK as a target with a panel of anti-ALK second generation CAR T cells
2. Determine the phenotypic profiles of ALK CAR T cells with different CAR structures
3. Functionally compare the lead ALK CAR T cell identified with a panel of other ALK CAR T cells which contain a previously published anti-ALK scFv
4. Investigate the combination of ALK into a dual-targeting CAR system combined with another CAR for neuroblastoma

2 Materials and Methods

2.1 Molecular techniques

2.1.1 Retrovirus for gene transfer

Retroviral vectors, such as gamma (γ)-retroviruses, are an efficient delivery tool for the transfer of nucleic acids, including gene sequences that encode CAR constructs (Maetzig et al., 2011). Retroviruses are capable of reverse transcribing their single stranded RNA genome, into double stranded DNA which can then be integrated in a stable manner into the host genome (Temin and Mizutani, 1970). The long-term expression of genes transferred in this way is possible; however non-specific incorporation of viral DNA throughout the host genome, and the generation of replication competent retrovirus in gene-modified cells can result in negative implications; some of which can be fatal (Vargas et al., 2016, Maetzig et al., 2011). In order to avoid this, genes which are essential for successful host infection are delivered in separate expression plasmids which lack other retroviral components; known as split packaging design (Maetzig et al., 2011). These essential genes encode viral proteins, including: *Gag* which encodes structural glycoproteins and is required for the assembly of viral particles, *pol* which encodes enzymes necessary for viral replication and integration into the host genome and *env* which produces envelope proteins embedded in the viral membrane that enable viral attachment to cellular receptors and fusion with target cells (Vargas et al., 2016).

The CAR constructs investigated in this PhD were previously cloned into SFG γ-retroviral plasmids, shown in Figure 2.1. These plasmids contain long terminal

repeats (LTR) and the psi packaging signal of moloney murine leukaemia virus (MoMLV), which are both necessary for the insertion of the viral genome into the host DNA, through driving transcription and encapsulation of the inserted genome into viral particles, respectively (Vargas et al., 2016). Along with this is an ampicillin resistance gene, which enabled the selection of successfully transduced clones. In this instance the gene of interest, a second generation ALK CAR, is co-expressed with an RQR8 molecule. RQR8 is an 136 amino acid protein that is recognised by the anti-CD34 antibody QBend10 and also renders T cells susceptible to lysis by the therapeutic monoclonal antibody rituximab (Philip et al., 2014). The CAR construct and RQR8 are separated by a T2A self cleaving peptide. This allows for the expression of RQR8 and the ALK construct as separate proteins encoded from a single open reading frame (ORF). Using a T2A between these two proteins, allows for equimolar production of the protein products within a single vector (Szymczak-Workman et al., 2012). Furthermore, this allows for the transduction efficacy to be assessed by RQR8 surface expression, through CD34 antibody binding.

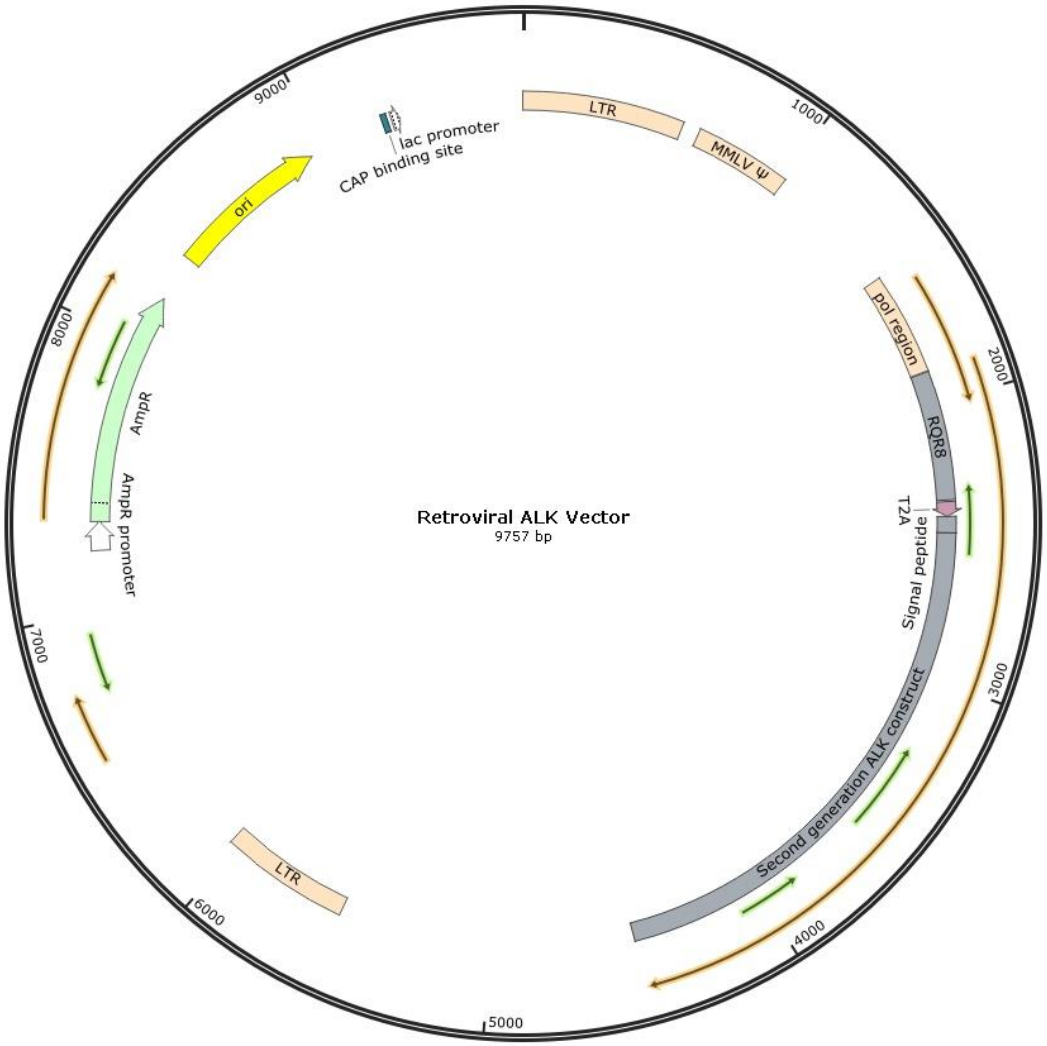

Figure 2.1 SFG γ-retroviral vector

A schematic illustrating the SFG γ-retroviral vector used within this project. The plasmid contains the second generation ALK CAR construct co-expressed with RQR8, separated by a T2A molecule. The CAR construct contains a CD28 costimulatory domain and CD3ζ endodomain along with stalk and transmembrane regions. The plasmid also contains LTR's and MoMLV packaging signal and ampicillin resistance gene.

2.1.2 Cloning products

All cloning strategies, oligonucleotides (gene blocks) and primers used in this thesis were designed using SnapGene (Version 4.2.11) and purchased from Integrated DNA Technologies (IDT) or ThermoFisher Scientific. Where gene blocks were used, they were initially amplified through polymerase chain

reaction (PCR) with the relevant primers to increase the amount of product available for further cloning. For this, and for cloning strategies, Phusion High-Fidelity PCR (NEB) was used, as per manufacturer's instructions, to produce blunt end products, which could be ligated together where necessary (section 2.1.5). A representative 50µL PCR reaction mastermix and PCR protocol are showed in Table 2.1 and

Table 2.2.

Table 2.1 50µL PCR reaction

Reagent	**Amount**
Nuclease Free Water	Up to 50µL
5x Phusion HF Buffer	10µL
10mM dNTPs	1µL
10µM Forward Primer	2.5µL
10µM Reverse Primer	2.5µL
DNA to be amplified	0.1-1 ng
Phusion DNA Polymerase	0.5µL

Total Volume	50µL

Table 2.2 General PCR cycling conditions

Step	Cycles	Temperature	Time
Initial Denaturation	1	98°C	30 seconds
Denaturation	15-35	98°C	5-10 seconds
Annealing		45-72°C	10-30 seconds
Extension		72°C	15-30 seconds per kb
Final Extension	1	72°C	5-10 minutes
Final	1	4°C	Forever

2.1.3 Detection of PCR product, extraction and purification

PCR products were separated by electrophoretic separation when required. Briefly, DNA products were mixed with 1x DNA loading buffer (NEB) and run by electrophoresis on a 1% agarose gel containing ethidium bromide at 120V for ~1 hour. The bands were identified for correct length by comparing the bands to a 1Kb plus DNA ladder (NEB) by visualising on a blue UV light transilluminator (VWR) in a dark room. If required for further cloning, the bands of interest were extracted from the gel using a scalpel. The extracted bands were purified with a

DNA purification kit (Wizard SV Gel and PCR Clean-Up System, Promega) as per manufacturer's instructions and the DNA was eluted into 25µL of nuclease-free water.

2.1.4 Double digestion

DNA fragments (inserts) and receiving vectors were double digested using the relevant restriction enzymes (incubation time and temperature of digestion dependant on the restriction enzymes used). These products were run on a 1% agarose gel and the required bands extracted and purified as previously described (Section 2.1.3). A representative 50µL double digest reaction is described in Table 2.3.

Table 2.3 50µL double digest reaction

Reagent	**Amount**
DNA	1µg
10x Buffer	5µL (1x)
Restriction Enzymes	1µL each (10 units)
Nuclease Free Water	Up to 50µL

2.1.5 Ligation reaction

The digested DNA products (insert and vector) were ligated at the following insert:vector ratios: 1:1, 2:1, 3:1, 5:1 and 7:1. The insert:vector ratio was calculated as follows:

Required mass insert (g) = insert:vector ratio x mass of vector (g) x ratio of insert to vector lengths

A vector alone reaction with no insert was used as a control. Briefly, the vector and insert were mixed with QuickLigase (NEB) on ice and incubated for 5 minutes at room temperature. If this reaction was being immediately transformed it was returned to ice (Section 2.1.7), or the reaction could be frozen until it was used at a later date. A representative 20µL ligation reaction is described in Table 2.4.

Table 2.4 20µL ligation reaction

Reagent	**Amount**
Quick Ligase Buffer (2x)	10µL
Digested DNA	Amount required as per formula above
Quick Ligase	1µL
Nuclease Free Water	Up to 20µL

2.1.6 Site-directed mutagenesis

Site-directed mutagenesis can be used to create direct targeted changes to a double stranded DNA plasmid, for example, when an enzyme restriction site must be inserted. For this the Q5 Site-Directed Mutagenesis Kit was used (NEB), as per manufacturer's instructions. Briefly, the NEBaseChanger (NEB) was used to determine the sequence of forward and reverse primers required. Following this, PCR amplification is required with the relevant primers created (as described in Section 2.1.2). The PCR product is then used with the kinase, ligase and DpnI (KLD) treatment for 5 minutes at room temperature. An example reaction is shown in).

Table 2.5. The product can then be transformed, as described in the following section (2.1.7).

Table 2.5 KLD treatment for site-directed mutagenesis

Reagent	**Amount**
PCR product	1µL
KLD Reaction Buffer (2x)	5µL (1x)
KLD Enzyme Mix (10x)	1µL (1x)
Nuclease-free water	3µL

2.1.7 Bacterial transformation

DNA plasmids and ligated DNA products that needed to be amplified were introduced into chemically competent 5-alpha high efficiency *E.Coli* (NEB) for expansion, as per manufacturer's instructions. Briefly, 1 µL of required DNA plasmid was added to 25 µL of competent cells and incubated on ice for 30 minutes. The cells were then heat shocked at 42°C for 35 seconds before incubation on ice for at least 2 minutes. Finally, the cells were added to 250 µL of SOC outgrowth medium and shaken at 200 RPM at 37°C for 40 minutes. This transformed bacteria was spread on agar plates containing ampicillin (100 µg/mL) and incubated at 37°C for ~16 hours. All plasmids contain an ampicillin resistance gene (Figure 2.1), and therefore only bacterial clones containing the desired

plasmid are expected to survive. Individual bacterial colonies can be picked for further expansion.

2.1.8 Small scale plasmid expansion (Miniprep)

Transformed bacterial colonies required for amplification were expanded in 5 mL of LB broth containing ampicillin (100 µg/mL) and cultured at 37°C at 200RPM shaking overnight. Plasmid DNA was extracted from the broth mix using a QIAprep Miniprep Kit (Quiagen), as per manufacturer's instructions.

2.1.9 Medium scale plasmid expansion (Midiprep)

For larger scale plasmid expansions transformed bacterial colonies were used to inoculate 200 mL of LB broth containing ampicillin (100 µg/mL) and cultured at 37°C at 200RPM shaking overnight. Plasmid DNA was extracted from the broth mix using a NucleoBond Xtra midi prep kit (Machery Nagel) as per manufacturer's instructions.

2.1.10 DNA quantification and sequencing

The amount of DNA was quantified using a spectrophotometer (Nanodrop ND1000) which measures at a wavelength of 260/280nm. Constructs and plasmids produced were all validated through DNA sequencing by Source BioScience (Nottingham, UK).

2.2 Cell culture and primary cell work

2.2.1 Maintenance of immortalised cell lines

All cell lines were cultured in a humidified incubator of 37°C with 5% CO_2, unless otherwise stated. They were all handled under sterile conditions in Biosafety Cabinet Class 2 hoods. When required, cell counting was performed using a haemocytometer (Immune systems) and Trypan Blue 0.4% (Gibco). Dead and dying cells take up Trypan Blue, which allowed for their exclusion and live cells were counted under a light microscope. All cell lines were genotyped by short tandem repeat (STR) analysis before use and confirmed negative for *mycoplasma* before and during use. Cell lines were cultured in one of the following media (see section 2.2.2 and 2.2.3 for more details):

RPMI Complete media

- RPMI-1640 media (Sigma)
- 10% foetal bovine serum (FBS) (Gibco)
- 20mM L-glutamine (Sigma)
- 100U/mL Penicillin/Streptomycin (Gibco)

IMDM Complete media

- Isocove's Modified Dulbecco Medium (IMDM) media (Sigma)
- 10% FBS
- 20mM L-glutamine
- 100U/mL Penicillin/Streptomycin
- 12mL HEPES buffer (Sigma)

2.2.2 Cell lines used within this project

A panel of neuroblastoma cell lines was characterised for antigen expression and used throughout this project (Table 2.6). Furthermore, the leukaemia cell line SUP-T1 wild type (WT) was often used as an antigen negative control, along with a number of SUP-T1 cell lines transduced with target antigens, including SUP-T1 ALK and SUP-T1 GD2 (Table 2.6). This allowed for matched antigen positive and negative cell lines. All cell lines displayed in Table 2.6 were cultured in RPMI-1640 Medium (Sigma), supplemented with 10% FBS and 2mM L-Glutamine, and split as required. For splitting of adherent cell lines, 3-5mL of 0.05% Trypsin-EDTA (Gibco) was added and cultured for 5 minutes in 37°C before neutralisation with culture medium. Cells were then washed in fresh RPMI and centrifuged at 1500RPM for 5 minutes, before being re-plated at optimal confluency.

Table 2.6 Cell Lines

Cell Line	**Origin**	**Characteristic**
SUP-T1 WT	T cell lymphoma	Suspension
SUP-T1 ALK	T cell lymphoma	Suspension
SUP-T1 GD2	T cell lymphoma	Suspension
SUP-T1 ALK_GD2	T cell lymphoma	Suspension
Jurkat	Acute T cell leukaemia	Suspension
Lan-1	Neuroblastoma	Adherent
Kelly	Neuroblastoma	Adherent
Lan-5	Neuroblastoma	Adherent
IMR32	Neuroblastoma	Adherent
SKNSH	Neuroblastoma	Adherent
SKNDZ	Neuroblastoma	Adherent
HEK293T	Embryonic Kidney	Adherent

2.2.3 HEK293T cells

Human embryonic kidney 293T (293T) cells are packaging cells which can be used to produce retroviruses through stable transfection. 293T cells were cultured and expanded when necessary in IMDM complete media. Cells were split when required using 3-5 mL of 0.05% Trypsin-EDTA (Gibco) for 3 minutes before neutralisation with culture medium (as described in 2.2.1).

2.2.4 Irradiation of cell lines

On occasions, cell lines were required without their growth capacity (for stimulation purposes, for example). To achieve this, cells were counted to desired concentrations and resuspended in 5mL of RPMI complete media. They were irradiated at 40 grays (Gy) with irradiator IBL 437C (94-468). Subsequently they were washed with RPMI complete media and centrifuged for 5 minutes at 1500RPM. Cells were resuspended in RPMI complete media and 10% DMSO and stored at -80°C for later use.

2.2.5 PBMC isolation

Healthy human peripheral blood mononuclear cells (PBMCs) were isolated from whole blood leucocyte cones (NHS Blood and Transplant, Colindale) via density gradient centrifugation using Lymphoprep (Stemcell). Blood was removed from cones and mixed 1:1 with Phosphate-Buffered Saline (PBS) (ThermoFisher). 25 mL of blood/PBS mix was slowly layered onto 20 mL of lymphoprep (ThermoFisher) before centrifuging for 20 minutes at 2400RPM with no break or acceleration. The buffy layer (containing the PBMCs) was transferred carefully into a new falcon tube using a Pasteur pipette. This was diluted in PBS and

centrifuged again at 1500RPM for 5 minutes. Red blood cells were lysed by resuspending the pellet in 5 mL of ammonium-chloride-potassium (ACK) lysing buffer (Lonza) for 10 minutes at room temperature. Cells were then washed again as before. The PBMC pellet was re-suspended in 50 mL of RPMI complete media and counted using a haemocytometer and Trypan Blue (as described in section 2.2.1).

2.2.6 Natural killer cell depletion and T cell activation and expansion

On the day of isolation, PMBCs were depleted of natural killer (NK) cells to prevent unspecific lysis of target cells in culture. NK cells express CD56, and can therefore be depleted using CD56 Microbeads (Miltenyi), as per manufacturer's instructions. Briefly, anti-$CD56^+$ magnetic beads were incubated with PBMCs before passing the cell/beads suspension through a magnetic column. The magnetic beads bind to the $CD56^+$ cells allowing for CD56- cells to pass through the column and be collected, while CD56+ cells remain on the column through positive selection. PBMCs were then activated with 0.5 µg/mL anti-CD3 and anti-CD28 functional-grade human antibodies (Miltenyi) to allow for specific alpha-beta (αβ) T cell expansion. T cells were expanded in RPMI complete media supplemented with 100 IU/mL Proleukin IL-2 (Novartis) every 2 days in 24 well plates at a concentration of $2x10^6$ T cells per well. T cells were typically expanded for 72 hours after activation, before used for transduction.

2.2.7 Retrovirus production

293T cells were plated at $1.5x10^6$ in 10cm plates (Corning) in 10 mL of IMDM complete media and left to adhere for ~30 hours. The following day, when the 293T cells were typically ~60-70% confluent, the cells were transiently

transfected. Initially, 470 µL of plain IMDM media was mixed with 30 µL of Genejuice (Merck) in a 15 mL falcon and left for 5 minutes. The components for triple transfection (shown below in Table 2.7) were added and incubated for a further 15 minutes. 500 µL of transfection mix was added dropwise to the plate of 293Ts, after removal of 4 mL of IMDM complete media. Retroviral supernatant was harvested once at 48 hours post transfection and placed in a falcon tube in the fridge overnight. The viral supernatant removed from the plate was replaced with fresh IMDM complete media, usually 6 mL. This was further harvested the following day (72 hour from transfection), and mixed with the 48 hour supernatant harvest. The viral supernatant was centrifuged at 1500RPM for 5 minutes to pellet any remaining 293T cells that may have been transferred, and used immediately for T cell transduction.

Table 2.7 Triple transfection reaction

Component	**Amount**
Gag-pol (gagpol)	4.6875 µg
Env (RD114)	3.125 µg
γ-retrovirus containing construct DNA	4.6875 µg
Total plasmid DNA	12.5 µg

2.2.8 T cell transduction

RetroNectin reagent (Takara) was used to improve T cell transduction, as it aids the co-localisation of target cells and virus particles. Non tissue culture treated 24 well plates (Costar) were coated with retronectin in PBS (final concentration of

1mg/mL) and incubated at 4°C for 24 hours. The retronectin was removed before the plates were used, and either replated or frozen in 50 mL falcons for future use (retronectin was used no more than twice). 1.5 mL of retroviral supernatant was added to each retronectin coated well. Following this, $3x10^5$ of expanded T cells resuspended in 500 µL of RPMI complete media was added to each well. This was further supplemented with IL-2 (100units/mL). The plates were centrifuged at 1000xg for 40 minutes, at room temperature before incubation at 37°C. Transduced T cells were harvested after 3 days and washed with RPMI complete media to remove any remaining virus. These transduced T cells were then cultured and expanded as per section 2.2.6, in RPMI complete media with IL-2 added every 2 days.

2.2.9 Production of SUP-T1 ALK_GD2

To create a double antigen positive control cell line, SUP-T1 ALK was transduced to also express GD2. To do this, retrovirus was produced as previously described in section 2.2.7 using a plasmid encoding GD2/GD3 synthase. This virus was used to transduce the SUP-T1 ALK cell line, as previously described in section 2.2.8. 3 days post transduction the cells were washed with RPMI complete media to remove any virus. Following this, cells were sorted by flow cytometry to identify the high ALK and high GD2 expressing population.

2.3 *In Vitro* Assays

2.3.1 Cytotoxicity assay

The cytotoxic activity of ALK CAR T cells against neuroblastoma and SUP-T1 cell lines was determined by using a radioactive four hour chromium (^{51}Cr)-release assay. Briefly, 1x10^{6} target cells were labelled with 20 µL ^{51}Cr (PerkinElmer) for 60 minutes at 37°C to allow for uptake into cells. Target cells were washed four times with RPMI complete media. Following this, target cells were co-cultured with effector CAR T cells at varying effector: target (E:T) ratios (10:1, 5:1, 2.5:1 and 1.25:1) for four hours at 37°C in 96 well V bottom plates (Grenier). After incubation, the plates were centrifuged at 1500RPM for 5 minutes and 150 µL of the supernatant was transferred to 96 well OptiPlate-96 HB (PerkinElmer). Following this, 50 µL of scintillation fluid was added per well and the plates were sealed and incubated overnight. ^{51}Cr release from lysed target cells was counted on 1450 MicroBeta Trilux Scintillation Counter (PerkinElmer). Untransduced (UT) T cells were used a negative control and target cells lysed with 1% Triton X-100 (Thermofisher) were used as a maximum ^{51}Cr release control. Specific levels of target cell lysis were calculated as follows:

$$\frac{(\text{Experimental } ^{51}\text{Cr Release} - \text{Spontaneous } ^{51}\text{Cr Release}) \text{ X } 100}{(\text{Maximum } ^{51}\text{Cr Release} - \text{Spontaneous } ^{51}\text{Cr Release})} = \% \text{ Lysis}$$

2.3.2 Detection of cytokines by ELISA

The presence of interleukin (IL)-2 and interferon gamma (IFNγ) in co-culture supernatant was detected using human IL-2 and human IFNγ enzyme-linked

immunoabsorbent assay (ELISA) kits (Invitrogen), as per manufacturer's instructions. ALK CAR T cells and target tumour cells were plated at a 1:1 E:T ratio in 48 well plates and co-cultured for 24 hours at 37°C. The following day, the plates were centrifuged and 600 µL of supernatant was removed and stored at -80°C if not analysed immediately. Briefly, 96 well ELISA plates were coated with human IL-2 or human IFNγ capture antibody and stored overnight at 4°C. Following blocking for 1 hour to prevent unspecific binding, samples and standards were loaded, followed by detection antibody and streptavidin. Human IFNγ standards were used to generate a standard curve with the range of 0-500 pg/mL, while the human IL-2 standards ranged from 0-250 pg/mL. Absorbance was measured at 450nm on a microplate reader (Tecan) and corrected by subtraction of background control values. During these experiments untransduced T cells were used as a negative control.

2.3.3 Short term proliferation assay

T cell proliferation on engagement with target cells was measured by the detection on cell trace dye by flow cytometry. In order to do this, transduced ALK CAR T cells were labelled with CellTrace Violet cell proliferation kit (ThermoFisher Scientific), as per manufacturer's instructions. Briefly, 1 µL cell trace stock solution was added to up to $1x10^6$ ALK CAR T cells resuspended in 1 mL of PBS (5 µM working concentration), and incubated for 20 minutes at 37°C protected from the light. After washing, these labelled T cells were plated into 48 well plates at an E:T of 1:1 with irradiated target cells, in a total of 1 mL RPMI complete media. Target cells were irradiated as described in section 2.2.4. 500 µL of supernatant was carefully removed and replaced with fresh RPMI complete media every two days. On day 4 and day 8 of co-culture, cells were removed from

the wells and ALK CAR T cell proliferation and cell phenotype were determined by flow cytometry, as described in sections 2.4.4 and 2.4.5. UT T cells were used a negative control, and ALK CAR T cells stimulated with PMA and Ionomycin were used as a positive control in these experiments.

2.3.4 Short term restimulation assay

ALK CAR T cells and irradiated target cells were plated at a 1:1 E:T ratio in 48 well plates in RPMI complete media. 500 µL of media was changed every two days as described in section 2.3.3. After 7 days of co-culture, the cells were washed and replated with the same stimulation conditions. After a further 24 hours of co-culture at 37°C, the supernatant was removed. The presence of IL-2 and IFNγ in the supernatant was measured as previously described in section 2.3.2.

2.3.5 Activation and degranulation marker assay

The surface expression of activation and degranulation markers by CAR T cells was investigated. For this assay, CAR T cells were plated as previously described in section 2.3.2. After 18 hours of co-cultured the cells were harvested and washed. The expression of CD69, CD25 and CD107a were determined by flow cytometry, as described in section 2.4.5.

2.3.6 Long term repeat stimulation proliferation assay

For long term proliferation assays, cell trace dyes could not be used as the proliferation dyes become too dilute after longer periods in culture with higher levels of cell divisions. For this experiment, ALK CAR T cells were plated in 48 well plates at a 1:1 E:T ratio with irradiated target cells, with a total of 1×10^6 cells

per well in 1 mL of RPMI complete media. 500 µL of supernatant was carefully removed and replaced with fresh RPMI complete media every two days. Every 7 days, ALK CAR T cell viability and counts were determined, as described in section 2.4.6. The remaining co-cultures were also restimulated, with the addition of 500,000 irradiated target cells.

2.4 Flow cytometry

2.4.1 Antibodies

Table 2.8 Antibodies/viability dyes used for flow cytometry

Specificity	Fluorochrome	Clone	Manufacturer	Dilution
CD3	BUV395	SK7	BD	3/50
αβTCR	BUV737	IP26	BD	3/50
αβTCR	FITC	BW242/412	Miltenyi/BD	3/50
CD34	APC	QBend10	BD	3/50
CD4	BV510	SK3	BD	3/50
CD8	PerCP-Cy5.5	RPA-T8	BD	3/50
CD45RO	Alexa Flouro 488	UCHL1	BD	3/50
CD62L (L-selectin)	BV650	DREG-56	BD	3/50
PD-1	PE	J105	BD	3/50
Tim3	Superbright702	F38-2E2	BD	3/50
Lag3	PEdazzle594	11C3C65	BD	3/50
CTLA-4	BV605	BNI3	BD	3/50
CD69	PE-Cy7	FN50	BD	3/50
CD25	Alexa Flouro 700	M-A251	BD	3/50
CD107a (LAMP-1)	Alexa Flouro 488	H4A3	Biolegend	3/50
ALK (mAb13)	Primary only	13	Gift (Marc Vigney)	2/50
Live/Dead	Near IR	N/A	ThermoFisher	1/100
Live/Dead	Zombie Yellow	N/A	Biolegend	1/100
Live/Dead	PI	N/A	BD	1/300

2.4.2 Detection of surface ALK

The expression of ALK on the surface of cell lines wad determined through flow cytometry. Briefly, up to 1 x 10^6 cells were removed from culture and washed with 2 mL of PBS and centrifuged for 5 minutes at 1500RPM. The supernatant was discarded and cells were incubated with anti-ALK mAb13 for 30 minutes (Table 2.8). Cells were washed as before, and stained with an APC labelled anti-mouse IgG antibody for a further 30 minutes. Cells were washed again and resuspended in 300 µL of PBS. All samples were analysed on a BD LSR II flow cytometer using Diva software (BD). For ALK surface expression, the median fluorescence intensity (MFI) was calculated and compared to controls. In all cases, compensation beads (OneComp eBeads Compensation Beads Thermofisher) were stained with the relevant antibodies (as per manufacturer's instructions) and used for the instrument's compensation, to prevent fluorescence spillover. All results were analysed on FlowJo software Version 10 (Treestar).

2.4.3 Detection of RQR8-ALK construct transduction efficacy

Within the constructs, RQR8 is co-expressed with the ALK CAR through the use of T2A molecule. The expression of RQR8 was determined through its binding to an anti-CD34 antibody, which could be quantified. Briefly, up to 1 x 10^6 T cells were removed from culture and washed with 2 mL of PBS and centrifuged for 5 minutes at 1500RPM. The supernatant was discarded and cells were incubated with a master mix containing FcR blocking reagent (ThermoFisher) and Zombie Yellow Fixable Viability Kit (Table 2.8) for 10 minutes. Cells were washed as before, and stained with a master mix containing antibodies against CD3, αβTCR, CD34 (Table 2.8) for 30 minutes. Cells were washed again and resuspended in

300 µL of PBS. All samples were collected on a BD LSR II Fortessa flow cytometer using Diva software (BD). In all cases, compensation beads (OneComp eBeads Compensation Beads Thermofisher) were stained with the relevant antibodies (as per manufacturer's instructions) and used for instrument's compensation, to prevent fluorescence spillover. All results were analysed on FlowJo software Version 10 (Treestar).

2.4.4 Short term proliferation

The proliferation of T cells labelled with cell trace violet (described in section 2.3.3) were detected via flow cytometry. Briefly, cultured T cells were removed from wells and washed with PBS by centrifuging for 5 minutes at 1500RPM. The supernatant was discarded and cells were stained with a Near IR fixable live dead dye (Table 2.8) as per manufacturer's instructions. Cells were incubated for 30 minutes and subsequently washed as before. They were then stained with a master mix containing antibodies against CD3, αβTCR, CD34 (Table 2.8) for 30 minutes. Cells were washed again and resuspended in 300 µL of PBS. All samples were analysed on a BD LSR II flow cytometer using Diva software (BD). In all cases, compensation beads (OneComp eBeads Compensation Beads Thermofisher) were stained with the relevant antibodies (as per manufacturer's instructions) and used for instrument's compensation, to prevent fluorescence spillover. All results were analysed on FlowJo software Version 10 (Treestar).

2.4.5 Detection of cell surface markers

Immunostaining for cell surface markers included the detection of CD4, CD8, CTLA-4, Tim3, Lag3, PD-1, CD69, CD25, CD45RO, CD107a and CD62L (Table 2.8). Briefly, cultured T cells were removed from wells and washed with PBS by

centrifuging for 5 minutes at 1500RPM. The supernatant was discarded and cells were stained with a Near IR fixable live dead dye (Table 2.8) as per manufacturer's instructions. Cells were incubated for 30 minutes and subsequently washed as before. They were then stained with a master mix containing the relevant antibodies and incubated for 30 minutes. Cells were washed again and resuspended in 300µL of PBS. When staining for the degranulation marker CD107a, an initial pre-incubation was required. Cells were incubated with a mastermix containing monensin (Biolegend) at a final concentration of 1 µL/mL and anti-CD107a antibody for 3 hours at 37°C. Following this cells were washed. Staining for other cell surface markers occurred subsequently, as previously described. All samples were collected on a BD LSR II flow cytometer using Diva software (BD). In all cases, compensation beads (OneComp eBeads Compensation Beads Thermofisher) were stained with the relevant antibodies (as per manufacturer's instructions) and used to prevent fluorescence spill over. All results were analysed on FlowJo software Version 10 (Treestar).

2.4.6 Long term proliferation

Long term proliferation was investigated by determining ALK CAR T cell counts. Briefly, cultured T cells were removed from wells and washed with PBS by centrifuging for 5 minutes at 1500RPM. The supernatant was discarded and cells were incubated with FcR blocking reagent for 10 minutes (Table 2.8). Cells were subsequently washed as before, and the supernatant was discarded. They were then stained with a master mix containing antibodies against αβTCR and CD34 (Table 2.8) for 30 minutes. Cells were washed again and resuspended in 300µL of PBS. Immediately before running, 1 µL of the live/dead dye PI was added. All

samples were collected on a FACSCalibur (BD) flow cytometer using CellQuest Pro software (BD). In all cases, compensation beads (OneComp eBeads Compensation Beads ThermoFisher Scientific) were stained with the relevant antibodies (as per manufacturer's instructions) and used for instrument's compensation, to prevent fluorescence spillover. All results were analysed on FlowJo software Version 10 (Treestar).

2.5 Data and statistical analysis

Data was analysed with GraphPad Prism 7, which was used to produce graphs and determine statistical analysis. Graphs are displayed at mean±SD unless otherwise stated. Statistical tests used are stated in the figure legends. For normally distributed numerical data, determined by Gaussian distribution on GraphPad Prism, parametric tests were used to determine significance of difference between groups. Analysis of variance (ANOVA) was used, unless otherwise stated. Significance is represented by: *$p<0.05$, ** $P<0.01$, *** $p<0.001$, **** $p<0.0001$.

3 Characterisation of ALK CAR T cells

3.1 Introduction

The selection of a target antigen for the development of T cell based therapies is of significant importance. Ideally, the target should be expressed highly and uniformly on malignant tissue with no expression on healthy cells. However, in the majority of cases CAR T cell therapies are produced against antigens that are overexpressed on malignant cells but also expressed at low levels in healthy tissues: these antigens are known as Tumour associated antigens (TAAs). The expression on healthy tissue gives rise to the risk of on-target off-tumour toxicity. GD2 as a target for CAR T cell therapy was described by Rossig *et al*., and the efficacy of anti-GD2 CAR T cells for the treatment of neuroblastoma was evaluated in a number of clinical trials (Rossig et al., 2001, Heczey et al., 2017, Pule et al., 2008). However, the targeting of GD2 presents a number of challenges. GD2 expression on healthy tissues has been shown on neurons, melanocytes and peripheral nerve fibres, posing further risk for on-target off-tumour toxicity (Alvarez-Rueda et al., 2011). A preclinical murine model showed severe lethal CNS toxicity caused by affinity matured GD2 CAR T cell infiltration and proliferation within the brain that resulted in neuronal destruction (Richman et al., 2018). Furthermore, sensorimotor demyelinating polyneuropathy and other central neuropathies have been observed with the use of anti-GD2 monoclonal antibody therapy (Richman et al., 2018, Alvarez-Rueda et al., 2011). Moreover, it has been shown that the 14.18 anti-GD2 scFv, included in a GD2-specific CAR, has the propensity to oligomerise, resulting in chronic phosphorylation of the CD3ζ domain and tonic signalling which is associated with increased activation,

exhaustion and higher levels of T cell apoptosis (Long et al., 2015). The lack of completely efficacious results, and potential for toxicities, indicates need to further develop current technologies, including evaluation of alternative target antigens for neuroblastoma. Efforts have gone into investigating other potential candidates such as L1 Cell Adhesion Molecule (L1-CAM), Glypican 2 (GPC2), and Neural Cell Adhesion Molecule (NCAM) (Crossland et al., 2018, Bosse et al., 2017, Park et al., 2007).

ALK may be another attractive target for immunotherapy. ALK has been identified as a potential oncogene contributing to the progression of neuroblastoma, and its expression is primarily restricted to the central and peripheral nervous system (Vernersson et al., 2006, Trigg and Turner, 2018). Importantly, its expression is mainly observed during foetal development and subsequently decreases with age (Iwahara et al., 1997). Activating mutations in the kinase domain of ALK, genomic amplification and increased WT ALK expression have all been identified in both familial and sporadic neuroblastoma cases. Genome analysis of primary and relapsed neuroblastoma tumours has also shown an increased frequency of ALK mutations at patient relapse (Trigg and Turner, 2018). Moreover, antibodies against the extracellular domain of ALK have demonstrated the ability to mediate cell lysis of neuroblastoma cell lines, *in vitro* (Moog-Lutz et al., 2005, Carpenter et al., 2012). Together, this demonstrates a clear rationale for investigating the development of an anti-ALK CAR T cell.

When designing a CAR construct, each incorporated domain can alter the functionality of the CAR itself. For example, the choice of spacer region (also referred to as a hinge or stalk), which connects the internal signalling domains to the antigen binding scFv, must be carefully considered. The distance between a

target cell and an effector cell is critical in mediating the efficient formation of a functional immune synapse, resulting in subsequent initiation of T cell signalling. The choice of spacer region is therefore influenced by multiple factors, including the length of the immune synapse, which is determined by the size of the target antigen and the location of the binding epitope recognised by the scFv (Srivastava and Riddell, 2015). While there is limited research regarding the implications of spacer length in CAR T cell efficacy, the domain is believed to play various roles in CAR T cell biological processes, including migration, tonic signalling and antigen recognition (Watanabe et al., 2016).

3.2 Aim

The aim of this research chapter is two-fold. Firstly, to assess the suitability of ALK as a target for CAR T cell therapy for neuroblastoma. Secondly, to characterise a panel of anti-ALK CAR T cells consisting of five different scFvs and two spacer regions of different structure and lengths. This will be assessed in a number of *in vitro* assays. An effective anti-ALK CAR T cell should be able to:

(i) Specifically lyse ALK expressing cells

(ii) Produce proinflammatory cytokines (namely IL-2 and IFNγ) in an ALK antigen-dependent manner

(iii) Proliferate in short and long term capacity, in an ALK antigen-dependent manner.

3.3 Results

3.3.1 ALK CAR Constructs

A panel of anti-ALK CAR constructs was previously produced within the research group. Briefly, mice were immunised with human ALK and their splenocytes were harvested once serum conversion had been confirmed. These splenocytes were used to create an scFv phage display library. Panning of this library identified five unique ALK specific binders which were then cloned into a scFv-Fc format. All five binders showed good levels of binding to both WT ALK expressed on neuroblastoma cell lines, and to cell lines transduced to express the ectodomain of ALK (data not shown). These ALK specific binders were then further cloned into second-generation CAR format (Figure 3.1). Nine anti-ALK CARs were generated containing either a CD8 stalk (CD8S) or a CH2CH3 spacer, herein referred to as an Fc spacer (FcS). The Fc spacer contains mutations to prevent unintended binding of innate immune cells expressing IgG Fc receptors (Hombach et al., 2010, Straathof et al., 2020).

ALK10-CD8-28ζ could not be cloned for unknown, but presumed technical reasons.

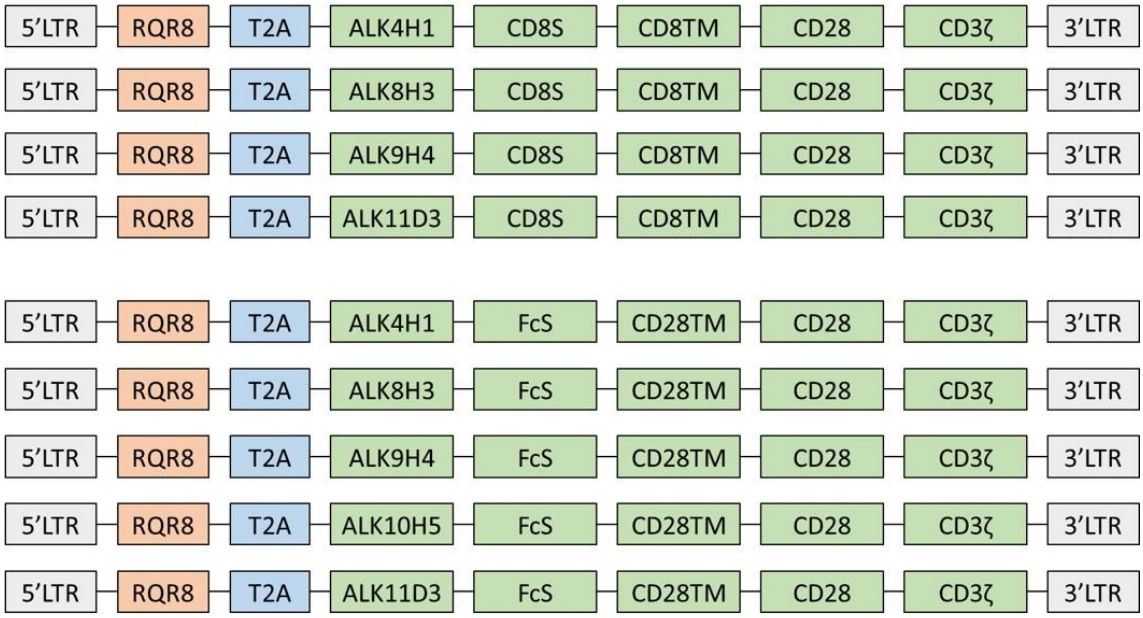

Figure 3.1 Design of second generation CAR constructs targeting ALK

Five different ALK scFvs were incorporated into SFG gamma-retroviral vector in the format of a second generation CAR. Each construct contains long terminal repeats (LTR) (grey) of the Moloney murine leukaemia virus (MoMLV), responsible for driving the transcription of the gene of interest. RQR8 (orange) is used as a marker of transduction (which binds the anti-CD34 antibody, clone QBEnd10) and acts as a safety switch, allowing T cells expressing the construct to be lysed with the addition of Rituximab (Philip et al., 2014). The CAR construct (green) includes the ALK-specific scFv binding domain (heavy and light chains joined with a glycine serine linker), spacer region (CD8 stalk or Fc spacer), transmembrane domain (CD8TM or CD28TM) along with CD28 and CD3ζ signalling domains. RQR8 and the CAR construct are separated by a Thosea asigna virus (self-cleaving peptide T2A) (blue), which allows efficient equimolar expression of both constructs on the surface of T cells.

3.3.2 Investigation of ALK expression on cell lines

It was crucial to confirm the surface expression of ALK on neuroblastoma cell lines in order to validate its use as a potential therapeutic target. Furthermore, identifying cell lines with varying ALK surface expression was important for investigating ALK CAR T cell functionality at different target antigen densities.

In order to investigate the above, ALK surface expression was determined on a panel of neuroblastoma cell lines and on cell lines that have been engineered to express the ALK ectodomain on their surface. In this latter case, wild type SUP-T1 (SUP-T1 WT) lymphoma cells were used. SUP-T1 WT cells were transduced with an SFG vector encoding the ectodomain and transmembrane domain of ALK, resulting in surface expression with the absence of the RTK intracellular signalling domains. These engineered cell lines were then sorted by flow cytometry to isolate a high ALK expressing population (SUP-T1 ALK) (generated by Maria Alonso Ferrero, UCL GOSH).

ALK surface expression was determined through median fluorescence intensity (MFI) measured by flow cytometry. For this purpose, the Mab13 antibody was used, a primary unconjugated antibody that binds the extracellular domain of ALK (gifted by Marc Vigney, Paris). It is should be noted that currently there is no commercially available antibody which binds the extracellular domain of ALK. Cell lines were incubated with Mab13, followed by an APC-labelled anti-mouse secondary antibody. No surface expression of ALK on SUP-T1 WT cells was seen in contrast with high expression on SUP-T1 ALK cells (Figure 3.2A). SUP-T1 WT and SUP-T1 ALK were used as negative and positive control cell lines, respectively. Varying levels of surface ALK expression were confirmed on Lan-5,

Kelly, SHS5Y, SKNDZ, Lan-1 and IMR32 neuroblastoma cell lines (Figure 3.2B). When average MFI across three individual experiments was investigated, Lan-5 had the brightest ALK expression with an average MFI of 3142±1148 (mean MFI±SD, n=3). IMR32 had the dimmest ALK expression with an average MFI of 1470±1053 (n=3).

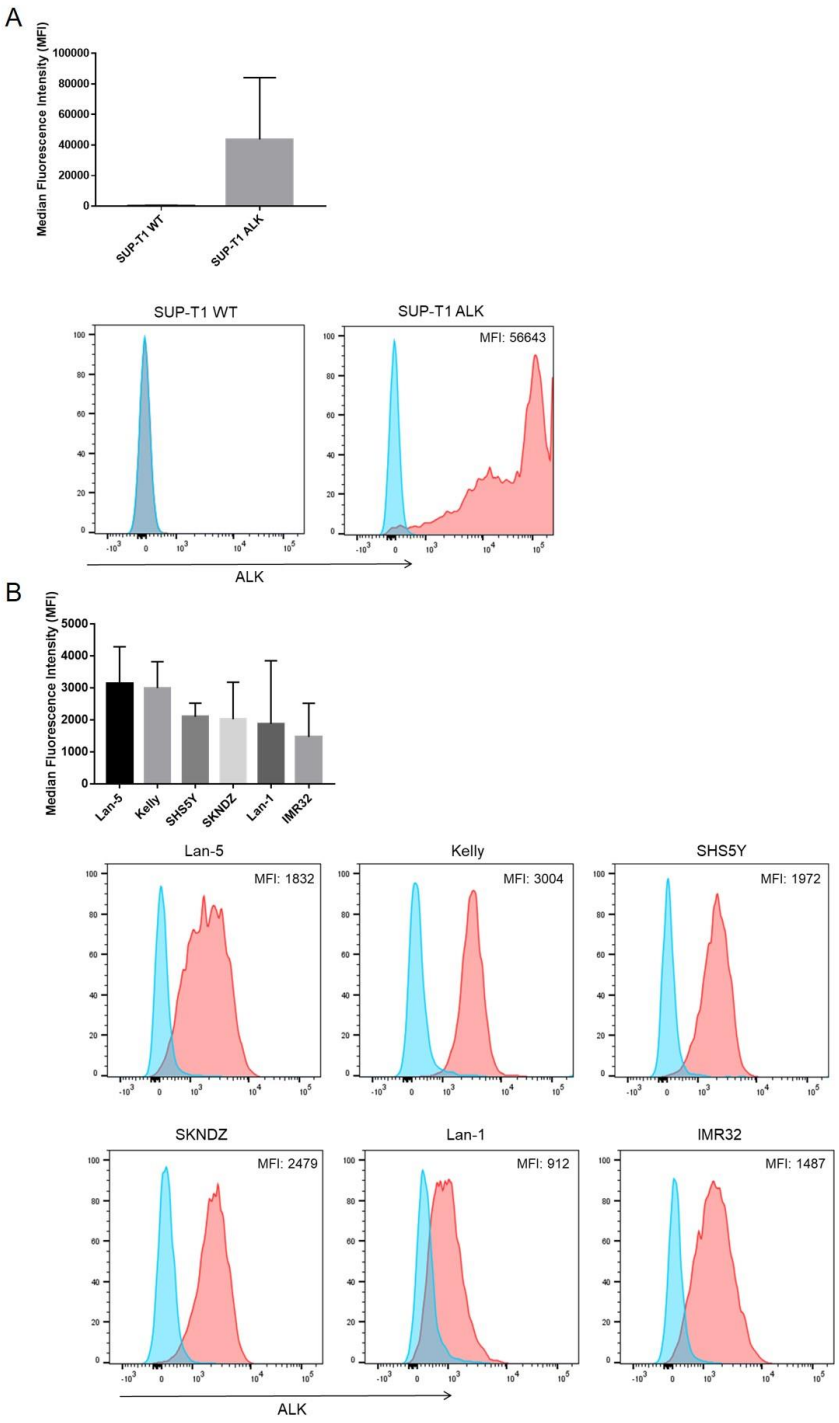

Figure 3.2 Surface expression of ALK in a panel of human cell lines

Surface ALK expression was determined by flow cytometry. Detection of ALK was achieved using Mab13 monoclonal primary antibody followed by APC anti-mouse secondary antibody (red histograms). Unstained cell lines were used as a control (blue histograms). Expression levels were quantified by MFI. (A) Detection of ALK on SUP-T1 cells transduced with the ALK ectodomain and further sorted for expression (SUP-T1 ALK), and on wild-type SUP-T1 (SUP-T1 WT). Mean MFI±SD (n=3 technical replicates) followed by representative histograms. (B) Mean MFI±SD (n=3 technical replicates) followed by representative histograms of ALK detection on a panel of neuroblastoma cell lines: Lan-5, Kelly, SHS5Y, SKNDZ, Lan-1 and IMR32.

3.3.3 Investigation of ALK CAR activity *in vitro*

As previously stated, the second aim of this research chapter was to characterise a panel of ALK CAR constructs in a number of *in vitro* assays. The CAR constructs used in these assays are as follows:

1. ALK4-CD8-28ζ
2. ALK4-Fc-28ζ
3. ALK8-CD8-28ζ
4. ALK8-Fc-28ζ
5. ALK9-CD8-28ζ
6. ALK9-Fc-28ζ
7. ALK10-Fc-28ζ
8. ALK11-CD8-28ζ
9. ALK11-Fc-28ζ

In the following experiments, untransduced (UT) T cells were used as a negative control.

3.3.3.1 Expression of ALK constructs on the surface of primary human T cells

Initially, it was investigated whether the nine above-mentioned ALK CAR constructs could be successfully expressed on the surface of primary human T cells. In order to investigate this, peripheral blood mononuclear cells (PBMCs) were isolated from healthy donors, and activated αβ T cells were transduced with retroviral supernatant produced from triple transfection of 293T cells with ALK CAR plasmids (2.2.7). Binding of anti-CD34 to RQR8, which is co-expressed with the CAR construct, was used as a marker of transduction in T cells. Surface

expression of RQR8 was seen in all T cell populations transduced to express the nine ALK constructs (Figure 3.3). Overall, the transduction efficacy ranged from 35±5% (mean±SD, n=3) to 84±34% (n=3). No statistically significant differences were observed between the transduction efficacies of the nine ALK CAR constructs.

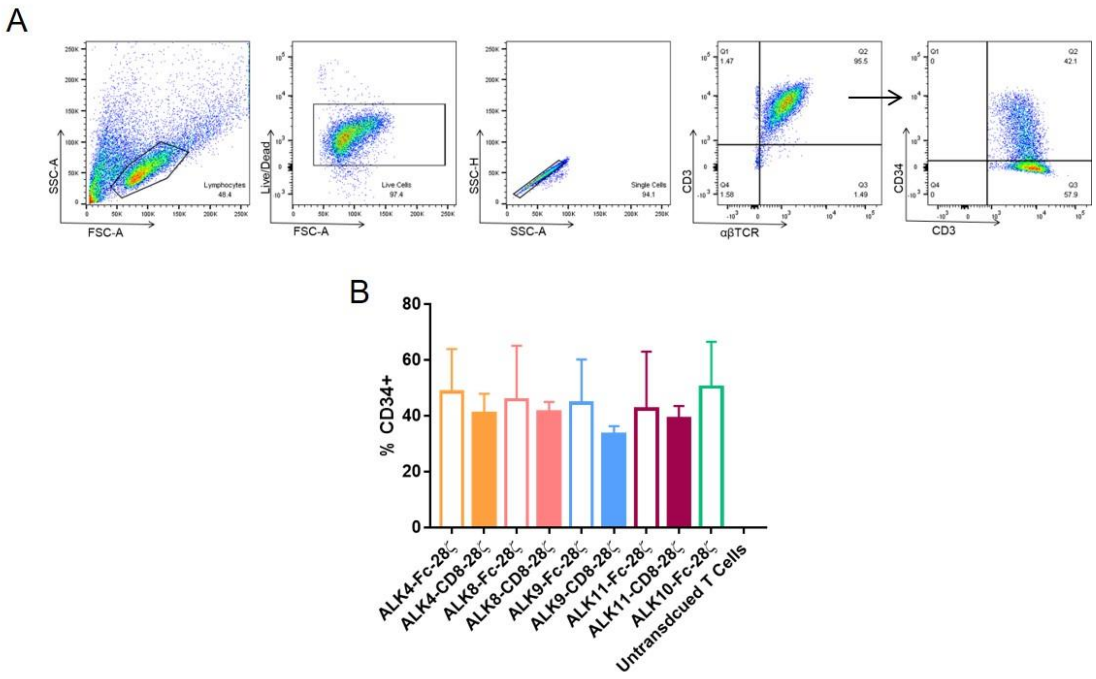

Figure 3.3 Transduction efficacy of ALK-RQR8 CAR constructs on primary αβ human T cells

Activated αβ T cells were transduced with retroviral supernatant to express the ALK CAR constructs Transduction efficacy was determined by quantifying the expression of the RQR8 marker gene co-expressed with the CAR construct. This was achieved by using an anti-CD34 APC antibody. Representative plots showing (A) the gating strategy to identify CD3+ αβTCR+ CD34+ T cells after the exclusion of doublets and dead cells. (B) Mean CD34 expression±SD (n=3 independent biological replicates). No statistically significant differences were found between CD34 expression levels as determined by one-way ANOVA followed by Tukey's post-hoc analysis.

3.3.3.2 Cytotoxic activity of ALK CAR T cells against a high ALK expressing cell line

Having confirmed the ALK CAR constructs could be detected on the surface of primary human T cells, their anti-tumour activity was assessed using a 4-hour chromium (^{51}Cr) release assay. This experiment allows a sensitive read out for cytotoxicity, in which target cells are labelled with a radioactive isotype and co-cultured for a short time with the effector CAR T cells. Upon target cell lysis, ^{51}Cr is released into the surrounding supernatant, which can be detected and correlated with the levels of target cell death.

Initially the high ALK expressing cell line SUP-T1 ALK, was used to investigate cell killing (Figure 3.2A). ALK CAR T cells were co-cultured with ^{51}Cr labelled SUP-T1 ALK and SUP-T1 WT at various effector:target (E:T) ratios (1.25:1, 2.5:1, 5:1 and 10:1). Minimal ^{51}Cr release was seen from UT T cells co-cultured with SUP-T1 ALK cells, or when ALK CAR T cells were co-cultured with the ALK-negative cell line, SUP-T1 WT (Figure 3.4A and Figure 3.4B). All ALK CAR T cells lysed the SUP-T1 ALK cell line to a degree, with ^{51}Cr release increasing along with E:T ratio. At a 10:1 E:T ratio, all nine anti-ALK CAR T cell populations induced significant ^{51}Cr release from the SUP-T1 ALK cell line compared to UT control T cells. The individual ALK CARs were also compared for significant differences between each other in terms of ^{51}Cr release at different E:T ratios. Only ALK9-CD8-28ζ demonstrated significantly increased levels of killing and only at one E:T ratio, these values are shown in Table 3.1.

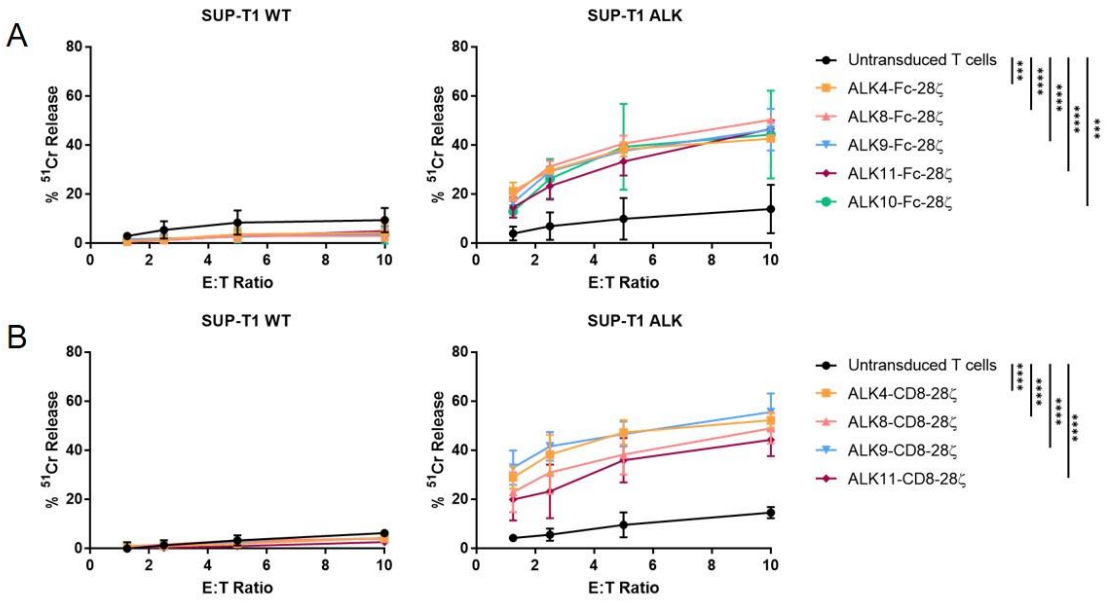

Figure 3.4 Cytotoxic activity of ALK CARs against SUP-T1 ALK and SUP-T1 WT cell lines

T cells transduced with ALK CARs expressing either an Fc (A) or a CD8 stalk (B) were co-cultured for four hours with 51Cr-labelled target cells (SUP-T1 WT or SUP-T1 ALK) at the following E:T ratios: 1.25:1, 2.5:1, 5:1 and 10:1. UT T cells were used as a negative control. Graphs show mean±SD (n=5 independent biological replicates). Two-way ANOVA was performed followed by Tukey's post-hoc analysis: *** p<0.001, **** p<0.0001 (Statistics displayed for 10:1 E:T only comparing ALK CAR to UT control T cells).

Table 3.1 Significant differences between ALK CAR T cells

ALK9-CD8-28ζ vs	E:T ratio	P value
ALK11-Fc-28ζ	1.25:1	* (p<0.1)
ALK10-Fc-28ζ	1.25:1	* (p<0.1)
ALK11-CD8-28ζ	2.5:1	* (p<0.1)
ALK11-Fc-28ζ	2.5:1	* (p<0.1)

3.3.3.3 Cytokine production by ALK CAR T cells co-cultured with a high ALK expressing cell line

Another way to investigate the function of CAR T cells is to determine their ability to produce proinflammatory cytokines on co-culture with target antigens. ALK CAR T cells were co-cultured at a 1:1 E:T ratio with the SUP-T1 ALK and SUP-T1 WT cell lines or cultured alone for 24 hours before the presence of cytokines in the supernatant was measured through ELISA.

ALK-Fc and ALK-CD8 CAR T cells co-cultured with SUP-T1 WT or alone, all demonstrated background production of IL-2 (Figure 3.5A and Figure 3.5B). In some cases, the level of IL-2 production was over 1000pg/mL. As this background IL-2 release was also seen from UT control T cells, which is much higher than expected for resting T cells, it likely represents contamination from previous T cell culture and expansion with IL-2. Despite this high background, ALK4-Fc-28ζ, ALK8-Fc-28ζ and ALK9-Fc-28ζ produced significantly higher levels of IL-2 than UT cells when co-cultured with SUP-T1 ALK cells: 2818±347 (mean pg/mL cytokine release±SD, n=3), 4000±400 pg/mL (n=3) and 3103±407 pg/mL (n=3), respectively (Figure 3.5A). Amongst the CARs with CD8 stalk, only ALK8-CD8-28ζ produced levels of IL-2 above that of the control UT T cells when co-cultured with SUP-T1 ALK cells, however this was not statistically significant (Figure 3.5B).

All five Fc spacer expressing ALK CAR T cells produced high levels of IFNγ when co-cultured with SUP-T1 ALK cells (Figure 3.5A). This trend was also seen with ALK-CD8 CAR T cells on co-culture with SUP-T1 ALK cells. However, only ALK8-

CD8-28ζ amongst the CD8 stalk CARs produced significantly higher level of IFNγ than UT T cells; 6320±4360 pg/mL (n=3) (Figure 3.5B).

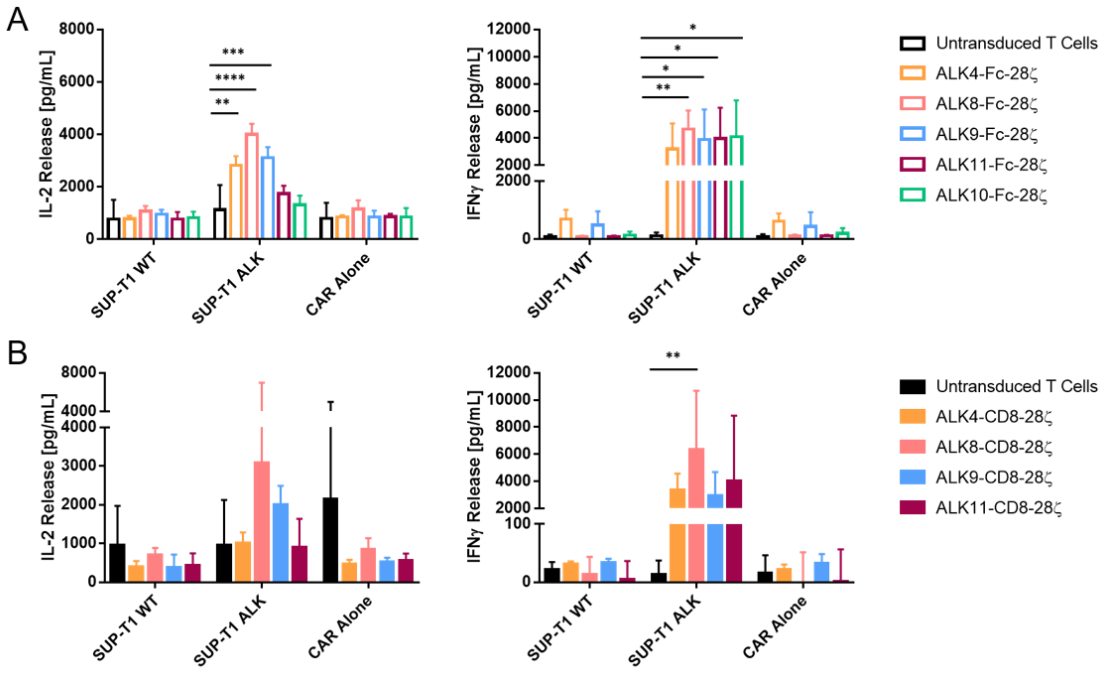

Figure 3.5 Quantification of IL-2 and IFNγ production by ALK CAR T cells co-cultured with a high ALK expressing cell line

IL-2 and IFNγ measured by ELISA from supernatant after 24 hour co-culture of ALK CAR T cells with target cells (SUP-T1 ALK or SUP-T1 WT) or alone at a 1:1 E:T ratio. The ALK CAR T cell constructs contained either an Fc (A) or a CD8 (B) spacer. Untransduced T cells were used as a negative control. Graphs show mean±SD (n=3 independent biological replicates). Two-way ANOVA was performed followed by Tukey's post-hoc analysis: * p<0.05, ** P<0.01, *** p<0.001, **** p<0.0001.

3.3.4 Further evaluation of ALK constructs against neuroblastoma cell lines

Based on the results found in Section 3.3.3, it was possible to exclude three ALK CAR T cells (ALK4-CD8-28ζ, ALK10-Fc-28ζ and ALK11-Fc-28ζ) from further analysis, based on their reduced cytokine production and lack of statistically significant differences between ALK CARs in the cytotoxicity assay. The following ALK CAR constructs were taken forward for further testing:

1. ALK4-Fc-28ζ
2. ALK8-Fc-28ζ
3. ALK8-CD8-28ζ
4. ALK9-Fc-28ζ
5. ALK9-CD8-28ζ
6. ALK11-CD8-28ζ

After demonstrating that ALK CAR T cells were able to lyse the SUP-T1 ALK cell line which was engineered to express high levels of surface ALK, the next step was to demonstrate specific killing of neuroblastoma cell lines which naturally express different levels of ALK. Compared to SUP-T1 ALK cells, neuroblastoma cell lines represent a more meaningful target as they have more physiologically relevant levels of surface ALK expression. For this set of experiments the following neuroblastoma cell lines were used, which express increasing levels of ALK surface expression; Lan-1 (average MFI: 1876), Kelly (average MFI: 2999) and Lan-5 (average MFI: 3142) (Figure 3.2). UT T cells were used as a negative control in these experiments.

3.3.4.1 Cytotoxic activity of ALK CAR T cells against a panel of neuroblastoma cell lines

As previously described, ALK CAR T cells were co-cultured at increasing E:T ratios with ^{51}Cr labelled target cells for four hours before ^{51}Cr release into the supernatant was determined. No lysis of the ALK negative cell line (SUP-T1 WT) was seen by any ALK CAR T cells, and UT control T cells elicited no cytotoxic effects on target neuroblastoma cell lines (Figure 3.6). The Lan-1 cell line has the lowest levels of ^{51}Cr release after co-culture with all ALK CAR T cells, while the Lan-5 cell line had the highest level of ^{51}Cr release. All ALK CAR T cells expressing an Fc spacer exhibited significantly higher levels of cytotoxic activity when co-cultured with Lan-1, Kelly and Lan-5 compared to control cells at a 10:1 E:T ratio (Figure 3.6A).

Similar results were observed when ALK CAR T cells expressing a CD8 stalk were co-cultured with Kelly and Lan-5 (Figure 3.6B). However, only ALK8-CD8-28ζ demonstrated statistically significant cytotoxicity when co-cultured with Lan-1 compared to UT T cells (19±10%, mean ^{51}Cr release±SD, n=5).

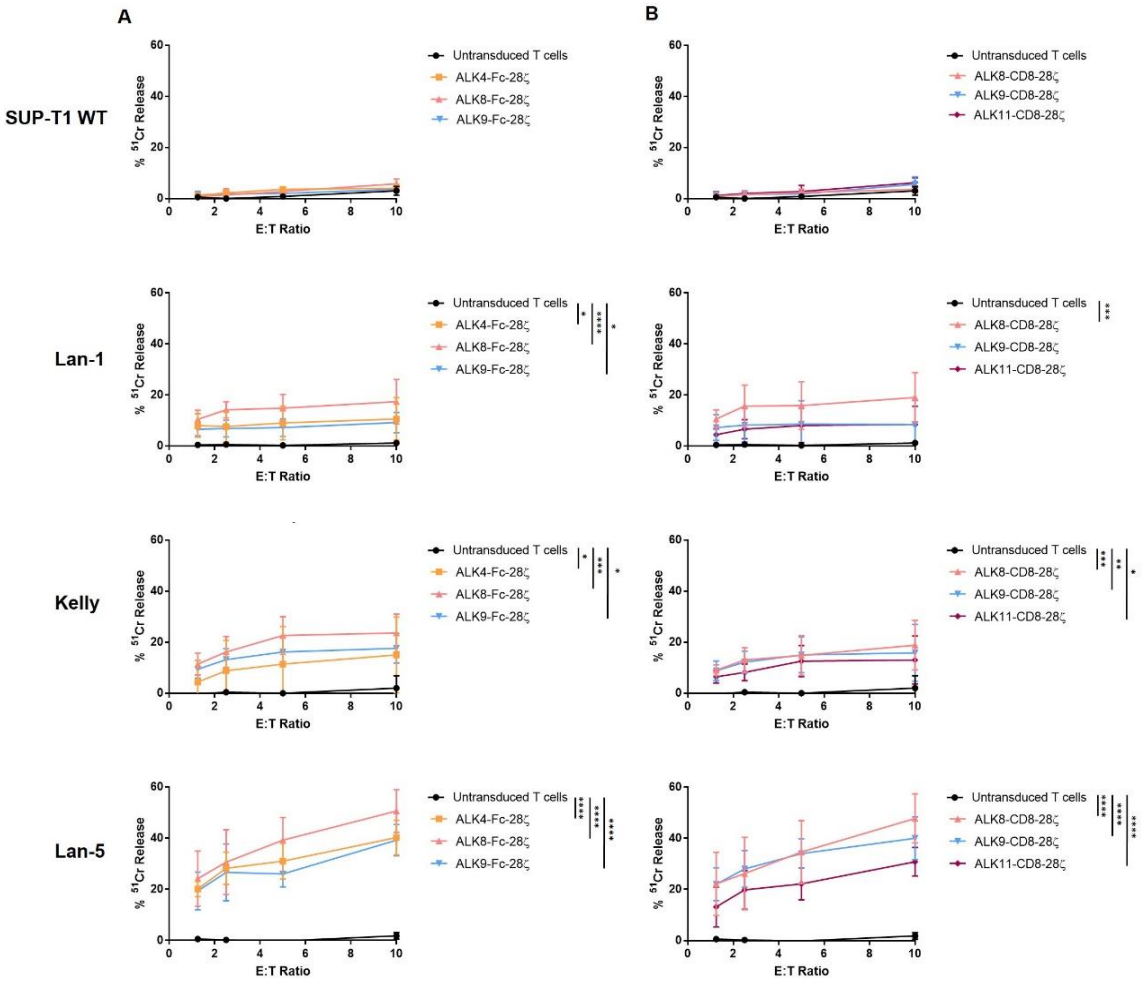

Figure 3.6 Cytotoxic activity of ALK CAR T cells co-cultured with neuroblastoma cell lines

ALK CAR T cells incorporating either an Fc (A) or a CD8 stalk (B) were co-cultured for four hours with ^{51}Cr-labelled target cells at increasing ALK target density (SUP-T1 WT, Lan-1, Kelly and Lan-5, respectively) at the following E:T ratios: 1.25:1, 2.5:1, 5:1 and 10:1. Untransduced T cells were used as a negative control. Graphs show mean ± SD (n=5 independent biological replicates). Two-way ANOVA was performed followed by Tukey's post-hoc analysis: * p<0.05, ** P<0.01, *** p<0.001, **** p<0.0001. (Statistics displayed for 10:1 E:T only).

Figure 3.7 displays the same data as above (Figure 3.6). In this case, the ALK CAR T cells with matched scFvs (ALK8 and ALK9) are displayed with either an Fc spacer or CD8 stalk region, for comparison purposes. In this way, the different stalk regions can be directly compared. Interestingly, at lower ALK antigen densities, namely when co-cultured with Lan-1, ALK8 CAR T cells lysed cells at similar levels, which was higher than ALK9 CAR T cells. When co-cultured with Kelly and Lan-5 cell lines, there were minimal differences between all four CAR

T cells, with ALK8-Fc-28ζ demonstrating slightly higher ^{51}Cr release from Kelly cells. When compared to each other, only ALK8-CD8-28ζ reached a statistically significant higher level of ^{51}Cr release compared to ALK9-CD8-28ζ when co-cultured with Lan-1 at a 10:1 E:T ratio (* $p<0.05$).

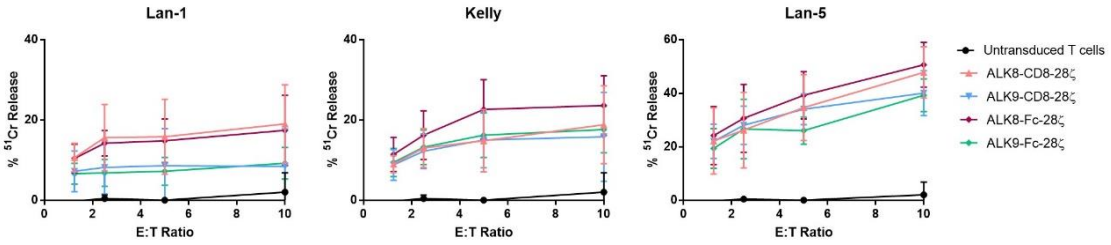

Figure 3.7 Comparison of ALK-Fc and ALK-CD8 CAR T cells with matched scFvs

This data is the same as shown in Figure 3.6, however only paired ALK scFvs are displayed. In this way matched ALK scFvs can be compared with different stalk regions.

3.3.4.2 Quantification of IL-2 and IFNγ produced from ALK CAR T cells co-cultured with a panel of neuroblastoma cell lines

As previously described, ALK CAR T cells were co-cultured with the neuroblastoma cell lines: Lan-1, Kelly or Lan-5, or SUP-T1 WT cells, or alone for 24 hours before the supernatant was measured for the presence of proinflammatory cytokines through ELISA.

ALK CAR T cells expressing the Fc spacer produced no levels of IL-2 when co-cultured with any cell lines (Figure 3.8A). Only ALK8-Fc-28ζ appeared to produce minimal levels of IL-2 when co-cultured with Kelly and Lan-5 cell lines (10pg/mL±7 and 12pg/mL±13, respectively). ALK CAR T cells expressing the Fc spacer produced IFNγ when co-cultured with Lan-1, Kelly and Lan-5 cell lines, however this was not statistically significant. Furthermore, ALK4-Fc-28ζ and ALK9-Fc-28ζ also produced low level IFNγ when co-cultured with SUP-T1 WT cells, and when cultured alone, suggesting there is some background activity.

ALK CAR T cells expressing CD8 stalks produced minimal levels of IL-2 on co-culture with neuroblastoma cell lines, apart from ALK8-CD8-28ζ which produced low levels IL-2 on co-culture with Lan-5, although not reaching statistical significance (Figure 3.8B). Furthermore, untransduced T cells appeared to produce IL-2 when co-cultured with Kelly, Lan-5 or when cultured alone. Only ALK8-CD8-28ζ and ALK9-CD8-28ζ showed an increase in mean IFNγ production compared to the untransduced control T cells, on co-culture with Lan-1, Kelly and Lan-5. Again, these results did not reach statistical significance.

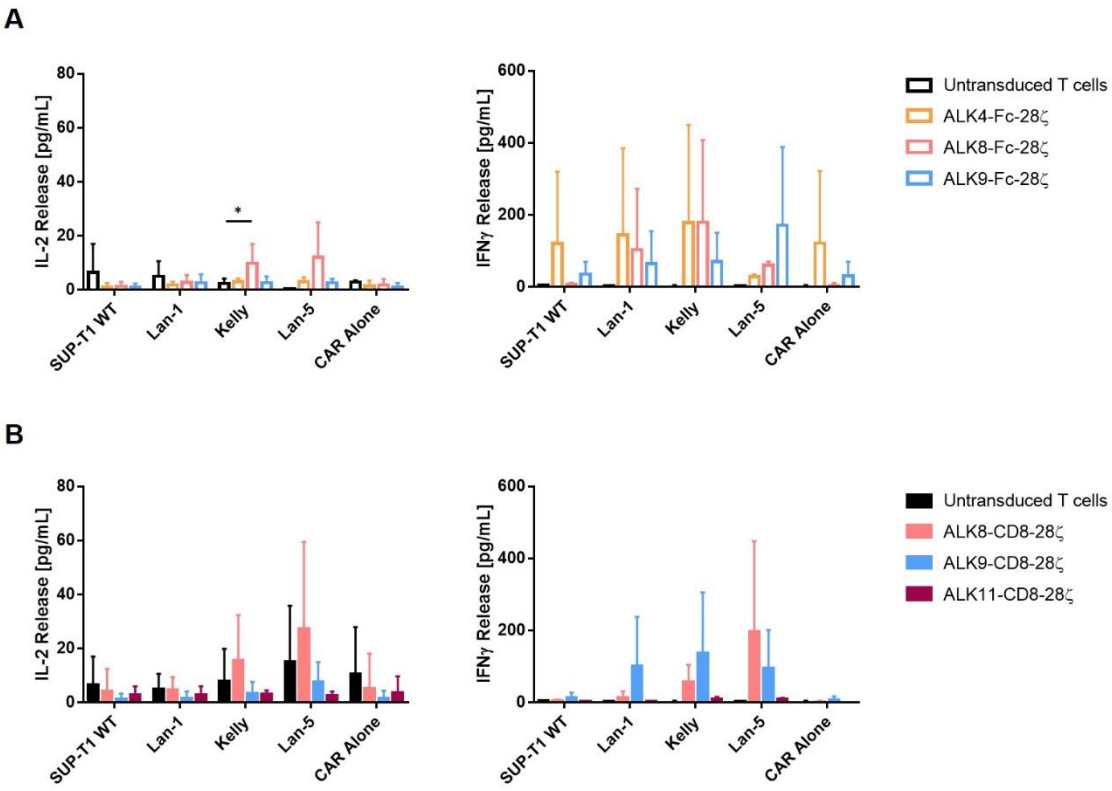

Figure 3.8 Quantification of IL-2 and IFNγ from ALK CAR T cells co-cultured with a panel of neuroblastoma cell lines

IL-2 and IFNγ measured by ELISA from supernatant after 24 hour co-culture of ALK CAR T cells incorporating either an Fc (A) or a CD8 (B) stalk and target cells (SUP-T1 ALK or SUP-T1 WT) or alone at a 1:1 E:T ratio. Untransduced T cells were used as a control. Graphs show mean ± SD (n=3-6 independent biological replicates). Two-way ANOVA was performed followed by Tukey's post-hoc analysis: * $p<0.05$.

3.3.5 Proliferation

An important characteristic of CAR T cells is their ability to proliferate on recognition of target antigens. It is equally important that CAR T cells don't proliferate independently or on recognition of unspecific antigens. To investigate this, ALK CAR T cells were co-cultured with ALK expressing cell lines, Lan-1, Kelly, Lan-5 or SUP-T1 ALK for increasing time periods, without the addition of IL-2. Proliferation was determined through the dilution of cell trace dyes, or by determining T cell counts. In this set of experiments, UT T cells or ALK CAR T cells were cultured alone, or with the ALK negative cell line, SUP-T1 WT, as negative controls. ALK CAR T cells stimulated with PMA and ionomycin were used as a positive control.

3.3.5.1 Short term proliferative capacity

Proliferation dyes such as cell trace violet can be used to monitor multiple generations through dye dilution, which indicates that a labelled population has undergone cell division. Cell trace violet-labelled ALK CAR T cells were co-cultured 1:1 with irradiated SUP-T1 WT, Lan-1, Kelly, Lan-5 or SUP-T1 ALK cell lines. After 4 and 8 days of co-culture, ALK CAR T cell proliferation was determined by cell trace violet dilution through flow cytometry. Figure 3.9 demonstrates a representative gating strategy to identify CD3+, αβTCR+, CD34+ T cells that have proliferated as per proliferation dye dilution, after the exclusion of dead cells and doublets.

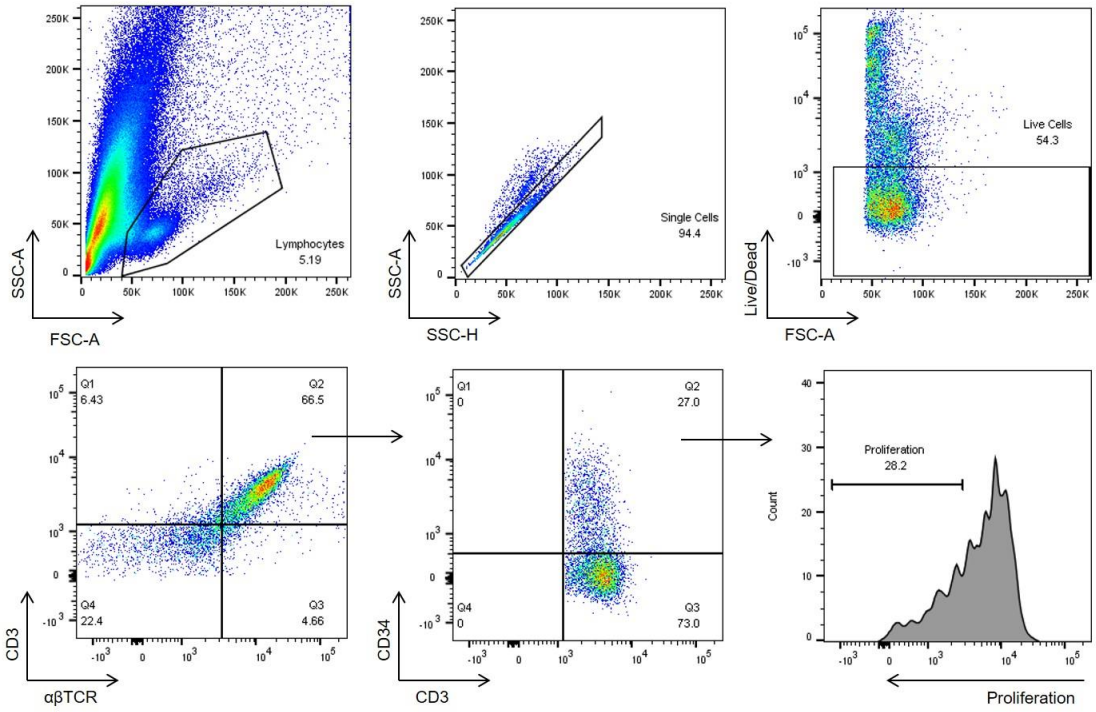

Figure 3.9 Representative gating strategy for proliferating cells

Gating strategy to identify CD3+, αβTCR+, CD34+ T cells after exclusion of dead and doublet cells. The proliferation gating is set on control UT T cells, and the dilution of cell trace violet indicates proliferation of a population.

In order to quantify this short term proliferation the change in MFI of cell trace violet compared to the untransduced T cell cultured alone for each experiment was determined; referred to as the delta MFI (ΔMFI). Figure 3.10 displays short term proliferation data after 4 days of co-culture. Commonly, there is donor to donor variability when biological samples are used. Figure 3.10A shows that donor 3 had a much lower response to PMA and ionomycin stimulation than donor 1 and donor 2, however this donor was still included in the following analysis.

Figure 3.10B displays representative histogram readouts of cell trace violet dilution for donor 1. ALK CAR T cells expressing an Fc spacer or a CD8 stalk were cultured alone, stimulated with PMA and ionomycin, or co-cultured with irradiated SUP-T1 WT, Lan-1, Kelly, Lan-5 or SUP-T1 ALK cell lines. In all cases the control UT T cells cultured alone did not proliferate, while ALK CAR T cells stimulated with PMA and ionomycin proliferated over the 4 days, as expected. Unexpectedly, the CARs containing an Fc spacer, ALK4-Fc-28ζ, ALK8-Fc-28ζ and ALK9-Fc-28ζ, appeared to proliferate regardless of the culture condition; when cultured alone, or co-cultured with SUP-T1 WT, Lan-1, Kelly, Lan-5 or SUP-T1 ALK. On the other hand, ALK8-CD8-28ζ, ALK9-CD8-28ζ and ALK11-CD8-28ζ demonstrated more restricted proliferation when cultured alone, or with the ALK negative cell line, SUP-T1 WT. Only ALK9-CD8-28ζ amongst those with CD8 stalks, appeared to demonstrate slight proliferation in these antigen-negative conditions but at a much lower extent than ALK CAR T cells expressing an Fc spacer. Furthermore, ALK8-CD8-28ζ, ALK9-CD8-28ζ and ALK11-CD8-28ζ demonstrated lower proliferation when co-cultured with Lan-1, a low ALK

expressing cell line, but higher levels of proliferation were seen when they were co-cultured in the presence of Kelly, Lan-5 and SUP-T1 ALK cell lines.

The ΔMFI for proliferation of ALK CARs after 4 days of co-culture is shown in Figure 3.10C. The ΔMFI for Fc spacer expressing CAR T cells suggests that all three CARs proliferated at similar levels regardless of the culture condition. In contrast, the ΔMFI for ALK CAR T cells expressing the CD8 stalk demonstrated more restricted patterns of proliferation, reflecting what was seen in the histograms (Figure 3.10B). All three CD8 stalk CARs had minimal proliferation when cultured alone, and with the antigen negative cell line, SUP-T1 WT. ALK11-CD8-28ζ and ALK9-CD8-28ζ demonstrated very low proliferative responses to Lan-1, and in the case of ALK9-CD8-28ζ the level of proliferation seen with Lan-1 was lower than that of the CAR cultured alone. Given the background proliferation from Fc spacer containing ALK CAR T cells, statistical differences were determined through one-way ANOVA comparing experimental conditions to the SUP-T1 WT control cell line.

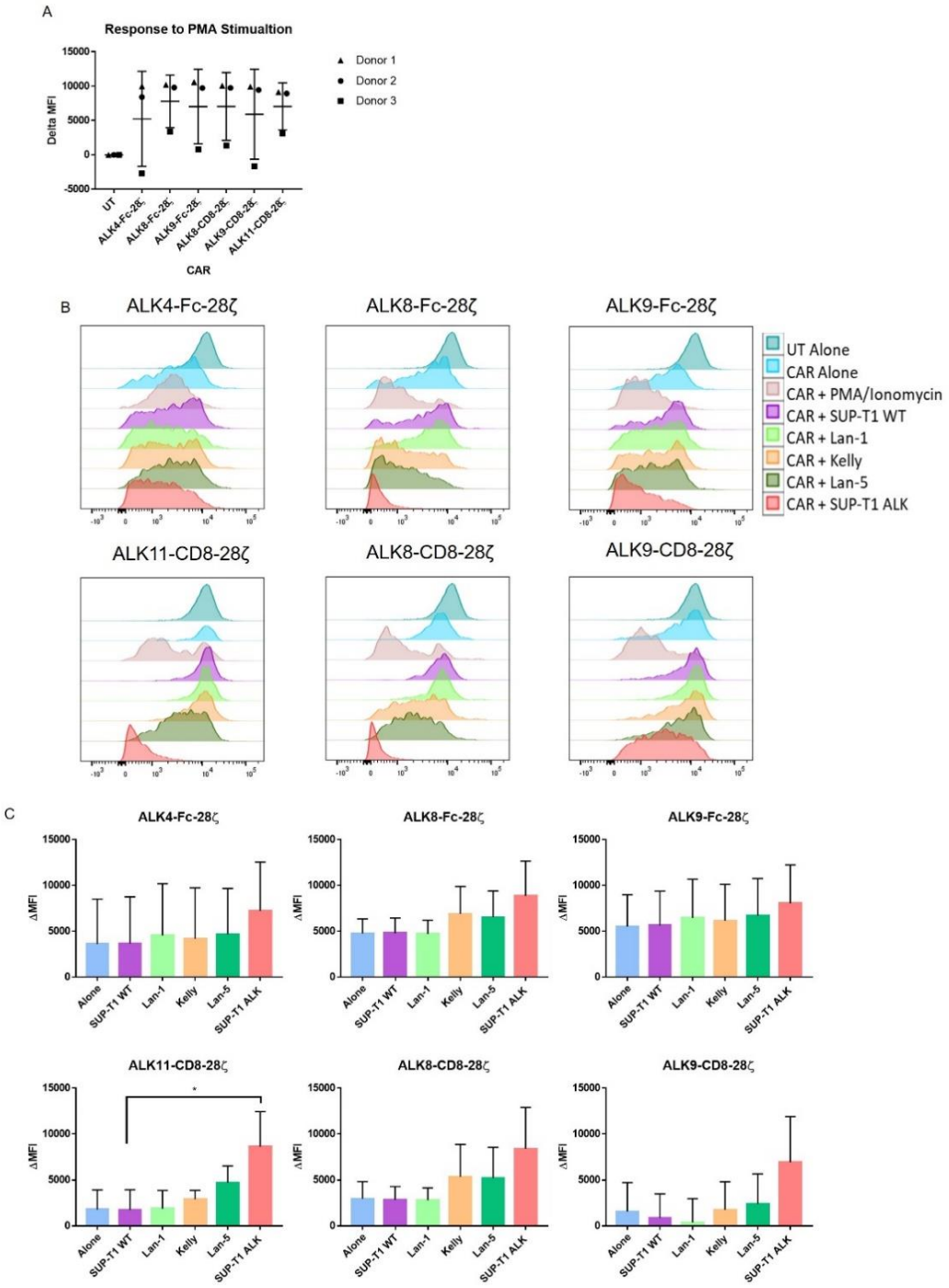

Figure 3.10 Proliferative capacity of ALK CAR T cells after 4 days of short term co-culture

ALK CAR or UT T cells labelled with cell trace violet proliferation dye were co-cultured with the following irradiated cell lines at a 1:1 E:T ratio: SUP-T1 WT, Lan-1, Kelly, Lan-5 and SUP-T1 ALK. UT T cells and ALK CAR T cells cultured alone were used as controls, along with PMA and ionomycin stimulation In these experiemnts, delta MFI (ΔMFI) was defined as the difference between the MFI of the indicated CAR and condition and the MFI of UT T cells with no targets. (A) The ΔMFI of the response to PMA and ionomycin stimulation from all three donors. (B) Representative histograms showing the cell trace violet dilution from CAR T cell populations in the aforementioned co-culture conditions. (C) Mean ΔMFI±SD for ALK CAR T cells (n=3 independent biological replicates). Statistical differences were determined by one-way ANOVA comparing experimental condition to control cell line, SUP-T1 WT: * $p<0.05$.

Figure 3.11 displays short term proliferation data from the same experiment after leaving the cells for 8 days of co-culture. Figure 3.11A shows a representative read out of cell trace violet dilution of ALK CAR T cells in co-culture conditions. As shown in Figure 3.10A, in all cases UT T cells cultured alone showed very little evidence of proliferation through cell trace violet dilution. ALK CAR T cells containing the Fc spacer region demonstrated cell trace violet dilution in every co-culture condition, including when cultured alone or with the ALK negative cell line, SUP-T1 WT, indicative of high background proliferation associated with the presence of these CARs. In contrast, ALK CAR T cells containing the CD8 stalk region demonstrated more restricted proliferation through proliferation dye dilution. As shown from the representative histograms, all CD8 stalk containing CAR T cells showed highest proliferation when co-cultured with the SUP-T1 ALK cell line. ALK8-CD8-28ζ also proliferated on co-culture with Lan-5 and Kelly cell lines, while ALK11-CD8-28ζ only proliferated with Lan-5 co-culture.

Figure 3.11B shows the mean ΔMFI for ALK CAR T cells. The ΔMFI reflects what is seen in the representative histograms and proliferation patterns at day 4 of co-culture (Figure 3.10). For Fc spacer containing ALK CAR T cells, proliferation is similar across every co-culture condition. In contrast, ALK CAR T cells containing a CD8 stalk region showed restricted proliferation patterns, with larger ΔMFI values against higher ALK expressing cell lines.

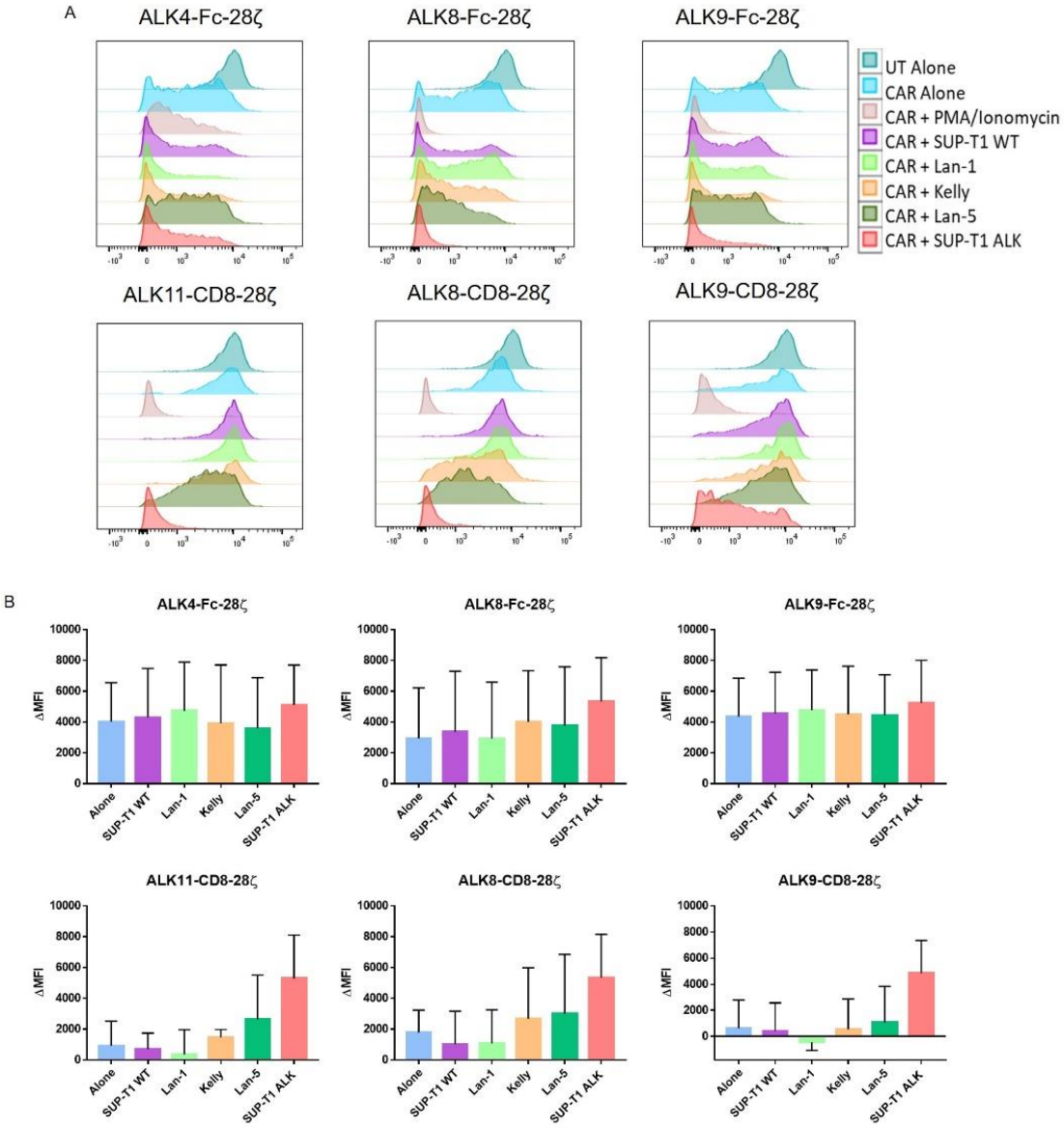

Figure 3.11 Proliferative capacity of ALK CAR T cells after 8 days of short term co-culture

ALK CAR or UT T cells labelled with cell trace violet proliferation dye were co-cultured with the following irradiated cell lines at a 1:1 E:T ratio: SUP-T1 WT, Lan-1, Kelly, Lan-5 and SUP-T1 ALK. UT T cells and ALK CAR T cells cultured alone were used as controls, along with PMA and ionomycin stimulation. (A) Representative histograms showing the cell trace violet dilution from CAR T cell populations in the aforementioned co-culture conditions. (B) Mean ΔMFI±SD for ALK CAR T cells (n=3 independent biological replicates). Statistical differences were determined by one-way ANOVA comparing experimental condition to control cell line, SUP-T1 WT.

3.3.5.2 Long term proliferative capacity with restimulation

An effective CAR T cell therapeutic for a solid cancer must be able to proliferate on initial recognition of a tumour antigen, and after prolonged exposure. It is not possible to track long term proliferation by use of cell trace dyes, due to dilution of the dye in culture over time which can cause uninterpretable results. Therefore, an initial pilot experiment was undertaken to see if ALK CAR T cells had long term proliferative capacity following repeated stimulation. ALK CAR T cells or untransduced T cells were co-cultured at a 1:1 E:T ratio with irradiated target cells; SUP-T1 WT, Lan-1, Kelly and Lan-5. ALK CAR T cell total count was determined once a week by flow cytometry, using a BD FACSCalibur instrument. The remaining T-cell populations were restimulated with an additional 500,000 irradiated target cells once a week for four weeks in total.

ALK CAR T cell numbers appeared to drop quickly after plating on day 0 to day 7 in culture when co-cultured with SUP-T1 WT, Lan-1, Kelly and Lan-5 cell lines (Figure 3.12). By day 14, there appeared to be minimal live ALK CAR T cells present, which remained the case at day 21 and 28, despite restimulation. A number of ALK CARs demonstrated significantly higher levels of CAR T cells present at day 7 than untransduced T cells, however this is not proliferation as T cell numbers were not increasing.

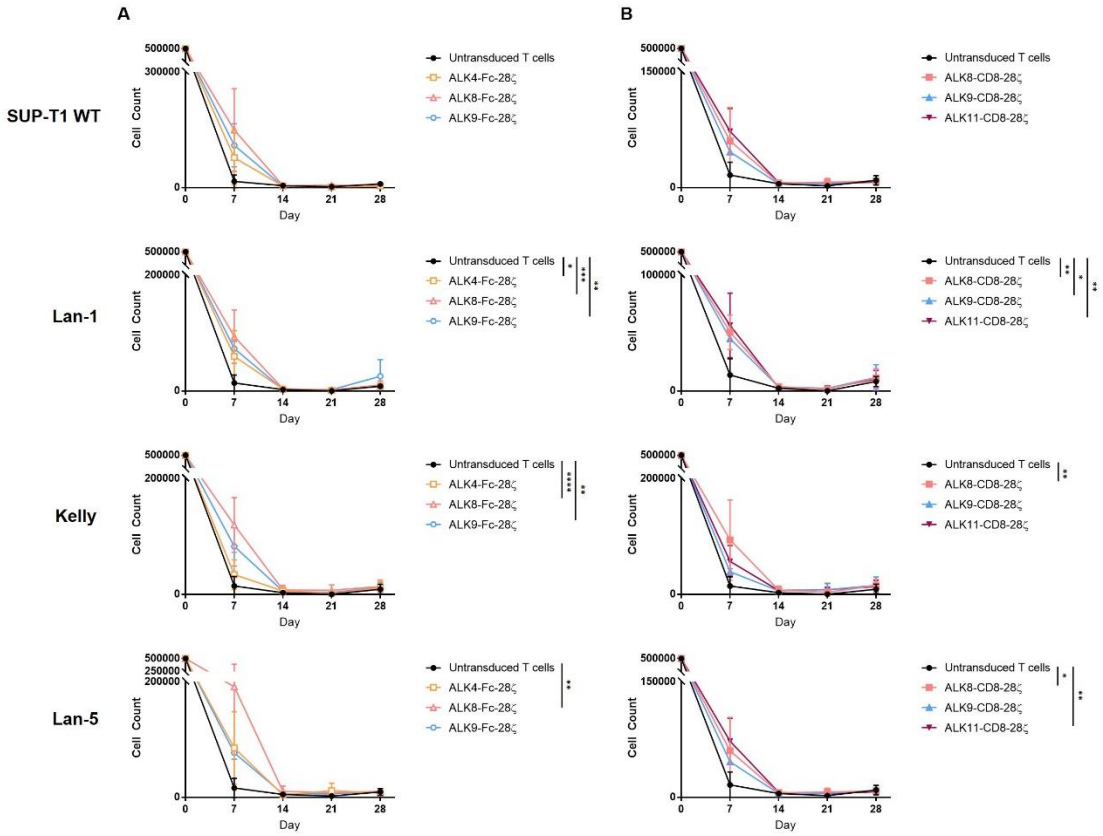

Figure 3.12 Long term proliferative capacity of ALK CAR T cells co-cultured with a panel of neuroblastoma cell lines

ALK CAR T cells were co-cultured with irradiated cell lines at 1:1 E:T. Untransduced T cells were used as a control. ALK CAR T cells were restimulated weekly by addition of 500,000 irradiated target cells. Cells were counted weekly for 4 weeks on FACSCalibur. Graphs show mean ± SD (n=2 independent biological replicates). Two-way ANOVA was performed followed by Tukey's post-hoc analysis: * p<0.05, ** P<0.01, *** p<0.001, **** p<0.0001. (Statistics displayed for Day 7, following time points showed no significant differences).

3.4 Discussion

The aim of this first chapter of research was to characterise a panel of ALK-specific CAR constructs based on their performance in a number of *in vitro* functional assays. For this purpose, nine different anti-ALK CARs were tested, comprising of five unique ALK binders combined with two spacer regions of different lengths; the Fc spacer and the CD8 stalk.

Initially, the levels of surface expressed ALK was determined on a panel of neuroblastoma cell lines. This was necessary for two reasons; to validate, albeit in a small sample, that ALK was expressed on the cell surface of neuroblastoma cells and could therefore be targeted by anti-ALK CAR T cells. Furthermore, it was important to identify a number of different neuroblastoma cell lines with a range of varied ALK surface expression so that subsequent experiments could compare CAR T cell reactivity against a range of different target antigen densities. In the first instance, attempts were made to quantify ALK antigen density on neuroblastoma cells by using a flow cytometry based quantification kit. Assays such as this, require a conjugated primary antibody. Currently, there is no commercially available antibody that can bind the extracellular domain of ALK. Mab13 is a primary unconjugated antibody that binds the ALK ectodomain, thought to be the glycine-rich region (Moog-Lutz et al., 2005). Attempts were made to conjugate this to a fluorochrome, such as APC. Despite the conjugation being performed as per protocol, there was intra-experimental variation in results suggesting unstable and incomplete conjugation. Based on this the results were uninterpretable (results not shown). This could be due to multiple reasons; including inefficient labelling and different degrees of contamination with

unlabelled antibody between independent experiments. Based on this, it was decided to determine the binding of primary mab13 and a secondary staining antibody to ALK by calculating the median fluorescence intensity (MFI). A range of ALK expression was identified on neuroblastoma cell lines (Figure 3.2B). ALK surface expression was also confirmed on a lymphoma cell line transduced to express the ALK ectodomain allowing for a high ALK expressing cell line with a matched ALK negative control (SUP-T1 ALK and SUP-T1 WT, respectively) (Figure 3.2A). The cell lines, Lan-1, Kelly and Lan-5 were taken forward for *in vitro* testing of ALK CARs based on their range of ALK expression from low to high. It has been noted, that cell lines do not represent the heterogeneity of antigen expression that can be seen in patient samples, and cultured cell lines have the capacity of antigen expression changes over time. Therefore, determining ALK expression on patient samples may represent a more accurate view of antigen expression in the wider setting.

It needed to be determined that ALK CAR constructs could be expressed on the surface of primary T cells, and that this could be measured accurately through flow cytometry. It has been previously demonstrated that the use of *Thosea asigna 2A* (T2A) self-cleaving peptide results in the equimolar expression of two constructs expressed within the same viral vector (Daniels et al., 2014, Wang et al., 2011, Szymczak et al., 2004). Chang *et al*., demonstrated that utilising a T2A molecule allowed for equal expression of truncated EGFR and a CD19 CAR, when EGFR was stained to demonstrate the EGFR-CAR transcript had been translated (Chang et al., 2015). They also commented that the use of reagents such anti-Fab antibodies that have the ability to bind an scFv only gave weak staining which was not accurate (Chang et al., 2015). Taking into consideration

the above reasons, ALK CAR constructs were co-expressed with an RQR8 molecule via a T2A peptide, which allows them to be translated as a single protein which is then cleaved at the T2A site (Chang et al., 2015, Philip et al., 2014) (Figure 3.1). This allows the indirect quantification of CAR expression via antibody staining of surface bound RQR8, without disrupting potential interactions between CAR molecules and their ligands. Based on this, surface binding of anti-CD34 to RQR8 was used as a determinant for transduction efficacy (Philip et al., 2014). It appeared that RQR8 was expressed on the surface of all ALK CAR transduced T cells at relatively similar levels, with no statistically significant differences between their expressions (Figure 3.3). This would suggest any differences in results seen with ALK CAR T cells was based on the activity of the CAR, rather than the level surface expression. However, this conclusion is based on the assumption that the different scFv and spacers will not alter stability or surface expression. This may not be an accurate conclusion, as later data demonstrate that an Fc spacer, as opposed to a CD8 stalk, can cause tonic signalling and antigen independent proliferation. Furthermore, this can potentially result in receptor internalisation, and therefore affect the surface expression level. Walker *et al*., discovered that ALK CAR and CD19 CAR T cells showed nearly complete CAR down-modulation upon co-incubation with tumours expressing high levels of cognate antigen in *in vitro* settings, which was further shown *in vivo* (Walker et al., 2017).

Others have investigated CAR expression by detecting different domains of the CAR construct, for example, binding of the Fc spacer using an anti-Fc antibody (Jena et al., 2013). However in this case, ALK CAR T cells don't contain the same spacer region and therefore this would not be an option. It was commented that

a major challenge in the CAR field is the lack of fast, sensitive and robust assays for the detection of CARs on the surface of immune effector cells (Gopalakrishnan et al., 2019). A sensitive novel luciferase-based detection assay was developed, in which a luciferase is joined in frame with an scFv which allows for a luminescent readout, demonstrated using the FMC63 CAR T cell (Gopalakrishnan et al., 2019). Other studies have detected CAR expressing T cells through staining with protein L, an immunoglobulin binding protein that binds to the variable light chains of a scFv without interfering with antigen binding site, or using anti-idiotype antibodies (Jena et al., 2013, Zheng et al., 2012). An alternative method of quantifying surface expression of ALK CAR constructs would be through the use of an ALK-Fc fusion protein. Upon incubation with the ALK CAR T cells, this will bind to the anti-ALK scFv; binding can then be detected with an anti-Fc antibody conjugated to a fluorochrome, and therefore detectable through flow cytometry.

Functionally, effective CAR T cells are expected to lyse target cells, produce proinflammatory cytokines and proliferate in an antigen-dependant manner. When co-cultured with a high expressing ALK+ cell line, SUP-T1 ALK, it was demonstrated that all nine ALK CAR T cells lysed target cells and induced ^{51}Cr release, particularly at high E:T ratios (Figure 3.4). This was antigen-dependent cytotoxic activity as ALK CAR T cells did not lyse the ALK-negative cell line (SUP-T1 WT), while UT T cells showed minimal cytotoxic activity against SUP-T1 ALK cells.

The production of IL-2 and IFNγ is imperative for the persistence and proliferation of CAR T cells *in vivo*. Furthermore, the production of IFNγ is associated with T cell activation, and therefore can be used as a measure of ALK CAR activation upon antigen engagement (van der Stegen et al., 2015). Importantly, antigen

independent activation of CAR T cells, resulting in the production of cytokines, is an indicator of CAR T cell tonic signalling. IL-2 and IFNγ production from ALK CAR T cells was observed, however to differing extents (Figure 3.5). Variable background levels of IL-2 were produced from all ALK CAR T cells cultured alone or when co-cultured with the ALK negative cell line, SUP-T1 WT (Figure 3.5A and Figure 3.5B). Furthermore, this was also seen for the resting UT control T cells, and was not replicated for IFNγ. Post transduction, before T cells are utilised in assays, they are expanded in the presence of IL-2. Despite T cell washing prior to experimental set up, this background production could be attributed to carry over contamination. Therefore, it is difficult to conclude that increased IL-2 production by ALK4-Fc-28ζ, ALK8-Fc-28ζ and ALK9-Fc-28ζ on co-culture with SUP-T1 ALK is truly significant (Figure 3.5A). Only ALK8-CD8-28ζ demonstrated much more production of IL-2 on co-culture with SUP-T1 ALK but the increase compared with UT control T cells did not reach significance (Figure 3.5B).

In the experiments shown, ALK11-Fc-28ζ, ALK10-Fc-28ζ, ALK4-CD8-28ζ and ALK11-CD8-28ζ co-cultured with SUP-T1 ALK cell lines secreted the same level of IL-2 as UT T cells in the same condition. All ALK CAR T cells secreted high levels of IFNγ on co-culture with SUP-T1 ALK cell lines, which wasn't observed when co-cultured with SUP-T1 WT cells or when cultured alone. This suggests that CAR T cell IFNγ production, and therefore activation, was ALK dependent. Based on the observation that ALK4-CD8-28ζ, ALK11-Fc-28ζ and ALK10-Fc-28ζ CAR T cells did not produce IL-2 above background level, they were excluded from further analysis.

Following this, the cytotoxic activity of ALK CAR T cells against neuroblastoma cell lines was investigated. It was important to determine the threshold of ALK

surface expression on target cells which is required for substantial levels of cell killing and cytokine release from ALK CAR T cells. Compared to the SUP-T1 ALK cell line used previously, neuroblastoma cell lines represent a more meaningful target as they present with more physiologically relevant levels of surface ALK. The level of target cell lysis appeared to correlate with the level of ALK target density, with the lowest levels of cell killing seen in the lowest ALK expressing cell line; Lan-1, and the highest levels of cell killing seen in the highest ALK expressing cell line; Lan-5 (Figure 3.6). ALK CARs containing the anti-ALK scFv 8 with both the Fc and the CD8 stalk region appeared to induce the highest level of ^{51}Cr release from Lan-1 and Kelly cell lines, indicated by the highest levels of significant differences between UT T cells at the 10:1 E:T ratio. Despite decreased levels of target cell killing at lower ALK antigen density, which in part is expected, investigating ALK CAR T cell function with lower ALK surface expression allowed for greater discrimination between individual ALK CAR T cells. As with a decreased level of cell killing, ALK CAR T cells co-cultured with Lan-1, Kelly or Lan-5 cell lines also had much lower, if any at all, levels of cytokine production (Figure 3.8). This highlights the importance of target antigen density on target cells; Wantanabe *et al*., demonstrated the level of CD20 expression on target cells required for cytokine production was 10 fold higher than that required for cytotoxic activity with a CD20 specific CAR T cell (Watanabe et al., 2015, Stone et al., 2012).

ALK target antigen density on neuroblastoma cell lines appears to be a limiting factor in the production of appreciable responses from ALK directed CAR T cells, for example, in the case of the Lan-1 cell line. This response is also likely to be dependent on multiple other factors, including surface CAR expression, scFv

affinity, spatial constraints; and tumour cell expression of adhesion and co-stimulatory ligands that provide signals distinct from the CAR (Srivastava and Riddell, 2015). There are, of course, methods to engineer CAR T cells to become more potent when low target antigen density is a concern. However, this could lead to increased toxicity due to the recognition of lower levels of the target antigen, which may be present on healthy tissue. TCRs have exquisite sensitivity to low antigen density. It is postulated that TCR sensitivity is mediated through a 'serial triggering' model, in which multiple TCRs detect the peptide-MHC complex through low affinity and short dissociation rates: 'K_{off}'. CARs which have higher affinity for their cognate peptide have been shown in some studies to actually reduce the cytolytic activity and sensitivity to low peptide concentrations relative to an αβTCR specific for the same epitope (Oren et al., 2014). There is, therefore, a fine balance that is required between target antigen density and the potency of a CAR T cell. For example, a lower efficacy CAR T cell may be better against a higher expressing target which is expressed at low levels on healthy tissue (Richards et al., 2018). Taking this together, it is possible that, given the low target density of ALK, use of a CAR against ALK as a single therapeutic agent may be inadequate. However, it may be possible to combine the specificity of ALK as a target, into a dual targeting therapy, and in this way providing a boost to an ALK targeting therapy. Furthermore, this differential response of CAR T cells to low and high antigen density may allow for the exploitation of a therapeutic window in which a low level of tumour antigen expression on normal tissue can be tolerated when targeting a tumour with high expression of the antigen (Walker et al., 2017).

As important as it is for CAR T cells to proliferate for an efficacious therapy, it is equally important that CAR T cells do not proliferate on recognition of unspecific antigens, or independent of any antigen recognition; a process known as tonic signalling. Moreover, T cells have limited replicative lifetimes, and therefore it is important that CAR T cells have as many antigen specific proliferations as possible. It is, however, a fine balance as T cell anergy, T cell exhaustion and activation-induced cell death (AICD) are triggered by excessive activation of the TCR during chronic infection or tumour progression (Kasakovski et al., 2018). Initially, short term proliferation was investigated utilising a cell trace dye after 4 and 8 days (Figure 3.10 and Figure 3.11). There was evidence of proliferation by all ALK CAR T cells; however there appears to be clear differences between ALK CAR T cells expressing an Fc spacer and those expressing a CD8 stalk. ALK CAR T cells expressing CD8 stalks show antigen specific proliferation, notably when co-cultured with Lan-5 and SUP-T1 ALK: higher ALK expressing cell lines. Importantly, these CD8 expressing ALK CARs do not show proliferation when cultured alone, or in the presence of an antigen negative cell line, SUP-T1 WT. Conversely, while Fc expressing CAR T cells also show proliferation when co-cultured with Lan-5 and SUP-T1 ALK cell lines, they also appear to proliferate in the presence of SUP-T1 WT and when cultured alone. Interestingly, the anti-ALK scFvs 8 and 9 were investigated with both the Fc and the CD8 stalks allowing a direct comparison, and clearly display the antigen dependent (CD8 stalk) and antigen independent (Fc spacer) proliferation patterns (Figure 3.7).

On investigation, there are multiple studies that demonstrate the role of an IgG derived spacer region in tonic signalling (Watanabe et al., 2016, Jonnalagadda et al., 2015, Hombach et al., 2007, Hombach et al., 2010, Gacerez et al., 2016,

Guest et al., 2005, Hombach et al., 2000). In a panel of CD19 CAR T cells, the incorporation of the IgG1-CH2CH3 spacer showed severe CD19-independent toxicity. It was shown to bind soluble mouse Fcγ-receptor (FcγR) I and mediated off-target T cell activation towards murine macrophages (Almasbak et al., 2015). Furthermore Hudecek *et al*., demonstrated the use of IgG4-CH2CH3 spacer in CD19 CARs conferred a lack of anti-tumour activity *in vivo* due to interaction between the Fc domain within the spacer and the Fc receptor-bearing myeloid cells, inducing AICD. They demonstrated *in vivo* persistence and anti-tumour activity could be restored by modifying distinct regions in the CH2 domain that are essential for Fc receptor binding (Hudecek et al., 2015). The binding of IgG derived spacer regions can therefore pose risks with activation of CAR T cells in areas where Fcγ receptors are more highly expressed. There are three different sub classes of Fcγ receptors: FcγRI (CD64), FcγRII (CD32) and FcγRIII (CD16), which are expressed by different immune cells and display different IgG binding affinities. CD64 and CD32 are mainly expressed by monocytes, macrophages, DCs and neutrophils whereas CD16 is expressed by NK cells (Watanabe et al., 2016). It would be interesting to consider what the Fc expressing ALK CAR T cells may be recognising and binding to within these experiments. After initial PBMC isolations, NK cells are depleted within the population. Furthermore, the expansion protocol is specific for αβ T cells, suggesting that other cell populations such as macrophages would not survive. NK T cells are a unique subset of T cells which express functional characteristics and surface markers of both conventional T cells and NK cells (Wu and Van Kaer, 2011). Interestingly they express CD16, as per NK cells; suggesting a potential interaction with ALK CAR T cells expressing the Fc spacer (Krijgsman et al., 2018). Furthermore, some

gammadelta (γδ) T cells express CD16 (Bodman-Smith et al., 2000). Activation and expansion of γδ T cells also utilises anti-CD3, in the same way αβ T cells are treated. This could offer another explanation as to a potential interaction between Fc spacers and receptors.

Hombach *et al*., modified their IgG1 Fc spacer region within the CAR and found it successfully avoided 'off-target' activation (Hombach et al., 2010). The Fc spacer used within our construct also contains these mutations to modify 'off-target' effects. When this Fc spacer was present with our CAR T cells, the mutations were not sufficient to remove antigen independent tonic signalling. Aside from causing AICD in CAR T cells, the cross-activation of FcγR+ immune cells may activate the innate immune system contributing to macrophage activation syndrome (MAS) and/or cytokine release syndrome (CRS) (Ajina and Maher, 2018). Furthermore, unconstrained activation of CAR T cells caused by chronic signalling has been shown to hinder the trafficking of CARs to the TME (Almåsbak et al., 2016). While we see this unspecific proliferation from Fc spacer containing ALK CAR T cells, it doesn't seem that there is unspecific cytokine production or killing of cell lines that don't express ALK. This suggests that the proliferation seen is due to the presence of the Fc spacer, rather than the scFv recognising unspecific antigens. It would be interesting to investigate the cytotoxicity of the ALK-Fc CAR T cells against an ALK negative cell line that expresses an Fcγ receptor. It has also been identified that AICD can be induced by the Fc spacer binding to innate immune cells, leading to decreased CAR T persistence in preclinical models (Hudecek et al., 2015, Hombach et al., 2010, Künkele et al., 2015).

The length of a spacer region can be critical in the functionality of a CAR as it can influence the formation of an efficient immunological synapse between target and effector cell. This also depends on the binding epitope to which the anti-ALK scFvs bind to. One study investigated the impact of epitope binding on immunoreceptor-triggered T cell activation. They concluded that the efficiency of T cell activation was determined by the position of the targeted epitope more than the binding efficiency of the scFv domain (Hombach et al., 2007). Given that different anti-ALK scFvs demonstrate different levels of cytoxicity and cytokine production at lower ALK target antigen densities, it would be interesting to map their binding epitopes on ALK. Furthermore, this may further influence the choice of spacer region used within the CAR construct. The structural and spatial elements of TCR recognition have evolved for precise regulation of the interaction between a T cell and its target cell, which can be difficult to recapitulate with synthetic receptors (Srivastava and Riddell, 2015). The distance between a CAR and their target antigen is important for effective initiation of T cell signalling, which depends on structural elements such as the location of the binding epitope and the spacer used between the scFv and the T cell membrane (Srivastava and Riddell, 2015). This was demonstrated through targeting a membrane-distal epitope on the receptor tyrosine kinase ROR1, which is expressed on many solid tumours, a CAR with a shortened extracellular spacer conferred superior recognition of ROR1+ tumour cells and induction of T cell effector functions compared to the same scFv with a longer spacer (Hudecek et al., 2013). It was thought that the use of a shorter spacer decreased the distance between the T cell and target cell, which maintained the exclusion of larger inhibitory molecules from the synapse (Hudecek et al., 2013). Therefore, the factors that determine

optimal synapse formation and CAR T cell triggering are complex and are determined by multiple factors such as location of epitope binding, size and flexibility of the spacer region and on and off rates of the binder.

Given that ALK CAR T cells demonstrated antigen driven short term proliferation after 8 days in co-culture, a pilot experiment was designed to investigate long term proliferation with repeated antigen stimulation. This initial experiment showed that ALK CAR T cell numbers dramatically reduce once T cells have been plated, which is not rescued with multiple antigen restimulations. This might suggest that the strength of the CAR signal is sufficient for a short term proliferation, but under long term conditions the production of IL-2 is not sufficient for longer term CAR survival. Given the high level of IL-2 production against the SUP-T1 ALK cell line, it would be interesting to do a repeat stimulation with this high ALK density cell line. Furthermore, to investigate the cytokine producing ability of the CARs after co-culture which is longer than 24 hours.

3.5 Conclusions and future directions

It appears that at high target antigen densities, all nine ALK CAR constructs displayed the ability to lyse ALK expressing cell lines and, to a varied extent, produce IL-2 and IFNγ. When co-cultured with neuroblastoma cell lines, with much lower target ALK density, CAR T cells had more limited cytotoxic activity and minimal cytokine production. Some anti-ALK scFvs showed high specificity, but low function in assays, suggesting ALK is still a good target for this therapy, but rather the ALK CAR itself requires enhancement. The anti-ALK scFv 8 combined with either a CD8 stalk or an Fc spacer conferred the highest level of cytotoxic activity at the lowest antigen levels, namely when co-cultured with Lan-1. ALK8-CD8-28ζ was therefore taken forward for investigation with a previously published anti-ALK CAR in Chapter 5.

CAR T cells expressing the Fc spacer region demonstrated unspecific proliferation when cultured alone, or with ALK negative cell lines, indicative of tonic signalling. Equally, ALK CAR T cells containing the same anti-ALK scFv but a CD8 stalk region, displayed no tonic effects as demonstrated by proliferation against the SUP-T1 WT cell line, but did show antigen dependent proliferation with ALK expressing cell lines. Based on this, the phenotype of CD8 stalk and Fc spacer expressing CAR T cells was investigated in the next research chapter.

4 Phenotyping of ALK CAR T cells

4.1 Introduction

Amongst other important factors; such as the efficient transduction of T cells that expand *ex vivo* with homing, persistence and cytotoxicity *in vivo* following infusion to a patient, the phenotype of a CAR T cell product is also an important consideration (Petersen et al., 2018). The question of which T cell subset should be used for ACT has remained a point of contention and controversy for many years now, in order to have optimal persistence and function. While both CD8+ cytotoxic T cells and CD4+ T helper cells play important roles in anti-tumour immunity, CD8+ T cells have received greater attention in the field of immunotherapy (Kuznetsova et al., 2019). Furthermore, activated and expanded T cells are classically used for CAR T cell studies since primary activation is a requirement for viral transduction, however these highly activated cells may be become terminally differentiated, displaying impaired proliferation and survival *in vivo*, and mediating short-term anti-tumour effects (Perret and Ronchese, 2008). Utilising less antigen-experienced T cell subtypes; such as naïve (T_N), stem cell memory (T_{SCM}) or central memory (T_{CM}) cells, for example, may be more beneficial (Klebanoff et al., 2012).

In the previous chapter I have described enhanced T cell proliferation in the absence of target antigen when CAR T cells contain an Fc spacer domain; a phenomenon that might be attributable to tonic signalling from the CAR or possibly related to Fc interaction with Fcγ receptors. Previously, published studies have demonstrated that tonic signalling is linked to CAR T cell dysfunction leading to ineffective CAR activity (Long et al., 2015, Frigault et al., 2015).

Therefore, I was interested to perform detailed immunophenotyping of the Fc and CD8 containing CARs to determine if there were differences in exhaustion, activation and differentiation markers.

4.2 Aims

The data presented in the previous chapter demonstrated that ALK CAR T cells expressing an Fc spacer had antigen-independent proliferation. In contrast, ALK CAR T cells with the same anti-ALK scFv but a CD8 stalk region showed restricted proliferation patterns; only proliferating in the presence of ALK antigen. I sought to investigate if the presence of an Fc spacer (ALK-Fc) compared to a CD8 stalk region (ALK-CD8) induced changes to the CAR T cell phenotype. This was explored by asking multiple questions:

(i) What are the differences in the CD4 and CD8 CAR T cell populations?

(ii) Are ALK-Fc CAR T cells more activated and exhausted than ALK-CD8 CAR T cells?

(iii) Do ALK-Fc CAR T cells express a more differentiated phenotype than ALK-CD8 CAR T cells?

In order to do this, the following CAR T cells were investigated in different culture conditions:

1. ALK8-CD8-28ζ
2. ALK8-Fc-28ζ
3. ALK9-CD8-28ζ
4. ALK9-Fc-28ζ

4.3 Results

For the following results, the aforementioned ALK CAR T cells were co-cultured in different conditions, and their phenotype was investigated through flow cytometry investigating a panel of exhaustion, activation and memory markers at day 4 and day 8 of co-culture.

4.3.1 CD4 and CD8 composition of ALK CAR T cells

Figure 4.1 shows a representative gating strategy to identify CD3+αβTCR+ T cells after exclusion of doublets and dead cells. The percentage of CD4+ and CD8+ T cells was determined from αβ T cell populations and CAR T cell populations, as determined by CD34 expression (Figure 4.1).

The percent of CD4 and CD8 cells were determined on day 4 and day 8 of ALK CAR T cell co-cultured with SUP-T1 WT or SUP-T1 ALK cells, or when cultured alone (Figure 4.2). There were broadly similar CD4+ and CD8+ populations between ALK8 αβ+ T cells and ALK8 αβ+CD34+ T cells, within each individual culture condition (Figure 4.2A and Figure 4.2B). By day 8 of co-culture alone, or with SUP-T1 WT, there was slightly higher levels of CD4+ T cells compared to CD8+ T cells within the ALK8-Fc-28ζ and ALK8-CD8-28ζ populations. This was seen in both ALK8 αβ+ T cell and ALK8 αβ+CD34+ T cell populations (Figure 4.2A and Figure 4.2B). In contrast, when ALK8-Fc-28ζ and ALK8-CD8-28ζ were co-cultured with SUP-T1 ALK cells, there was an increase in the proportion of CD8+ T cell populations with a concomitant decrease in CD4+ T cell populations by day 8 of co-culture. Notably, there were no significant differences in the CD4+ and CD8+ populations between ALK8-Fc-28ζ and ALK8-CD8-28ζ within the same culture conditions.

There were broadly similar CD4+ and CD8+ ratios between ALK9 αβ+ T cells and ALK9 αβ+CD34+ T cells, within each individual culture condition (Figure 4.2C and Figure 4.2D). When ALK9-Fc-28ζ was cultured alone, or with SUP-T1 WT, the CD4+ and CD8+ populations changed very little between day 4 and day 8. However, for ALK9-CD8-28ζ in the same culture conditions, there were slightly higher levels of CD4+ populations by day 8 (Figure 4.2C and Figure 4.2D). This trend was also reflected in ALK8-CD8-28ζ in the same culture conditions (Figure 4.2A and Figure 4.2B). Unlike when ALK8 was co-cultured in the presence of target antigen, with SUP-T1-ALK, ALK9-Fc-28ζ and ALK9-CD8-28ζ demonstrated minimal changes in CD4+ and CD8+ populations between time points, and when compared to each other. Again, there was no statistically significant differences between ALK9-Fc and ALK9-CD8 CAR T cell populations.

Taken together these data are consistent with ALK8 containing CARs inducing preferential expansion of CD8+ cells in the presence of antigen, an observation that was not found with the ALK9 containing CARs.

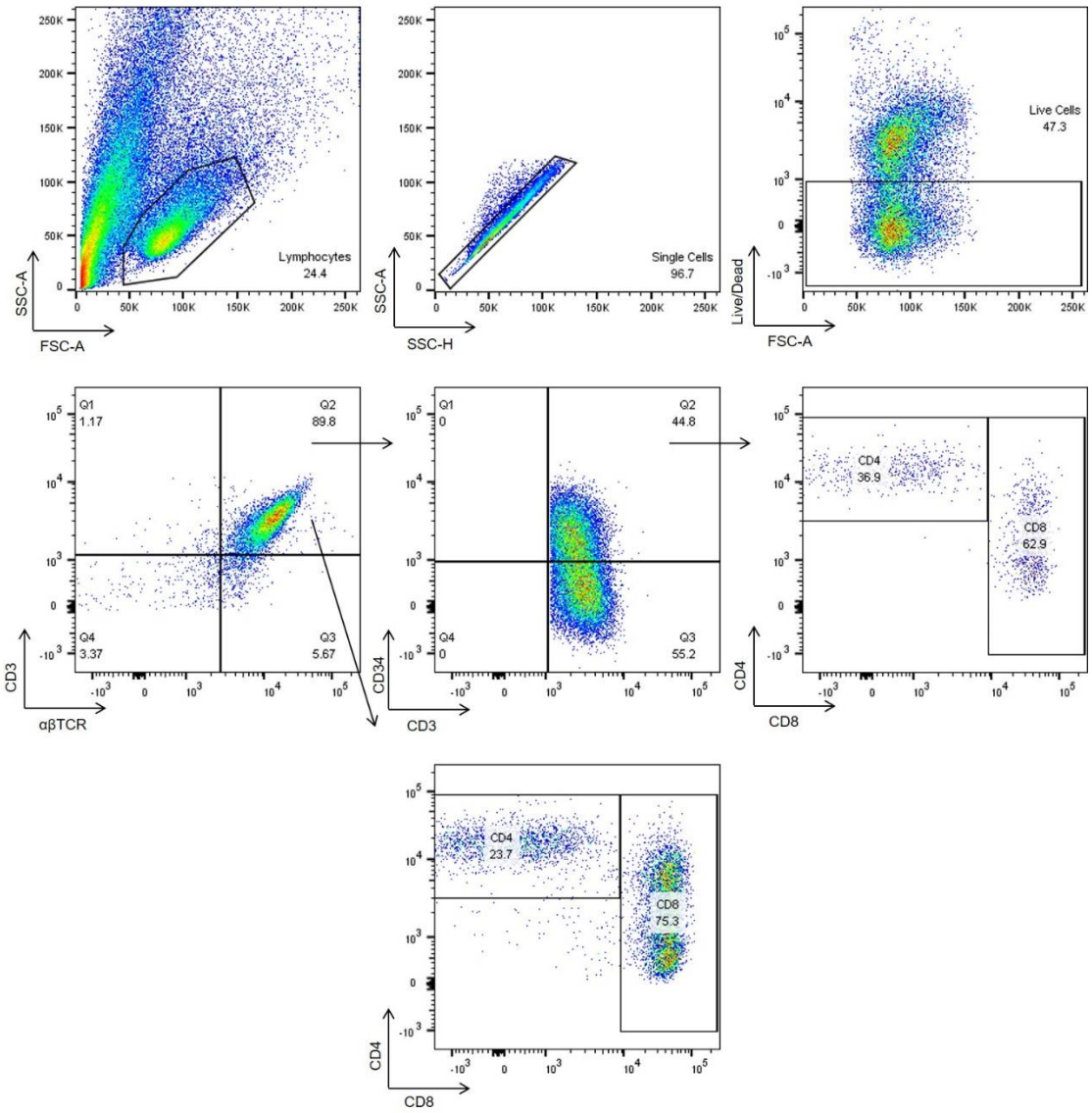

Figure 4.1 Gating strategy to identify CD4+ and CD8+ T cell populations

ALK CAR T cells were co-cultured in different conditions before CD4+ and CD8+ populations were determined at day 4 and day 8. A representative plot identifying the CD3+αβTCR+ T cell population, after the exclusion of dead cells and doublet cell populations. The CD4+ and CD8+ populations were then identified from the CD3+αβTCR+ population, or in the ALK CAR specific CD34+ population.

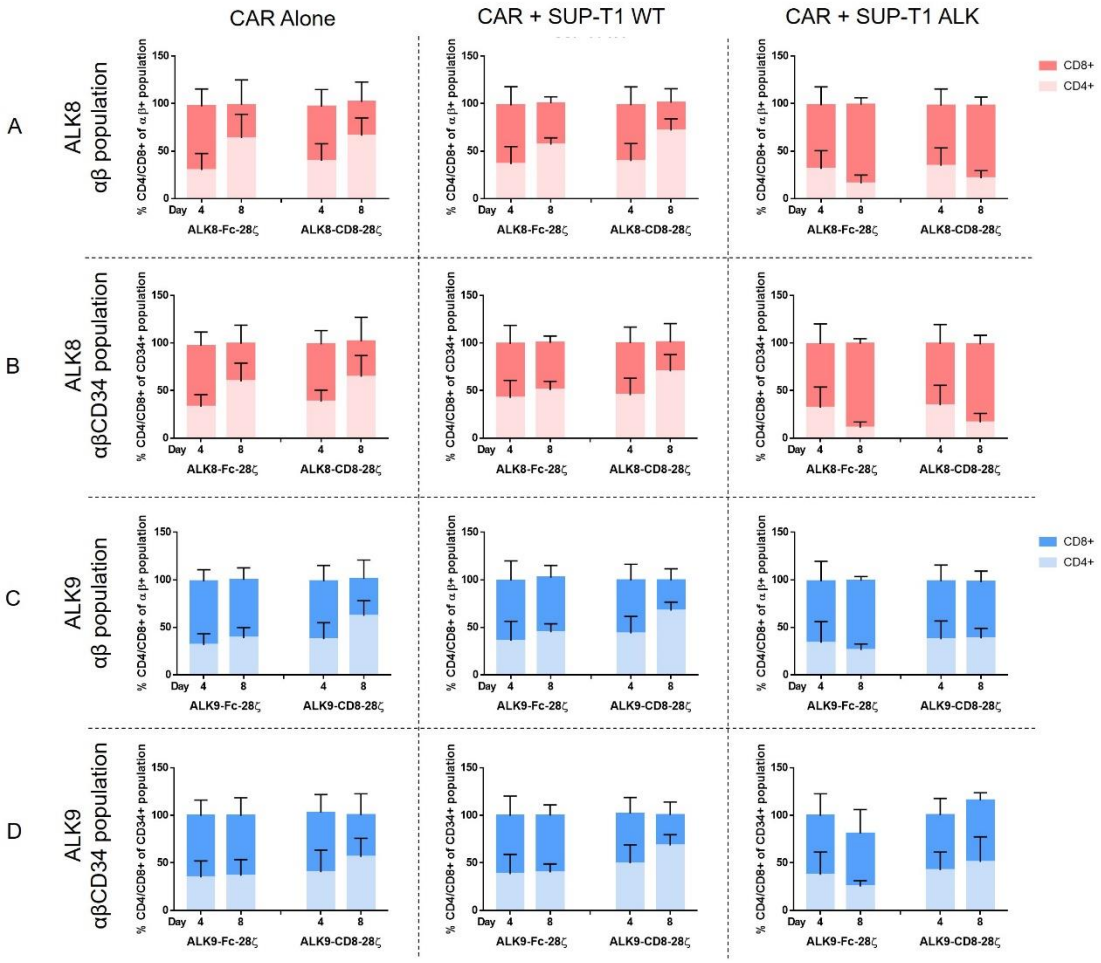

Figure 4.2 CD4 and CD8 populations within αβ+ and CAR+ populations in Fc and CD8 ALK CAR T cells

CD4+ and CD8+ populations were identified in ALK CAR populations co-cultured in different conditions. CD4+ and CD8+ populations in ALK8-Fc-28ζ and ALK8-CD8-28ζ in αβ+ (A) and CD34+ populations (B) cultured alone or with SUP-T1 WT and SUP-T1 ALK cell lines. CD4+ and CD8+ populations in ALK9-Fc-28ζ and ALK9-CD8-28ζ in αβ+ (C) and CD34+ populations (D) cultured alone or with SUP-T1 WT and SUP-T1 ALK cell lines. Data displayed is mean±SD (n=3 independent biological replicates). No statistical differences were found between CD4+ and CD8+ populations when comparing between ALK8-Fc-28ζ and ALK8-CD8-28ζ, and between ALK9-Fc-28ζ and ALK9-CD8-28ζ, determined by two-way ANOVA followed by Tukey's post-hoc analysis.

While there were no significant differences between CD4+ and CD8+ populations between ALK-Fc and ALK-CD8 expressing CAR T cells, the proliferative capacity of these two populations was investigated. In order to do this, the change in mean fluorescence intensity for cell trace violet between untransduced T cells cultured

alone and CAR T cells plus target (ΔMFI) after 8 days of co-culture was calculated (Figure 4.3).

When ALK8-CD8-28ζ was co-cultured with SUP-T1 WT, CD4+ CAR T cells demonstrated a low level of proliferation, while CD8+ CAR T cells showed a decreased in ΔMFI indicative of less proliferation than the untransduced control cells (Figure 4.3A). ALK9-CD8-28ζ CAR T cells also demonstrated this pattern in decreased ΔMFI on co-culture with SUP-T1 WT (Figure 4.3C). Conversely, when ALK8-Fc-28ζ and ALK9-Fc-28ζ were cultured with SUP-T1 WT cells, there appeared to be proliferation from both CD4+ and CD8+ CAR T cells (Figure 4.3B and Figure 4.3D). All ALK CAR T cells demonstrated that on co-culture with SUP-T1 ALK, both CD4+ and CD8+ T cell populations proliferated, however CD4+ CAR T cells had higher levels of proliferation. The proliferation was similar across both ALK8 and ALK9 CAR T cells with SUP-T1 ALK, regardless of the spacer region included. No statistically significant differences were found.

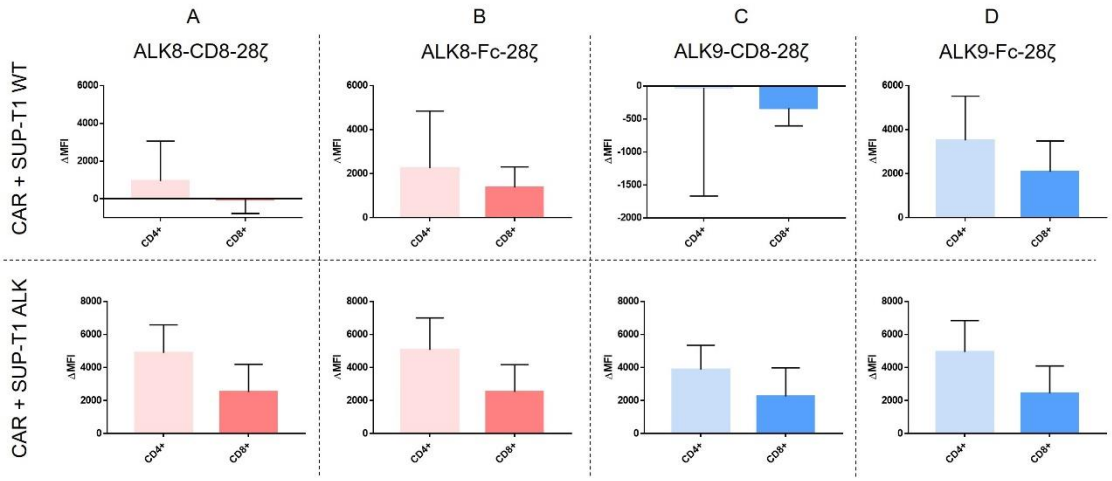

Figure 4.3 ΔMFI at day 8 of CD4+ and CD8+ CAR T cells

The ΔMFI of cell trace violet labelled CD4+ and CD8+ CAR T cells was determined at day 8 of co-culture compared to the untransduced control T cells cultured alone for (A) ALK8-CD8-28ζ, (B) ALK8-Fc-28ζ, (C) ALK9-CD8-28ζ and (D) ALK9-Fc-28ζ when co-cultured with SUP-T1 WT and SUP-T1 ALK. Data displayed is mean±SEM (n=3 independent biological replicates). No statistical differences were found between CD4+ and CD8+ populations determined by two-way ANOVA followed by Tukey's post-hoc analysis.

4.3.2 Activation and exhaustion of ALK CAR T cells

ALK CAR T cells containing an Fc spacer demonstrated antigen-independent proliferation when co-cultured with the ALK negative cell line, SUP-T1 WT. In contrast, ALK CAR T cells with the same anti-ALK scFv but combined with a CD8 stalk did not demonstrate this proliferation pattern. Based on this, it was hypothesised that ALK-Fc CAR T cells would be more activated and exhausted than ALK-CD8 CAR T cells. To investigate this, ALK CAR T cells containing the same anti-ALK scFv with either an Fc spacer or CD8 stalk region were co-cultured with SUP-T1 WT and SUP-T1 ALK cell lines. The expression of activation markers (CD69 and CD25) and exhaustion markers (PD-1, Lag3, CTLA-4 and Tim3) was determined by flow cytometry at day 4 and day 8 of co-culture. For this, CD3+αβTCR+ T cells were identified after the exclusion of dead cells and doublets from lymphocyte populations (Figure 4.4A). Activation markers (Figure 4.4B) and exhaustion markers (Figure 4.4C) were determined from ALK CAR T cell populations, based on CD34 expression, and from CD4+ and CD8+ ALK CAR T cell populations.

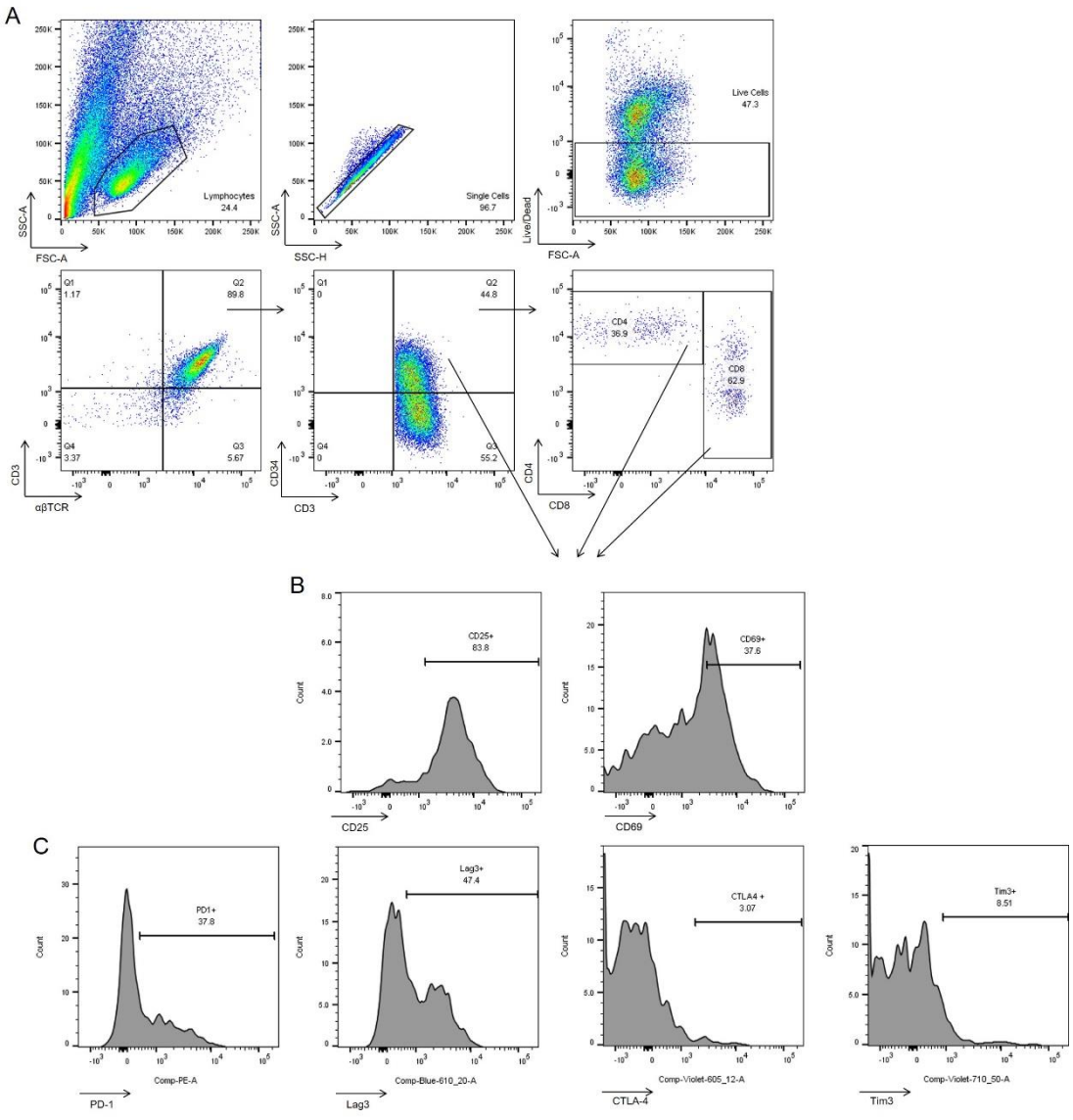

Figure 4.4 Gating strategy to identify activation and exhaustion markers in CAR T cell populations

ALK CAR T cells were co-cultured in different conditions activation and exhaustion markers were determined at day 4 and day 8. (A) Shows a representative plot identifying the CD3+αβTCR+ T cell population, after the exclusion of dead cells and doublet cell populations. ALK CAR T cells were identified through CD34 expression followed by individual CD4+ and CD8+ ALK CAR T cell populations. Within these populations CD25 and CD69 (B) and PD-1, Lag3, CTLA-4 and Tim3 (C) were identified.

Activation and exhaustion after 4 days

Figure 4.5 and Figure 4.6 show representative histograms from one donor for activation and exhaustion marker expression after ALK-Fc and ALK-CD8 CAR T

cells with the same anti-ALK scFvs were co-cultured with SUP-T1 WT and SUP-T1 ALK cell lines for 4 and 8 days, respectively.

We first evaluated differences in activation and exhaustion marker expression between CAR binders with CD8 and Fc spacers respectively, after culture with target cells for 4 days. Representative histograms from one donor are shown in Figure 4.5. When ALK8-CD8-28ζ was co-cultured with SUP-T1 WT, which should not activate the T cell through CAR engagement, there were minimal differences of activation and exhaustion marker expression between the CAR T cells and control UT T cells (Figure 4.5A). The same trends could be seen with ALK8-Fc-28ζ co-cultured with SUP-T1 WT, with the exception of the activation marker CD25, which appeared to be upregulated (Figure 4.5A). This differential activation was not demonstrated by ALK9-CD8-28ζ and ALK9-Fc-28ζ when co-cultured with SUP-T1 WT, indeed both CARs had similar activation and exhaustion marker expression as control UT T cells (Figure 4.5B). When ALK8 and ALK9 were co-cultured with SUP-T1 ALK cell lines, there appeared to be no notable differences in expression patterns in activation and exhaustion markers between Fc spacer and CD8 stalk expressing CAR T cells (Figure 4.5C and Figure 4.5D). In some cases, co-culture with SUP-T1 ALK induced upregulation of marker expression compared with the untransduced control. For example, ALK8-Fc-28ζ and ALK8-CD8-28ζ expressed higher CD25 expression than control UT T cells, however ALK8-Fc-28ζ also had this upregulation on co-culture with SUP-T1 WT (Figure 4.5A and Figure 4.5C). Moreover, both ALK8 and ALK9 with either an Fc spacer or a CD8 stalk, demonstrated upregulation of Lag3 and CTLA-4 when CAR T cells were co-cultured with SUP-T1 ALK compared to co-culture with SUP-T1 WT cells (Figure 4.5).

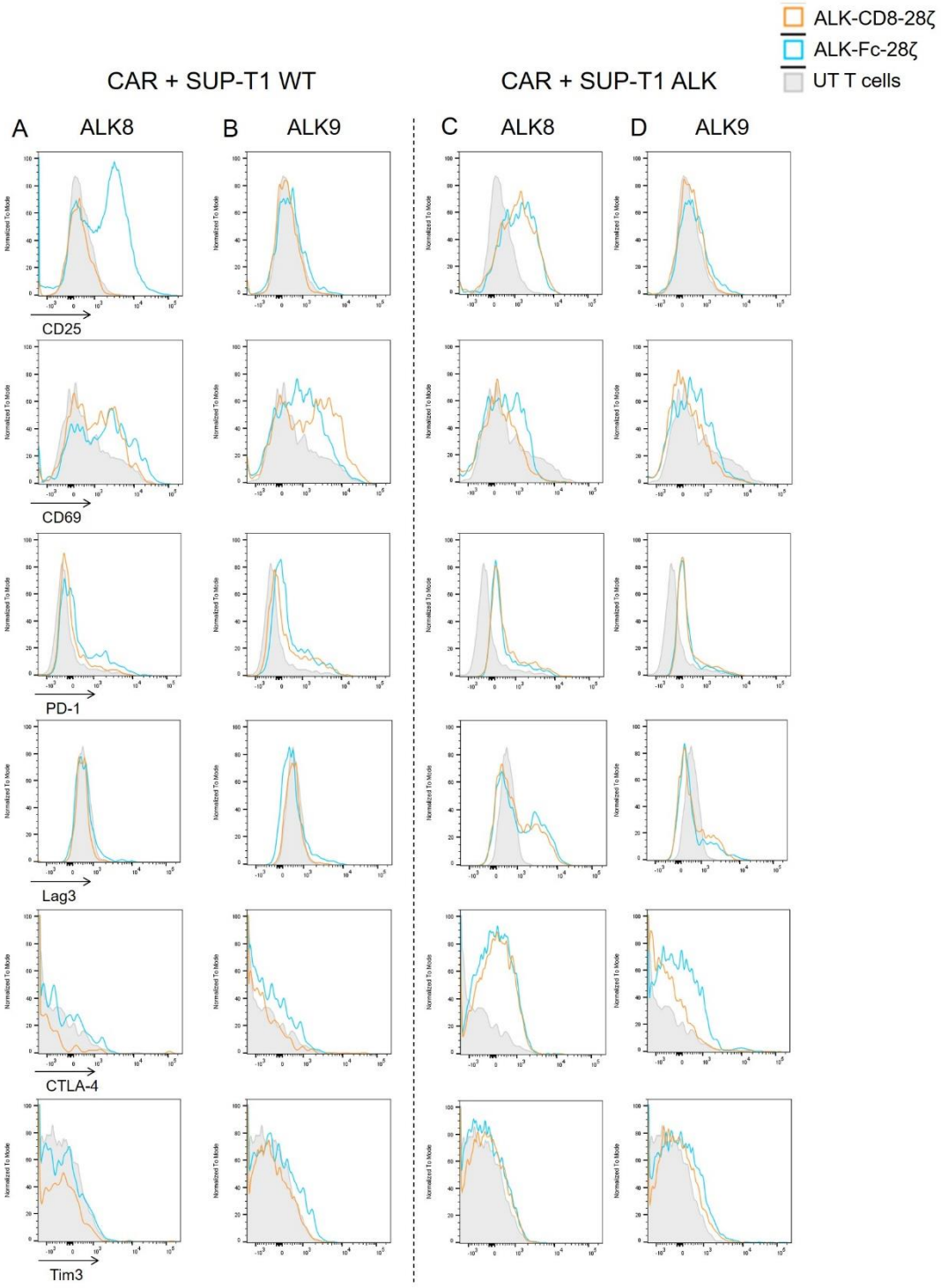

Figure 4.5 Representative histogram readout of activation and exhaustion marker expression after 4 days.

ALK CAR T cells containing either a CD8 stalk or an Fc spacer with matched anti-ALK scFvs were co-cultured with SUP-T1 WT and SUP-T1 ALK cells for 4 days. Expression of activation markers (CD25 and CD69) and exhaustion markers (PD-1, Lag3, CTLA-4 and Tim3) were determined and compared to UT T cells cultured in the same condition.

Activation and exhaustion after 8 days

We next evaluated the same activation and exhaustion marker expression after 8 days of culture with target cells. Representative histograms from one donor are shown in Figure 4.6. ALK8-CD8-28ζ and ALK8-Fc-28ζ co-cultured with SUP-T1 WT had similar expression of CD25, PD-1, Lag3 and Tim3 as UT T cells, also cultured with SUP-T1 WT (Figure 4.6A). Interestingly, CD69 is upregulated with both ALK8 and ALK9 with either stalk regions, both in the presence and absence of antigen. Furthermore, ALK8-Fc-28ζ demonstrated higher CTLA-4 expression than ALK8-CD8-28ζ and control UT T cells, in the absence of target antigen. This trend was also seen with ALK9 CAR T cells co-cultured with SUP-T1 WT for 8 days (Figure 4.6B). When ALK8 and ALK9 CAR T cells were co-cultured with SUP-T1 ALK (Figure 4.6C and Figure 4.6D), the expression patterns of CD25, CD69, PD-1, Lag3 and Tim3 remained unchanged from co-culture with SUP-T1 WT cells. However, the expression of CTLA-4 by ALK8-CD8-28ζ and ALK9-CD8-28ζ was upregulated to match that of their Fc spacer containing counterparts on co-culture with SUP-T1 ALK cells (Figure 4.6C and Figure 4.6D).

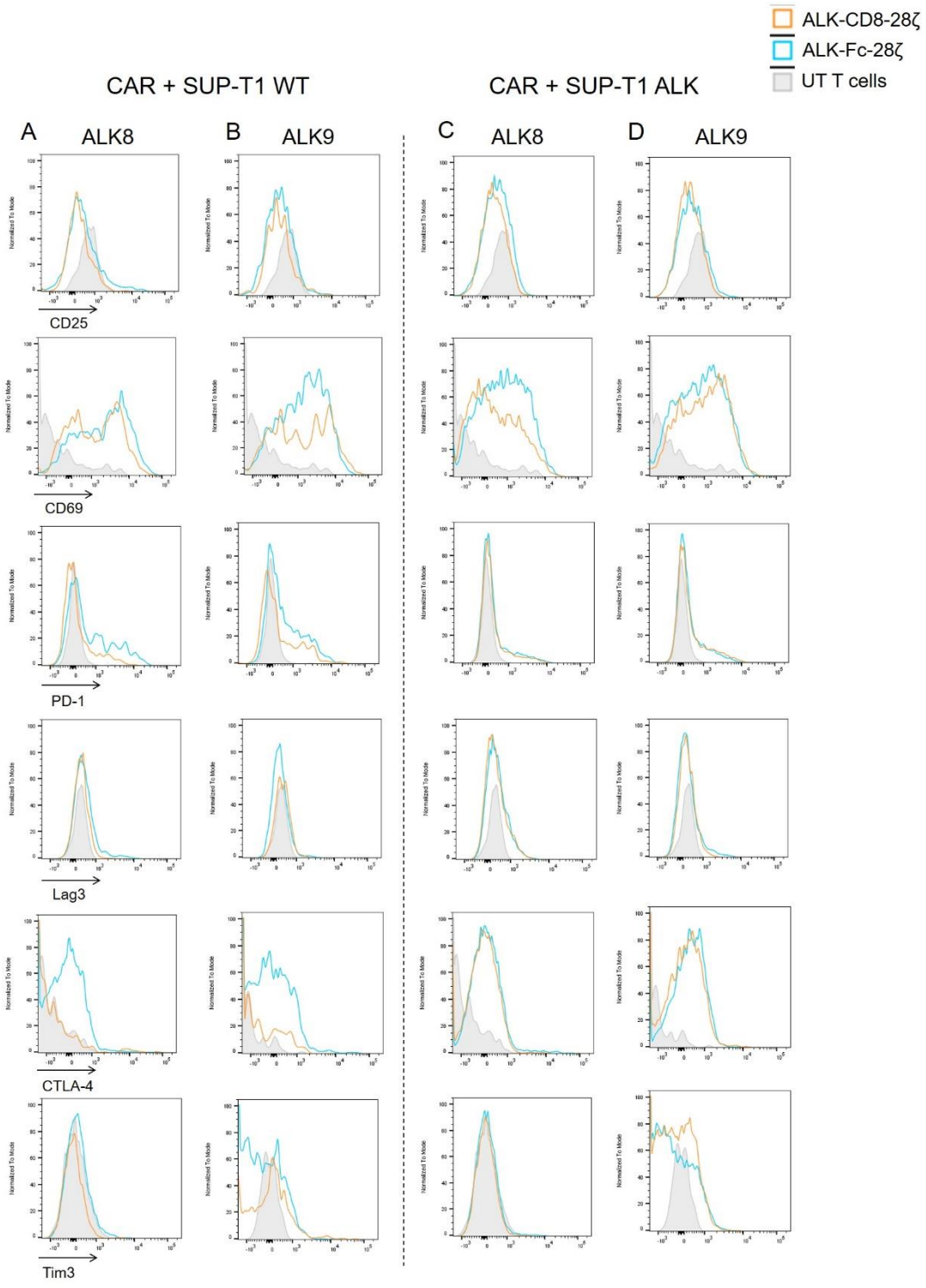

Figure 4.6 Representative histogram readout of activation and exhaustion marker expression after 8 days.

ALK CAR T cells containing either a CD8 stalk or an Fc spacer with matched anti-ALK scFvs were co-cultured with SUP-T1 WT and SUP-T1 ALK cells for 8 days. Expression of activation markers (CD25 and CD69) and exhaustion markers (PD-1, Lag3, CTLA-4 and Tim3) were determined and compared to UT T cells cultured in the same condition.

Change in CD25 expression

In the representative histogram shown in Figure 4.5, ALK8-Fc-28ζ demonstrated marker upregulation of CD25, which was not replicated by the ALK8-CD8-28ζ CAR. To determine if this observation was a generalisable finding, we next plotted the mean activation marker expression averaged over three independent donors.

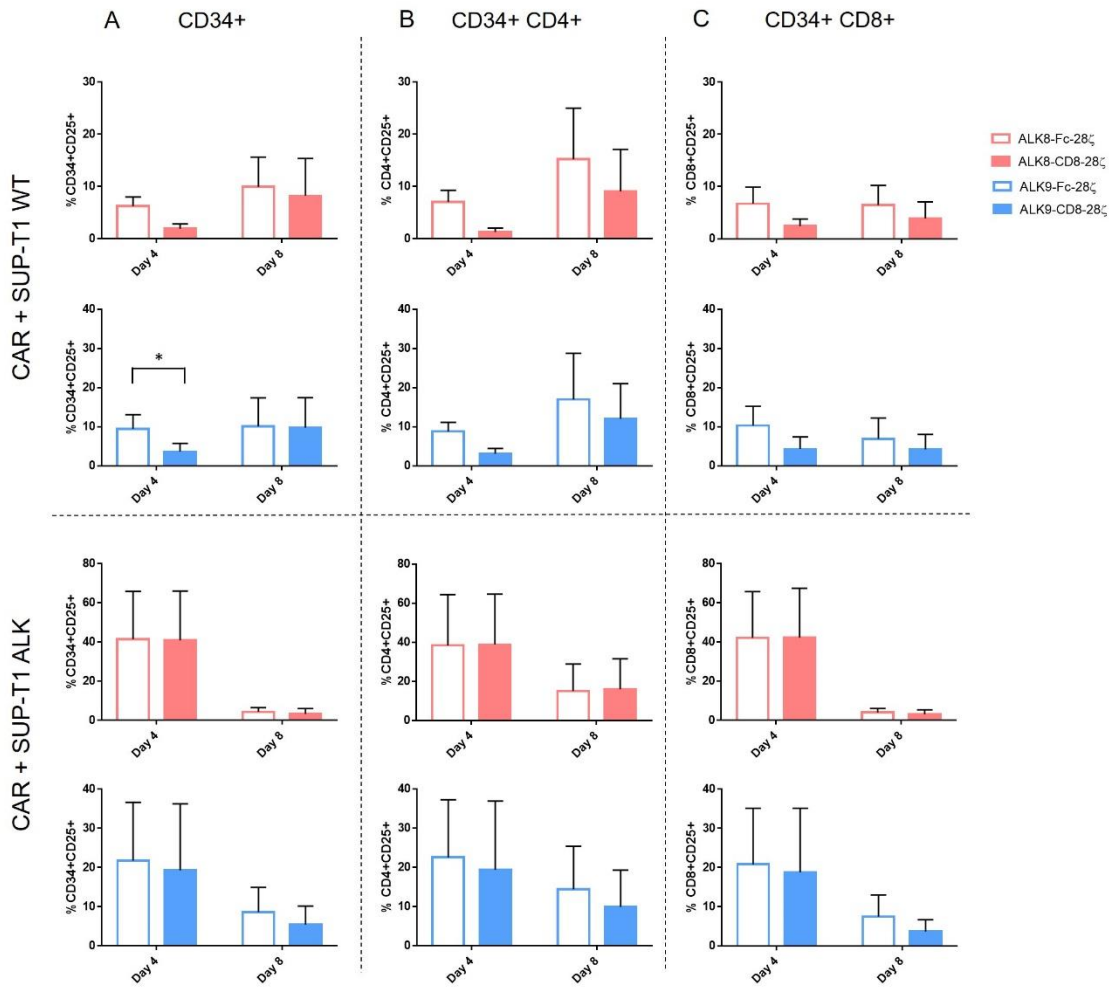

Figure 4.7 shows the percentage of CD25+ cells in ALK CAR T cell populations and individual CD4+ and CD8+ ALK T cell populations when co-cultured with SUP-T1 WT and SUP-T1 ALK cells. As we were particularly interested in differences between Fc spacer and CD8 spacer for each CAR and cell lines condition these have been depicted as open and filled columns on the graphs respectively.

At day 4 of co-culture with SUP-T1 WT cells, ALK8-Fc-28ζ and ALK9-Fc-28ζ demonstrated higher expression of CD25 than ALK8-CD8-28ζ and ALK9-CD8-28ζ, respectively, consistent with antigen-independent activation restricted to the CARs with an Fc spacer (Figure 4.7A). This differential expression was however no longer apparent by day 8 of co-culture. When co-cultured with SUP-T1 ALK cells, both spacers conferred similar activation and no difference between spacers was observed with CD25 expression on ALK-Fc and ALK-CD8 CAR T cells being very similar. The number of cells expressing CD25 was markedly reduced by day 8 of co-culture, compared to day 4 consistent with activation decreasing by 8 days following stimulus.

When looking at the ALK CAR T cell CD4+ populations, the same trend was identified. CARs containing an Fc spacer (ALK8-Fc-28ζ and ALK9-Fc-28ζ) demonstrated higher expression of CD25 than ALK8-CD8-28ζ and ALK9-CD8-28ζ, respectively, on co-culture with SUP-T1 WT cells at day 4, consistent with antigen-independent activation (Figure 4.7B). By day 8 of co-culture, this trend was still present and the number of CD4+ ALK CAR T cells expressing CD25 had increased. In contrast, when co-cultured with SUP-T1 ALK, CD25 expression was similar between ALK-Fc and ALK-CD8 expressing CAR T cells at day 4, which reduced by day 8 of co-culture.

Within the ALK CAR T cell CD8+ populations, the trend was as described above. ALK-Fc CAR T cells demonstrate higher CD25 than ALK-CD8 CAR T cells at day 4 of co-culture with SUP-T1 WT cell line, consistent with CAR T cell activation in the absence of antigen, specifically with the Fc spacer (Figure 4.7C). Unlike with CD4+ populations, there was no notable differences in CD25 expression between day 4 and day 8 in the CD8+ CAR T cell population. When co-cultured with SUP-

T1 ALK, there were no notable differences between ALK-Fc and ALK-CD8 CAR T cell populations. CD25 surface expression was much higher at day 4, which was markedly reduced by day 8.

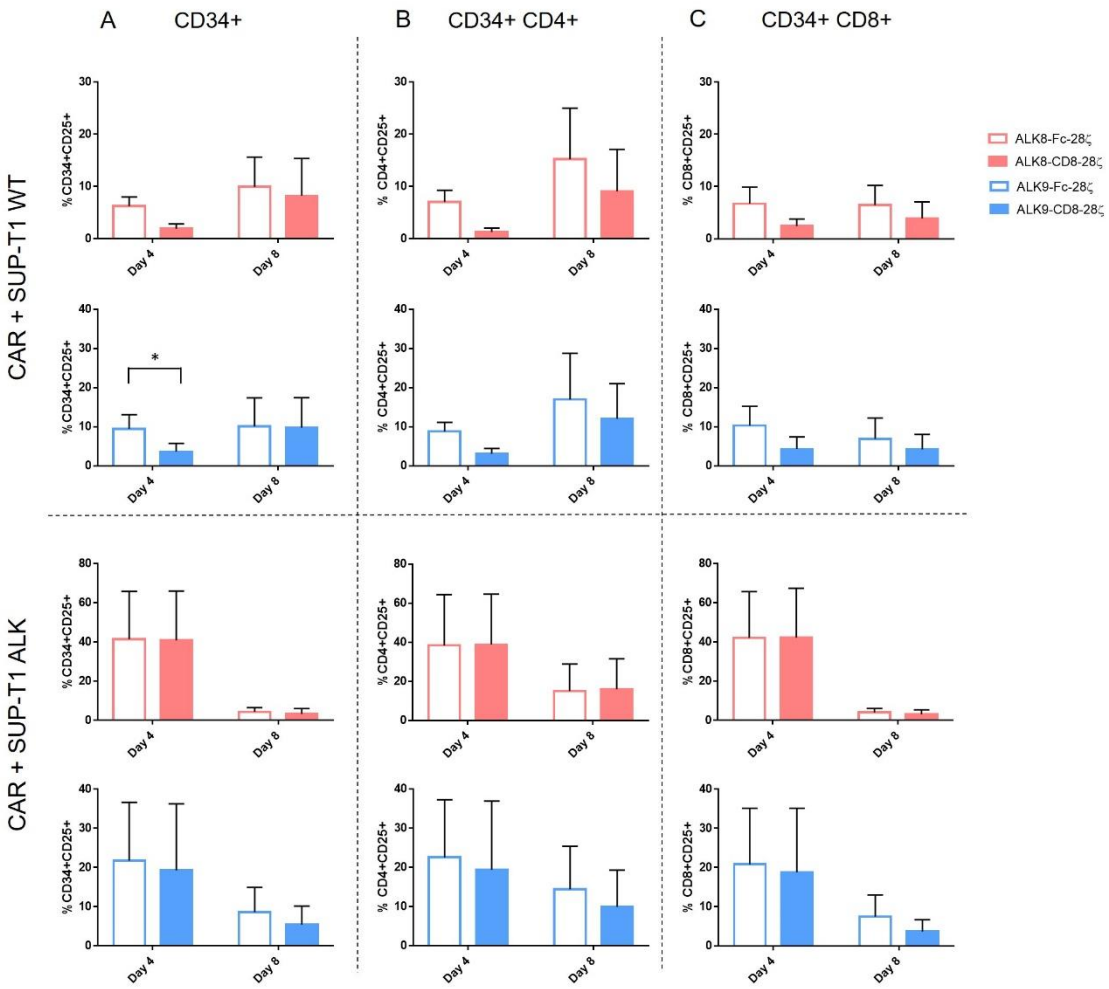

Figure 4.7 Expression of CD25 in CAR populations

Surface CD25 expression was determined by flow cytometry. The percent of cells positive for CD25 were identified in (A) CAR T cell populations as a whole, by CD34+ expression, or in the CD4+ (B) and CD8+ (C) CAR T cell populations. Data is shown as mean expression±SEM (n=3 independent biological replicates). Two-way ANOVA was performed followed by Tukey's post-hoc analysis: * $p<0.05$ (Statistics displayed only for ALK-Fc CAR vs ALK-CD8 CAR within each culture condition).

Change in CD69 expression

To investigate if the antigen-independent upregulation of CD69, which was observed with both ALK8 and ALK9 combined with both stalks at day 4 and day

8 (Figure 4.5 and Figure 4.6), was a generalizable finding over biological replicates, the mean values across 3 independent donors was plotted (Figure 4.8b). This was also compared to the expression of CD69 on control untransduced T cells, at day 4 and day 8, when co-cultured with SUP-T1 WT and SUP-T1 ALK, of the three donors (Figure 4.8a). CD69 was expressed by untransduced T cells, which increased slightly from day 4 to day 8, on co-culture with both SUP-T1 WT and SUP-T1 ALK (Figure 4.8a).

When comparing CD69 expression on CAR T cells cultured with SUP-T1 WT and SUP-T1 ALK, there was no statistical differences between populations with different stalk regions (Figure 4.8b). However, the mean value decreased for both binders and both spacers and at both time points in the presence of the antigen. Hence, CD69 is upregulated post T cell transduction, and is then downregulated in the presence of culturing with the ALK antigen (SUP-T1 ALK).

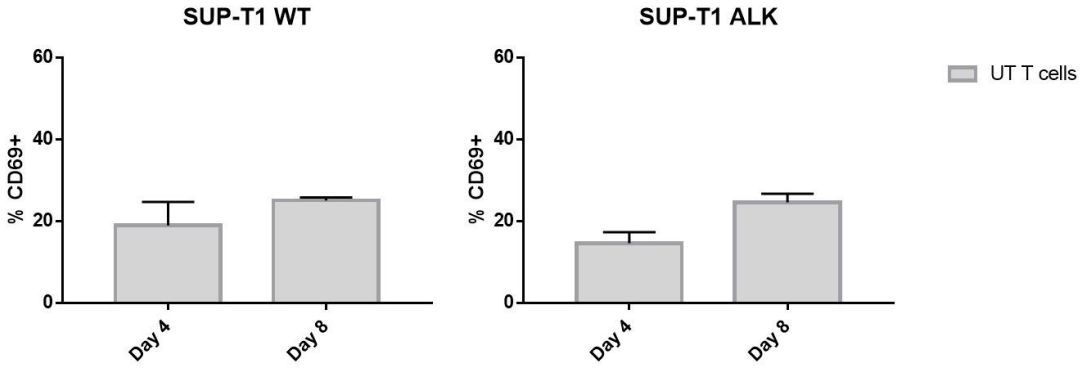

Figure 4.8a Expression of CD69 in untransduced T cell popoulations

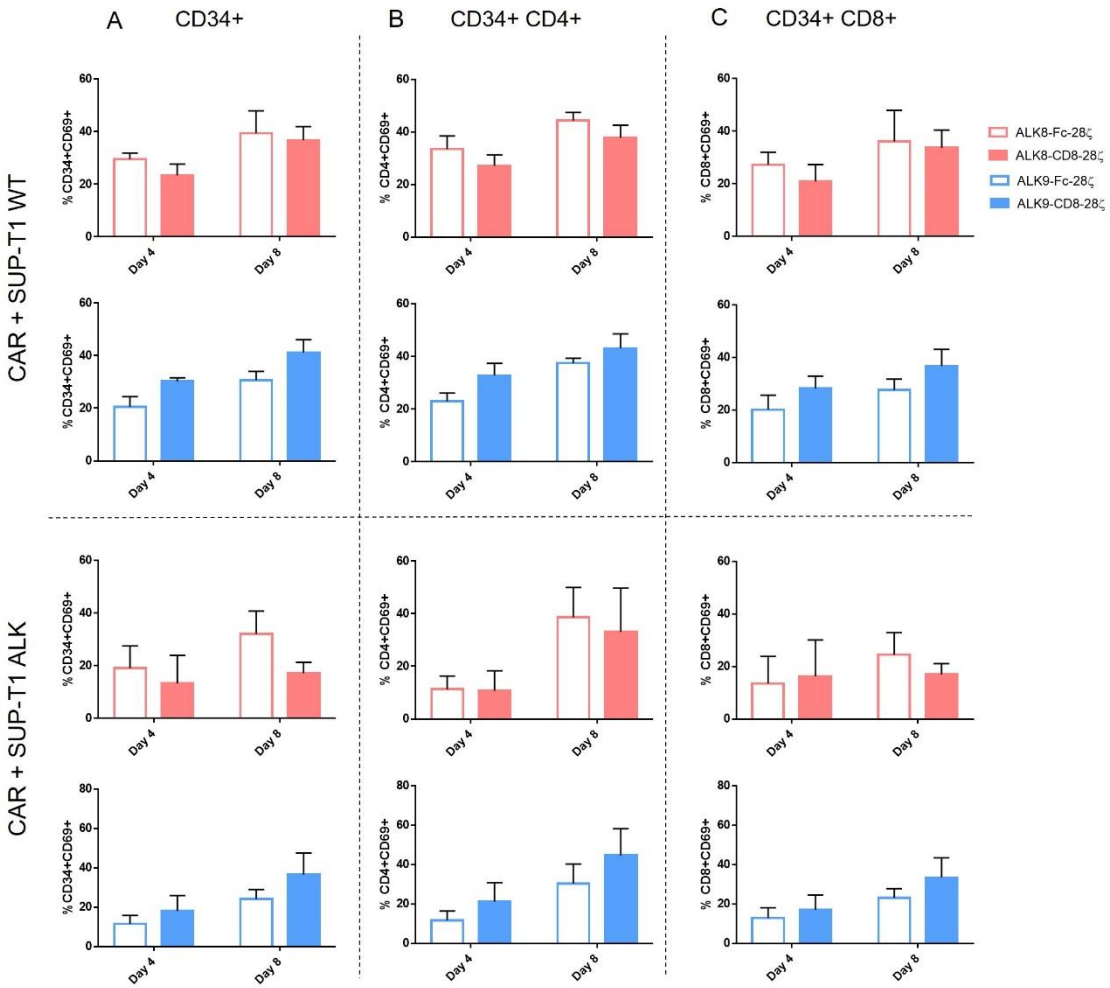

Figure 4.8b Expression of CD69 in CAR T cell populations

Figure 4.8 Expression of CD69 in T cell populations

Surface CD69 expression was determined by flow cytometry in untransduced T cells (a) and within CAR T cell populations (b). Within the CAR T cell populations, CD69 was determined on the population as a whole by CD34+ expression (A), or in the CD4+ (B) and CD8+ (C) populations. No statistical differences were found by two-way ANOVA followed by Tukey's post-hoc analysis comparing ALK-Fc CAR vs ALK-CD8 CAR within each culture condition. Data is shown as mean expression±SEM (n=3 independent biological replicates).

Expression of PD-1 and Tim3 exhaustion markers

Following this, the expression of cell surface markers associated with exhaustion was evaluated in the different CAR T cells through the expression of PD-1 and Tim3 (Figure 4.9). ALK-Fc and ALK-CD8 CAR T cells were co-cultured with SUP-T1 WT and SUP-T1 ALK cell lines for 4 and 8 days. Previously, PD-1 high and Tim3 double positive cells have been linked with a terminal exhaustion phenotype. Therefore, in this case, the most exhausted and dysfunctional T cells were determined as double positive for PD-1 and Tim3, while the least exhausted were double negative.

At day 4 of co-culture with SUP-T1 WT, there were minimal differences between ALK-Fc and ALK-CD8 exhaustion phenotypes with the majority of CAR T cells being PD-1-/Tim3- (Figure 4.9A). There was an indication that ALK8-Fc-28ζ was had higher marker expression than ALK8-CD8-28ζ, however the only statistical difference was that ALK8-CD8-28ζ CAR T cells had a significantly higher proportion of PD-1-/Tim3- cells. By day 8 of co-culture there was still a large proportion of ALK CAR T cells that were double negative for exhaustion markers, with a small increase in PD-1+/Tim3+ cells within the ALK9-Fc-28ζ population (Figure 4.9B).

When CAR T cells were co-cultured with SUP-T1 ALK, ALK8 CAR T cells had higher proportions of PD-1 and Tim3 expression compared to on co-culture with SUP-T1 WT, and compared to ALK9 CAR T cells on co-culture with SUP-T1 ALK although these differences did not reach statistical significance (Figure 4.9C). Interestingly, by day 8 ALK8 CAR T cells demonstrated lower expression of exhaustion markers, when culture in the presence of antigen, with higher levels

of PD-1-/Tim3- CAR T cells, while ALK9 had higher levels of PD-1-/Tim3+ cells, albeit not reaching statistical significance (Figure 4.9D). There were no other statistically significant differences between ALK-CD8 and ALK-Fc expressing CAR T cells.

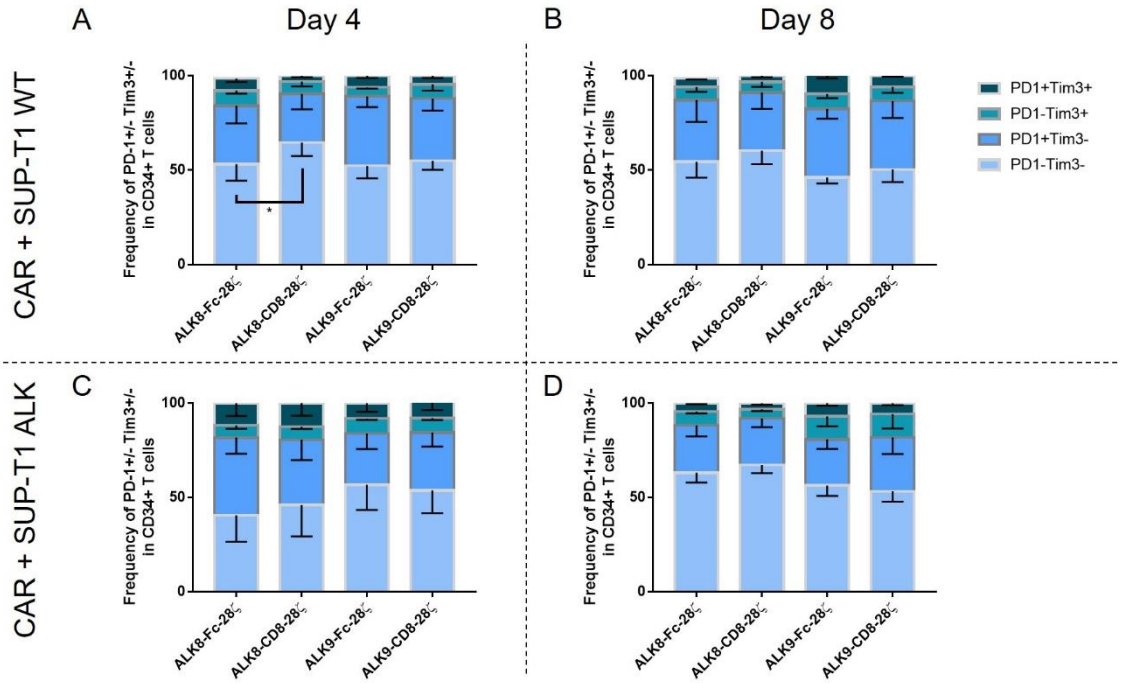

Figure 4.9 PD-1 and Tim3 expression

Surface expression of PD-1 and Tim3 was determined by flow cytometry. The percent of cells positive was determined on ALK CAR T cells cultured with SUP-T1 WT at day 4 (A) and day 8 (B) and SUP-T1 ALK at day 4 (C) and day 8 (D) of co-culture. Data is shown as mean expression±SEM (n=3 independent biological replicates). Statistical differences determined by two-way ANOVA followed by Tukey's post-hoc analysis comparing CD8 stalk and Fc spacer expressing CAR T cells for each phenotype and within each culture condition: * $p<0.05$.

4.3.3 Differentiation of ALK CAR T cells

Next, the differentiation of ALK CAR T cells, comparing ALK-CD8 CAR T cells with ALK-Fc CAR T cells was investigated. Given the unspecific proliferation of ALK-Fc CAR T cells when cultured with the ALK negative cells, it was hypothesised that these Fc spacer containing CAR T cells may be more differentiated when compared to the ALK CAR containing the same scFv, but a CD8 stalk region. This was investigated at day 4 and day 8 of co-culture with SUP-T1 WT and SUP-T1 ALK cells, using flow cytometry. The stage of T cell differentiation was determined by the expression of CD45RO and L-selectin (CD62L) (Figure 4.10). The expression of CD62L and CD45RO was determined in the ALK CAR T cell population, determined by CD34 expression, and in the individual CD4+ and CD8+ ALK CAR T cell populations as depicted in Figure 4.11.

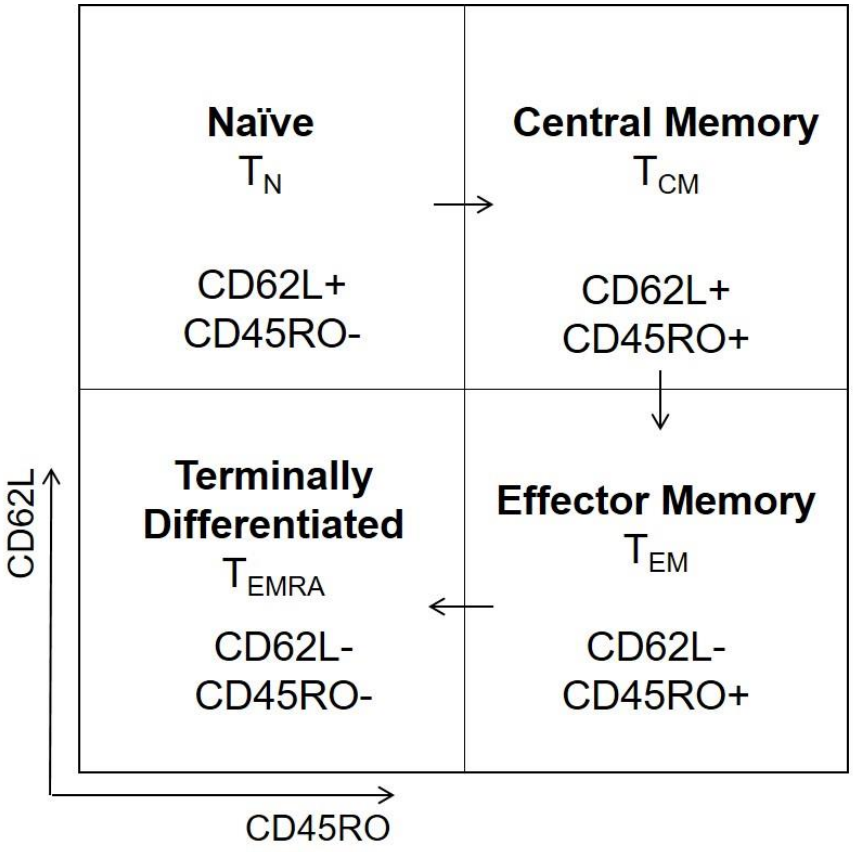

Figure 4.10 T cell differentiation stages

The differentiation stage of T cells was determined by the markers L-selectin (CD62L) and CD45RO. Naïve T cells (T_N) were defined as being CD62L+ and CD45RO-, central memory T cells (T_{CM}) as CD62L+ and CD45RO+, effector memory T cells (T_{EM}) as CD62L- and CD45RO+ and terminally differentiated (T_{EMRA}) as CD62L- and CD45RO-.

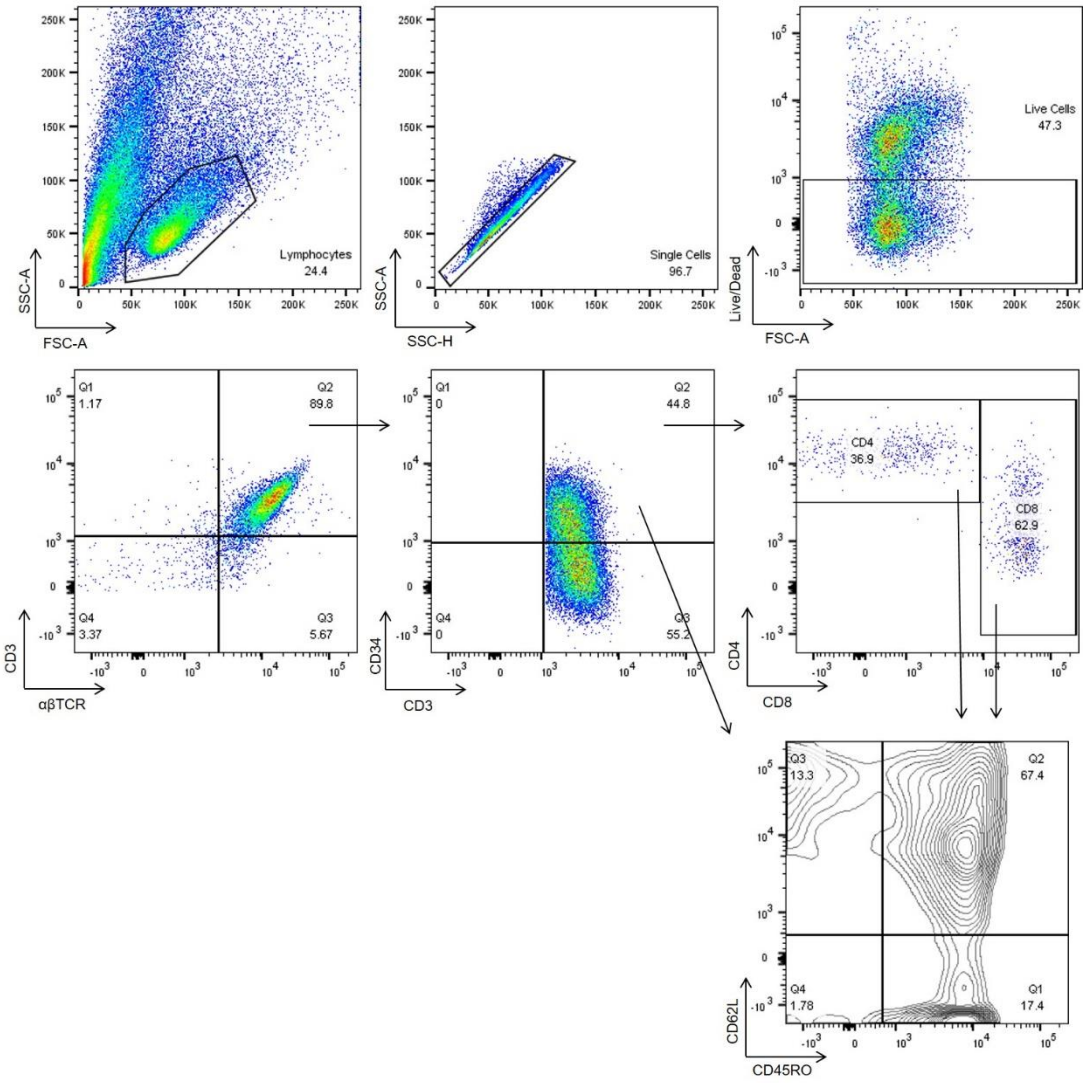

Figure 4.11 Gating Strategy for T cell differentiation

Representative gating strategy identifying CD3+, αβTCR+ T cells from the lymphocyte population after the exclusion of dead cells and doublets. ALK CAR T cells were identified through the surface expression of CD34 and the CD4 and CD8 populations were further identified. The differentiation stage was determined through the expression of L-selectin (CD62L) and CD45RO: T_N (CD62L+CD45RO-), T_{CM} (CD62L+CD45RO+), T_{EM} (CD62L-CD45RO+) and T_{EMRA} (CD62L-CD45RO-).

Figure 4.12 and Figure 4.13 show the differentiation of ALK8 and ALK9 CAR T cells at day 4 and day 8 respectively of co-culture with SUP-T1 WT and SUP-T1 ALK cell lines. The stage of differentiation was determined in the bulk ALK CAR population, determined by CD34+ (A), or within the individual CD4+ (B) and CD8+ (C) ALK CAR T cell populations.

First we looked at the memory phenotype of CARs at day 4 of co-culture. All CAR T cells both in the presence of antigen (SUP-T1 ALK) and without antigen (SUP-T1 WT) express a predominant phenotype of T_{EM}, followed by T_{CM}, along with very low numbers of T_N and T_{EMRA} CAR T cells (Figure 4.12). This is consistent across bulk CAR T cell population determined by CD34 (A), and CD4+ (B) and CD8+ CAR T cells (C). Interestingly, while T_N were low across all CARs, the highest levels of residual naïve T cells were within the CD8 stalk CAR T cell populations without antigen stimulation. This is consistent with the loss of naïve T cells following antigen stimulation (CAR + SUP-T1 ALK), or with the leakiness of the Fc spacer expressing CAR T cells in the presence and absence of antigen. When antigen is added, all CAR T cells expressed lower levels of T_{CM}, with increasing levels of T_{EM} CAR T cells. This is consistent across all CAR T cells with different stalk regions, and within whole CAR, CD4+ CAR and CD8+ CAR populations (Figure 4.12A, B and C), indicative of CARs being activated and differentiating in the presence of the SUP-T1 ALK cell line.

By day 8 of co-culture, interestingly there were more T_N CAR T cells compared to day 4; perhaps representing the emergence of new T_N T cells within the populations. This was found across both ALK8 and ALK9 populations, and within the CD34+ whole CAR, CD4+ CAR and CD8+ CAR populations (Figure 4.13A, B and C). The pattern of T_{CM} and T_{EM} CAR T cells demonstrated the same shift

from central to effector in the presence of antigen. This shift was most noticeable in ALK8 CAR T cells, compared to ALK9 CAR T cells, although not reaching statistical significance.

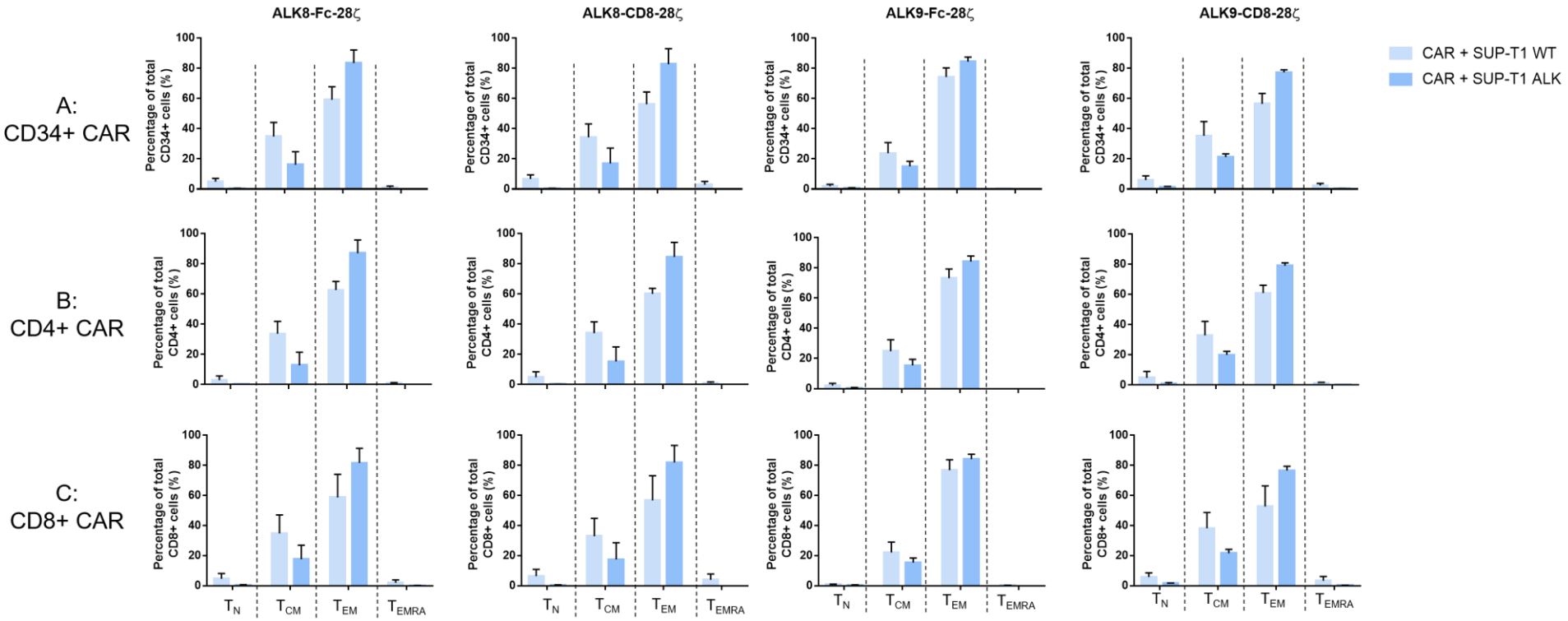

Figure 4.12 Differentiation of ALK CAR T cells after four days of co-culture.

Stratification of ALK CAR T cells co-cultured for four days with SUP-T1 WT (light blue bars) and SUP-T1 ALK (dark blue bars) cells into different differentiation status based on expression of the markers CD45RO and L-selectin (CD62L). The differentiation phenotype was determined in whole ALK CD34+ CAR population (A) and in the CD4+ (B) and CD8+ (C) CAR populations. Fc spacer and CD8 stalk expressing CAR T cells are displayed separately. Graphs show mean±SEM (n=3 independent biological replicates). No statistical differences were found using two-way ANOVA followed by Tukey's post-hoc analysis to compare the differentiation status between Fc spacer and CD8 stalk expressing ALK CAR T cells from the same co-culture conditions.

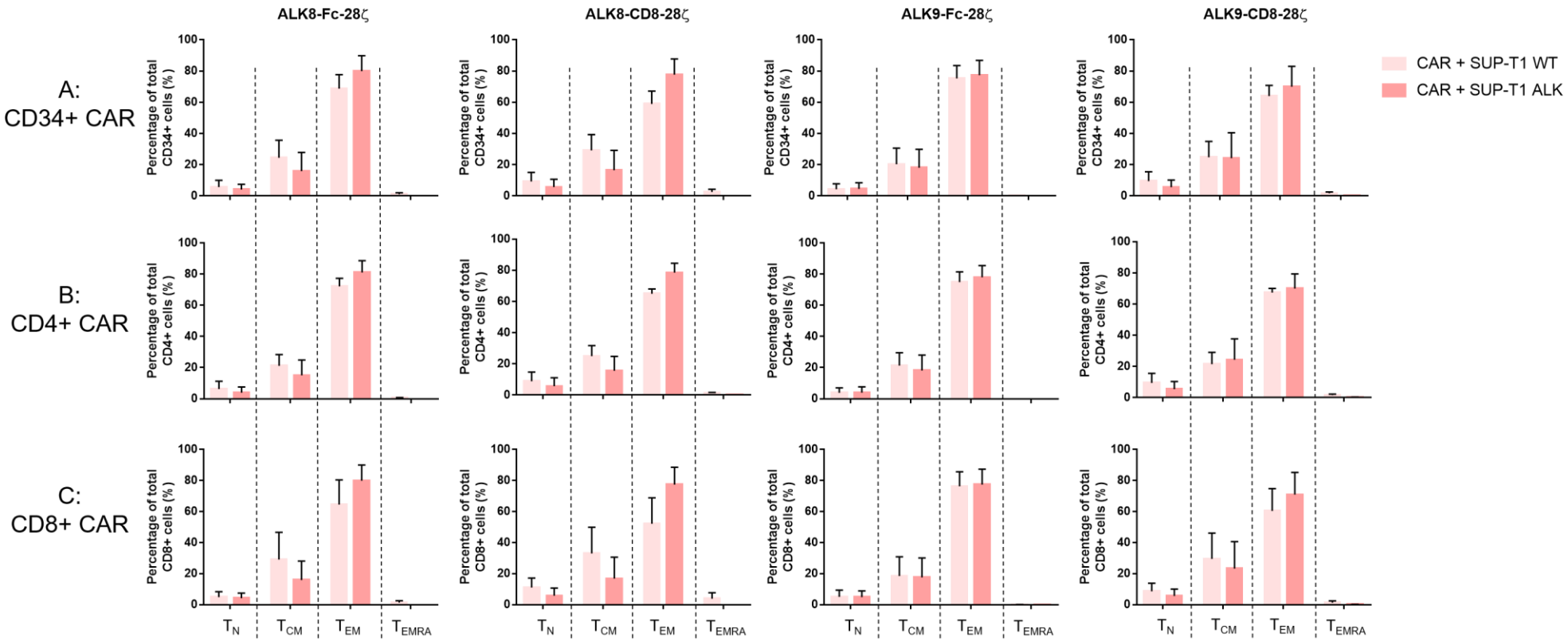

Figure 4.13 Differentiation of ALK CAR T cells after eight days of co-culture.

Stratification of ALK CAR T cells co-cultured for eight days with SUP-T1 WT (light pink bars) and SUP-T1 ALK (dark pink bars) cells into different differentiation status based on expression of the markers CD45RO and L-selectin (CD62L). The differentiation phenotype was determined in whole ALK CD34+ CAR population (A) and in the CD4+ (B) and CD8+ (C) CAR populations. Fc spacer and CD8 stalk expressing CAR T cells are displayed separately. Graphs show mean±SEM (n=3 independent biological replicates). No statistical differences were found using two-way ANOVA followed by Tukey's post-hoc analysis to compare the differentiation status between Fc spacer and CD8 stalk expressing ALK CAR T cells from the same co-culture conditions.

4.4 Discussion

CD4 and CD8 populations

In the first results chapter it was demonstrated that ALK-Fc CAR T cells proliferated in an antigen-independent manner, indicative of tonic signalling, while ALK-CD8 CAR T cells did not. It has been documented in literature that tonic signalling results in functionally exhausted and ineffective CAR T cells (Long et al., 2015). Based on this and the differences in ALK-Fc and ALK-CD8 CAR T cells, the aim of this chapter was to investigate if there were any phenotypic differences between the two CAR populations.

Initially, the proportions of CD4+ and CD8+ T cells were investigated, when CAR T cells were cultured alone or with ALK negative and ALK positive cell lines, namely SUP-T1 WT or SUP-T1 ALK. The CD4+ and CD8+ populations were investigated in αβ+ populations and in αβ+CD34+ (Figure 4.1) populations, to determine if the addition of a CAR construct caused any changes. Broadly, for ALK8 there was an increase in CD4+ populations over the co-culture when ALK8-Fc-28ζ and ALK8-CD8-28ζ were cultured alone or with SUP-T1 WT. When co-cultured with the antigen positive cell line, SUP-T1 ALK, there was enrichment of the CD8+ populations over the co-culture. This CD8+ CAR enrichment in the presence of antigen stimulus is interesting, which has not generally been noted in CAR T cell expansion studies before. There were no statistical differences between the ALK8-Fc and ALK8-CD8 populations, or between total αβ and αβCD34 populations.

In the case of ALK9, both ALK9-Fc-28ζ and ALK9-CD8-28ζ cultured alone or with SUP-T1 WT had the same expression patterns; higher CD8+ populations at day

4 that decreased by day 8 only in the CD8 stalk containing CAR T cells (Figure 4.2C and Figure 4.2D). As with ALK8, ALK9 CAR T cells had higher expansion, or relative survival, of CD4+ CAR T cell populations between day 4 and day 8 in the absence of antigen. However, in contrast to ALK8, when ALK9 was co-cultured with SUP-T1 ALK, there was no enrichment for CD8+ T cells. This was observed in both αβ and αβCD34 populations, and regardless of spacer region used. This may suggest that ALK8 and ALK9 may induce slight differences in CAR T cell activity.

No statistically significant differences were found between any CD8 stalk and Fc spacer CAR populations, suggesting the inclusion of an Fc spacer over a CD8 stalk did not induce any differences between the proportions of CD4 and CD8 populations of CAR T cells.

It has previously been demonstrated that Fc containing CARs proliferate in an antigen independent manner when co-cultured with SUP-T1 WT cells, compared to their matching counterpart containing a CD8 stalk (section 3.3.5). Figure 4.3B and Figure 4.3D demonstrates that both the CD4+ and CD8+ ALK-Fc CAR populations are proliferating in an antigen-independent manner. Interestingly, when examining CARs with Fc spacers, the addition of antigen (SUP-T1 ALK) increased the proliferation only for the CD4+ ALK-Fc CAR populations, while the CD8+ CARs with Fc spacer populations demonstrated similar ΔMFIs in both presence and absence of antigen.

When looking at the CD8 stalk containing CARs, ALK8-CD8-28ζ CD4+ CAR T cells showed low level proliferation on co-culture with SUP-T1 WT cells, which was not observed in the CD8+ population, or the ALK9-CD8-28ζ CD4+ and CD8+

populations (Figure 4.3A and Figure 4.3C). Indeed with ALK9-CD8-28ζ there is a small decrease in ΔMFI, which is more pronounced for the CD4+ subpopulation suggesting that the UT control T cells cultured alone are proliferating more in this instance (an inhibitory effect of the unstimulated CAR). As expected, all ALK CAR T cells proliferated on co-culture with the SUP-T1 ALK cell line, however in all cases CD4+ CAR populations demonstrated higher ΔMFIs.

While differences in CD4 and CD8 populations have been investigated here, it is well documented that immune elimination of tumour cells requires the close cooperation of both CD8+ cytotoxic and CD4+ T helper cells (Hombach et al., 2006). CD8+ T cells are classically thought of as the most important T cell subset based on cytotoxicity, it has been documented a major hurdle in immunotherapy by adoptively transferred CD8+ T cells is their dependency on CD4+ T cells, which boost antitumor activity by recruiting further effector cells and are required the expansion of CD8+ cells by providing cytokines and costimulation, augmenting priming, persistence, memory formation and trafficking of cytotoxic effectors (Hombach et al., 2006, Janssen et al., 2003, Shedlock and Shen, 2003, Guedan et al., 2018b). Liadi *et al*., investigated the difference between CD4+ and CD8+ CAR T cells, and demonstrated that while CD4+ CAR T cells can participate in killing and multiple-killing, they do so at a lower rate than CD8+ CAR T cells, most likely due to the lower Granzyme B content (Liadi et al., 2015). While the CD4 and CD8 populations have broadly been investigated here in terms of their proliferation patterns, it would be interesting to look at their impact in more detail. For example, by selecting on these populations and utilising them in *in vitro* assays such as cytotoxicity and cytokine producing abilities.

Activation and exhaustion markers

Following on from this, the activation and exhaustion status of ALK CAR T cells was investigated. It was hypothesised that ALK-Fc containing CAR T cells would have a higher expression of activation and exhaustion markers than ALK-CD8 CAR T cells, based on the observation of antigen independent proliferation of ALK-Fc containing CAR T cells (section 3.3.5). This ligand independent activity, indicative of tonic signalling, results in deleterious impacts on CAR T cell function and survival, which may lead to a significant disparity between *in vitro* cytolytic capacity and *in vivo* anti-tumour efficacy (Ajina and Maher, 2018). This is, in part, caused by the exhaustion of T cells, which induces low proliferative capacity, cytokine producing capabilities, high rates of apoptosis and expression of high inhibitory receptors such as PD-1, Tim3 and Lag3 (Long et al., 2015).

Activation markers, namely CD69 and CD25 (Figure 4.4B), and exhaustion markers, namely PD-1, Lag3, CTLA-4 and Tim3 (Figure 4.4C), were measured through flow cytometry. These markers were measured on αβ+CD34+ CAR T cells as a whole, and on CD4+ and CD8+ populations also. In general, representative histograms demonstrate that when co-cultured with either SUP-T1 WT or SUP-T1 ALK cells for 4 days, ALK-Fc and ALK-CD8 CAR T cells showed no difference in exhaustion and activation marker expression (Figure 4.5). Of note, ALK8-Fc-28ζ showed a higher expression of the CD25 marker, compared to ALK8-CD8-28ζ and UT control T cells, when incubated with the ALK negative cell line, SUP-T1 WT (Figure 4.5A). Despite this, it was not consistent with the other donors investigated. By day 8 of co-culture, there was still minimal differences between ALK-Fc and ALK-CD8 expressing CAR T cells (Figure 4.6). CTLA-4 was more highly expressed on ALK8-Fc and ALK9-Fc

compared to ALK8-CD8 and ALK9-CD8, when co-cultured with SUP-T1 WT in one donor, however again this was not consistent between donors (data not shown). CD25 and CD69 expression were quantified in Figure 4.7 and Figure 4.8b Expression of CD69 in CAR T cell populations

Figure 4.8. While it showed there were some differences in expression between ALK-Fc and ALK-CD8 CAR T cells, namely CD25 expression when co-cultured with SUP-T1 WT (Figure 4.7A, B and C), there were no statistical differences between ALK-Fc and ALK-CD8 CAR T cells. Of course, the difference in CD25 expression is interesting, particularly because this difference occurs without the presence of stimulating antigen. On co-culture with SUP-T1 ALK, these differences are not found.

Interestingly, when ALK8 and ALK9 CAR T cells were incubated with SUP-T1 ALK cells, ~40% of ALK8 CAR T cells (both Fc spacer and CD8 stalk containing) express CD25 compared to ~20% of ALK9 CAR T cells in the same condition. As this appears to be irrelevant to the stalk region used, this may suggest some other part of the CAR architecture is inducing a higher level of activation, on antigen engagement. Long *et al*., demonstrated that on *ex vivo* expansion, a second generation GD2-28ζ CAR showed higher levels of CD25 expression compared to a CD19-28ζ CAR. Furthermore, along with increased activation, these GD2-28ζ CAR T cells showed a cell surface and transcriptional prolife consistent with exhaustion, including higher expression of Tim3 and Lag3 (Long et al., 2015). It was demonstrated that this tonic signalling and subsequent profile was related to CAR aggregation, due to GD2 scFv clustering based on interactions within the scFv framework regions (Long et al., 2015). Perhaps the differences in CD25 expression found between ALK8 and ALK9, could be attributed to the scFv, rather

than the presence of the Fc spacer. Despite this, it has also been evidenced that the presence of an Fc spacer can induce chronic activation, identified through elevated CD25 levels (Watanabe et al., 2016). This interplay between CAR architecture and the evidence of tonic activity suggests there are multiple things to consider when identifying a source of over activity. As previously discussed, mapping of the epitope binding of the individual anti-scFvs would be interesting (section 3.4), as this may offer a potential explanation, and identify any differences between the anti-ALK scFv 8 or 9. Interestingly, Long *et al*., demonstrated that replacing the CD28 domain with 41-BB domain ameliorated exhaustion, suggesting the signalling induced by different costimulatory endodomains can impact on phenotype.

With regard to CD69, there were no differences in expression between ALK-Fc and ALK-CD8 CAR T cells, or when co-cultured with SUP-T1 WT compared to SUP-T1 ALK. (Figure 4.5 and Figure 4.6). However, there were differences between CAR transduced and UT control T cells (Figure 4.8). This may suggest that CD69 is consistently upregulated following transduction of the CAR, independent of the presence of target antigen, and then appears to decrease when CAR T cells are activated by the presence of the antigen. Interestingly, this doesn't seem to be the case for CD25 expression, which is dependent on antigen engagement of the CAR.

The level of CAR T cell exhaustion was investigated here by determining the surface expression of PD-1 and Tim3 (Figure 4.9). The highest level of exhaustion was identified as PD-1+/Tim3+ populations, and the least through double negative populations. While there appeared to be minimal differences between ALK8-Fc and ALK8-CD8, and ALK9-Fc and ALK9-CD8 on co-culture

with SUP-T1 ALK at day 4 and day 8 (Figure 4.9C and D), ALK8 showed differences on co-culture with the ALK negative cell line (Figure 4.9A). This suggests that there were a higher level of more exhausted ALK8-Fc CAR T cells than ALK8-CD8 cells at day 4. While this finding was significant, there were other minimal differences. It is well documented that chronic CAR activation and tonic signalling hinders efficient functioning of CAR activity (Long et al., 2015, Lynn et al., 2019). Importantly here, the were no major differences between ALK-Fc and ALK-CD8 CAR T cells, suggesting that the presence of the Fc spacer did not induce major differences between exhaustion and activation marker expression, despite impacting proliferative capacity.

Overall, looking at the expression of Tim3 and PD-1 demonstrated at ALK8-Fc-28ζ had higher exhaustion marker expression than ALK8-CD8-28ζ in the absence of antigen, consistent with antigen independent activity of the Fc spacer region. An interesting observation was that by day 8 in the presence of antigen, the total exhausted populations of ALK8 CAR T cells appears to decrease from day 4 (Figure 4.9C and D). One potential explanation for this is the reduction in exhausted cells at day 4 due to lack of proliferation, which are replaced by proliferating CAR T cells by day 8, which are less exhausted.

Differentiation markers

Efficacy of CAR T cell therapy requires the long-term maintenance of transferred cells, which depends on the presence and persistence of memory T cells. The differentiation state of the T cells selected can also influence the function and their migratory properties *in vivo* (Srivastava and Riddell, 2018). CAR T cells displaying tonic signalling are associated with accelerated T cell differentiation,

exhaustion and impaired antitumour effects. It was therefore hypothesised that ALK-Fc CAR T cells would express a more differentiated phenotype than that of ALK-CD8 CAR T cells. This was investigated through the surface expression of L-selectin (CD62L) and CD45RO in Fc spacer and CD8 stalk expressing CAR T cells with matched anti-ALK scFvs, co-cultured with antigen negative and positive cell lines.

At day 4 of co-culture, the differentiation status of ALK CAR T cells was the same between different CAR T populations, for example the number of T_{CM} and T_{EM} ALK8-Fc-28ζ CAR T cells was the same between CD4+, CD8+ and CD34+ populations within the same co-culture condition (Figure 4.12). This trend could also be said for the other ALK CAR T cells. Across all four ALK CAR T cells, co-culture with SUP-T1 ALK over SUP-T1 WT induced an increase in T_{EM} CAR T cells with a decreased in T_{CM} CAR T cells suggesting antigen stimulation induces a higher level of differentiation, as expected. When comparing the phenotype between ALK-Fc and ALK-CD8 CAR T cells, ALK9-Fc-28ζ had significantly higher expression of the T_{EM} phenotype than ALK9-CD8-28ζ on co-culture with SUP-T1 WT cells (Figure 4.12A and Figure 4.12B). This suggests that the Fc containing CAR T cells are more differentiated than the CD8 containing CAR T cells, however this wasn't present in the ALK8 CAR populations, and no significant differences were found between ALK9-Fc and ALK9-CD8 with other T cell phenotypes.

By day 8 of co-culture, the phenotype of ALK8 CAR T cells followed the same trend, with higher T_{CM} CAR T cells when co-cultured with the antigen negative cell line, and higher levels of T_{EM} CAR T cells on co-culture with SUP-T1 ALK, across CD4+, CD8+ and CD34+ CAR populations (Figure 4.13). By day 8, with

both SUP-T1 WT and SUP-T1 ALK co-culture conditions, ALK9-Fc-28ζ and ALK9-CD8-28ζ appeared to have the same memory phenotypes, despite the addition of ALK stimulation. This could suggest that ALK9 CAR T cells are activated and differentiating when ALK isn't present, on co-culture with SUP-T1 WT cells, or alternatively on ALK stimulation with SUP-T1 ALK cells, ALK9 CAR T cells don't differentiate. Overall, for all CARs in all culture conditions, there were few T_N and T_{EMRA} and higher proportions of T_{EM} than T_{CM}. This is consistent with other studies in CAR T cells by which cells are activated by OKT3 for their transduction (Barrett et al., 2014).

Accumulating data suggests that engineering less differentiated T_N and/or T_{CM} cells, or culturing T cells in conditions that preserve these phenotypes, provides CAR T cell products with superior persistence *in vivo* (Srivastava and Riddell, 2018). Hinrichs *et al*., demonstrated that deriving effector cells from T_N cells gave rise to better effector populations that mediated superior effector functions upon transfer and did not acquire the expression of the marker of terminal differentiation, KLRG-1 (Hinrichs et al., 2009). Furthermore, these naïve derived effector cells displayed minimal effector differentiation, high levels of CD27 and retained longer telomeres; characteristics that suggest greater proliferative potential and have been linked to greater efficacy in clinical trials (Hinrichs et al., 2009). The use of T_{CM} have superior antitumor function relative to T_{EM} in xenograft models of haematological malignancies due to superior persistence and proliferation (Berger et al., 2008, Sommermeyer et al., 2016). Despite this, T_{EM} express higher levels of chemokine receptors and adhesion molecules required for homing to inflamed peripheral tissues and may be better poised to enter solid tumour sites.

The classic model of differentiation has been refined with the identification of memory stem cells (T_{SCM}), which identify as a weekly differentiated T cell subset that sits between naïve and central memory subsets (Gattinoni et al., 2011). This rare type of memory lymphocyte is believed to be endowed with the stem cell-like ability to self-renew with extreme longevity and therefore has implications for CAR T cell therapies (Gattinoni et al., 2011, Cieri et al., 2013). It may be interesting to identify if this population was present within our ALK CAR T cells, and equally investigate further individual phenotypic populations in *in vitro* assays.

Overall phenotype discussion

Previously, clinical trials using CAR T cells have used cell products prepared from unselected 'bulk' T cells, however, preclinical studies indicate that some T cell subtypes show distinct properties *in vivo*, such as enhanced proliferative capacity and increased antitumour effects (Guedan et al., 2018b, Gattinoni et al., 2011). Both CD4+ T helper cells and CD8+ cytotoxic T cells play important roles in antitumour immunity, with CD8+ T cells assumed to be primary effectors due to their enhanced cytotoxic properties (Kuznetsova et al., 2019). While it has also been demonstrated that CD4+ CAR T cells can participate in killing, they also play an essential role in the promotion of cytotoxicity and it is therefore argued that an equal ratio of CD4 and CD8 CAR T cells is optimal for adoptive transfer (Liadi et al., 2015, Turtle et al., 2016, Sommermeyer et al., 2016). A recent review discussed different CAR T products for glioblastoma treatment, one trial utilised uniformly expanded CD8+ T cells with an activated effector phenotype and found limited persistence in patients (Brown et al., 2015). A follow up study utilised a different phenotype, enriched for T_{CM} cells by selecting on CAR T cells expressing L-selectin (CD62L+) based on evidence of long term persistence upon *in vivo*

transfer (Brown et al., 2016, Brown et al., 2018). Furthermore, enriching for memory T cells in CD19 CAR T cell therapy resulted in 93% complete remission rates being reached (Hay et al., 2017). Studies of adoptive T cell transfer in mice and nonhuman primates suggest that although T_{EM} cells have robust cytolytic function, only T_{CM} cells and other less differentiated T cell subsets, such as T_N cells, are critical for *in vivo* expansion, survival and long-term persistence. As T cells become more differentiated they lose costimulatory receptor expression and tissue homing capacity (Gattinoni et al., 2005). It is clear that the composition of CAR T cell products has a profound influence on functional and therapeutic efficacy, and it is therefore something to consider when designing future experiments.

4.5 Conclusions and future directions

Chronic T cell activation is observed in certain combinations of scFv, hinge and costimulatory domains and may be increased due to high levels of CAR expression. Based on previous indications of tonic signalling with the presence of an Fc spacer, the phenotypic differences between ALK-CD8 and ALK-Fc expressing CAR T cells was investigated. Despite demonstrating minimal changes between ALK-CD8 and ALK-Fc CAR T cells there are a number of interesting points:

a. Increased CD8+ populations with CAR antigen stimulation in ALK8-CD8-28ζ
b. Increased CD25 activation with Fc spacer at day 4, despite only being present in one donor
c. Increased T_{CM} to T_{EM} transition with antigen stimulation in ALK8-CD8-28ζ

In the future it may be interesting to isolate specific phenotypes and undertake *in vitro* assays to identify further differences, for example, isolate CD4+ and CD8+ CAR T cells for use compared to bulk CD34+ populations.

5 Comparison of lead ALK-CAR with a previously published ALK CAR

5.1 Introduction

Commonly when investigating a new treatment, the experimental drug will be compared to a 'gold standard'. For example, the current gold standard for CAR T cell therapy is the anti-CD19 CAR; Kymriah and Yescarta. Studies in this area, for example investigating alternative anti-CD19 scFvs, will use one of the two FDA approved FMC63 CD19 CAR T cell as a comparison to validate research against (Ghorashian et al., 2019, Sommermeyer et al., 2017). In this way, comparing new therapies to the current gold standard important new developments can be identified. For example, all published clinical trials targeting CD19 have utilised scFvs derived from murine anti-human mAbs. However, recent research demonstrated that numerous human derived anti-human CD19 scFvs with similar binding characteristics to FMC63 showed improved *in vitro* functions against tumour lines and *in vivo* activity in a xenograft model (Sommermeyer et al., 2017). Based on this, fully human anti-CD19 CAR T cells were recently investigated in a clinical trial (Brudno et al., 2020).

A number of trials are investigating the potential of CAR T cell therapy for neuroblastoma, nevertheless none of these are targeting ALK, and therefore we are lacking a gold standard therapy for clinical comparison. However, another research group recently explored the utility of targeting ALK as a CAR-based immunotherapy, providing us with an alternate CAR for functional comparison (Walker et al., 2017). In this publication, three unique anti-ALK scFvs were investigated, in combination with CD28-CD3ζ or CD8α-4-1BB-CD3ζ signalling

endodomains. The lead construct containing an ‘ALK48’ scFv and a 4-1BBζ signalling domain was taken forward for further investigation. This CAR contained a CD8 derived hinge and transmembrane (H/TM) region, compared to longer CARs created containing the CH2CH3 spacer regions. These longer CARs showed considerably diminished cytokine production and cytolytic activity and were therefore not investigated further (Walker et al., 2017). ALK48-4-1BBζ demonstrated the ability to lyse ALK expressing tumour cell lines and produced IFNγ upon ALK antigen stimulation (Walker et al., 2017). However, there was limited IL-2 production, which had a sharp threshold for appreciable cytokine production that was higher than that required for IFNγ cytokine secretion. Furthermore, it appeared to lack potent *in vivo* anti-tumour activity in two xenograft models of neuroblastoma, and the authors postulated that low antigen density is a major limitation for the use of ALK as a target for CAR T cells (Walker et al., 2017). Although ALK48-4-1BBζ cannot be considered a gold standard for ALK CAR T cell therapy, it is of interest to compare our novel ALK binders to determine relative efficacy and to determine if different ALK binders may exceed the activation threshold for antigen-low targets.

5.2 Aims

The data described in chapters 3 and 4 aimed to characterise a panel of anti-ALK CAR T cells in a number of *in vitro* experiments. Of particular importance is the observation that the anti-ALK binder 8 combined with either an Fc or a CD8 stalk region and CD28ζ signalling domains, demonstrated the greatest ability to lyse ALK expressing cells at the lowest target antigen density, namely the Lan-1 cell line. Furthermore, ALK8-CD8-28ζ was found to proliferate in an antigen-specific manner at this low antigen density. Based on this, ALK8-CD8-28ζ was taken forward for use within this chapter of research, in which it was directly compared to a previously published anti-ALK scFv in combination with different backbones, acting as a comparator for anti-ALK CAR T cells. Therefore, the first aim of this chapter was to generate a panel of ALK48-based CAR T cells with different backbone combinations. The second aim was to ask a number of questions:

(i) Is the ALK48 CAR function affected by changing the spacer region and signalling endodomain?

(ii) Is ALK8 superior to ALK48 with its optimal spacer and endodomains, in a low antigen neuroblastoma setting?

To do this I performed a series of co-cultures with a range of ALK surface density to evaluate cytotoxic potential, cytokine production and short term proliferative responses.

5.3 Results

5.3.1 Generation of ALK48 CAR constructs

In order to produce a panel of CAR constructs including the ALK48 scFv combined with different spacer regions and the CD28ζ signalling domains, a cloning strategy was devised displayed in Figure 5.1. To do this, the ALK9-CD8-28ζ CAR was used as a backbone for inserting new gene sequences based on the presence of certain restriction sites which would allow for cloning by restriction digest (Figure 5.1A). The sequences of ALK48 scFv and the CD8H/TM region were provided by Robbie Majzner (Stanford, USA) (Figure 5.1B). Based on this, the following DNA gene blocks were produced (shown in green in Figure 5.1C):

1. XhoI-ALK48-Fc-CD28TM-BsiWI
2. XhoI-ALK48-NotI
3. XhoI-ALK48-CD8H/TM-BsiWI

This allowed for the production of three novel ALK48 CARs: ALK48-Fc-28ζ, ALK48-CD8-28ζ and ALK48-28ζ (Figure 5.1C). The former two CARs will therefore contain the ALK48 scFv with regions as per the panel of novel ALK constructs investigated in results chapter 1. The latter CAR was produced to contain the ALK48 scFv with no spacer apart from the CD8H/TM published in Walker *et al*. However, ALK48-28ζ contains the CD28 co-stimulatory domain, in place of 4-1BB. The DNA sequences were validated through restriction digest and sanger sequencing (Source Bioscience).

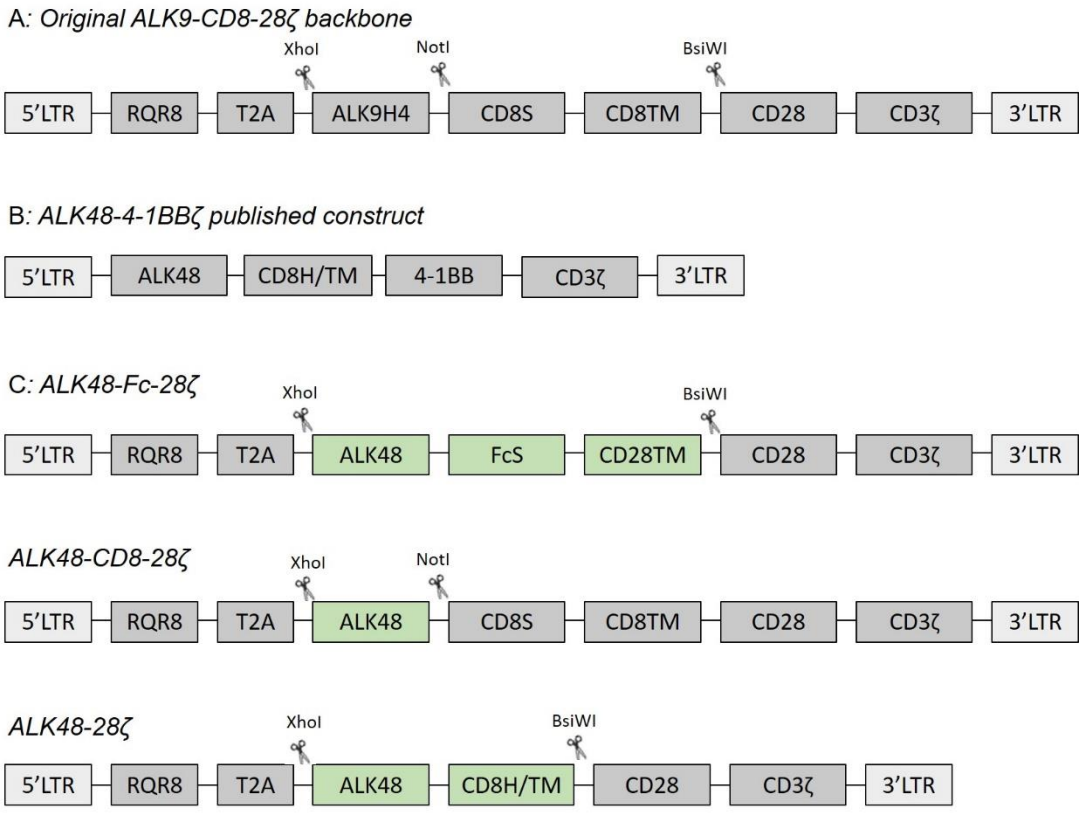

Figure 5.1 Design of the ALK48 CAR T cell panel

The ALK9-CD8-28ζ CAR was used as a backbone for molecular cloning based on the position of the restriction sites XhoI, NotI and BsiWI (A). The sequences of the ALK48 scFv and the CD8H/TM domain (B) were combined with the ALK9-CD8-28ζ backbone (A) through the production of DNA gene blocks (indicated in green) and insertion through restriction cloning. Based on this, the following novel ALK CAR constructs were produced: ALK48-Fc-28ζ, ALK48-CD8-28ζ and ALK48-28ζ (C).

5.3.2 Expression of ALK48 constructs on the surface of primary human T cells

After the ALK48 CAR constructs were validated for the correct DNA sequences, it was necessary to investigate their expression on the surface of primary human T cells. To do this, PBMCs were isolated from healthy donors and activated αβ T cells were transduced with gamma-retroviral supernatant produced from triple transfection of 293T cells with the ALK48 CAR plasmids. As previously described, the binding of anti-CD34 to RQR8, which is co-expressed with the CAR construct, was used as a marker of successful transduction in T cells. This binding was detected through flow cytometry. No statistical differences were observed between the transduction efficacies of the four ALK CAR constructs (Figure 5.2).

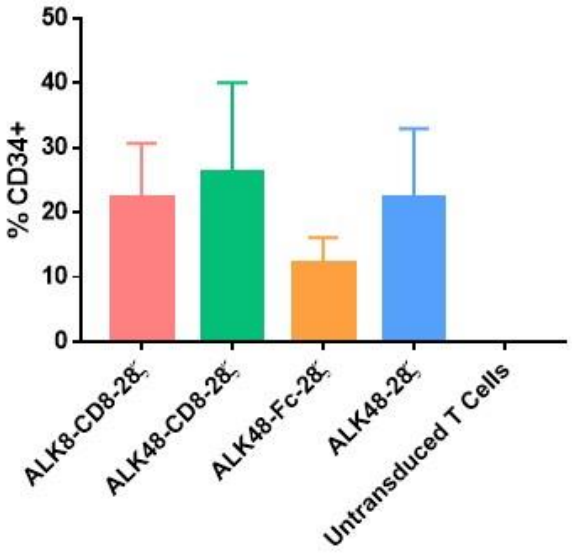

Figure 5.2 Transduction efficacy of ALK-RQR8 CAR constructs on primary αβ human T cells

Activated αβ T cells were transduced to express the ALK CAR constructs with gamma-retroviral supernatant, and the transduction efficacy was determined by quantifying the expression of the RQR8 marker gene co-expressed with the CAR construct. This was achieved through the binding of the anti-CD34 APC antibody. Mean CD34 expression±SD is displayed (n=3-4). No statistically significant differences were found between CD34 expression levels as determined by one-way ANOVA followed by Tukey's post-hoc analysis.

5.3.3 Cytotoxic activity of ALK48 and ALK8 CAR T cells

Having confirmed that CD34 could be detected on the surface of primary human T cells, their anti-tumour activity was assessed using a 4-hour ^{51}Cr release assay. Target cells, in this case SUP-T1 WT, Lan-1, Kelly, Lan-5 and SUP-T1 ALK cell lines, were labelled with ^{51}Cr and co-cultured with effector CAR T cells at various E:T ratios (1.25:1, 2.5:1, 5:1 and 10:1). After four hours, the ^{51}Cr released from lysed cells was recorded. The experiment was replicated in 3-4 independent donors and the respective transduction efficiencies are as depicted in figure 5.2. Minimal lysis of SUP-T1 WT control cells by any of the CAR T cell subtypes (Figure 5.3A) was observed while UT T cells did not present significant anti-tumour activity against ALK expressing cell lines (Figure 5.3B). ALK48-Fc-28ζ and ALK48-28ζ appeared to induce no ^{51}Cr release when co-cultured with Lan-1, Kelly, Lan-5 or SUP-T1 ALK at any E:T ratio. Conversely, ALK8-CD8-28ζ and ALK48-CD8-28ζ demonstrated similar levels of cytotoxicity against all ALK expressing cell lines. At 10:1 E:T ratio, both of these CAR T cells exhibited significantly higher levels of ^{51}Cr release than UT T cells when co-cultured with Lan-1, Kelly and SUP-T1 ALK cell lines. Only ALK8-CD8-28ζ had significantly higher levels of Lan-5 killing compared to UT T cells. In the case of ALK8-CD8-28ζ and ALK48-CD8-28ζ, the level of ^{51}Cr release was higher when ALK target density was higher (Figure 3.2). For example, at a 10:1 E:T ratio ALK8-CD8-28ζ and ALK48-CD8-28ζ co-cultured with Lan-1 resulted in 26±15% (mean±SD, n=4) and 19±12% (n=4) killing compared to when co-cultured with SUP-T1 ALK which resulted in 42±12% (n=4) and 41±22% (n=4), respectively. Despite these differences, there was no statistically significant differences between the cytotoxicity of ALK8-CD8-28ζ and ALK48-CD8-28ζ.

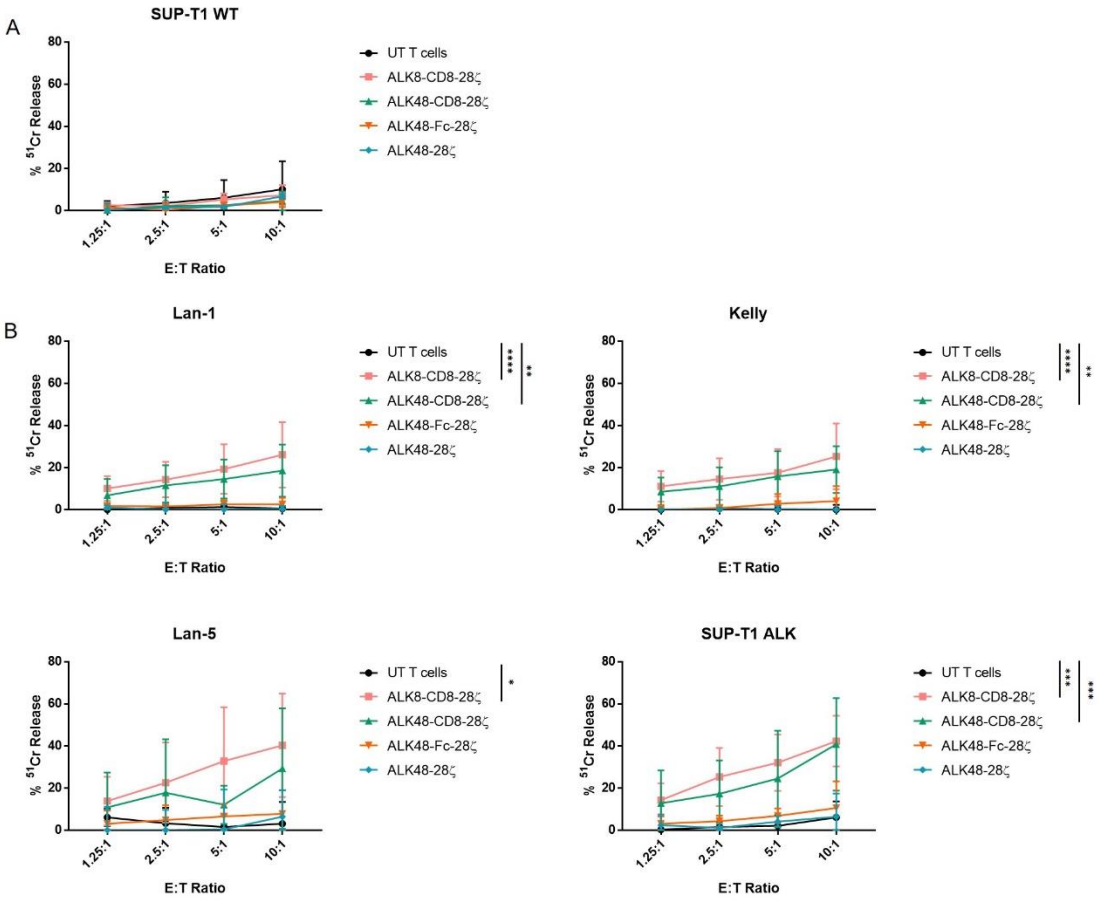

Figure 5.3 Cytotoxicity of ALK CARs against neuroblastoma and SUP-T1 WT and SUP-T1 ALK cell lines

T cells transduced with ALK8-CD8-28ζ, ALK48-CD8-28ζ, ALK48-Fc-28ζ and ALK48-28ζ were co-cultured with SUP-T1 WT (A) or ALK expressing cell lines (B) at the following E:T ratios: 1.25:1, 2.5:1, 5:1 and 10:1. UT T cells were used a negative control. Graphs show mean±SD (n=3-4). Two-way ANOVA was performed followed by Tukey's post-hoc analysis: * p<0.1, ** p<0.01, *** p<0.001, **** p<0.0001 (Statistics displayed for 10:1 E:T only).

5.3.4 Donor response to PMA/Ionomycin stimulation

While it was found that ALK8-CD8-28ζ and ALK48-CD8-28ζ were cytotoxic against neuroblastoma cell lines (Figure 5.3), when these ALK CAR T cells were utilised in subsequent cytokine and proliferation assays there was variable response to PMA and ionomycin stimulation. During these experiments, CAR and UT T cells stimulated with PMA and ionomcyin acts as a positive control to check the health of the T cell. Figure 5.4A shows the response to PMA and ionomycin stimulation of the three donors used for the above experiments. The ΔMFI compared to UT T cells cultured alone clearly shows that two out of three donors had minimal response to stimulation. While donor variability is common, the lack of stimulatory response combined with the relatively low transduction efficacies for these CARs (Figure 5.2) makes it difficult to conclude information from these results.

In order to produce more accurate *in vitro* results, assays were repeated with new donors which had a higher transduction efficacy and response to PMA and ionomycin stimulation (Figure 5.4). As described previously (section 2.2.8), activated αβ T cells were transduced with γ-retroviral supernatant produced from triple transfection of 293T cells with the ALK48 CAR plasmids. The binding of anti-CD34 to RQR8 was determined by flow cytometry. The transduction efficacies were higher than previously produced (Figure 5.2). The ΔMFI of ALK CAR T cells stimulated with PMA and ionomycin (Figure 5.4B) was greater than previous donors used (Figure 5.4A). Unfortunately, at this time the facilities to repeat a ^{51}Cr cytotoxicity assay with the following repeat transductions were not available, these donors are used for the following experiments described for the rest of the chapter.

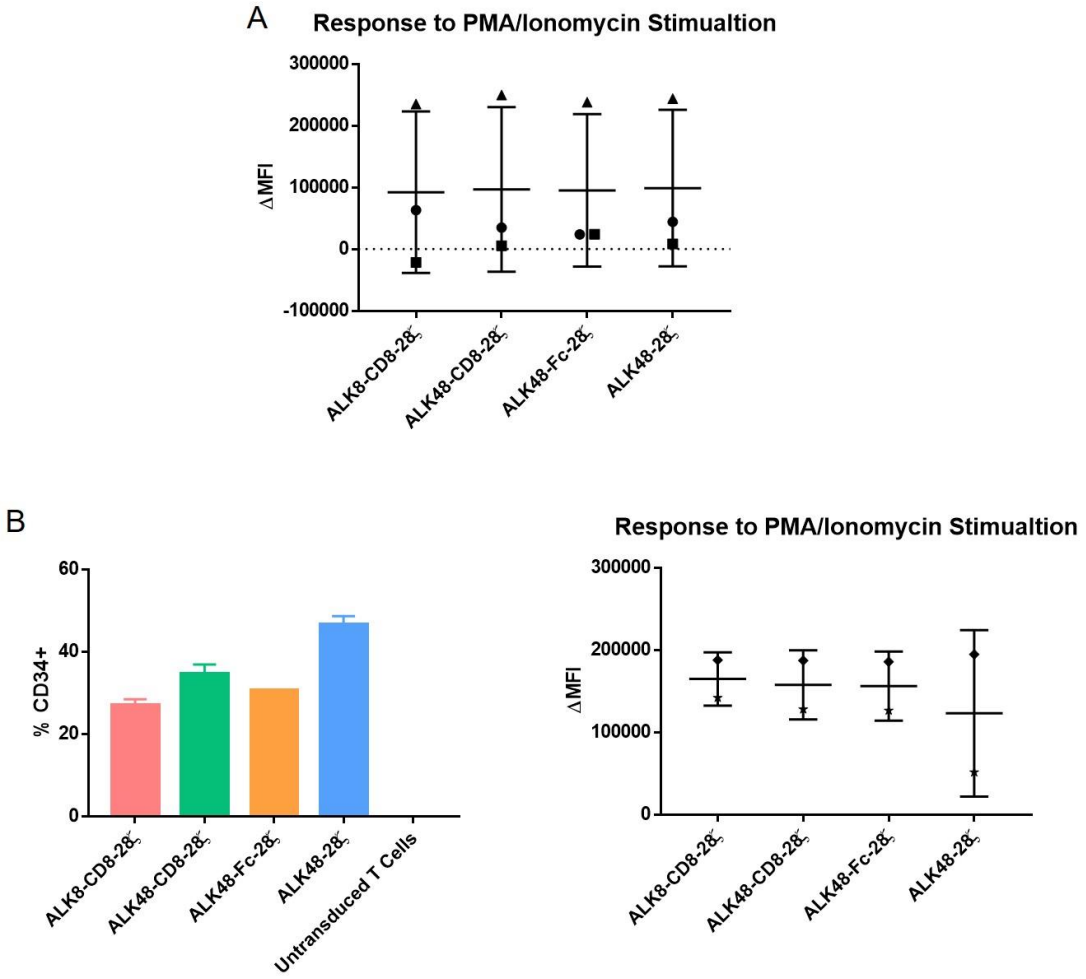

Figure 5.4 ΔMFI of donors in response to PMA and Ionomycin

ALK CAR T cells were labelled with cell trace violet and proliferation was determined through dilution of this dye. ALK CAR T cells stimulated with PMA and ionomycin were used as a positive control. The ΔMFI of these cells was determined by comparing the MFI to that of UT T cells cultured alone. (A) Two out of three of the original donors demonstrate no proliferation in response to PMA and ionomycin stimulation, when compared to UT T cells cultured alone from the same donor. Data shows mean ΔMFI±SD, each donor represented by different symbol, n=3 of independent biological replicates. Based on this, a further two donors were utilised for further experiments (B). Activated αβ T cells were transduced to express ALK CAR constructs with γ-retroviral supernatant. The transduction efficacy was determined by quantifying the expression of the RQR8 marker gene which is co-expressed with the CAR constructs. Data shows mean CD34 expression±SD is displayed. ΔMFI of ALK CAR T cells demonstrates proliferative response to PMA and ionomycin stimulation. Data shows mean ΔMFI±SD, each donor represented by different symbol, n=2 of independent biological replicates.

5.3.5 Cytokine production

The following experiments utilised the two final donors, not the original three donors used for the cytotoxicity assay. The ability of ALK48 CARs to produce proinflammatory cytokines on co-culture with ALK-expressing target cells was investigated. For this, ALK CAR T cells were co-cultured with irradiated SUP-T1 WT, Lan-1, Kelly, Lan-5 or SUP-T1 ALK cell lines (section 3.3.4.2). The presence of IL-2 and IFNγ was measured in the supernatant by ELISA after 24 hour co-culture (Figure 5.5A) and after restimulation with the same targets following a 7 day co-culture (Figure 5.5B).

When ALK CAR T cells were co-cultured with target cells for 24 hours no IL-2 was produced on co-culture with SUP-T1 WT, Lan-1, Kelly or Lan-5 cell lines (Figure 5.5A). On co-culture with SUP-T1 ALK, only ALK8-CD8-28ζ produced IL-2. ALK CAR T cells and UT control T cells produced similar levels of IL-2 when stimulated with PMA and ionomycin. In terms of IFNγ production after 24 hour co-culture, only ALK8-CD8-28ζ appeared to produce IFNγ on co-culture with Kelly, Lan-5 and SUP-T1 ALK cell lines. There was a slight indication of IFNγ production from ALK48 CAR T cells on co-culture with SUP-T1 ALK, however this was much lower than that produced by ALK8-CD8-28ζ. On stimulation with PMA and ionomycin, UT control T cells, ALK8-CD8-28ζ, ALK48-Fc-28ζ and ALK48-28ζ all produced IFNγ, but ALK48-CD8-28ζ did not.

ALK CAR T cells were co-cultured with target cells for 7 days, before antigen restimulation. To do this, ALK CARs were co-cultured with cell lines and subsequently washed after 7 days, to remove any cytokines previously produced, and re-plated with the original stimulation conditions. After 24 hours the

supernatant was harvested for evaluation of cytokines by ELISA (Figure 5.5B). IL-2 was only produced from ALK CAR and UT T cells after restimulation with PMA and ionomycin. There was low level of IFNγ production from ALK48-CD8-28ζ and ALK48-Fc-28ζ when co-cultured with Kelly cells, however this was also true of UT control T cells suggesting it could be background production. As with IFNγ production after 24 hour co-culture (Figure 5.5A), ALK8-CD8-28ζ produced IFNγ on co-culture with SUP-T1 ALK, and all T cell populations produced IFNγ on PMA and ionomycin stimulation, apart from ALK48-CD8-28ζ. Only ALK48-Fc-28ζ demonstrated IFNγ production when cultured alone. As this work was carried out in only two donors it was not possible to investigate statistical significance.

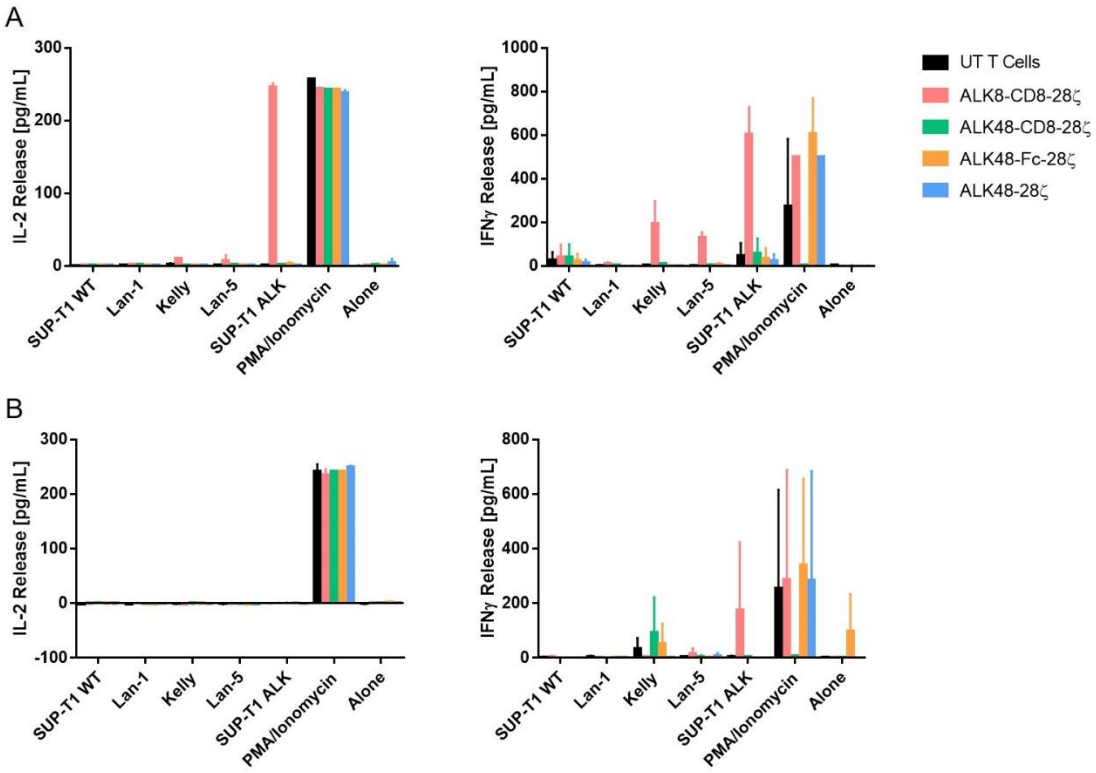

Figure 5.5 Quantification of IL-2 and IFNγ production by ALK CAR T cells

IL-2 and IFNγ production measured by ELISA from supernatant after 24 hour co-culture (A) or 7 day co-culture with restimulation (B). ALK CAR T cells or UT T cells were co-cultured with SUP-T1 WT, Lan-1, Kelly, Lan-5 or SUP-T1 ALK cell lines, alone or with PMA and Ionomycin stimulation. UT T cells were used as a control. Graphs show mean±SD (n=2 of independent biological replicates). No statistical analysis was performed.

5.3.6 Short term proliferative capacity

The short term proliferative capacity of the ALK48 CARs was investigated as previously described (section 3.3.5.1). The ALK CAR T cells were labelled with cell trace violet, a proliferation dye traceable through flow cytometry. These labelled CAR T cells were co-cultured at a 1:1 ratio with irradiated SUP-T1 WT, Lan-1, Kelly, Lan-5 or SUP-T1 ALK cell lines. After 4 and 8 days of co-culture, CAR T cell proliferation was determined by cell trace violet dilution by flow cytometry. ALK CAR T cells were stimulated with PMA and ionomycin as a positive control. ALK CAR T cells and UT T cells were cultured alone as negative controls. The ΔMFI of ALK CAR T cell proliferation compared to that of UT T cells cultured alone was determined, as previously described (section 3.3.5.1), in order to quantify the proliferation of the ALK CARs.

Figure 5.6 shows the short term proliferation after 4 days of co-culture. Figure 5.6A displays a representative histogram readout of cell trace violet dilution from one donor. No proliferation was seen from UT T cells or CAR T cells cultured alone. While only ALK8-CD8-28ζ and ALK48-28ζ appeared to have a small shift in proliferation when stimulated with PMA and ionomycin on the histograms (Figure 5.6A), the ΔMFI demonstrated both donors responded to this stimulation (Figure 5.6B). ALK8-CD8-28ζ demonstrated the greatest shift in cell trace violet labelled population when co-cultured with SUP-T1 ALK, with smaller shifts in proliferation on co-culture with Kelly and Lan-5 cell lines (Figure 5.6A). These patterns were not reflected by the ALK48 CAR T cells.

The MFI of cell trace violet was compared to the MFI of the UT T cell control for each experiment (Figure 5.6B). The ΔMFI reflects what is seen in the histograms

for ALK8-CD8-28ζ with increasing proliferation from co-culture with Lan-1 through to SUP-T1 ALK. This pattern of ΔMFI was also reflected by ALK48-CD8-28ζ, but to a lesser extent. The ΔMFI for ALK48-Fc-28ζ and ALK48-28ζ suggests there is limited evidence of proliferation at day 4 co-culture. However, as previously stated, there was evidence of that all four ALK CAR T cells responded to PMA and ionomycin stimulation. However, it is difficult to make conclusive statements as statistics can't be determined for two donors.

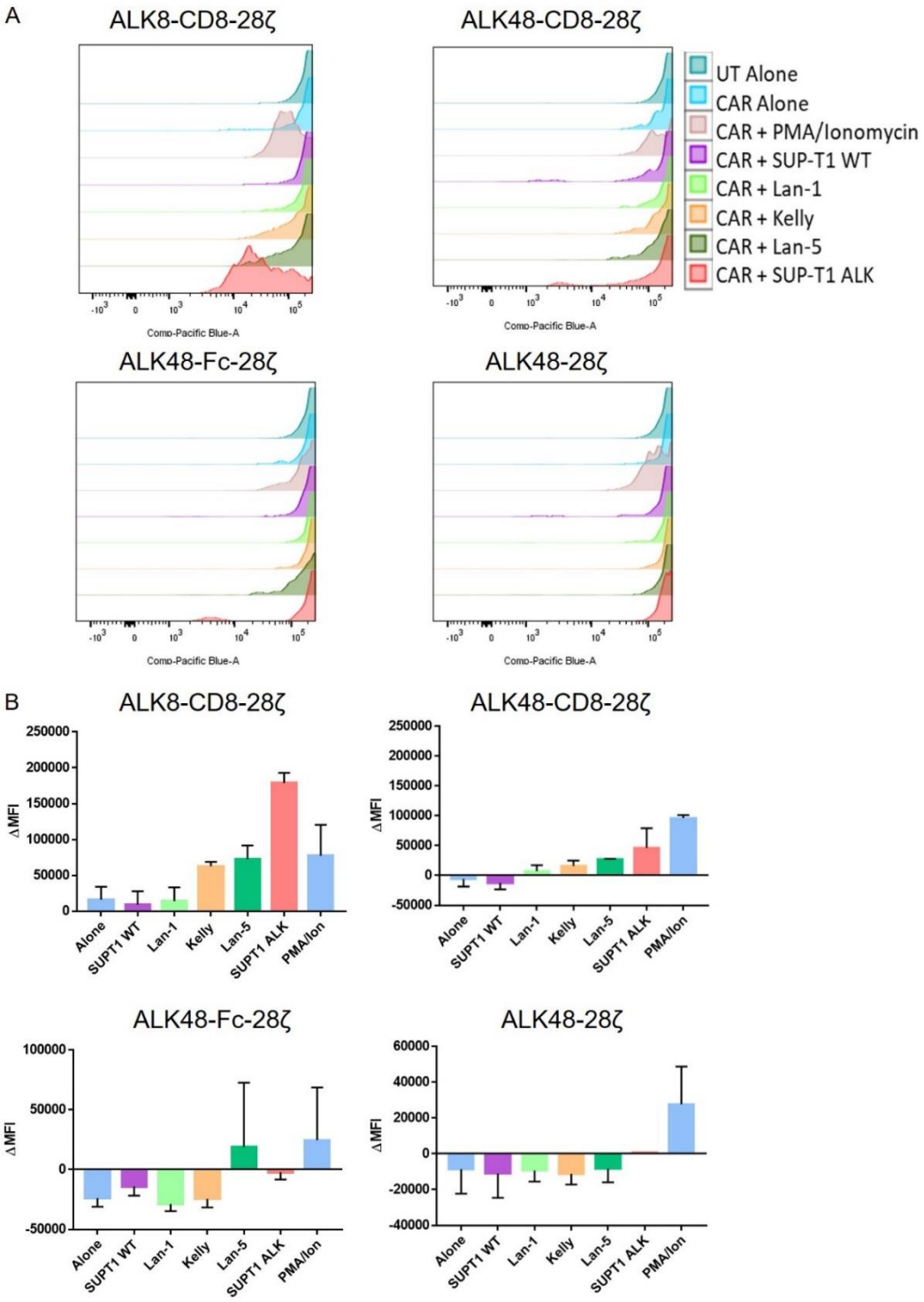

Figure 5.6 Proliferative capacity of ALK CAR T cells after 4 days of short term co-culture

ALK CAR T cells or UT T cells were labelled with cell trace violet and cultured alone, or with irradiated target cells (SUP-T1 WT, Lan-1, Kelly, Lan-5 or SUP-T1 ALK cell lines) at a 1:1 ratio. The dilution of cell trace violet was determined by flow cytometry after 4 days. (A) shows representative histograms showing dilution of cell trace violet. (B) shows the mean ΔMFI±SD compared to the UT T cell alone control. (n=2 independent biological replicates). No statistical analysis was performed.

Figure 5.7 shows the short term proliferation of ALK CAR T cells after 8 days in co-culture. Figure 5.7A displays a representative histogram readout of cell trace violet dilution from one donor. As shown at day 4 of co-culture (Figure 5.7A), UT T cells and CAR T cells cultured alone did not show evidence of proliferation after 8 days. In contrast, all ALK CAR T cells showed cell trace violet dilution, indicative of proliferation, when stimulated with PMA and ionomycin. ALK8-CD8-28ζ showed minimal proliferation when co-cultured with SUP-T1 WT or Lan-1, however increasing cell trace violet dilution was found with Kelly, Lan-5 and SUP-T1 ALK. ALK48-CD8-28ζ and ALK48-Fc-28ζ also demonstrated cell trace violet dilution on co-culture with SUP-T1 ALK, and with Lan-5 to a lesser extent. Interestingly, the proliferation against SUP-T1 ALK by the aforementioned CAR T cells appeared to have two different populations, one demonstrating proliferation and another not. In contrast, ALK48-28ζ showed minimal proliferation from all co-culture conditions, with a very small shift seen when co-cultured with SUP-T1 ALK cells.

Figure 5.7B shows the mean ΔMFI over 8 days of co-culture averaged over the two independent donors. As shown at day 4 (Figure 5.7B), the ΔMFI for ALK8-CD8-28ζ reflects what is shown in the histograms, suggesting the highest level of CAR T cell proliferation with the SUP-T1 ALK cell line. ALK48-CD8-28ζ and ALK48-Fc-28ζ also demonstrated the highest level of proliferation against SUP-T1 ALK, but to a much lesser extent. Importantly, all four ALK CAR T cells demonstrate a proliferative response to PMA and ionomycin stimulation, reflected in the ΔMFI.

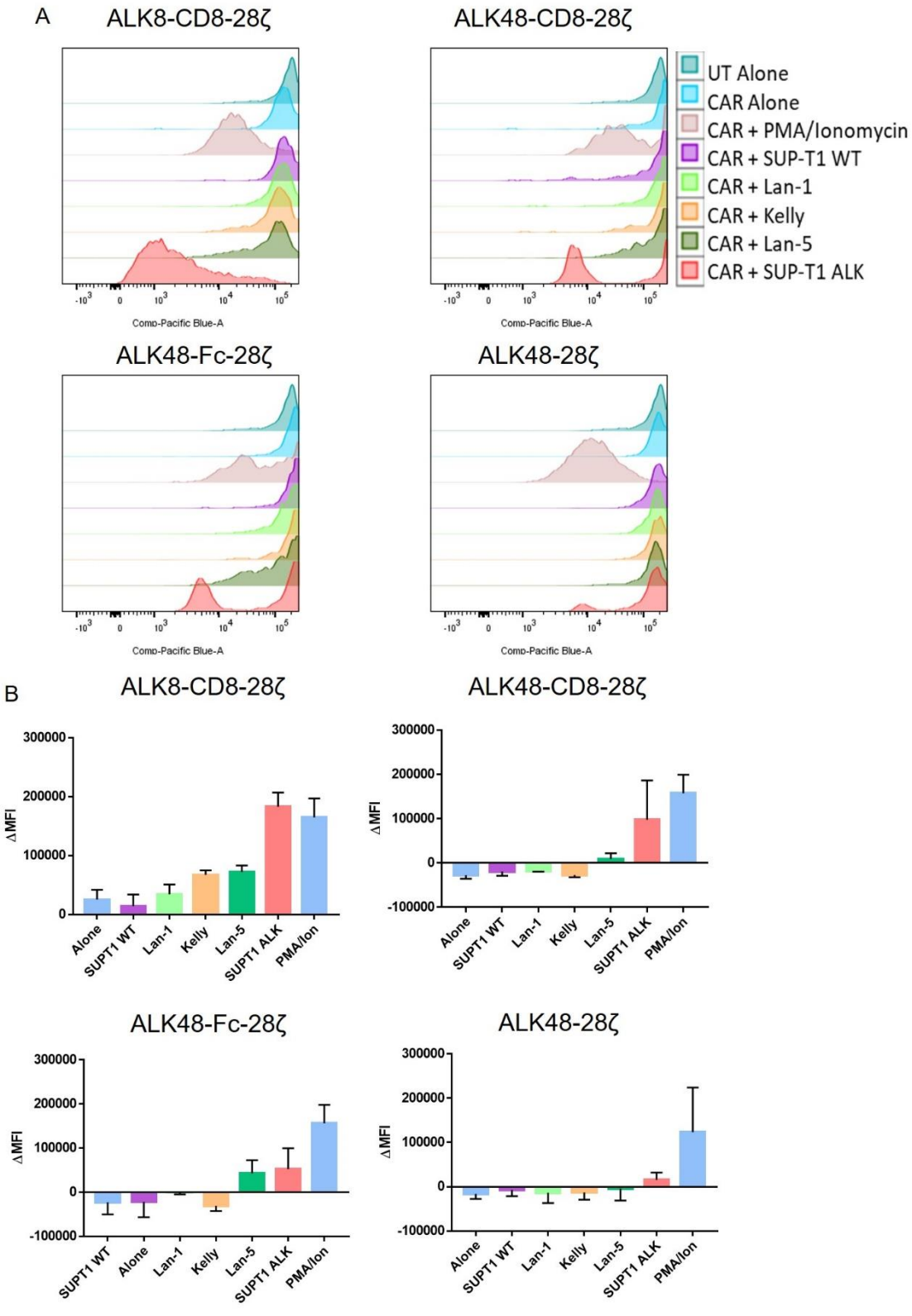

Figure 5.7 Proliferative capacity of ALK CAR T cells after 8 days of short term co-culture

ALK CAR T cells or UT T cells were labelled with cell trace violet and cultured alone, or with irradiated target cells (SUP-T1 WT, Lan-1, Kelly, Lan-5 or SUP-T1 ALK cell lines) at a 1:1 ratio. The dilution of cell trace violet was determined by flow cytometry after 8 days. (A) shows representative histograms showing dilution of cell trace violet. (B) shows the mean ΔMFI±SD compared to the UT T cell alone control. (n= 2 independent biological replicates). No statistical analysis was performed.

5.4 Discussion

Previously there have been no CAR based immunotherapies targeting ALK for use in neuroblastoma that have been evaluated in a clinical trial setting. Based on this, it was decided to utilise a previously published and characterised anti-ALK CAR T cell for functional comparison with the ALK CAR taken forward from our group. Following the characterisation of the panel of anti-ALK CAR T cells in Chapter 3 and 4, the anti-ALK scFv 'ALK8' combined with either an Fc or a CD8 spacer conferred the highest cytotoxicity at the lowest ALK antigen target density, namely against the Lan-1 cell line. Based on the indication of tonic activity of ALK CARs combined with an Fc spacer, and the restricted, antigen-dependent proliferation patterns seen with ALK8-CD8-28ζ, this CAR combination was taken forward to be compared with a panel of ALK48 CARs.

The published CAR, ALK48-4-1BBζ, has previously demonstrated the ability to lyse ALK expressing tumour cell lines and produce IFNγ upon ALK antigen stimulation (Walker et al., 2017). We therefore aimed to compare the published ALK48 scFv, with our ALK8 scFv in a panel of *in vitro* experiments. A panel of three ALK48 CAR constructs were designed and produced, combining the ALK48 scFv into CAR constructs containing the transmembrane domains, spacer regions and endodomains of our ALK CAR constructs, creating ALK48-CD8-28ζ and ALK48-Fc-28ζ (Figure 5.1C). Furthermore, a final ALK48 CAR was produced, containing the published CD8 hinge/transmembrane (H/TM) region and the CD28ζ signalling domain used within our CARs (Figure 5.1C). This is based on the published ALK48-4-1BBζ CAR which contains only a short CD8 hinge sequence as spacer. In this way, a complete ALK48 panel was created to

validate ALK8-CD8-28ζ against. The panel of ALK48 CAR constructs was created through restriction cloning. These constructs were sequenced for the correct DNA sequences and confirmed to be accurately cloned. Whist both the vector and the endodomains (CD28 in our construct and 4-1BB in Walker *et al*) differ from Walker *et al*'s., experiments, it was important to compare like with like in order to evaluate the contribution of the respective ScFvs towards CAR T cell activation. Whilst it is possible that the published binder, ALK48, might function more optimally in a different vector and endodomain, we are able to draw inferences about target antigen activation thresholds of the different binders. Of course, by using a CD28 co-stimulatory domain, as opposed to the 4-1BB endodomain, it would be expected that the ALK48 CARs produced for this chapter may act differently compared to the lead ALK48 construct previously documented (Walker et al., 2017). The functional differences of the use of CD28 vs a 4-1BB co-stimulatory domain are discussed previously (section 1.4.1.3). CD28 is well known to provide a stronger proinflammatory response and short term proliferative capacity while 4-1BB demonstrate enhanced long term proliferation and persistence (Kawalekar et al., 2016).

After production of the ALK48 CAR construct panel, it needed to be determined if they could be expressed on the surface of primary αβ T cells. Despite the transduction efficacies being generally quite low, ranging from 12±4% to 26±14% (mean±SD, n=4), there was still evidence of surface expression detected through anti-CD34 binding. Anti-CD34 binds the RQR8 domain contained within the CAR constructs, which is co-expressed with the CAR gene by a T2A molecule. The use of RQR8 co-expressed with the CAR gene by T2A molecule for determining transduction efficacy is discussed previously (section 3.4). The transduction

efficacy of ALK8-CD8-28ζ as determined by CD34 expression was at least double in Chapter 3 (Figure 3.3), suggesting the low levels of transduction found during these experiments with all constructs could be donor related or due to technical reasons. Of course, it has been documented that low transduction efficacies have an impact on CAR functionality. Walker *et al*., demonstrated that not only does target antigen density limit CAR T cell function, such as decreased IL-2 production with lower target antigen density, but surface CAR expression level can impact T cell signal strength and ultimately also limit CAR T cell function (Walker et al., 2017). Furthermore, it was suggested this was through the CAR being lost from the surface after antigen encounter through internalisation (Walker et al., 2017). Of course, the link between CAR functionality and target antigen density is well documented (Weijtens et al., 2000, Anurathapan et al., 2014, Caruso et al., 2015, Turatti et al., 2007). There is also building evidence to suggest that CARs undergo rapid down modulation after engagement with their target antigens (Caruso et al., 2015, Hamieh et al., 2019). Therefore, having low levels of CAR transduced T cells, as seen in this set of experiments, may impact the results due to a diminished effector population.

After it was successfully demonstrated that ALK48 CAR constructs could be expressed on the surface of primary αβ T cells, their cytotoxic potential was investigated through a ^{51}Cr release assay (Figure 5.3). While ALK8-CD8-28ζ and ALK48-CD8-28ζ acted in a similar manner when co-cultured with ALK expressing cell lines, ALK48-Fc-28ζ and ALK48-28ζ induced no cytotoxicity from any cell lines, in the same manner as the UT T cell control. Interestingly, Walker *et al*., also investigated the use of an Fc (CH2CH3) region combined with their ALK48 scFv, termed ‘long’ CARs. They found that the long ALK48 CAR could be

expressed on the surface of T cells, but showed considerably diminished cytokine production and cytolytic activity compared with ALK48 with CD8 hinge transmembrane (Walker et al., 2017). Despite seeing a lack of activity with an ALK48 long CAR, the incorporation of an Fc region into our ALK CARs previously investigated, demonstrated no cytotolytic differences to ALK CAR T cells containing the same ALK scFv and a CD8 stalk (Figure 3.4). It is therefore difficult to say whether the lack of activity by ALK48-Fc-28ζ is based on the incorporation of the Fc spacer. Perhaps the combination of ALK48 and an Fc spacer inducing a lack of CAR activity suggests the differences between our anti-ALK scFvs and ALK48 could be impacting these results, as ALK-Fc combinations demonstrated cytotoxicity in our hands. Furthermore, the published ALK48-4-1BBζ CAR contained only a very short spacer comprising the CD8 H/TM domain, which is also present in the ALK48-28ζ that was produced and evaluated in this assay. Again, it is therefore difficult to conclude that the lack of cytotoxic activity seen by ALK48-28ζ was due to the presence of the CD8 H/TM domain.

When these ALK CAR T cells were investigated in further *in vitro* assays, it was found that two out of three donors had a minimal proliferative response to PMA and ionomycin stimulation after 8 days, compared to UT T cells cultured alone (Figure 5.4A). In this case, PMA and ionomycin is used as a positive control to check the health of the T cell. The lack of proliferative response to this stimulation suggests the results produced from these donors may not be reliable. Based on this, two further donors were investigated for the subsequent cytokine and proliferation experiments. Unfortunately due to lab closures, the facilities to repeat a ^{51}Cr based killing assay were unavailable. The surface expression of the CAR T cells was determined through anti-CD34 binding (Figure 5.4B). In this

case, the transduction efficacy was increased for each CAR compared to initial efficacies (Figure 5.2). The smallest increase being ALK8-CD8-28ζ; 20±9% (n=3) to 27±1% (n=2), and the largest increase being ALK48-28ζ; 24.5±12% (n=3) to 46.5±2% (n=2). These new donors' also demonstrated higher proliferative responses to PMA and ionomycin stimulation after 8 days, suggesting they are responding as expected (Figure 5.4B).

The ability of the ALK48 CAR T cells to produce cytokines was investigated by co-culturing CAR T cells with target cells for 24 hours, or for 7 days with additional antigen restimulation (Figure 5.5). After 24 hours of co-culture with cell lines there was no IL-2 production from ALK48 CAR T cells (Figure 5.5A). Only ALK8-CD8-28ζ demonstrated IL-2 production when co-cultured with the high ALK expressing cell line, SUP-T1 ALK (av 246pg/mL IL-2 release, n=2). While this is clearly higher than ALK48 CAR T cells, ALK8-CD8-28ζ has previously produced much higher levels of IL-2 levels when co-cultured with SUP-T1 ALK (Figure 3.5). When stimulated with PMA and ionomycin, all CAR T cells and UT T cells produced similar levels of IL-2, as expected. In a similar manner, only ALK8-CD8-28ζ produced IFNγ on 24 hour co-culture with Kelly and Lan-5 cell lines. On co-culture with SUP-T1 ALK cells, there was some low level IFNγ production from ALK48 CAR T cells, however this was similar to what was seen from UT T cells, suggesting this is background release. Only ALK8-CD8-28ζ produced a relatively high level of IFNγ on SUP-T1 ALK co-culture (av 602pg/mL IFNγ release, n=2), but again this is lower than previously produced (Figure 3.5). Interestingly, all T cell populations produced IFNγ when stimulated with PMA and ionomycin, apart from ALK48-CD8-28ζ. This lack of cytokine production from ALK CAR T cells on co-culture with lower ALK expressing cell lines, namely Lan-1 and Kelly, again

highlights the importance of target antigen density in the stimulation and subsequent activation of CAR T cells. Many papers have investigated the threshold for CAR T activation. Watanabe *et al*., looked at the density of CD20 required for anti-CD20 CAR T cell to become activated, and demonstrated that as low as ~200 CD20 molecules per cell was required to induce target cell lysis (Watanabe et al., 2015). Furthermore, it was demonstrated that target antigen density required to induce T cell proliferation and cytokine production was higher than that required to induce CAR mediated lysis: for example, ~5,000 CD20 molecules per cell were needed for cytokine production and T cell proliferation (Watanabe et al., 2015). This suggests CAR T cells have hierarchical T cell signalling thresholds for cell lysis, proliferation and individual cytokine production (Watanabe et al., 2018). This was further confirmed with a CAR targeting a tumour glycoepitope of murine OTS8 and CD22 for use in leukaemia (Stone et al., 2012, Ramakrishna et al., 2019).

The ability of ALK CAR T cells to produce IL-2 and IFNγ after restimulation was also investigated (Figure 5.5B). In this case, ALK CAR T cells were co-cultured with target cells for 7 days before washing and restimulation with the same culture conditions. After 24 hours, ALK CAR T cells and UT T cells only produced IL-2 when stimulated with PMA and ionomycin. In terms of IFNγ production, as with 24 hour co-culture (Figure 5.5A) all ALK CARs and UT T cells, apart from ALK48-CD8-28ζ, produced IFNγ on PMA and ionomycin stimulation. There was low level release from ALK48-CD8-28ζ when cultured with Kelly cells, but not with SUP-T1 ALK which has higher ALK expression, or when stimulated with PMA and ionomycin. This suggests this result may be background release. Equally, ALK48-Fc-28ζ demonstrated release low level IFNγ when co-cultured with Kelly

cells and alone, along with when stimulated with PMA and ionomycin. Interestingly, chapter 3 results demonstrated that Fc spacer containing CAR T cells proliferated when cultured alone, but didn't produce IFNγ. Nevertheless, the IFNγ production here is relatively low, and could be attributed to background release.

The short term proliferation of the ALK48 CAR T cells was investigated at day 4 and day 8 of co-culture by cell trace violet dilution, determined through flow cytometry (Figure 5.6 and Figure 5.7). After 4 days of co-culture, ALK48 CAR T cells showed no evidence of proliferation in the representative histogram plots, with potentially slight population shifts when stimulated with PMA and ionomycin (Figure 5.6A). Only ALK8-CD8-28ζ proliferated on co-culture with SUP-T1 ALK cells. In order to quantify the change in proliferation of CAR T cells compared to UT T cells from the same donor cultured alone, the ΔMFI was determined (Figure 5.6B). The ΔMFI shows all four CAR T cells responded to PMA and ionomycin stimulation, as expected. ALK8-CD8-28ζ showed similar patterns of proliferation as shown in chapter 3 (section 3.3.5.1), with the highest proliferation with the high ALK expressing cell line, SUP-T1 ALK. This trend was also seen with ALK48-CD8-28ζ, but to a much lesser extent. The proliferation patterns were similar at day 8 of co-culture (Figure 5.7), however there was a more pronounced response to PMA and ionomycin stimulation. ALK48 CAR T cells showed a greater response to SUP-T1 ALK co-culture, however the histograms demonstrate two different populations of proliferating and non-proliferating cells. While the histograms only show one donor, this phenomenon was also present for the second donor. Interestingly, this didn't appear to be the case for ALK8-CD8-28ζ, or for any other ALK CAR T cells investigated in chapter 3 results (Figure 3.10

and Figure 3.11). It would be interesting to look at the phenotype of these responders and non-responders, for example, the CD4 and CD8 populations. This could offer an explanation as to why some appear to be proliferating more than others.

The differences between the ALK8 scFv and the ALK48 scFv are unknown, apart from their DNA sequences. Of course, the differences we see in their functionality in this panel of *in vitro* assays could also be due to the differences in the scFv, for example, to which epitope of the ALK antigen they recognise and bind to. Mapping of epitope binding of the scFvs would therefore be an interesting experiment to validate potential reasons between functional differences. The binding epitope on the target antigen also influences the distance between the CAR-bound epitope and the target cell membrane influences the synapse formation between the target cell and the CAR expressing T cell. One method of investigating this is to produce truncated isoforms of ALK, removing certain parts of the ALK antigen, for example parts of the ectodomain which are believed to be involved in ligand binding. These isoforms can be expressed on the surface of an ALK negative cell line, such as 293Ts, and ALK CAR binding can be assessed. In this way, Sotillo *et al*., investigated the binding of the FMC63 CD19 CAR T scFv to different truncated isoforms of CD19 (Sotillo et al., 2015).

The data produced in this chapter, along with the data produced in chapter 3, suggest there is a complex relationship between target antigen density, CAR surface expression level and CAR T cell composition. To an extent it is expected that as the level of target antigen density increases or decreases, the level of target recognition by a CAR and subsequent killing, cytokine release and proliferation will also increase or decrease, respectively. Walker *et al*.,

demonstrated this by utilising a panel of NALM-6 leukaemia lines overexpressing ALK at different densities, showing that there is a critical role for target antigen density in limiting CAR efficacy, in agreement with previous reports showing impaired CAR T cell lytic capacity at low antigen densities (Walker et al., 2017). It was concluded that antigen density governs several aspects of ALK CAR T cell function, and it has a substantial impact on the efficacy of CAR T cell anti-tumour responses *in vivo* (Walker et al., 2017). In cases where target antigen density has been modulated, for example, through the use of Bryostatin1 to upregulate the expression of CD22 on leukaemia and lymphoma cell lines, it was seen to improve the *in vitro* and *in vivo* functionality of an anti-CD22 CAR T cell (Ramakrishna et al., 2019). Based on the importance of target antigen density, it would be a beneficial experiment to quantify the number of ALK molecules per cell for the cell lines used. Previously, the relative expression of ALK, as per MFI, was used as a marker of how bright a cell line was for ALK surface expression (Figure 3.2). In this way, a more accurate determination of the threshold surface of ALK target density could be determined.

The difference in results found could also be attributed to the different CAR structures that are included within this assay. The ALK CARs which contained the CD8 transmembrane domain and CD8 stalk region, namely ALK8-CD8-28ζ and ALK48-CD8-28ζ (Figure 5.1C), acted in an almost identical manner in the cytotoxicity experiment (Figure 5.3). In contrast, no cytotoxic activity was seen by ALK48-Fc-28ζ or ALK48-28ζ. With regards to anti-CD19 CAR T cells, it has previously been shown that CARs expressing a CD8α hinge and transmembrane domains produced lower levels of cytokines and exhibited lower levels of AICD

compared to CARs expressing a CD28 hinge and transmembrane domains (Alabanza et al., 2017).

5.5 Conclusions and future directions

The combination of the previously published anti-ALK scFv, ALK48, with different stalk and hinge regions was compared to ALK8-CD8-28ζ. While ALK48 combined with a CD8 stalk acted in a similar manner to ALK8-CD8-28ζ in terms of cytotoxicity, ALK8-CD8-28ζ demonstrated higher levels of cytokine production and proliferation. ALK48 combined with an Fc spacer or the published hinge/transmembrane region demonstrated little activity in the assays described above.

As described previously, the ALK target density is too low on neuroblastoma cell lines for full activation of the second generation ALK-CAR constructs described. Given the restrictive nature of the anti-ALK8 scFv, and the indication that ALK8-CD8-28ζ may be more effective than the previously published ALK scFv in the same CAR combination, ALK8-CD8 was taken forward for use in a dual targeting CAR system.

6 Utilising ALK in a dual-targeting CAR

6.1 Introduction

The data described in the previous chapters has highlighted the importance of target antigen density in the functionality of CAR T cell therapies. In the case of ALK, we have shown decreased functionality of multiple second generation ALK CAR T cells when target antigen density is lower, in line with what has previously been documented in the literature (Walker et al., 2017). The thresholds of antigen expression required to activate CARs has been investigated in multiple pre-clinical models (Yoshida et al., 2016, Watanabe et al., 2015, Majzner et al., 2020). At low target antigen densities, it was demonstrated that CARs produce lower levels of IL-2 or IFNγ, regardless of the addition of co-stimulatory domains or alterations to the scFv binding affinity, demonstrating its critical role in efficient CAR functioning (Chmielewski et al., 2011). Despite this, when ALK antigen density was high enough, anti-ALK CAR T cells demonstrated cytotoxic activity, proliferation and proinflammatory cytokine production in an antigen-dependent manner. Furthermore, anti-ALK CAR T cells expressing a CD8 stalk region as opposed to an Fc spacer, demonstrated clear antigen-dependant proliferative capacity in a short-term setting.

Based on this, the final chapter of this thesis aimed to investigate how ALK could be utilised in a dual-targeting CAR system. By combining an anti-ALK CAR with another CAR also specific for a neuroblastoma associated antigen, such as GD2, the functionality of the ALK CAR could potentially be increased. In this way, the T cell ‘signal 1’ (CD3ζ) is physically dissociated from the costimulatory ‘signal 2’ into two separate CAR constructs of differing antigen specificity (Lanitis et al.,

2013). This dual-targeting system has multiple benefits over a single monotherapy CAR T cell. While potentially increasing the functionality of ALK as a target for neuroblastoma, the specificity of the therapy should also be increased. In theory, CAR T cell reactivity will be in a setting when only both target antigens are present, sparing the destruction of single positive tissues. This approach has previously been described for different antigenic targets (Lanitis et al., 2013, Wilkie et al., 2012, Kloss et al., 2013) but never previously using ALK CAR or targeting neuroblastoma.

6.2 Aim

The first aim of this chapter was to create a single endodomain anti-ALK CAR T cell containing CD3ζ signalling domain only, for combination with a GD2-Fc-28 single endodomain CAR. The second aim was to determine if expressing these single constructs together could increase the following on co-culture with double antigen positive cells:

(i) Production of pro-inflammatory cytokines

(ii) Activation and degranulation marker expression

(iii) Level of proliferation

6.3 Results

6.3.1 Production of ALK8-CD8-ζ

Within the lab group a GD2-Fc-28 single endodomain construct had already been produced (Figure 6.1A) (generated by Wisidagamage Don Nisansala Dilrukshi and Pierre Abramowski, UCL GOSH). This construct contains the RQR8 domain, which can be detected through binding of the anti-CD34 antibody. Based on this, a cloning strategy was devised to produce a single endodomain anti-ALK construct combined with CD3ζ alone. Based on Chapter 3, the anti-ALK scFv 'ALK8' combined with the CD8 stalk was chosen to be used. Given the RQR8 domain was present with GD2-Fc-28, a myc tag was added in order to allow for surface detection with an anti-myc antibody. In order to have the ALK8-CD8-ζ construct in the same backbone as GD2-Fc-28, the restriction site BstBI was added into the original GD2-CD8-28ζ second generation CAR T cell through site-directed mutagenesis (Figure 6.1B). Based on this, and the position of the MluI restriction site, the following geneblock was designed and produced by IDT:

1. BstBI-myc-ALK8H3-CD8-CD8TM-CD3ζ-MluI

Subsequently, the geneblock was inserted into the GD2 CAR backbone through restriction cloning to create ALK8-CD8-ζ (Figure 6.1C). The DNA sequences were all validated through restriction digest and Sanger sequencing (Source Bioscience).

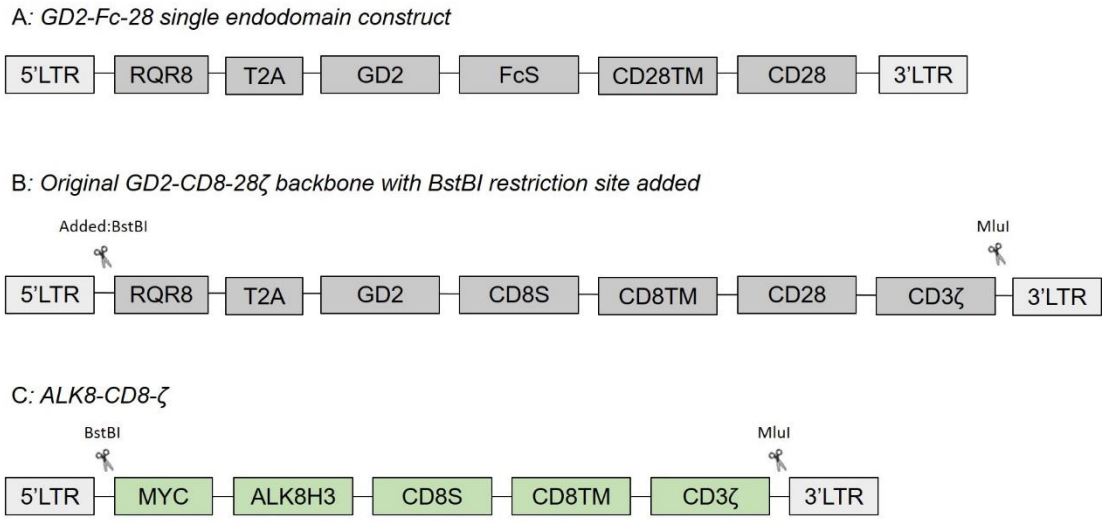

Figure 6.1 Design of ALK single endodomain construct

ALK8-CD8-ζ was designed and produced through restriction cloning. (A) the anti-GD2 scFv was combined with an Fc spacer region (FcS), a CD28 transmembrane domain (CD28TM) and a CD28 endodomain. This construct was co-expressed with an RQR8 domain by use of a T2A self-cleaving peptide, allowing for surface detected through anti-CD34 binding. (B) the original second generation anti-GD2 CAR construct, which contains an MluI restriction site after the CD3ζ endodomain. The restriction site BstBI was added before the RQR8 domain, using site directed mutagenesis. (C) geneblock encoding 'BstBI-Myc-ALK8-CD8S-CD8TM-CD3ζ-MluI' was created and inserted into GD2-CD8-28ζ backbone (B) using restriction cloning.

6.3.2 Production of an ALK and GD2 positive control cell line

In previous chapters the lymphoma cell line, SUP-T1, has been utilised as a matched control cell line for ALK expression. In order to produce a double positive control cell line, the SUP-T1 ALK cell line was transduced with an oncoretroviral SFG vector encoding both GD3 synthase and GM2/GD2 synthase separated by a T2A peptide. These enzymes are required for the stable surface expression of the GD2 ganglioside. The SUP-T1 ALK cell line was transduced with γ-retroviral supernatant produced from triple transfection of 293T cells with the GD2 plasmid. Following transduction, the cell line was sorted by flow cytometry to select on the high ALK and high GD2 expressing cells, detected through APC and FITC staining, respectively (Figure 6.2A). This expression was further confirmed after a week in cell culture conditions, post cell sort by flow cytometry (Figure 6.2B).

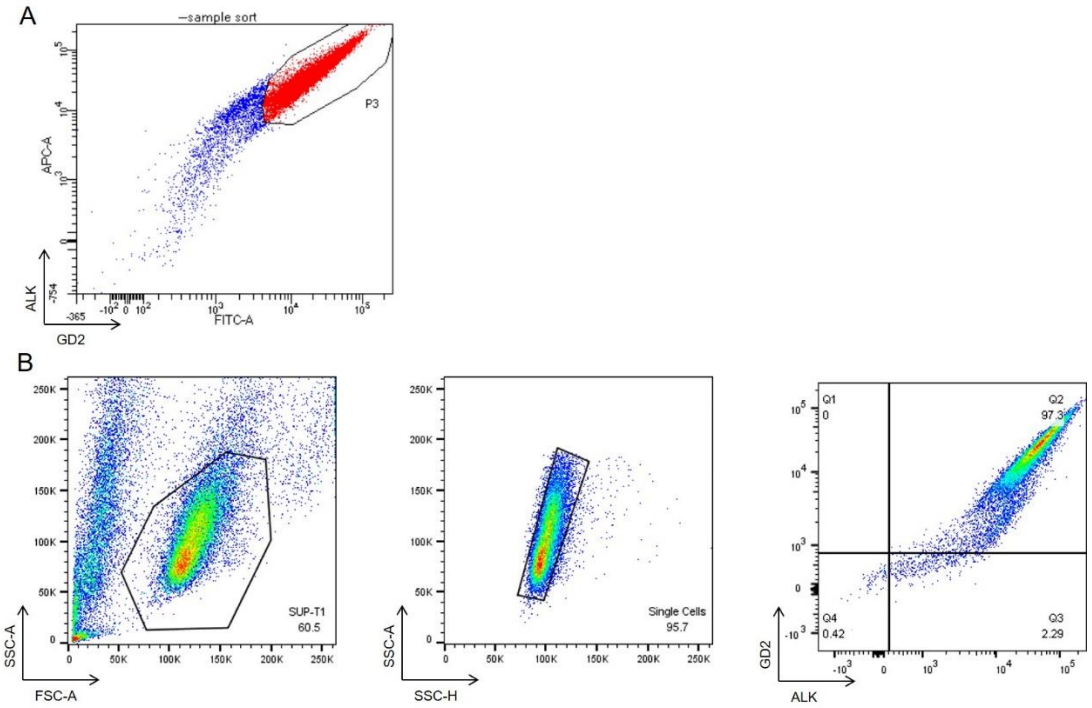

Figure 6.2 Production of SUP-T1 ALK_GD2

The SUP-T1 ALK cell line was transduced to express GD2 using retroviral supernatant. This cell line was sorted to identify high ALK and high GD2 expressing cells by flow cytometry (A). (B) Confirmation of GD2 and ALK expression on the SUP-T1 ALK_GD2 cell line after one week in cell culture. ALK+GD2+ populations were identified from the single cell lymphocyte population.

6.3.3 Expression of ALK and GD2 on neuroblastoma cell lines

While ALK expression was previously described (section 3.3.3.1), the expression of surface GD2 has not been characterised for this thesis. For that reason, the surface expression of both ALK and GD2 was determined through flow cytometry. ALK and GD2 were expressed on all neuroblastoma cell lines Lan-1, Kelly and Lan-5, as expected (Figure 6.3A). SUP-T1 WT was confirmed negative for both ALK and GD2 (Figure 6.3B). SUP-T1 ALK was confirmed positive for ALK and negative for GD2. SUP-T1 GD2 was confirmed negative for ALK and positive for GD2. Finally, SUP-T1 ALK_GD2 was confirmed positive for both ALK and GD2.

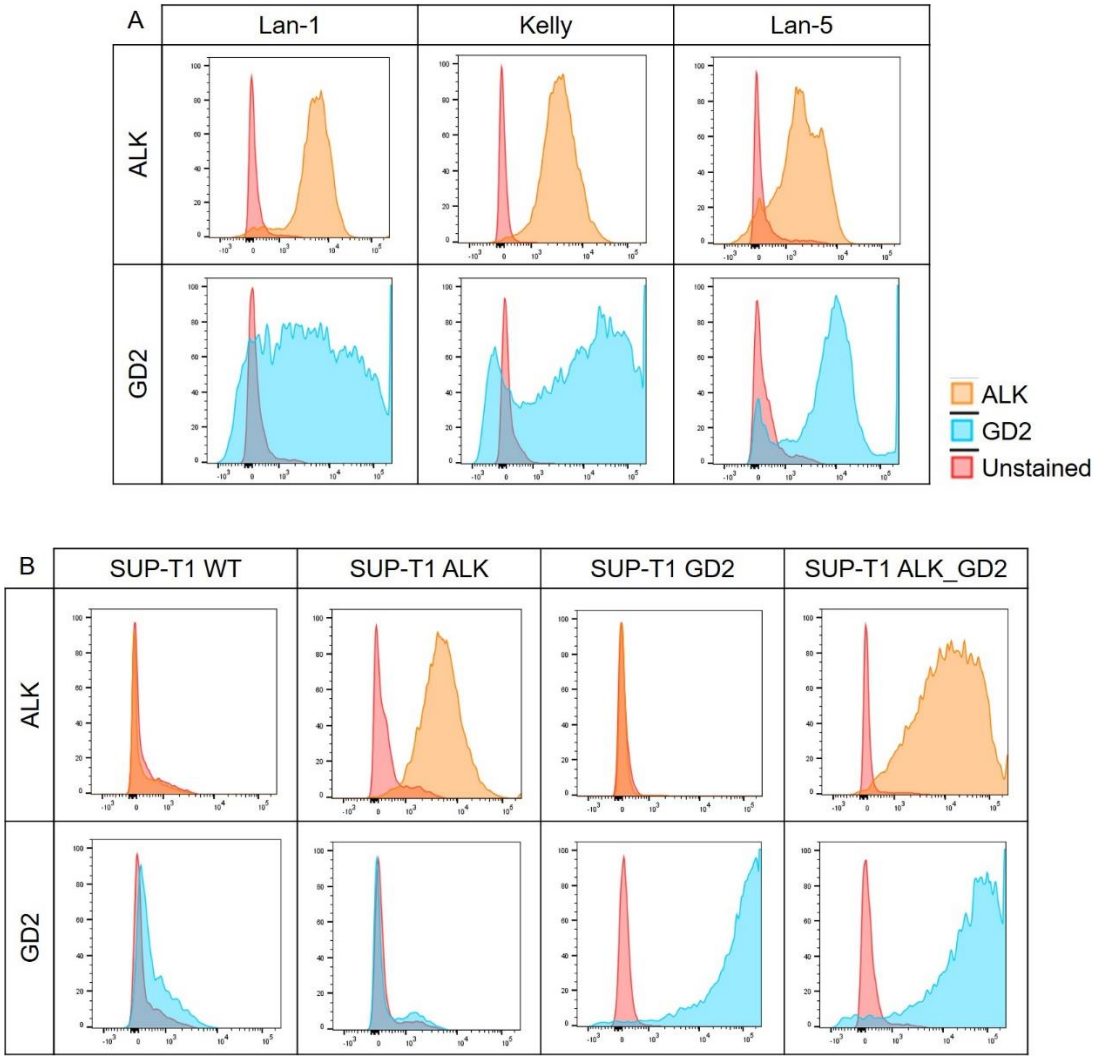

Figure 6.3 Relative expression of GD2 and ALK on cell lines

The surface expression of ALK and GD2 was determined by flow cytometry on (A) neuroblasotma cell lines and (B) control SUP-T1 cell lines. Median fluorescence intensity (MFI) is displayed against unstained controls (n=1 independent experiments).

6.3.4 Confirmation of surface expression

After producing ALK8-CD8-ζ I wanted to confirm it could be expressed on the surface of cells and detected through flow cytometry. Furthermore, I wanted to confirm that both ALK8-CD8-ζ and GD2-Fc-28 could be expressed on cells at the same time through mixing of single construct virus for transduction. As previously discussed, the surface detection of constructs containing the RQR8 domain, present in GD2-Fc-28, is through the binding of anti-CD34 to this domain. As ALK8-CD8-ζ contains a myc tag, surface expression of this construct was determined through anti-myc binding. Therefore, binding of anti-CD34 to RQR8, and anti-myc to the myc tag, were used as a marker of successful co-transduction.

In order to do this, γ-retrovirus was produced through the triple transfection of 293T cells with the ALK8-CD8-ζ and GD2-Fc-28 plasmids. Following this, Jurkats were transduced with virus for the single CAR constructs, and with mixed virus from the two single CAR constructs (herein referred to as the double CAR). Figure 6.4A demonstrates that the ALK8-CD8-ζ could successfully be expressed on the surface of Jurkat cells, detected through anti-myc staining. Furthermore, this staining was unaffected by the presence of anti-CD34 staining. Figure 6.4B demonstrates that ALK8-CD8-ζ and GD2-Fc-28 can be detected on the surface of Jurkat cells through anti-myc and anti-CD34 staining, respectively. Moreover, Jurkats transduced to express the double CAR can be detected on the surface with both anti-myc and anti-CD34 staining.

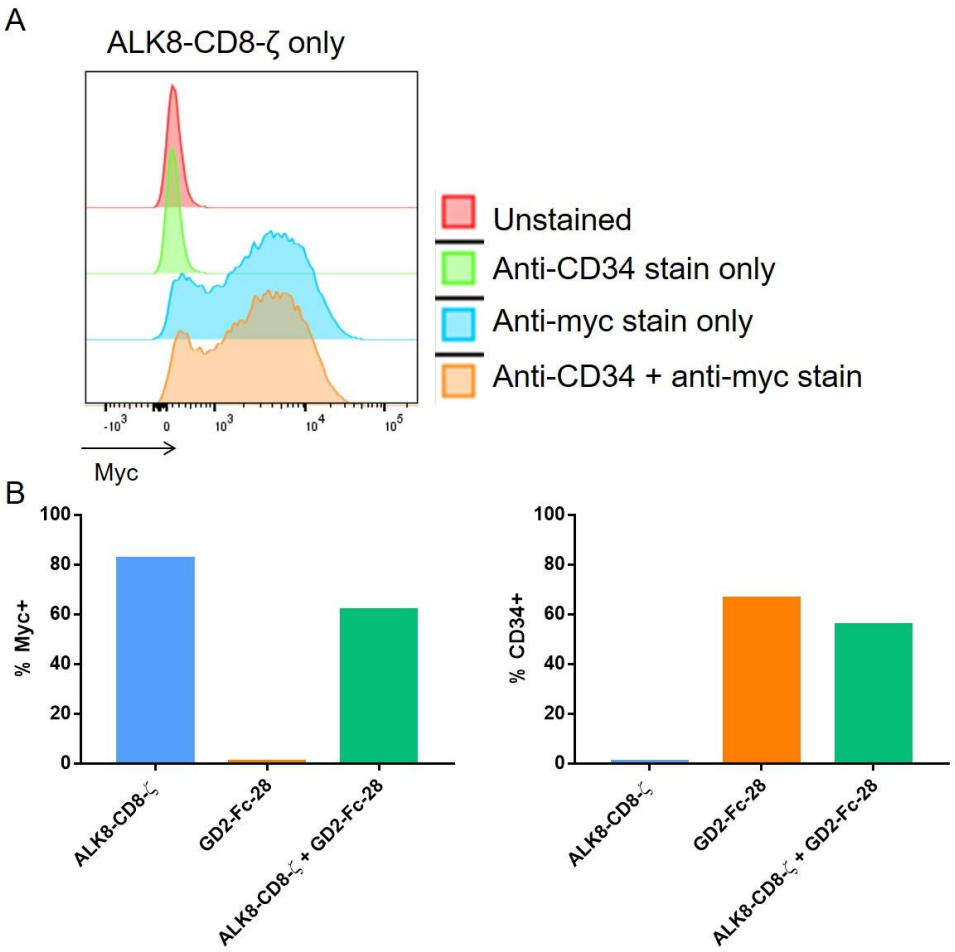

Figure 6.4 Expression of single endodomain and double CAR on Jurkat cells

Jurkat cells were transduced to express ALK8-CD8-ζ, GD2-Fc-28 or the double CAR with γ-retrovirus produced from the triple transfection of 293Ts. (A) ALK8-CD8-ζ could successfully be detected on the surface of Jurkat cells through the binding of an anti-myc antibody, detected through flow cytometry. (B) Surface expression of ALK8-CD8-ζ was detected through anti-myc staining, GD2-Fc-28 was detected through anti-CD34 staining, and the double CAR was detected through both anti-myc and anti-CD34 staining, through flow cytometry (n=1).

6.3.5 Expression on primary T cells

Next the expression of ALK8-CD8-ζ alone, GD2-Fc-28 alone and the double CAR was investigated on primary T cells. PMBCs were isolated from healthy donors, and activated αβ T cells were transduced with retroviral supernatant produced from triple transfection of 293T cells with CAR plasmids. Surface expression of constructs was investigated on CD3+αβTCR+ cells identified through flow cytometry (Figure 6.5A). Single positive myc and CD34 populations could successfully be detected on the surface of αβ T cells through flow cytometry (Figure 6.5B). Similarly, where T cells were transduced to express the double CAR, double positive populations for CD34 and myc could be identified (Figure 6.5B). Overall, the transduction efficacies ranged from 42±15% for the double CAR (mean ± SD, n=3), 60±8% for GD2-Fc-28 (n=3) and 66±8% for ALK8-CD8-ζ (n=3) (Figure 6.5C).

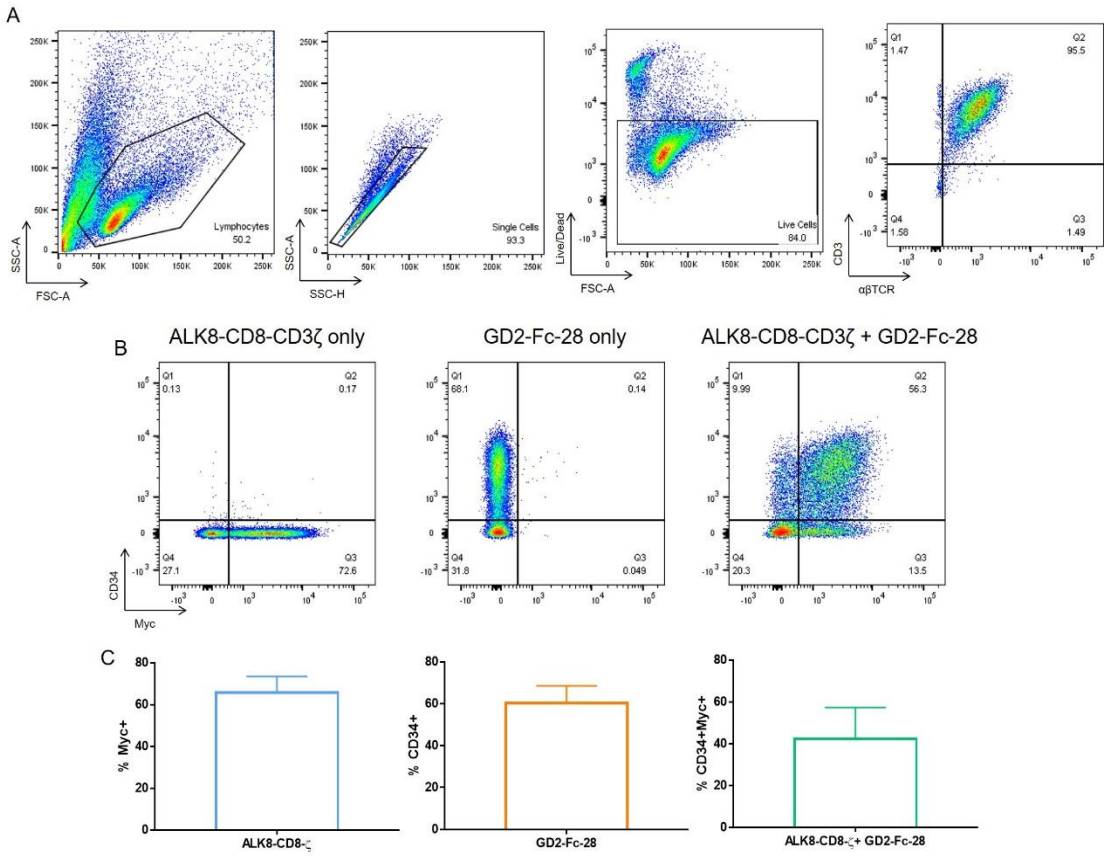

Figure 6.5 Transduction efficacy of ALK and GD2 CAR constructs on primary αβ human T cells

Activated αβ T cells were transduced to express the CAR constructs with retroviral supernatant. Transduction efficacy was determined by quantifying the expression of the RQR8 marker gene and the myc tag. This was achieved by using an anti-CD34 APC antibody and anti-myc PE antibody. (A) Representative plots showing the gating strategy to identify CD3+ αβTCR+ T cells after exclusion of doublets and dead cells. (B) Single ALK and GD2 constructs and double construct can be detected by anti-myc and anti-CD34 staining. (C) Mean expression±SD (n= 3 of individual donors). No statistically significant differences were found between CD34 and myc expression levels by one-way ANOVA followed by Tukey's post-hoc analysis.

6.3.6 Short term effector functions

6.3.6.1 Activation and degranulation markers

The activation of CAR T cells on engagement with ALK and GD2 antigens was investigated through the surface expression of CD69 and CD25 markers. Furthermore, the degranulation of CAR T cells was investigated by measuring the intensity of CD107a surface expression on co-culture of CAR T cells with GD2 and ALK expressing cell lines. CD107a is a marker of T cell degranulation that is exposed to the T cell surface when activated cytotoxic T cells secrete perforins and granzymes against targets, and is therefore a quantitative indicator of lytic function by T cells (Brownrigg et al., 2019, Betts et al., 2003). In this research chapter it was not possible to undertake ^{51}Cr based cytotoxicity assays, and therefore investigating CD107a acted as a surrogate readout. In order to do this, CAR T cells were co-cultured with the neuroblastoma cell lines: Lan-1, Kelly or Lan-5 (Figure 6.6), or the SUP-T1 cell lines: SUP-T1 WT, SUP-T1 GD2, SUP-T1 ALK or SUP-T1 ALK_GD2 (Figure 6.7). After 18 hours of co-culture, the expression of CD69, CD25 and CD107a was determined on CAR T cells through flow cytometry.

Figure 6.6A and Figure 6.6B show the expression of activation markers from CAR T cells. There is a clear shift in the percent of CD25+ CAR T cells when the double CAR was co-cultured with Lan-1, Kelly and Lan-5 cell lines, despite only demonstrating significance compared to GD2-Fc-28 on co-culture with Lan-5 (Figure 6.6). There was minimal CD25 expression from control UT T cells in all conditions, or GD2-Fc-28 when co-cultured with Kelly or Lan-5 cells. Low level CD25 expression was found from ALK8-CD8-ζ in all culture conditions, and when

GD2-Fc-28 was co-cultured with Lan-1 cells (Figure 6.6A). The double CAR demonstrated significantly higher CD69 expression compared to ALK8-CD8-ζ when co-cultured with Lan-1, Kelly and Lan-5 cell lines, following a similar trend to CD25 expression (Figure 6.6B). GD2-Fc-28 also expressed CD69 on co-culture with neuroblastoma cell lines, which was above that of ALK8-CD8-ζ and the control, UT T cells. As with activation markers, the double CAR demonstrated higher expression of CD107a than ALK8-CD8-ζ, GD2-Fc-28 and UT T cells (Figure 6.6C). Both ALK8-CD8-ζ and GD2-Fc-28 expressed CD107a to similar levels as each other. However, the differences in CD107a expression did not reach statistical significance.

Figure 6.7 shows the expression of CD69, CD25 and CD107a on co-culture with SUP-T1 cell lines. Figure 6.7A shows the expression of CD25 on CAR T cells. There was low background CD25 expression from control UT T cells on co-culture with all cell lines. The largest increase is found when ALK8-CD8-ζ and the double CAR are engaged, namely when co-cultured with SUP-T1 GD2 and SUP-T1 ALK_GD2. Here, there was no evidence that costimulation through the use of the double CAR increased the expression of CD25.

Figure 6.7B shows the expression of CD69 on CAR T cells on co-culture with target cells. Unlike with CD25, there was a higher background level of CD69 expression on control UT T cells, on co-culture with all target cells. The largest increase in CD69 expression was seen when costimulation was provided by the double CAR, most notably when co-cultured with SUP-T1 ALK_GD2. In this instance, ALK8-CD8-ζ on co-culture with cell lines does not increase CD69 expression, apart from on co-culture with SUP-T1 ALK_GD2. Interestingly, GD2-

Fc-28 alone also has increased CD69 expression on co-culture with SUP-T1 GD2 and SUP-T1 ALK_GD2.

Figure 6.7C displays the expression of CD107a. As with CD25 expression, there was low background CD107a expression on control UT T cells. Both ALK8-CD8-ζ and GD2-Fc-28 alone was sufficient to induce modest CD107a expression, in the absence of antigen (SUP-T1 WT). The addition of antigen through target cells does not cause great changes to CD107a expression by ALK8-CD8-ζ or GD2-Fc-28. However, the addition of the costimulation through the double CAR increased the expression of CD107a on co-culture with SUP-T1 ALK_GD2, although not significant.

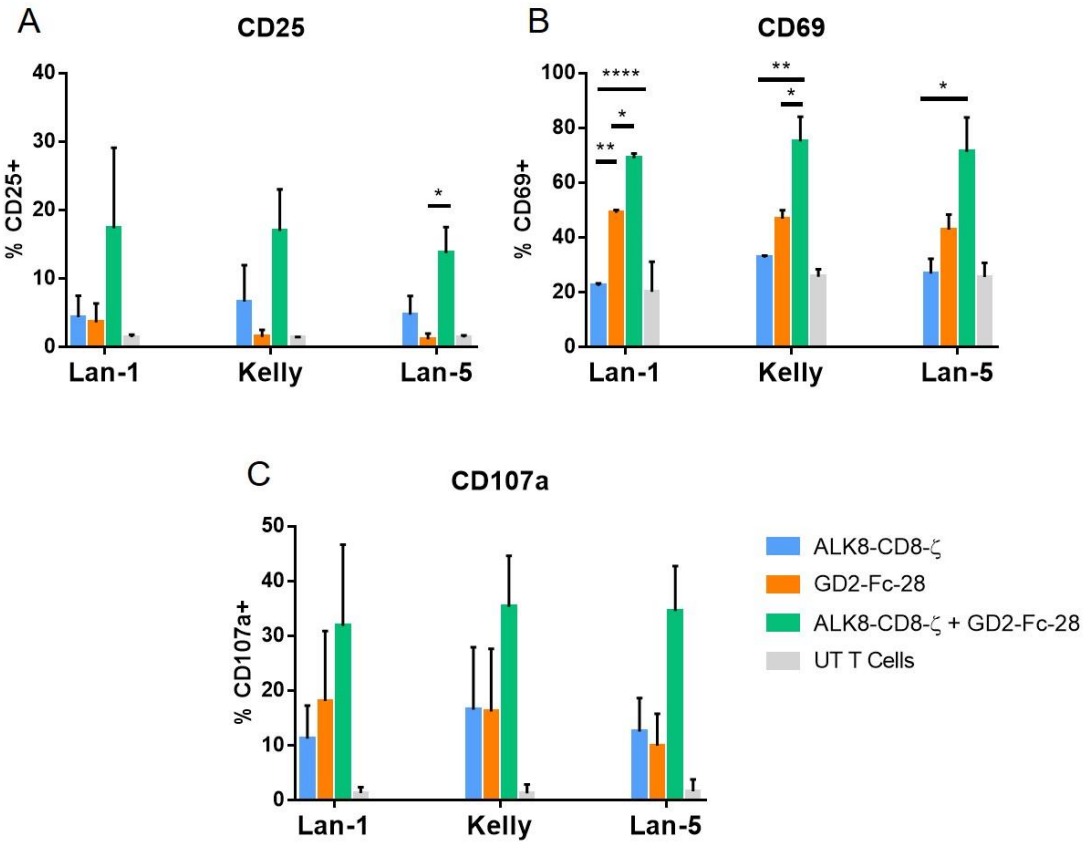

Figure 6.6 Activation and degranulation marker expression of CAR T cells on 18 hour co-culture with neuroblastoma cell lines

Surface expression of CD69 and CD25, activation markers, and CD107a, a degranulation marker, were investigated in ALK8-CD8-ζ, GD2-Fc-28 and double CAR populations. Untransduced (UT) T cells were included as a control for comparison purposes. Expression of (A) CD25, (B) CD69 and (C) CD107a were determined using flow cytometry analysis, performed after 18 hour co-culture with the following neuroblastoma cell lines; Lan-1, Kelly and Lan-5. Data shown is mean±SEM (n= 3 of individual donors). Statistical analysis was performed with one-way ANOVA comparing double CAR to ALK8-CD8-ζ and GD2-Fc-28, followed by Tukey's post-hoc analysis: * p<0.05, ** P<0.01, *** p<0.001, **** p<0.0001.

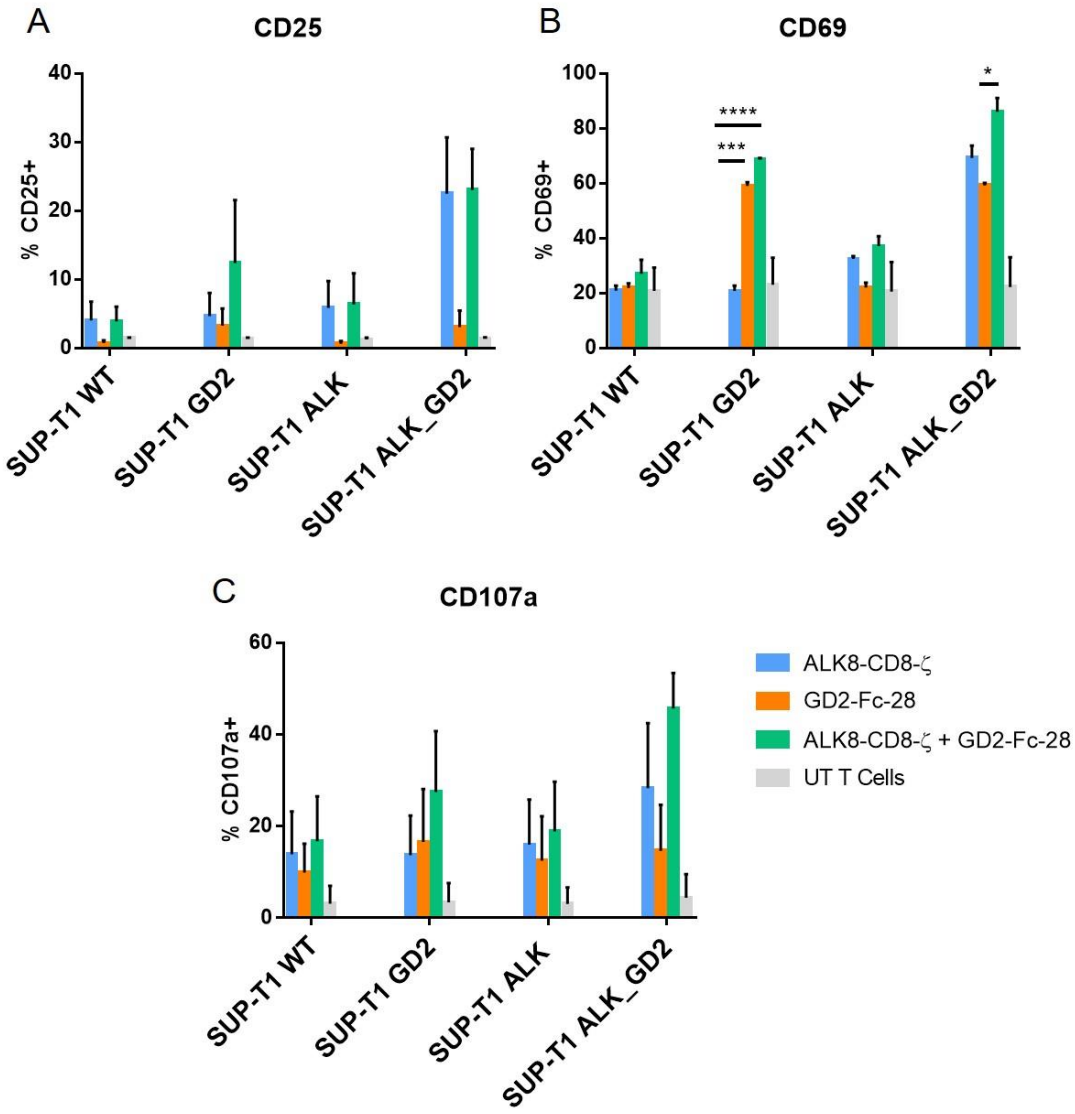

Figure 6.7 Activation and degranulation marker expression of CAR T cells on 18 hour co-culture with SUP-T1 cell lines

Surface expression of CD69 and CD25, activation markers, and CD107a, a degranulation marker, were investigated in ALK8-CD8-ζ, GD2-Fc-28 and double CAR populations. Untransduced (UT) T cells were included as a control for comparison purposes. Expression of (A) CD25, (B) CD69 and (C) CD107a were determined using flow cytometry analysis, performed after 18 hour co-culture on co-culture with SUP-T1 cell lines expressing no antigen (SUP-T1 WT), single positive for GD2 or ALK (SUP-T1 GD2 and SUP-T1 ALK), or double positive for GD2 and ALK (SUP-T1 ALK_GD2). Data shown is mean±SEM (n= 3 of individual donors). Statistical analysis was performed with one-way ANOVA comparing double CAR to ALK8-CD8-ζ and GD2-Fc-28, followed by Tukey's post-hoc analysis * $p<0.05$, ** $P<0.01$, *** $p<0.001$, **** $p<0.0001$.

6.3.6.2 Cytokine production

The production of IL-2 and IFNγ was investigated after 24 hours of co-culture. CAR T cells were co-cultured with neuroblastoma and SUP-T1 cell lines at a 1:1 E:T ratio, before cytokine levels were determined through ELISA.

When CAR T cells were co-cultured with Lan-1, Kelly and Lan-5, only the double CAR showed any production of IL-2 (Figure 6.8A). While the double CAR also produced the highest levels of IFNγ on co-culture with the same cell lines, there was also low level release from GD2-Fc-28 on culture with Lan-1, from UT control T cells on co-culture with Lan-1, Kelly and Lan-5, and from ALK8-CD8-ζ on co-culture with Lan-5 (Figure 6.8B). Despite this, the double CAR produced significantly more IFNγ than both single CARs on Kelly and Lan-5 co-culture.

On co-culture with SUP-T1 cell lines, IL-2 was only produced by the double CAR on incubation with SUP-T1 ALK_GD2, along with low level production from ALK8-CD8-ζ in the same culture condition (Figure 6.8C). In a similar trend, the largest amount of IFNγ was produced by the double CAR on co-culture with SUP-T1 ALK_GD2, with low level production from ALK8-CD8-ζ (Figure 6.8D).

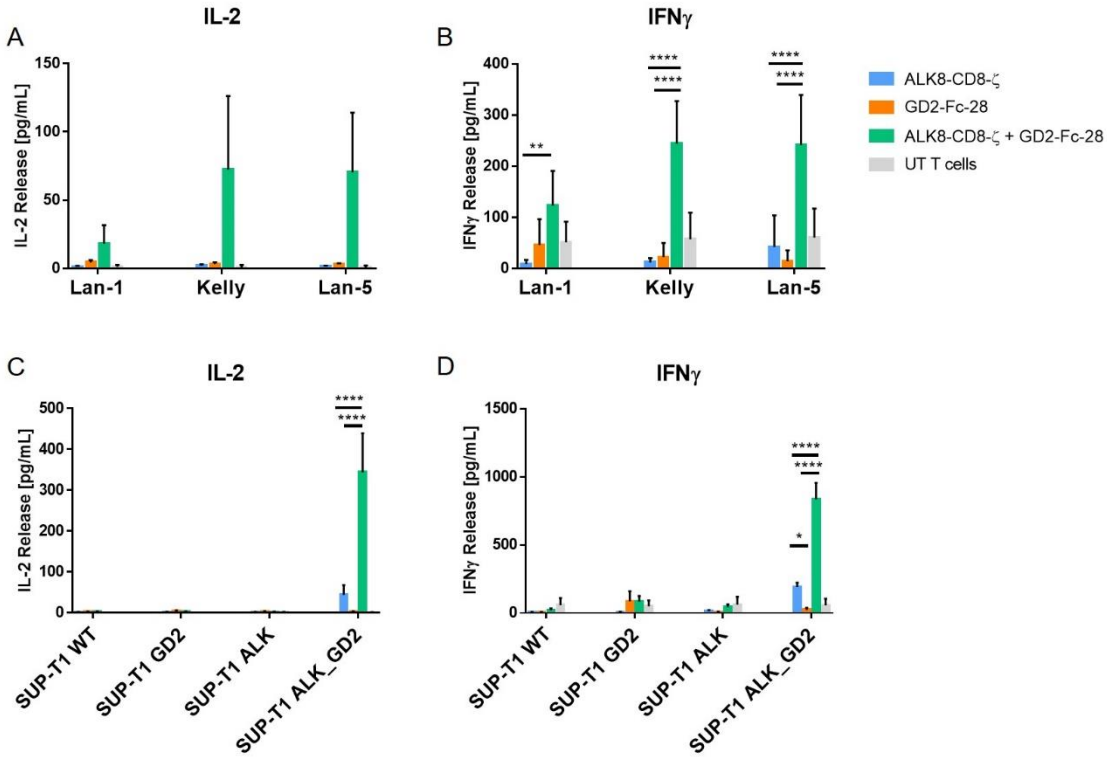

Figure 6.8 Short term cytokine production

IL-2 and IFNγ measured by ELISA from supernatant after 24 hour co-culture of CAR T cells with neuroblastoma cell lines (A-B), or SUP-T1 WT, SUP-T1 GD2, SUP-T1 ALK or SUP-T1 ALK_GD2 (C-D). Untransduced T cells were used as a negative control. Data shows mean±SD (n=3 independent biological replicates). Two-way ANOVA was performed followed by Tukey's post-hoc analysis: * p<0.05, ** P<0.01, *** p<0.001, **** p<0.0001.

6.3.7 Long term effector function

6.3.7.1 Proliferative capacity

Following on from this, the proliferative capacity of the double CAR was investigated, compared to ALK8-CD8-ζ and GD2-Fc-28. Cell trace violet labelled CAR T cells were co-cultured with irradiated SUP-T1-WT, SUP-T1 ALK, SUP-T1 GD2 and SUP-T1 ALK_GD2 and neuroblastoma cell lines, before being analysed through flow cytometry after 4 and 8 days. Figure 6.9 and Figure 6.10 show representative histogram read outs for cell trace violet dilution from one donor, followed by the mean ΔMFI of all three donors. In this case, the ΔMFI of CAR T cells was defined as the difference between the MFI of CAR T cells in co-culture conditions and the MFI of that CAR T cell cultured alone for the same length of time. This was to take into account for any background proliferation that might have been seen in any conditions.

After 4 days of co-culture with neuroblastoma cell lines, the double CAR showed a higher level of proliferation than ALK8-CD8-ζ and GD2-Fc-28 alone (Figure 6.9A). Interestingly, GD2-Fc-28 demonstrated low level proliferation on co-culture with neuroblastoma cell lines, which was also seen from ALK8-CD8-ζ cultured with Lan-5. On co-culture with the antigen negative SUP-T1 WT cell line, the ΔMFI decreased for all CAR T cells, suggesting no proliferation above the background proliferation was seen (Figure 6.9B). The double CAR demonstrated higher proliferation levels on incubation with SUP-T1 GD2 and SUP-T1 ALK cell lines, however this was more pronounced on co-culture with SUP-T1 GD2 cells: showing statistically higher proliferation compared to ALK8-CD8-ζ. While the double CAR also demonstrated increased proliferation on incubation with SUP-

T1 ALK_GD2, there was proliferation from ALK8-CD8-ζ and GD2-Fc-28 CAR T cells also (Figure 6.9B).

The proliferation trends at day 8 reflect those from day 4 of co-culture. The double CAR continued to show higher levels of proliferation when co-cultured with Lan-1, Kelly and Lan-5 cell lines, but to a lesser extent (Figure 6.10A). GD2-Fc-28 also continued to demonstrate low level proliferation when co-cultured with neuroblastoma cell lines, along with ALK8-CD8-ζ on co-culture with Lan-5. These patterns were also reflected in the representative histograms. The ΔMFI of CAR T cells on day 8 of co-culture (Figure 6.10B) with SUP-T1 cell lines also remained similar to day 4 of co-culture (Figure 6.9B). While GD2-Fc-28 and ALK8-CD8-ζ showed no proliferation against SUP-T1 WT, the double CAR showed low level activity which is also seen in the representative histogram. Proliferation against the SUP-T1 GD2 cell line was still evident from GD2-Fc-28 and the double CAR at day 8, which was also seen in the representative histograms. This background proliferation from GD2-Fc-28 was no longer evident on co-culture with SUP-T1 ALK, unlike at day 4 (Figure 6.9B), however both ALK8-CD8-ζ and the double CAR demonstrated proliferation against this cell line. On co-culture with the double positive cell line, SUP-T1 ALK_GD2, the representative histogram showed proliferation from all three CAR T cells, with the greatest proliferative shift from the double CAR, followed by ALK8-CD8-ζ and finally by GD2-Fc-28. This is also reflected in the ΔMFI, however the differences are minimal.

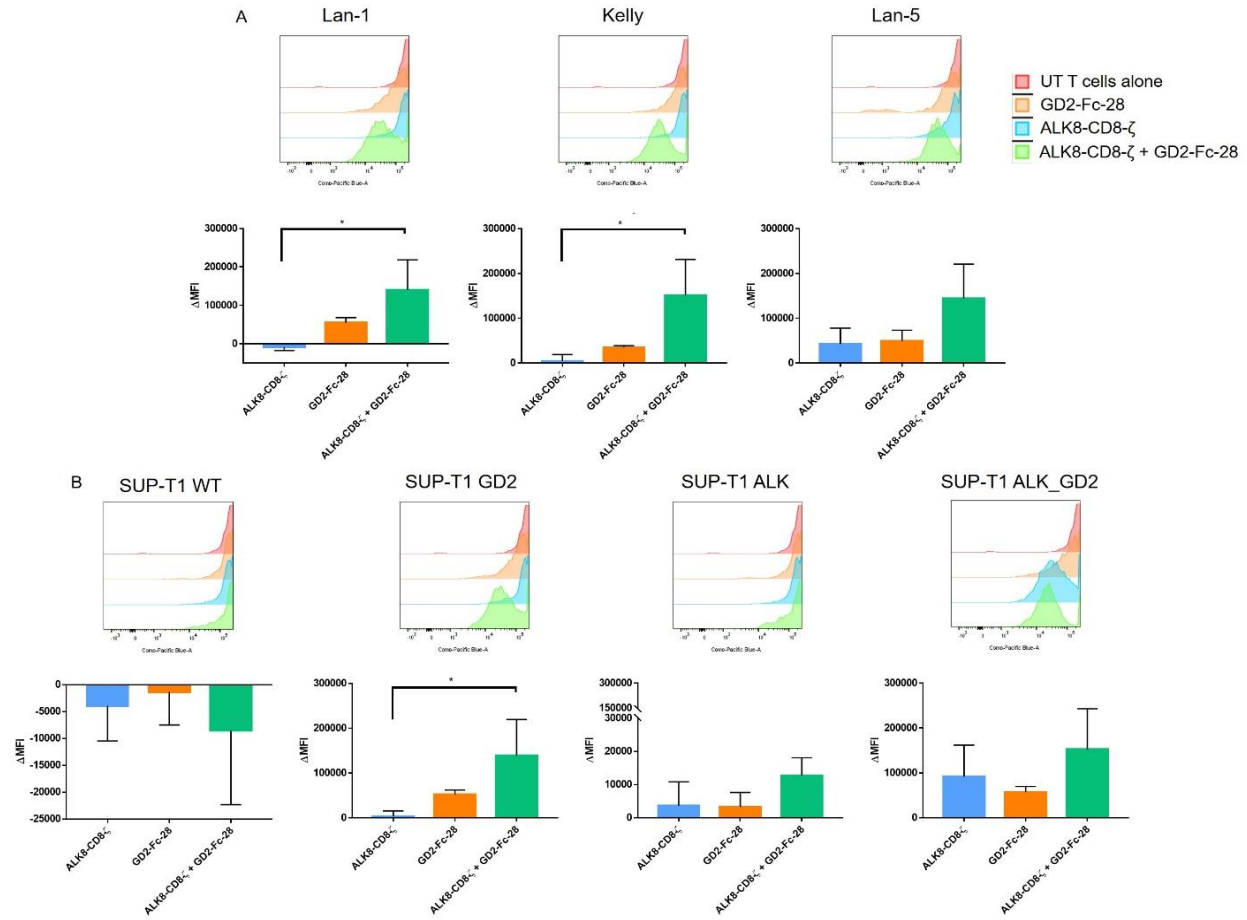

Figure 6.9 Proliferation at 4 days of co-culture

CAR T cells or UT T cells were labelled with cell trace violet dye and co-cultured with irradiated cell lines at a 1:1 E:T ratio for 4 days. Representative histograms from one donor and mean ΔMFI±SD for CAR T cells were determined on co-culture with (A) neuroblastoma cell lines: Lan-1, Kelly and Lan-5, or (B) SUP-T1 WT, SUP-T1 ALK, SUP-T1 GD2 and SUP-T1 ALK_GD2. (n=3 independent biological replicates). One-way ANOVA was performed followed by Tukey's post-hoc analysis: * $p<0.05$.

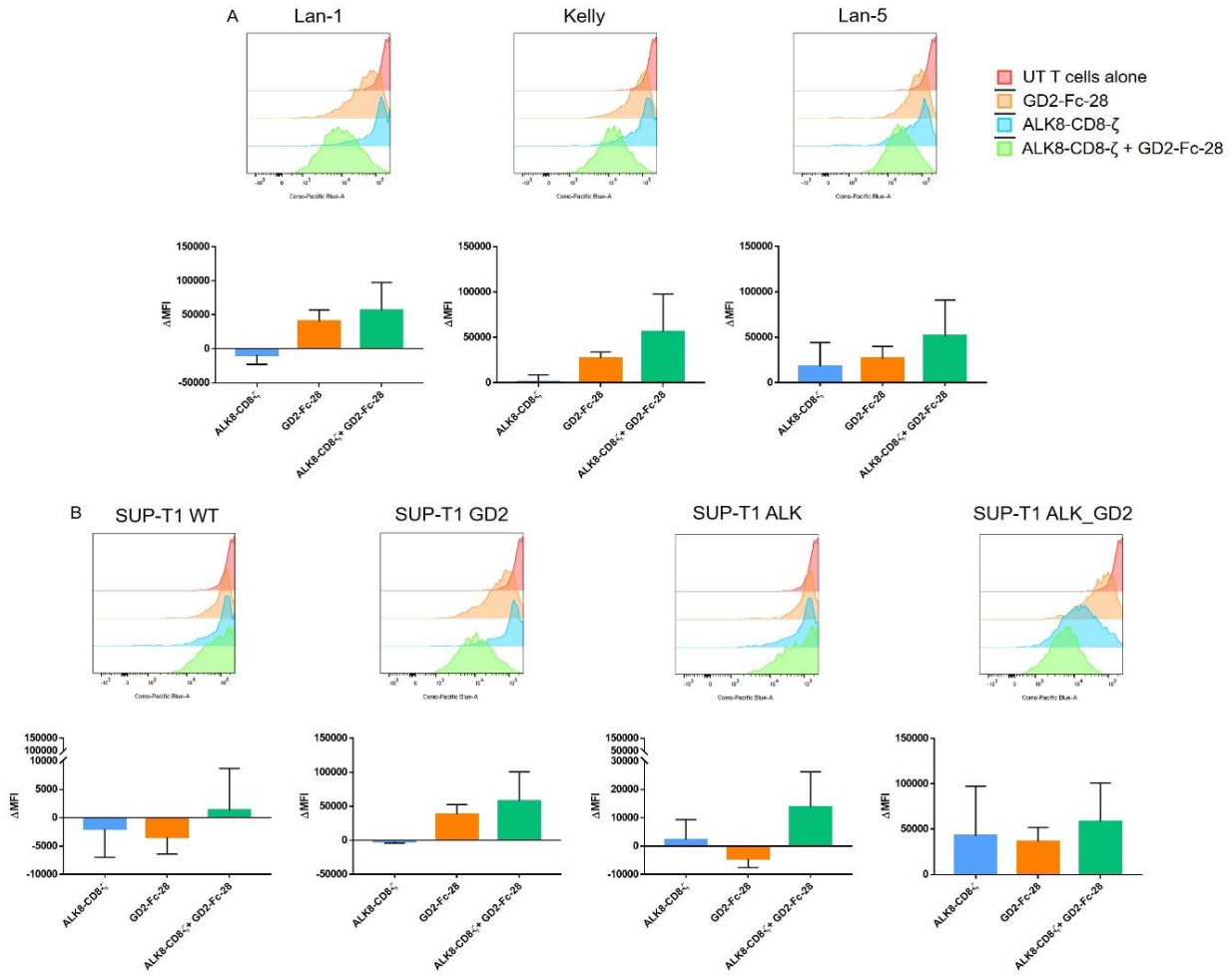

Figure 6.10 Proliferation after 8 days of co-culture

CAR T cells or UT T cells were labelled with cell trace violet dye and co-cultured with irradiated cell lines at a 1:1 E:T ratio for 8 days. Representative histograms from one donor and mean ΔMFI±SD for CAR T cells were determined on co-culture with (A) neuroblastoma cell lines: Lan-1, Kelly and Lan-5, or (B) SUP-T1 WT, SUP-T1 ALK, SUP-T1 GD2 and SUP-T1 ALK_GD2. (n=3 independent biological replicates). One-way ANOVA was performed followed by Tukey's post-hoc analysis.

6.3.7.2 Cytokine Production

To investigate ability of cells to produce cytokine in an antigen-dependent way following antigen-dependent expansion, CAR T cells were co-cultured with irradiated target cells; Lan-1, Kelly, Lan-5, SUP-T1 WT, SUP-T1 GD2, SUP-T1 ALK and SUP-T1 ALK_GD2. After 7 days of co-culture, cells were washed and replated with the original plating conditions. After a further 24 hours of co-culture, the supernatant was harvested and IL-2 and IFNγ was measured through ELISA.

Despite the double CAR showing significantly higher levels of IL-2 production on co-culture with Kelly cells compared to ALK8-CD8-ζ and GD2-Fc-28, the levels are so low this must considered as background (Figure 6.11A). IFNγ was produced by the double CAR on culture with all neuroblastoma cell lines to varying levels, while the single endodomain CARs did not produce cytokine (Figure 6.11B). On co-culture with SUP-T1 cell lines, the double CAR only produced IL-2 and IFNγ on co-culture with SUP-T1 ALK_GD2, which was significantly higher than ALK-CD8-ζ and GD2-Fc-28 (Figure 6.11C and Figure 6.11D).

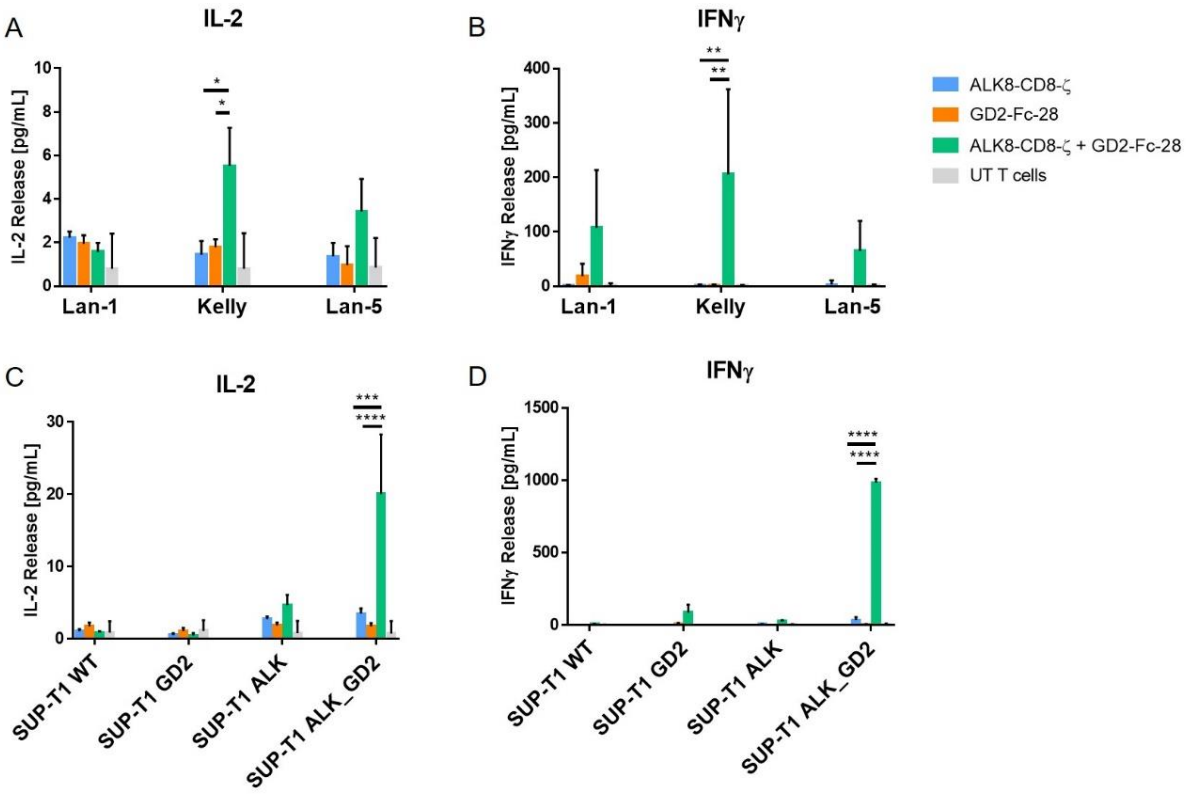

Figure 6.11 Long term cytokine production

IL-2 and IFNγ measured by ELISA from supernatant after 7 hour co-culture of CAR T cells with neuroblastoma cell lines (A-B), or SUP-T1 WT, SUP-T1 GD2, SUP-T1 ALK or SUP-T1 ALK_GD2 (C-D). Untransduced T cells were used as a negative control. Data shows mean±SD (n=3 independent biological replicates). Two-way ANOVA was performed followed by Tukey's post-hoc analysis: * p<0.05, ** P<0.01, *** p<0.001, **** p<0.0001.

6.4 Discussion

Previously, we have demonstrated that second generation anti-ALK CAR T cells as a monotherapy do not produce sufficient responses in low target antigen density settings. This has been well documented for both CARs targeting ALK and other tumour associated antigens (Walker et al., 2017, Ramakrishna et al., 2019, Chmielewski et al., 2011, Watanabe et al., 2015). Despite this, at higher target antigen densities, when anti-ALK scFvs were combined with a CD8 stalk region, there was evidence of antigen-dependant cytotoxic activity, production of proinflammatory cytokines and short term proliferation. A strategy used to improve the therapeutic index of CAR based immunotherapy involves the use of T cells with dual antigen specificity. In this setting, two complementary CARs are co-expressed in the same T cell population, each directed to a distinct tumour target, and engineered to provide complementary signals. In previous investigations, the rationale is to optimise T cell homing and tumour specificity, which in turn reduces 'on-target off-tumour' toxicity, where targeted antigens are also expressed on healthy tissues. However in this chapter, by combining co-stimulation with another neuroblastoma expressed antigen, in this case GD2, the aim was to selectively enhance the activity of the ALK CAR T cell. Due to the physical dissociation of CD3ζ and the co-stimulatory CD28 domain into two separately targeted CAR T cells, the specificity of this system is also enhanced. As such, the use of this dual targeting CAR in the same T cell should result in activation, cytotoxicity and proliferation only in a setting of ALK and GD2 expression: namely against neuroblastoma.

While GD2 was already combined into a co-stimulatory only construct within the lab: GD2-Fc-28, it was decided that the ‘ALK8’ scFv combined with a CD8 stalk region was to be constructed into a CD3ζ only construct. Of course, GD2 could have been combined into the CD3ζ construct and ALK in the co-stimulatory only construct. However, it has previously been documented that within dual targeting CAR systems it is possible for first generation CAR T cells conferring signal 1 only, to become activated at the site of both target antigens, but subsequently continue to exert effects post activation at sites of single antigen expression (Kloss et al., 2013). Kloss *et al*., further demonstrated that by diminishing the efficiency of T cell activation to a level where it is ineffective in the absence of simultaneous chimeric costimulatory receptor (CCR) recognition of the second antigen, this problem can be eradicated (Kloss et al., 2013). Based on the diminished activity of the second generation ALK CAR T cell when target antigen density was lower, it therefore made sense to combine ALK into the CD3ζ only construct (Figure 6.1). As the GD2 single construct contained the RQR8 domain it was necessary to produce ALK8-CD8-ζ with an alternative tag for surface detection. It was successfully demonstrated that ALK8-CD8-ζ could be detected on the surface of Jurkat cells and primary αβ T cells through binding of anti-myc detected through flow cytometry (Figure 6.4 and Figure 6.5).

The most effective way to produce a double construct expressing CAR T cell, herein referred to as the double CAR, was considered. In the above approach, the transduction was achieved by combining γ-retrovirus from two separate constructs, giving a mean transduction efficacy of 42±15% (n=3) (Figure 6.5). It has been commented that transduction with two different vectors per T cell might enhance the risk of insertional mutagenesis by various genetic integrations

(Zimmermann et al., 2020). It may be beneficial to produce an 'all-in-one' vector, which would allow for constitutive expression of both constructs for any T cell infected with virus. Expression of two constructs with the use of a T2A molecule, or an IRES, would ensure equimolar expression, while equal expression cannot be guaranteed with two separate virus infections. Furthermore, within the double transduced populations, there will inevitably be the presence of single positive T CAR T cells also. While the double CAR T cells produced here were only utilised in flow based assays, where it was possible to identify the double myc+ and CD34+ populations, the use of double CAR T cells within non flow based assays would raise problems with identifying a truly double positive population. While it wasn't possible to undertake ^{51}Cr assays for this chapter of work due to lab closure, it would have required flow based cell sorting to identify double CAR+ T cells before undertaking this kind of killing experiment. Furthermore, flow based cell sorting could pose a risk of unwanted CAR T cell activation, before cells have been utilised in assays. Despite this, the transduction efficacy achieved for the double CAR was relatively high (Figure 6.5), in some cases higher than previously achieved for a single second generation CAR T cell (Figure 3.3), potentially as the separate vectors were smaller than the second generation ALK CAR constructs. Furthermore, clear effector differences were seen between the single ALK8-CD8-ζ and GD2-Fc-28 CAR populations compared to the double CAR transduced T cells, suggesting double transduction identified by myc and CD34 was accurate.

In vitro activity of the double CAR T cells was initially tested with the neuroblastoma cell lines Lan-1, Kelly and Lan-5, which all express ALK and GD2 antigen (Figure 6.3A). Furthermore, while the control cell lines SUP-T1 WT, SUP-

T1 ALK and SUP-T1 GD2 were already available for use, it was preferable to incorporate a double antigen positive control cell line with high double antigen expression. SUP-T1 ALK_GD2 was produced and high double positive antigen expression was confirmed by flow cytometry (Figure 6.2). The control cell lines were confirmed either positive or negative for ALK and GD2, as expected (Figure 6.3B).

Initially short term effector functions between the three CAR T cells were compared consisting of co-cultures with neuroblastoma cell lines and control SUP-T1 cell lines, before determining activation and degranulation levels, and cytokine production (Figure 6.6, Figure 6.7 and Figure 6.8). CD25 and CD69 are activation markers which are upregulated on activation and restimulation, but are generally low on resting CAR T cells (Gargett et al., 2016). On co-culture with neuroblastoma cell lines, there was a general shift showing that the double CAR had a higher percentage of CD25 and CD69 expressing cells, compared to ALK8-CD8-ζ and GD2-Fc-28 CAR T cells (Figure 6.6A and Figure 6.6B). This suggests that at these lower ALK antigen expressing cell lines, the double CAR can induce a higher production of proinflammatory cytokines which requires the engagement of both targeted antigens. While there was minimal expression of CD25 on ALK8-CD8-ζ and GD2-Fc-28 CAR T cells and control UT T cells, there was a clear low level expression of CD69 on the aforementioned cells (Figure 6.6A and Figure 6.6B). The upregulation on ALK8-CD8-ζ CAR T cells was in line with that of UT control T cells, suggesting this could be a level of background activation, however there was further upregulation on GD2-Fc-28 CAR T cells (Figure 6.6B). While these chimeric costimulatory receptors (CCR) are required to achieve robust CAR T cell expansion, function, persistence and antitumor activity in combination, they

do not provide a T cell activation signal alone (Sadelain et al., 2013). The upregulation of CD69 on GD2-Fc-28 CAR T cells is therefore unexpected. While the Fc spacer is combined with the second generation GD2 targeting CAR T cell currently being evaluated in a clinical trial (Straathof et al., 2020). I have previously demonstrated that in combination with a second generation ALK CAR T cell the Fc spacer may be responsible for antigen-independent proliferation of CAR T cells (section 3.3.5.1). This could offer a potential explanation as to why there is an increased level of CD69 expression here. As previously discussed, Long *et al*., demonstrated that second generation GD2-28ζ CAR aggregate on the surface of T cells due to their scFv framework which is responsible for their tonic signalling, in an antigen-independent manner (Long et al., 2015). This may also offer an explanation into this higher level of activation seen with GD2-Fc-28.

As previously mentioned, the use of the double CAR in a ^{51}Cr cytotoxicity assay within this set of experiments was not possible at this time. Instead, the levels of surface CD107a were measured. This degranulation marker could be used as a 'surrogate' readout to a killing assay. It has been commented that measuring degranulation directly may be a more direct measurement of T cell cytotoxicity, while ^{51}Cr release assay is actually an indirect measurement of T cell functionality (Betts et al., 2003). Cytotoxic lymphocytes mediate killing of target cells through two major pathways: a granule-dependent method involving perforin and granzyme production, and a granule-independent method involving fas-fasL pathways (Betts et al., 2003). Perforin and granzyme are pre-formed lytic lysosomes located within the cytoplasm which are surrounded by a lipid bilayer containing lysosomal associated membrane glycoproteins (LAMPs), including CD107a (LAMP-1) (Peters et al., 1991). Activated T cells results in the migration

of granules to the plasma membrane and release of granule contents into the immunological synapse resulting in death of target cells, and exposing CD107a as a surface marker which can subsequently be measured (Betts et al., 2003). Surface expression of CD107a was determined after short term co-culture of CAR T cells with neuroblastoma cell lines, and was found to be expressed more highly on double CAR T cells in every culture condition (Figure 6.6C). The engagement of both GD2 and ALK by the double CAR induces a higher level of degranulation, suggesting T cells are more cytotoxic against double positive cell lines when the double CAR is present. Again, there was also an upregulation of CD107a expression of ALK8-CD8-ζ and GD2-Fc-28 CAR T cells, which wasn't present on control UT T cells. This suggests this isn't a background level of expression, and the presence of the single construct CAR T cells is inducing this CD107a upregulation. First generation CAR T cells can induce cytotoxic effects against target cells, however they either fail to persist or become anergic, as tumour cells frequently lack requisite ligands for costimulation (Lanitis et al., 2013). While we did see a shift in CD107a surface expression between CAR T cell populations, perhaps the timings for such an experiment were too long. Betts *et al*., suggests significant expression of cell surface CD107a can be observed as early as 30 minutes following stimulation of primary CD8+ T cells, and reaches a maximum by 4 hours (Betts et al., 2003). Importantly, the double CAR demonstrated an increased upregulation in CD25, CD69 and CD107a compared to ALK8-CD8-ζ and GD2-Fc-28 in a double antigen positive neuroblastoma setting.

Figure 6.7 shows the same experiment, however the target cells, SUP-T1 WT, have been manipulated to express high levels of GD2 alone, ALK alone, or high levels of both. The percentage of double CAR T cells expressing CD25 was

upregulated more highly on co-culture with SUP-T1 GD2 and SUP-T1 ALK_GD2, also shown with ALK8-CD8-ζ CAR T cells (Figure 6.7A). The activity seen from the single ALK8-CD8-ζ CAR T cell isn't completely unexpected. First generation constructs, such as this, are capable of providing a comparable stimulatory signal to that of the entire CD3 complex (Haynes et al., 2001, Irving and Weiss, 1991). However, in *in vivo* settings they are insufficient to sustain antitumor responses, due to lack of proliferation and cytokine production from T cells (Brocker and Karjalainen, 1995). CD69 was also upregulated on double CAR expressing T cells in response to co-culture with SUP-T1 GD2, along with expression on GD2-Fc-28 (Figure 6.7B). Clearly, the presence of the GD2 antigen on target cells engaging with the anti-GD2 scFv, is inducing activation, even in the absence of signal 1: in the case of GD2-Fc-28 alone. While there was a small increase in CD69 activation by double CAR T cells on co-culture with the SUP-T1 ALK_GD2 cell line, both ALK8-CD8-ζ and GD2-Fc-28 also had high levels of CD69 expression (Figure 6.7B). Perhaps the upregulation on GD2-Fc-28 could be due to previous activation. One possible explanation is that all CAR T cells have previously been activated with anti-CD3 and anti-CD28 9 days prior to being used in the proliferation assay. While there is an assumption that the response to this stimulation will have slowed by then, these CAR T cells subsequently engage with an antigen and form an immune synapse, which could induce a level of activation, even without the presence of CD3ζ.

The expression of CD107a was more highly upregulated on the double CAR co-cultured with SUP-T1 ALK_GD2, however there was also upregulation on the double CAR co-cultured with SUP-T1 WT, SUP-T1 GD2 and SUP-T1 ALK (Figure 6.7C). Equally, there was also CD107a expression on ALK8-CD8-ζ and GD2-Fc-

28 on co-culture with these SUP-T1 cell lines, albeit at lower levels than the double CAR. The expression on UT control T cells is low, suggesting the degranulation seen from the single endodomain CARs is not background. This could be due to multiple reasons previously discussed, such as first generation CAR signalling on engagement of antigen, or previous activation of CAR T cells resulting in signalling on antigen engagement. The fact there is evidence of degranulation by the double CAR in the presence of single antigen positive cell lines, could suggest there is clustering of the two CAR receptors and subsequent activation of both on engagement of single antigen. This, however, does not explain why there is evidence of degranulation in the presence of SUP-T1 WT cells.

The production of IL-2 and IFNγ were determined after 24 hours of co-culture with neuroblastoma cells (Figure 6.8A and B) or with SUP-T1 cell lines (Figure 6.8C and D). Clearly, IL-2 was only produced when the double CAR was incubated with Lan-1, Kelly and Lan-5 cell lines, to varying degrees (Figure 6.8A). This trend was also seen with IFNγ, with the highest production consistently being from the double CAR (Figure 6.8B), suggesting both antigens require engagement from the double CAR for proinflammatory cytokine production. In contrast to IL-2, control UT T cells in all conditions, along with ALK8-CD8-ζ co-cultured with Lan-5 and GD2-Fc-28 co-cultured with Lan-1, produced some low level background IFNγ. As previously mentioned, first generation CAR T cells do have the capability to become activated and signal, which could explain why ALK8-CD8-ζ produced IFNγ on co-culture with the highest ALK expressing neuroblastoma cell line, Lan-5. When CAR T cells were co-cultured with SUP-T1 cell lines, IL-2 was only produced by the double CAR incubated with the double antigen positive cell line,

SUP-T1 ALK_GD2, as expected (Figure 6.8C). ALK8-CD8-ζ also produced low levels of IL-2 on co-culture with this cell line. In some ways this could be expected, due to the high target antigen density of ALK on this cell line. However, the SUP-T1 ALK_GD2 was produced from the SUP-T1 ALK cell line, and therefore the antigen density of ALK on these cell lines would be expected to be the same. One possible explanation is that the brightness of ALK surface expression may be dimmer on SUP-T1 ALK, due to the long standing nature of culturing. When SUP-T1 ALK_GD2 was produced, only the highest ALK expressing cells were sorted by flow cytometry to create the new population. Perhaps the surface expression of ALK on the SUP-T1 ALK_GD2 cell line is therefore higher than that on the SUP-T1 ALK cell line. In future, it would be beneficial to sort SUP-T1 ALK by flow cytometry to ensure a highly bright ALK surface antigen density. With regard to IFNγ production, again the double CAR when co-cultured with SUP-T1 ALK_GD2 only produced a high level of cytokine (Figure 6.8D). There was low levels of IFNγ from UT control T cells, from GD2-Fc-28 and double CAR on co-culture with SUP-T1 GD2, and from ALK8-CD8-ζ on co-culture with SUP-T1 ALK_GD2. The low level reactivity from GD2-Fc-28 against SUP-T1 GD2 could be attributed to the tonic nature of both the GD2 scFv and the Fc spacer, however in previous publications this tonic signalling has been shown to be antigen-independent also (Long et al., 2015). This suggests it should be witnessed in every co-culture condition, which interestingly isn't the case.

In order to investigate longer term effects of CAR T cells, proliferation was investigated at day 4 and day 8, along with cytokine production after 7 days of co-culture and antigen restimulation. In previous chapters, the ΔMFI of CAR T cells was determined by comparing the MFI of CAR T cells with the MFI of UT

control T cells cultured alone. While there was some background proliferation from the CAR T cells in these assays, the main aim here was to investigate if there was a difference between single endodomain CARs and the double CAR. Therefore, the ΔMFI was determined by comparing the MFI of CAR T cells in a co-culture condition with the MFI of the matched CAR T cell cultured alone. After 4 days, the proliferation of cell trace violet labelled CAR T cells was determined by flow cytometry on co-culture with neuroblastoma cell lines (Figure 6.9A) and with SUP-T1 control cell lines (Figure 6.9B). Figure 6.9A demonstrates that on co-culture with Lan-1, Kelly and Lan-5, there was a higher level of proliferation by the double CAR, suggesting full proliferative activation requires the presence of both antigens and both CARs in co-culture. It is also encouraging that the ΔMFI appears similar across all neuroblastoma cell lines, including Lan-1 which is the lowest ALK expressing cell line (Figure 3.2). Interestingly, GD2-Fc-28 appeared to show a low level of proliferation on co-culture with these cell lines also. While it is thought that these CCR CARs should not be able to signal, there are a number of possible explanations for this background activity. As previously mentioned, these CAR T cells have previously been activated 9 days prior to being used in the proliferation assay. While there is an assumption that the response to this stimulation will have slowed by then, these CAR T cells subsequently engage with an antigen and form an immune synapse, which could induce a level of proliferation, even without the presence of CD3ζ. Furthermore, the GD2-Fc-28 construct contains both the 14g2a scFv and an Fc spacer region. Long *et al*., has previously demonstrated that the 14g2a scFv can aggregate and cluster due to interactions with the scFv framework resulting in tonic T cell activation (Long et al., 2015). Both the data produced in chapter 3 and within the

literature, has documented the activity of the Fc spacer which can induce tonic signalling.

Figure 6.9B shows the proliferation of CAR T cells against SUP-T1 cell lines. As per the representative histograms, there appears to be no proliferation against the double antigen negative SUP-T1 WT cell line. The ΔMFI shows that the proliferation here against the double negative cell line was lower than that in the CAR alone. In theory, there should be no proliferation of CAR T cells on co-culture with SUP-T1 GD2 and SUP-T1 ALK. In contrast, we can see double CAR proliferation on co-culture with both these cell lines, which is more pronounced against the GD2 antigen. Furthermore, there is evidence of background GD2-Fc-28 proliferation with SUP-T1 GD2, and both single endodomain CARs against SUP-T1 ALK. Perhaps, proliferation could be explained here by clustering and interaction between scFvs or other CAR architecture. It has already been demonstrated that the anti-GD2 scFv can interact (Long et al., 2015). Furthermore, it is documented that CARs containing hinge and transmembrane regions of CD8α containing of cysteine residues result in CD8α dimerization (Salzer et al., 2020, Hennecke and Cosson, 1993).

Considering SUP-T1 ALK_GD2 expresses the highest level of double antigen based on cell sorting, it would be expected to induce the biggest increase in proliferation by the double CAR. However, both ALK8-CD8-ζ and GD2-Fc-28 demonstrate proliferation against SUP-T1 ALK_GD2. While it is known that first generation CAR T cells are capable of activation and subsequent signalling on antigen engagement, it is well regarded that costimulation is required for full T cell activation, subsequent effector functions, such as proliferation and the prevention of AICD and anergy (Lanitis et al., 2013, Chmielewski et al., 2011,

Gong et al., 1999). Moreover, if it is truly engagement of ALK on this cell line by ALK8-CD8-ζ that is inducing this response, we must question why the same level of proliferation was not seen when ALK8-CD8-ζ was co-cultured with SUP-T1 ALK. One explanation was discussed before, regarding the production of SUP-T1 ALK_GD2, which may have identified more highly ALK expressing cells.

CAR T cell proliferation after 8 days of co-culture is displayed in Figure 6.10. On co-culture with neuroblastoma cell lines, the trend of proliferation follows day 4 co-culture (Figure 6.9A), however the proliferation by the double CAR is less pronounced (Figure 6.10A). Equally, proliferation patterns on co-culture with SUP-T1 cell lines also reflected on day 8 also reflected what was seen at day 4 (Figure 6.9B), however the double CAR demonstrated low level proliferation on co-culture with SUP-T1 WT cells and GD2-Fc-28 no longer appeared to proliferate with SUP-T1 ALK (Figure 6.10B). Importantly, there is evidence that the use of the double CAR induces higher proliferation than single endodomain CAR T cells against neuroblastoma cell lines with lower antigen expression, namely Lan-1, which has the lowest ALK surface density (Figure 3.2). It is interesting to consider why the double CAR did not show to increase the functionality on co-culture with SUP-T1 ALK_GD2, which has of course been engineered to express high levels of ALK and GD2. While this shows stronger activation by cells expressing both target antigens, there is often significant activation by cells expressing single antigen alone and tuning of antigen expression and affinity is often required to observe strong discrimination between dual- and single-antigen target cells (Lim and June, 2017).

Finally, the long term cytokine producing ability of CAR T cells was investigated after 7 day co-culture and CAR T cell restimulation (Figure 6.11). While the

double CAR produced slightly higher levels of IL-2 on co-culture with Kelly and Lan-5 neuroblastoma cell lines, the level of production was so low that it must be classed as low background production (Figure 6.11A). In contrast, the production of IFNγ from the double CAR on co-culture with Lan-1 and Kelly cell lines (Figure 6.11B) was comparable to that after 24 hours of co-culture (Figure 6.8B). Furthermore, there was no background IFNγ production from the single endodomain CARs, suggesting there was minimal background activation. The IL-2 production from the double CAR on co-culture with SUP-T1 ALK_GD2 was also significantly higher than the single endodomain CARs, however the levels here still remain low, and it is difficult to claim effective functioning of the CAR (Figure 6.11C). Encouragingly, the double CAR produced a large level of IFNγ on co-culture with SUP-T1 ALK_GD2, which was not reflected in the single positive SUP-T1 cell lines, or SUP-T1 WT (Figure 6.11D). Equally, there was no background IFNγ production from the single endodomain CARs on co-culture with any SUP-T1 cell lines. This suggests that the double CAR must be present and engaged with both antigens for effective cytokine production from the CAR T cells. Importantly, after 7 days of co-culture and subsequent restimulation, this cytokine producing ability is not completely hampered in the case of IFNγ.

While second generation single antigen targeting CAR T cells have reaped outstanding results in some settings, there are drawbacks. The enhanced potency of these second generation CARs containing costimulatory domains can be associated with autoimmunity due to on-target toxicities against normal tissues expressing low levels of the TAA of choice (Lanitis et al., 2013). Furthermore, the targeting of one TAA can induce selection pressures and contribute towards antigen negative disease relapse; a phenomenon described

with CD19 second generation CAR T cell therapy (Nie et al., 2020). This has been reported as a cause of failure in both preclinical and clinical studies using adoptively transferred T cells with single antigen specificity to treat heterogeneous tumours types (Anurathapan et al., 2014, Riker et al., 1999). As previously discussed, the main aim of this chapter was to selectively boost the function of an anti-ALK CAR by combining it with another neuroblastoma targeted CAR, based on limited *in vitro* activity of a second generation anti-ALK CAR T cell at low antigen densities, however dual targeting CAR systems appear to have multiple other benefits.

There are of course multiple things that need to be considered when designing this dual CAR system. There are numerous neuroblastoma associated antigens that could have been utilised in this assay, which should be considered carefully. Kloss *et al*., initially demonstrated that first generation CAR T cells can become activated at sites of double antigen expression, but continue to exert effects at sites of single antigen expression, despite the co-stimulatory receptor not being engaged. This was rectified by reducing the affinity of the scFv in the first generation CAR (Kloss et al., 2013). This demonstrates the importance of understanding target antigen densities and designing the combination of CAR T cells as such, with consideration to the affinity of each scFv to its target. Therefore, understanding the ALK scFv affinities would be of importance. Furthermore, understanding complete expression profiles of ALK and GD2 on healthy and malignant tissues would be a key finding in order to make sure there is no overlap on on-target toxicity on healthy tissues.

Furthermore, effective CAR T cell function depends on the formation of an optimal immune synapse (Watanabe et al., 2018). Structural and spatial elements of TCR

recognition have evolved for precise regulation of the interaction between a T cells and its target cell, and this can be challenging to recapitulate with synthetic receptors (Srivastava and Riddell, 2015). Recent work has revealed that activation of canonical TCR chains is critically dependent on the size of the MHC ligand being recognised, with signalling attenuating sharply when the TCR:peptide-MHC (pMHC) ligand pair size exceed WT dimensions (Choudhuri et al., 2005). The spatial distance between CARs and their target antigens is of equally importance for effective initiation of T cell signalling, but this depends on an entirely different set of structural elements related to the location of the epitope on the target molecule and the spacer domain between the scFv and the T cell membrane (Srivastava and Riddell, 2015). As previously discussed in this thesis, the epitope mapping of our anti-ALK scFvs has not been undertaken, and therefore we do not know the optimal length of spacer region to utilise. By combining with another CCR CAR T cell, the size of the antigens being targeted together and the architecture of the CAR T cells must be considered carefully. Of course, the size of the antigens themselves will differ, for example, CD22 is a large extracellular domain must be considered whereas CD20 is a tetrapanin-like protein with a small extracellular domain while CD22 is comprised of seven Ig-like domain (James et al., 2008). By honing the immune synapse of the double CAR through utilising stalk regions of relevant length, the double CAR system could be augmented. There are therefore multiple components to be considered, differences in specificity, affinity, and stoichiometry of CARs, as well as different model systems may be influencing factors (Lanitis et al., 2013).

6.5 Conclusions and Future directions

This proof of concept chapter has proved that the use of a double CAR can induce double antigen-dependent activation, degranulation, cytokine production and proliferation. In the future, this should be directly compared side by side with ALK8-CD8-28ζ second generation CAR. Furthermore, increased understanding of the length of the immune synapse which includes ALK and GD2 is vital, along with a deeper understanding of epitope binding and scFv affinity which can inform further decisions regarding CAR architecture. Furthermore, potential consideration to the changing of the GD2-Fc spacer region, based on evidence throughout this PhD of tonic signalling, and literature such as Long *et al*. Depending on which antigen is more highly expressed on healthy tissue, it is possible to arrange the choice of target on CAR specifically. For example, recognition of the antigen combined with costimulation alone will induce singular transmission of CD28 signal, but in the absence of CD3ζ activating signalling, the dual-targeting CAR T cell will not become activated (Lanitis et al., 2013).

7 Discussion

7.1 Final conclusions

The aim of this PhD project was to develop a CAR T cell immunotherapy which targets ALK, for potential use in neuroblastoma. While the panel of nine anti-ALK second generation CAR T cells demonstrated cytotoxic activity and proinflammatory cytokine production at high ALK target densities, at lower target densities the functionality decreased. Moreover, ALK CAR T cells containing Fc spacers domains demonstrated unspecific proliferative capabilities, indicative of tonic signalling, while matched anti-ALK scFvs combined in CARs with a CD8 stalk region demonstrated restricted and antigen dependent proliferation patterns. While these CARs acted differently in a proliferative setting, there were minimal differences when the phenotypes of these matched CARs were investigated, namely looking at activation and exhaustion levels and their memory phenotype. A previously published anti-ALK scFv (ALK48) was incorporated into another panel of ALK CAR T cells which contained various stalk lengths, allowing for an *in vitro* side by side comparison with the lead CAR identified from this thesis (ALK8-CD8-28ζ). While ALK48 combined with an Fc spacer region or the previously published hinge/transmembrane region demonstrated little *in vitro* activity, ALK48-CD8-28ζ and ALK8-CD8-28ζ demonstrated similar cytotoxic behaviour. On further investigation ALK8-CD8-28ζ had higher IL-2 and IFNγ production and higher levels of ALK specific proliferation. Given the limited activity of the second generation ALK CARs at low antigen densities, ALK was combined into a dual-targeting CAR system along with GD2, another well characterised neuroblastoma associated antigen. It was demonstrated that both ALK and GD2 were required to be engaged by the double

CAR to induce increased levels of proliferation, activation, degranulation and proinflammatory cytokine production. This offers a potential solution to the problem of how to boost the activity of an anti-ALK CAR at low target antigen densities, which appears to be the case with neuroblastoma.

7.2 Future directions

It has clearly been demonstrated that the functionality of an ALK CAR T cell is hampered by the low target antigen density of ALK on target cells. Having identified methods using our co-CAR approach, we can also consider methods to enhance functionality through augmentation of CAR T cell survival.

7.2.1 Augmenting CAR T cell proliferation

Administering Cytokines

Investigators have evaluated the addition of cytokines as drugs, given to the host following T cell adoptive transfer. Early studies in tumour infiltrating lymphocytes expanded in IL-2 involved the co-administration of high dose IL-2, which was deemed to be essential for their persistence following adoptive transfer (Rosenberg, 2014). However, high dose IL-2 is known to induce toxicity and enhanced potential to for regulatory T cell induction, which limits its scope in the CAR T cell field (Zhang et al., 2005).

Engineering Cytokine Signalling

Engineering CAR T cells to produce cytokines locally is a potential way to overcome lack of persistence, and toxicity from exogenous cytokine addition. Armoured CAR T cells are typically modified second generation CAR T cells that have been further optimised to inducibley or constitutively secrete active cytokines or express ligands that further armour CAR T cells to improve efficacy and persistence. The choice of the ‘armour’ agent can be decided based on knowledge of the TME (Yeku and Brentjens, 2016). Hurton and colleagues generated CAR T cells co-expressing an IL-15 chimeric receptor which

demonstrated longer *in vivo* persistence, for up to 65 days after removal of antigen stimulus (Hurton et al., 2016).

Targeting Immunosuppressive Mechanisms

Targetable evasion mechanisms include the TGFβ and PD-1 pathways. Kloss et al., reported that blockade of TGFβ through co-expression of an anti-PSMA CAR with dominant-negative TGFβII resulted in improved anti-tumour efficacy and enhanced CAR T cell proliferation (Kloss et al., 2018). While clinical experience of combining CAR T cells with checkpoint inhibitor antibodies remain limited, strategies to target PD-1 at the genomic locus in combination with CAR expression in T cells using CRISPR/Cas9 technology are beginning to be evaluated in the clinic (Cherkassky et al., 2016).

7.2.2 Strategies to increase sensitivity

Changes to ITAMs/CD3

The functional diversity of ITAMs has been demonstrated through CAR T cells, which mostly utilise the CD3ζ cytoplasmic domain as a fixed module to deliver a major activation signal (Wu et al., 2020). Manipulation of the CD3 cytoplasmic domain is an alternative option for increasing the functionality of a low antigen density targeting CAR T cell. Traditional CD3ζ signalling domains contain three ITAMs, however it's been demonstrated they have different contributions to the anti-tumour function of CAR T cells (Feucht et al., 2019). Furthermore, Wu *et al.,* investigated the use of CD3ε, δ or γ in CARs and demonstrated CD3ε incorporation yielded a CAR with improved signalling prolife and tumour control (Wu et al., 2020). One important consideration is that lowering the activation threshold through increased numbers of ITAMs would most likely require an scFv

and CAR construct of high specificity which doesn't demonstrate tonic signalling or on-target off-tumour effects, due to the increased sensitivity of the CAR.

Change of CAR transmembrane domain

The importance of CAR architecture is something discussed throughout this thesis. The role of the transmembrane domain, which is often the least considered domain, has been demonstrated to impact the CAR expression level and stability on the T cell compared to other domains such as the hinge (Fujiwara et al., 2020). Furthermore, it was demonstrated that replacing a CD8 derived hinge and transmembrane region of a 4-1BB second generation CAR T cell, with a CD28 derived hinge and transmembrane region, actually lowers the threshold for CAR reactivity, despite identical signalling molecules (Majzner et al., 2020). The structure of the CAR T cells used within this thesis do vary, for example the Fc spacer containing CAR T cells contain a transmembrane region derived from CD28, while the CD8 stalk CAR T cells contain a CD8 transmembrane region (Figure 3.1). In the future, it would be worthwhile considering the overall structure of the CAR for more thorough comparisons and the optimal combination for low antigen density targeting.

Changes to CAR expression level

The level of surface CAR expression is another limiting factor that can impede CAR functionality due to impacts on signal strength. In the future, it would be useful to investigate the impact of increased transduction efficacies on *in vitro* results. Populations of different transduction efficacies can be identified by selecting on CAR+ T cells through CD34 selection.

7.2.3 Strategies to decrease antigen density threshold

CAR dosing combined with ALK inhibitors

Given the impact of antigen density on the function of ALK CAR T cells, it would be expected that methods to increase this would subsequently increase the activity of CARs, demonstrated with CAR T cells targeting CD22 (Ramakrishna et al., 2019). Crizotonib, an ALK inhibitor, has been shown increase the surface expression of ALK on neuroblastoma cell lines (Carpenter et al., 2012). In the future, it would be interesting to combine dual dosing with ALK inhibitors and anti-ALK CAR T cells to look for improved efficacy.

AJINA, A. & MAHER, J. 2018. Strategies to Address Chimeric Antigen Receptor Tonic Signaling. *Mol Cancer Ther,* 17**,** 1795-1815.
ALABANZA, L., PEGUES, M., GELDRES, C., SHI, V., WILTZIUS, J. J. W., SIEVERS, S. A., YANG, S. & KOCHENDERFER, J. N. 2017. Function of Novel Anti-CD19 Chimeric Antigen Receptors with Human Variable Regions Is Affected by Hinge and Transmembrane Domains. *Molecular therapy : the journal of the American Society of Gene Therapy,* 25**,** 2452-2465.
ALARCÓN, B., MESTRE, D. & MARTÍNEZ-MARTÍN, N. 2011. The immunological synapse: a cause or consequence of T-cell receptor triggering? *Immunology,* 133**,** 420-425.
ALMÅSBAK, H., AARVAK, T. & VEMURI, M. C. 2016. CAR T Cell Therapy: A Game Changer in Cancer Treatment. *Journal of immunology research,* 2016**,** 5474602-5474602.
ALMASBAK, H., WALSENG, E., KRISTIAN, A., MYHRE, M. R., SUSO, E. M., MUNTHE, L. A., ANDERSEN, J. T., WANG, M. Y., KVALHEIM, G., GAUDERNACK, G. & KYTE, J. A. 2015. Inclusion of an IgG1-Fc spacer abrogates efficacy of CD19 CAR T cells in a xenograft mouse model. *Gene Ther,* 22**,** 391-403.
ALVAREZ-RUEDA, N., DESSELLE, A., COCHONNEAU, D., CHAUMETTE, T., CLEMENCEAU, B., LEPRIEUR, S., BOUGRAS, G., SUPIOT, S., MUSSINI, J.-M., BARBET, J., SABA, J., PARIS, F., AUBRY, J. & BIRKLÉ, S. 2011. A Monoclonal Antibody to O-Acetyl-GD2 Ganglioside and Not to GD2 Shows Potent Anti-Tumor Activity without Peripheral Nervous System Cross-Reactivity. *PLOS ONE,* 6**,** e25220.
ANURATHAPAN, U., CHAN, R. C., HINDI, H. F., MUCHARLA, R., BAJGAIN, P., HAYES, B. C., FISHER, W. E., HESLOP, H. E., ROONEY, C. M., BRENNER, M. K., LEEN, A. M. & VERA, J. F. 2014. Kinetics of Tumor Destruction by Chimeric Antigen Receptor-modified T Cells. *Molecular Therapy,* 22**,** 623-633.
ARTYOMOV, M. N., LIS, M., DEVADAS, S., DAVIS, M. M. & CHAKRABORTY, A. K. 2010. CD4 and CD8 binding to MHC molecules primarily acts to enhance Lck delivery. *Proceedings of the National Academy of Sciences,* 107**,** 16916-16921.
BARR, E. K. & APPLEBAUM, M. A. 2018. Genetic Predisposition to Neuroblastoma. *Children (Basel, Switzerland),* 5**,** 119.
BARRETT, D. M., SINGH, N., LIU, X., JIANG, S., JUNE, C. H., GRUPP, S. A. & ZHAO, Y. 2014. Relation of clinical culture method to T-cell memory status and efficacy in xenograft models of adoptive immunotherapy. *Cytotherapy,* 16**,** 619-30.
BENMEBAREK, M.-R., KARCHES, C. H., CADILHA, B. L., LESCH, S., ENDRES, S. & KOBOLD, S. 2019. Killing Mechanisms of Chimeric Antigen Receptor (CAR) T Cells. *International journal of molecular sciences,* 20**,** 1283.
BERGER, C., JENSEN, M. C., LANSDORP, P. M., GOUGH, M., ELLIOTT, C. & RIDDELL, S. R. 2008. Adoptive transfer of effector CD8+ T cells derived from central memory cells establishes persistent T cell memory in primates. *The Journal of clinical investigation,* 118**,** 294-305.
BETTS, M. R., BRENCHLEY, J. M., PRICE, D. A., DE ROSA, S. C., DOUEK, D. C., ROEDERER, M. & KOUP, R. A. 2003. Sensitive and viable identification of antigen-specific CD8+ T cells by a flow cytometric assay for degranulation. *Journal of Immunological Methods,* 281**,** 65-78.
BODMAN-SMITH, M. D., ANAND, A., DURAND, V., YOUINOU, P. Y. & LYDYARD, P. M. 2000. Decreased expression of FcgammaRIII (CD16) by gammadelta T cells in patients with rheumatoid arthritis. *Immunology,* 99**,** 498-503.
BOSSE, K. R. & MARIS, J. M. 2016. Advances in the translational genomics of neuroblastoma: From improving risk stratification and revealing novel biology to identifying actionable genomic alterations. *Cancer,* 122**,** 20-33.
BOSSE, K. R., RAMAN, P., ZHU, Z., LANE, M., MARTINEZ, D., HEITZENEDER, S., RATHI, K. S., KENDSERSKY, N. M., RANDALL, M., DONOVAN, L.,

MORRISSY, S., SUSSMAN, R. T., ZHELEV, D. V., FENG, Y., WANG, Y., HWANG, J., LOPEZ, G., HARENZA, J. L., WEI, J. S., PAWEL, B., BHATTI, T., SANTI, M., GANGULY, A., KHAN, J., MARRA, M. A., TAYLOR, M. D., DIMITROV, D. S., MACKALL, C. L. & MARIS, J. M. 2017. Identification of GPC2 as an Oncoprotein and Candidate Immunotherapeutic Target in High-Risk Neuroblastoma. *Cancer cell,* 32**,** 295-309.e12.

BOSSI, R. T., SACCARDO, M. B., ARDINI, E., MENICHINCHERI, M., RUSCONI, L., MAGNAGHI, P., ORSINI, P., AVANZI, N., BORGIA, A. L., NESI, M., BANDIERA, T., FOGLIATTO, G. & BERTRAND, J. A. 2010. Crystal structures of anaplastic lymphoma kinase in complex with ATP competitive inhibitors. *Biochemistry,* 49**,** 6813-25.

BRESLER, S. C., WEISER, D. A., HUWE, P. J., PARK, J. H., KRYTSKA, K., RYLES, H., LAUDENSLAGER, M., RAPPAPORT, E. F., WOOD, A. C., MCGRADY, P. W., HOGARTY, M. D., LONDON, W. B., RADHAKRISHNAN, R., LEMMON, M. A. & MOSSE, Y. P. 2014. ALK mutations confer differential oncogenic activation and sensitivity to ALK inhibition therapy in neuroblastoma. *Cancer Cell,* 26**,** 682-94.

BROCKER, T. & KARJALAINEN, K. 1995. Signals through T cell receptor-zeta chain alone are insufficient to prime resting T lymphocytes. *The Journal of experimental medicine,* 181**,** 1653-1659.

BROWN, C. E., AGUILAR, B., STARR, R., YANG, X., CHANG, W.-C., WENG, L., CHANG, B., SARKISSIAN, A., BRITO, A., SANCHEZ, J. F., OSTBERG, J. R., D'APUZZO, M., BADIE, B., BARISH, M. E. & FORMAN, S. J. 2018. Optimization of IL13Rα2-Targeted Chimeric Antigen Receptor T Cells for Improved Anti-tumor Efficacy against Glioblastoma. *Molecular therapy : the journal of the American Society of Gene Therapy,* 26**,** 31-44.

BROWN, C. E., ALIZADEH, D., STARR, R., WENG, L., WAGNER, J. R., NARANJO, A., OSTBERG, J. R., BLANCHARD, M. S., KILPATRICK, J., SIMPSON, J., KURIEN, A., PRICEMAN, S. J., WANG, X., HARSHBARGER, T. L., D'APUZZO, M., RESSLER, J. A., JENSEN, M. C., BARISH, M. E., CHEN, M., PORTNOW, J., FORMAN, S. J. & BADIE, B. 2016. Regression of Glioblastoma after Chimeric Antigen Receptor T-Cell Therapy. *The New England journal of medicine,* 375**,** 2561-2569.

BROWN, C. E., BADIE, B., BARISH, M. E., WENG, L., OSTBERG, J. R., CHANG, W.-C., NARANJO, A., STARR, R., WAGNER, J., WRIGHT, C., ZHAI, Y., BADING, J. R., RESSLER, J. A., PORTNOW, J., D'APUZZO, M., FORMAN, S. J. & JENSEN, M. C. 2015. Bioactivity and Safety of IL13Rα2-Redirected Chimeric Antigen Receptor CD8+ T Cells in Patients with Recurrent Glioblastoma. *Clinical cancer research : an official journal of the American Association for Cancer Research,* 21**,** 4062-4072.

BROWN, M. P., EBERT, L. M. & GARGETT, T. 2019. Clinical chimeric antigen receptor-T cell therapy: a new and promising treatment modality for glioblastoma. *Clinical & translational immunology,* 8**,** e1050-e1050.

BROWNRIGG, L. M., TAN, D. B., BOSIO, E. & STURM, M. 2019. A simple rapid car T-cell cytotoxicity and degranulation flow cytometric assay. *Cytotherapy,* 21**,** S35.

BRUDNO, J. N., LAM, N., VANASSE, D., SHEN, Y.-W., ROSE, J. J., ROSSI, J., XUE, A., BOT, A., SCHOLLER, N., MIKKILINENI, L., ROSCHEWSKI, M., DEAN, R., CACHAU, R., YOUKHARIBACHE, P., PATEL, R., HANSEN, B., STRONCEK, D. F., ROSENBERG, S. A., GRESS, R. E. & KOCHENDERFER, J. N. 2020. Safety and feasibility of anti-CD19 CAR T cells with fully human binding domains in patients with B-cell lymphoma. *Nature Medicine,* 26**,** 270-280.

BURNET, M. 1957. Cancer: a biological approach. III. Viruses associated with neoplastic conditions. IV. Practical applications. *British medical journal,* 1**,** 841-847.

CANTRELL, D. 2015. Signaling in lymphocyte activation. *Cold Spring Harbor perspectives in biology,* 7**,** a018788.
CARPENTER, E. L., HAGLUND, E. A., MACE, E. M., DENG, D., MARTINEZ, D., WOOD, A. C., CHOW, A. K., WEISER, D. A., BELCASTRO, L. T., WINTER, C., BRESLER, S. C., VIGNY, M., MAZOT, P., ASGHARZADEH, S., SEEGER, R. C., ZHAO, H., GUO, R., CHRISTENSEN, J. G., ORANGE, J. S., PAWEL, B. R., LEMMON, M. A. & MOSSÉ, Y. P. 2012. Antibody targeting of anaplastic lymphoma kinase induces cytotoxicity of human neuroblastoma. *Oncogene,* 31**,** 4859-4867.
CARUSO, H. G., HURTON, L. V., NAJJAR, A., RUSHWORTH, D., ANG, S., OLIVARES, S., MI, T., SWITZER, K., SINGH, H., HULS, H., LEE, D. A., HEIMBERGER, A. B., CHAMPLIN, R. E. & COOPER, L. J. N. 2015. Tuning Sensitivity of CAR to EGFR Density Limits Recognition of Normal Tissue While Maintaining Potent Antitumor Activity. *Cancer research,* 75**,** 3505-3518.
CHAILYAN, A., MARCATILI, P. & TRAMONTANO, A. 2011. The association of heavy and light chain variable domains in antibodies: implications for antigen specificity. *The FEBS journal,* 278**,** 2858-2866.
CHANG, Z. L., LORENZINI, M. H., CHEN, X., TRAN, U., BANGAYAN, N. J. & CHEN, Y. Y. 2018. Rewiring T-cell responses to soluble factors with chimeric antigen receptors. *Nature chemical biology,* 14**,** 317-324.
CHANG, Z. L., SILVER, P. A. & CHEN, Y. Y. 2015. Identification and selective expansion of functionally superior T cells expressing chimeric antigen receptors. *Journal of translational medicine,* 13**,** 161-161.
CHEN, DANIEL S. & MELLMAN, I. 2013. Oncology Meets Immunology: The Cancer-Immunity Cycle. *Immunity,* 39**,** 1-10.
CHERKASSKY, L., MORELLO, A., VILLENA-VARGAS, J., FENG, Y., DIMITROV, D. S., JONES, D. R., SADELAIN, M. & ADUSUMILLI, P. S. 2016. Human CAR T cells with cell-intrinsic PD-1 checkpoint blockade resist tumor-mediated inhibition. *J Clin Invest,* 126**,** 3130-44.
CHIARLE, R., VOENA, C., AMBROGIO, C., PIVA, R. & INGHIRAMI, G. 2008. The anaplastic lymphoma kinase in the pathogenesis of cancer. *Nat Rev Cancer,* 8**,** 11-23.
CHMIELEWSKI, M. & ABKEN, H. 2020. TRUCKS, the fourth-generation CAR T cells: Current developments and clinical translation. *ADVANCES IN CELL AND GENE THERAPY,* 3**,** e84.
CHMIELEWSKI, M., HOMBACH, A. A. & ABKEN, H. 2011. CD28 cosignalling does not affect the activation threshold in a chimeric antigen receptor-redirected T-cell attack. *Gene Ther,* 18**,** 62-72.
CHOUDHURI, K., WISEMAN, D., BROWN, M. H., GOULD, K. & VAN DER MERWE, P. A. 2005. T-cell receptor triggering is critically dependent on the dimensions of its peptide-MHC ligand. *Nature,* 436**,** 578-582.
CIERI, N., CAMISA, B., COCCHIARELLA, F., FORCATO, M., OLIVEIRA, G., PROVASI, E., BONDANZA, A., BORDIGNON, C., PECCATORI, J., CICERI, F., LUPO-STANGHELLINI, M. T., MAVILIO, F., MONDINO, A., BICCIATO, S., RECCHIA, A. & BONINI, C. 2013. IL-7 and IL-15 instruct the generation of human memory stem T cells from naive precursors. *Blood,* 121**,** 573-84.
CLAMBEY, E. T., DAVENPORT, B., KAPPLER, J. W., MARRACK, P. & HOMANN, D. 2014. Molecules in medicine mini review: the alphabeta T cell receptor. *J Mol Med (Berl),* 92**,** 735-41.
CROSSLAND, D. L., DENNING, W. L., ANG, S., OLIVARES, S., MI, T., SWITZER, K., SINGH, H., HULS, H., GOLD, K. S., GLISSON, B. S., COOPER, L. J. & HEYMACH, J. V. 2018. Antitumor activity of CD56-chimeric antigen receptor T cells in neuroblastoma and SCLC models. *Oncogene,* 37**,** 3686-3697.
CURRAN, K. J., SEINSTRA, B. A., NIKHAMIN, Y., YEH, R., USACHENKO, Y., VAN LEEUWEN, D. G., PURDON, T., PEGRAM, H. J. & BRENTJENS, R. J. 2015.

Enhancing Antitumor Efficacy of Chimeric Antigen Receptor T Cells Through Constitutive CD40L Expression. *Molecular Therapy,* 23**,** 769-778.
DANIELS, R. W., ROSSANO, A. J., MACLEOD, G. T. & GANETZKY, B. 2014. Expression of multiple transgenes from a single construct using viral 2A peptides in Drosophila. *PloS one,* 9**,** e100637-e100637.
DELLA CORTE, C. M., VISCARDI, G., DI LIELLO, R., FASANO, M., MARTINELLI, E., TROIANI, T., CIARDIELLO, F. & MORGILLO, F. 2018. Role and targeting of anaplastic lymphoma kinase in cancer. *Molecular Cancer,* 17**,** 30.
DOTTI, G., GOTTSCHALK, S., SAVOLDO, B. & BRENNER, M. K. 2014. Design and development of therapies using chimeric antigen receptor-expressing T cells. *Immunol Rev,* 257**,** 107-26.
DRENT, E., THEMELI, M., POELS, R., DE JONG-KORLAAR, R., YUAN, H., DE BRUIJN, J., MARTENS, A. C. M., ZWEEGMAN, S., VAN DE DONK, N., GROEN, R. W. J., LOKHORST, H. M. & MUTIS, T. 2017. A Rational Strategy for Reducing On-Target Off-Tumor Effects of CD38-Chimeric Antigen Receptors by Affinity Optimization. *Mol Ther,* 25**,** 1946-1958.
DU, H., HIRABAYASHI, K., AHN, S., KREN, N. P., MONTGOMERY, S. A., WANG, X., TIRUTHANI, K., MIRLEKAR, B., MICHAUD, D., GREENE, K., HERRERA, S. G., XU, Y., SUN, C., CHEN, Y., MA, X., FERRONE, C. R., PYLAYEVA-GUPTA, Y., YEH, J. J., LIU, R., SAVOLDO, B., FERRONE, S. & DOTTI, G. 2019. Antitumor Responses in the Absence of Toxicity in Solid Tumors by Targeting B7-H3 via Chimeric Antigen Receptor T Cells. *Cancer Cell,* 35**,** 221-237.e8.
DUNN, G. P., BRUCE, A. T., IKEDA, H., OLD, L. J. & SCHREIBER, R. D. 2002. Cancer immunoediting: from immunosurveillance to tumor escape. *Nat Immunol,* 3**,** 991-8.
DWIVEDI, A., KARULKAR, A., GHOSH, S., RAFIQ, A. & PURWAR, R. 2019. Lymphocytes in Cellular Therapy: Functional Regulation of CAR T Cells. *Frontiers in immunology,* 9**,** 3180-3180.
DZIERAN, J., RODRIGUEZ GARCIA, A., WESTERMARK, U. K., HENLEY, A. B., EYRE SÁNCHEZ, E., TRÄGER, C., JOHANSSON, H. J., LEHTIÖ, J. & ARSENIAN-HENRIKSSON, M. 2018. MYCN-amplified neuroblastoma maintains an aggressive and undifferentiated phenotype by deregulation of estrogen and NGF signaling. *Proceedings of the National Academy of Sciences*.
ESHHAR, Z. & GROSS, G. 1990. Chimeric T cell receptor which incorporates the anti-tumour specificity of a monoclonal antibody with the cytolytic activity of T cells: a model system for immunotherapeutical approach. *The British journal of cancer. Supplement,* 10**,** 27-29.
ESHHAR, Z., WAKS, T., GROSS, G. & SCHINDLER, D. G. 1993. Specific activation and targeting of cytotoxic lymphocytes through chimeric single chains consisting of antibody-binding domains and the gamma or zeta subunits of the immunoglobulin and T-cell receptors. *Proc Natl Acad Sci U S A,* 90**,** 720-4.
FEUCHT, J., SUN, J., EYQUEM, J., HO, Y.-J., ZHAO, Z., LEIBOLD, J., DOBRIN, A., CABRIOLU, A., HAMIEH, M. & SADELAIN, M. 2019. Calibration of CAR activation potential directs alternative T cell fates and therapeutic potency. *Nature Medicine,* 25**,** 82-88.
FRIGAULT, M. J., LEE, J., BASIL, M. C., CARPENITO, C., MOTOHASHI, S., SCHOLLER, J., KAWALEKAR, O. U., GUEDAN, S., MCGETTIGAN, S. E., POSEY, A. D., ANG, S., COOPER, L. J. N., PLATT, J. M., JOHNSON, F. B., PAULOS, C. M., ZHAO, Y., KALOS, M., MILONE, M. C. & JUNE, C. H. 2015. Identification of Chimeric Antigen Receptors That Mediate Constitutive or Inducible Proliferation of T Cells. *Cancer Immunology Research,* 3**,** 356-367.
FUJIWARA, K., TSUNEI, A., KUSABUKA, H., OGAKI, E., TACHIBANA, M. & OKADA, N. 2020. Hinge and Transmembrane Domains of Chimeric Antigen Receptor Regulate Receptor Expression and Signaling Threshold. *Cells,* 9.

GACEREZ, A. T., ARELLANO, B. & SENTMAN, C. L. 2016. How Chimeric Antigen Receptor Design Affects Adoptive T Cell Therapy. *Journal of cellular physiology,* 231**,** 2590-2598.

GALLUZZI, L., CHAN, T. A., KROEMER, G., WOLCHOK, J. D. & LOPEZ-SOTO, A. 2018. The hallmarks of successful anticancer immunotherapy. *Sci Transl Med,* 10.

GARGETT, T., YU, W., DOTTI, G., YVON, E. S., CHRISTO, S. N., HAYBALL, J. D., LEWIS, I. D., BRENNER, M. K. & BROWN, M. P. 2016. GD2-specific CAR T Cells Undergo Potent Activation and Deletion Following Antigen Encounter but can be Protected From Activation-induced Cell Death by PD-1 Blockade. *Molecular therapy : the journal of the American Society of Gene Therapy,* 24**,** 1135-1149.

GATTINONI, L., KLEBANOFF, C. A., PALMER, D. C., WRZESINSKI, C., KERSTANN, K., YU, Z., FINKELSTEIN, S. E., THEORET, M. R., ROSENBERG, S. A. & RESTIFO, N. P. 2005. Acquisition of full effector function in vitro paradoxically impairs the in vivo antitumor efficacy of adoptively transferred CD8+ T cells. *J Clin Invest,* 115**,** 1616-26.

GATTINONI, L., LUGLI, E., JI, Y., POS, Z., PAULOS, C. M., QUIGLEY, M. F., ALMEIDA, J. R., GOSTICK, E., YU, Z., CARPENITO, C., WANG, E., DOUEK, D. C., PRICE, D. A., JUNE, C. H., MARINCOLA, F. M., ROEDERER, M. & RESTIFO, N. P. 2011. A human memory T cell subset with stem cell-like properties. *Nat Med,* 17**,** 1290-7.

GAUDINO, S. J. & KUMAR, P. 2019. Cross-Talk Between Antigen Presenting Cells and T Cells Impacts Intestinal Homeostasis, Bacterial Infections, and Tumorigenesis. *Frontiers in immunology,* 10**,** 360-360.

GHORASHIAN, S., KRAMER, A. M., ONUOHA, S., WRIGHT, G., BARTRAM, J., RICHARDSON, R., ALBON, S. J., CASANOVAS-COMPANY, J., CASTRO, F., POPOVA, B., VILLANUEVA, K., YEUNG, J., VETHAROY, W., GUVENEL, A., WAWRZYNIECKA, P. A., MEKKAOUI, L., CHEUNG, G. W., PINNER, D., CHU, J., LUCCHINI, G., SILVA, J., CIOCARLIE, O., LAZAREVA, A., INGLOTT, S., GILMOUR, K. C., AHSAN, G., FERRARI, M., MANZOOR, S., CHAMPION, K., BROOKS, T., LOPES, A., HACKSHAW, A., FARZANEH, F., CHIESA, R., RAO, K., BONNEY, D., SAMARASINGHE, S., GOULDEN, N., VORA, A., VEYS, P., HOUGH, R., WYNN, R., PULE, M. A. & AMROLIA, P. J. 2019. Enhanced CAR T cell expansion and prolonged persistence in pediatric patients with ALL treated with a low-affinity CD19 CAR. *Nat Med,* 25**,** 1408-1414.

GONG, M. C., LATOUCHE, J. B., KRAUSE, A., HESTON, W. D., BANDER, N. H. & SADELAIN, M. 1999. Cancer patient T cells genetically targeted to prostate-specific membrane antigen specifically lyse prostate cancer cells and release cytokines in response to prostate-specific membrane antigen. *Neoplasia (New York, N.Y.),* 1**,** 123-127.

GOPALAKRISHNAN, R., MATTA, H., CHOI, S., NATARAJAN, V., PRINS, R., GONG, S., ZENUNOVIC, A., NARASAPPA, N., PATEL, F., PRAKASH, R., CHAUDHARY, V., SIKRI, V., CHITNIS, S. D., KOCHEGAROV, A., WANG, D., FALAT, M., KAHN, M., KEERTHIPATI, P. S., SHARMA, N., LENKA, J., STIEBEN, T. M., BRAUN, J., BATRA, A., PURVIS, K., ITO, K., LEE, J. H., JERONIMO, A., ZAMORA, H. M., MEMBRENO, A., QIU, Q., PESHIN, S., NAMBURU, L. & CHAUDHARY, P. M. 2019. A novel luciferase-based assay for the detection of Chimeric Antigen Receptors. *Scientific Reports,* 9**,** 1957.

GOYETTE, J., NIEVES, D. J., MA, Y. & GAUS, K. 2019. How does T cell receptor clustering impact on signal transduction? *Journal of Cell Science,* 132**,** jcs226423.

GRIFFITHS, G. M., TSUN, A. & STINCHCOMBE, J. C. 2010. The immunological synapse: a focal point for endocytosis and exocytosis. *Journal of Cell Biology,* 189**,** 399-406.

GUAN, J., UMAPATHY, G., YAMAZAKI, Y., WOLFSTETTER, G., MENDOZA, P., PFEIFER, K., MOHAMMED, A., HUGOSSON, F., ZHANG, H., HSU, A. W., HALENBECK, R., HALLBERG, B. & PALMER, R. H. 2015. FAM150A and FAM150B are activating ligands for anaplastic lymphoma kinase. *Elife,* 4**,** e09811.

GUEDAN, S., CALDERON, H., POSEY, A. D., JR. & MAUS, M. V. 2018a. Engineering and Design of Chimeric Antigen Receptors. *Molecular therapy. Methods & clinical development,* 12**,** 145-156.

GUEDAN, S., POSEY, A. D., JR., SHAW, C., WING, A., DA, T., PATEL, P. R., MCGETTIGAN, S. E., CASADO-MEDRANO, V., KAWALEKAR, O. U., URIBE-HERRANZ, M., SONG, D., MELENHORST, J. J., LACEY, S. F., SCHOLLER, J., KEITH, B., YOUNG, R. M. & JUNE, C. H. 2018b. Enhancing CAR T cell persistence through ICOS and 4-1BB costimulation. *JCI insight,* 3**,** e96976.

GUEST, R. D., HAWKINS, R. E., KIRILLOVA, N., CHEADLE, E. J., ARNOLD, J., O'NEILL, A., IRLAM, J., CHESTER, K. A., KEMSHEAD, J. T., SHAW, D. M., EMBLETON, M. J., STERN, P. L. & GILHAM, D. E. 2005. The role of extracellular spacer regions in the optimal design of chimeric immune receptors: evaluation of four different scFvs and antigens. *J Immunother,* 28**,** 203-11.

HALLBERG, B. & PALMER, R. H. 2013. Mechanistic insight into ALK receptor tyrosine kinase in human cancer biology. *Nature Reviews Cancer,* 13**,** 685-700.

HALLBERG, B. & PALMER, R. H. 2016. The role of the ALK receptor in cancer biology. *Annals of Oncology,* 27**,** iii4-iii15.

HAMIEH, M., DOBRIN, A., CABRIOLU, A., VAN DER STEGEN, S. J. C., GIAVRIDIS, T., MANSILLA-SOTO, J., EYQUEM, J., ZHAO, Z., WHITLOCK, B. M., MIELE, M. M., LI, Z., CUNANAN, K. M., HUSE, M., HENDRICKSON, R. C., WANG, X., RIVIÈRE, I. & SADELAIN, M. 2019. CAR T cell trogocytosis and cooperative killing regulate tumour antigen escape. *Nature,* 568**,** 112-116.

HAY, K. A., HANAFI, L.-A., LI, D., GUST, J., LILES, W. C., WURFEL, M. M., LÓPEZ, J. A., CHEN, J., CHUNG, D., HARJU-BAKER, S., CHERIAN, S., CHEN, X., RIDDELL, S. R., MALONEY, D. G. & TURTLE, C. J. 2017. Kinetics and biomarkers of severe cytokine release syndrome after CD19 chimeric antigen receptor-modified T-cell therapy. *Blood,* 130**,** 2295-2306.

HAYNES, N. M., SNOOK, M. B., TRAPANI, J. A., CERRUTI, L., JANE, S. M., SMYTH, M. J. & DARCY, P. K. 2001. Redirecting mouse CTL against colon carcinoma: superior signaling efficacy of single-chain variable domain chimeras containing TCR-zeta vs Fc epsilon RI-gamma. *J Immunol,* 166**,** 182-7.

HECK, J. E., RITZ, B., HUNG, R. J., HASHIBE, M. & BOFFETTA, P. 2009. The epidemiology of neuroblastoma: a review. *Paediatr Perinat Epidemiol,* 23**,** 125-43.

HECZEY, A., LOUIS, C. U., SAVOLDO, B., DAKHOVA, O., DURETT, A., GRILLEY, B., LIU, H., WU, M. F., MEI, Z., GEE, A., MEHTA, B., ZHANG, H., MAHMOOD, N., TASHIRO, H., HESLOP, H. E., DOTTI, G., ROONEY, C. M. & BRENNER, M. K. 2017. CAR T Cells Administered in Combination with Lymphodepletion and PD-1 Inhibition to Patients with Neuroblastoma. *Molecular Therapy,* 25**,** 2214-2224.

HENNECKE, S. & COSSON, P. 1993. Role of transmembrane domains in assembly and intracellular transport of the CD8 molecule. *J Biol Chem,* 268**,** 26607-12.

HINRICHS, C. S., BORMAN, Z. A., CASSARD, L., GATTINONI, L., SPOLSKI, R., YU, Z., SANCHEZ-PEREZ, L., MURANSKI, P., KERN, S. J., LOGUN, C., PALMER, D. C., JI, Y., REGER, R. N., LEONARD, W. J., DANNER, R. L., ROSENBERG, S. A. & RESTIFO, N. P. 2009. Adoptively transferred effector cells derived from naive rather than central memory CD8+ T cells mediate superior antitumor immunity. *Proc Natl Acad Sci U S A,* 106**,** 17469-74.

HOMBACH, A., HEUSER, C., GERKEN, M., FISCHER, B., LEWALTER, K., DIEHL, V., POHL, C. & ABKEN, H. 2000. T cell activation by recombinant FcepsilonRI

gamma-chain immune receptors: an extracellular spacer domain impairs antigen-dependent T cell activation but not antigen recognition. *Gene Ther,* 7**,** 1067-75.

HOMBACH, A., HOMBACH, A. A. & ABKEN, H. 2010. Adoptive immunotherapy with genetically engineered T cells: modification of the IgG1 Fc 'spacer' domain in the extracellular moiety of chimeric antigen receptors avoids 'off-target' activation and unintended initiation of an innate immune response. *Gene Ther,* 17**,** 1206-13.

HOMBACH, A., KÖHLER, H., RAPPL, G. & ABKEN, H. 2006. Human CD4⁺ T Cells Lyse Target Cells via Granzyme/Perforin upon Circumvention of MHC Class II Restriction by an Antibody-Like Immunoreceptor. *The Journal of Immunology,* 177**,** 5668-5675.

HOMBACH, A. A., SCHILDGEN, V., HEUSER, C., FINNERN, R., GILHAM, D. E. & ABKEN, H. 2007. T cell activation by antibody-like immunoreceptors: the position of the binding epitope within the target molecule determines the efficiency of activation of redirected T cells. *J Immunol,* 178**,** 4650-7.

HUANG, H. 2018. Anaplastic Lymphoma Kinase (ALK) Receptor Tyrosine Kinase: A Catalytic Receptor with Many Faces. *International journal of molecular sciences,* 19**,** 3448.

HUANG, M. & WEISS, W. A. 2013. Neuroblastoma and MYCN. *Cold Spring Harb Perspect Med,* 3**,** a014415.

HUDECEK, M., LUPO-STANGHELLINI, M. T., KOSASIH, P. L., SOMMERMEYER, D., JENSEN, M. C., RADER, C. & RIDDELL, S. R. 2013. Receptor affinity and extracellular domain modifications affect tumor recognition by ROR1-specific chimeric antigen receptor T cells. *Clin Cancer Res,* 19**,** 3153-64.

HUDECEK, M., SOMMERMEYER, D., KOSASIH, P. L., SILVA-BENEDICT, A., LIU, L., RADER, C., JENSEN, M. C. & RIDDELL, S. R. 2015. The nonsignaling extracellular spacer domain of chimeric antigen receptors is decisive for in vivo antitumor activity. *Cancer Immunol Res,* 3**,** 125-35.

HUGHES, M. M., YASSAI, M., SEDY, J. R., WEHRLY, T. D., HUANG, C.-Y., KANAGAWA, O., GORSKI, J. & SLECKMAN, B. P. 2003. T cell receptor CDR3 loop length repertoire is determined primarily by features of the V(D)J recombination reaction. *European Journal of Immunology,* 33**,** 1568-1575.

HURTON, L. V., SINGH, H., NAJJAR, A. M., SWITZER, K. C., MI, T., MAITI, S., OLIVARES, S., RABINOVICH, B., HULS, H., FORGET, M. A., DATAR, V., KEBRIAEI, P., LEE, D. A., CHAMPLIN, R. E. & COOPER, L. J. 2016. Tethered IL-15 augments antitumor activity and promotes a stem-cell memory subset in tumor-specific T cells. *Proc Natl Acad Sci U S A,* 113**,** E7788-e7797.

IRVING, B. A. & WEISS, A. 1991. The cytoplasmic domain of the T cell receptor zeta chain is sufficient to couple to receptor-associated signal transduction pathways. *Cell,* 64**,** 891-901.

IWAHARA, T., FUJIMOTO, J., WEN, D., CUPPLES, R., BUCAY, N., ARAKAWA, T., MORI, S., RATZKIN, B. & YAMAMOTO, T. 1997. Molecular characterization of ALK, a receptor tyrosine kinase expressed specifically in the nervous system. *Oncogene,* 14**,** 439-49.

JAMES, S. E., GREENBERG, P. D., JENSEN, M. C., LIN, Y., WANG, J., TILL, B. G., RAUBITSCHEK, A. A., FORMAN, S. J. & PRESS, O. W. 2008. Antigen Sensitivity of CD22-Specific Chimeric TCR Is Modulated by Target Epitope Distance from the Cell Membrane. *The Journal of Immunology,* 180**,** 7028-7038.

JANOUEIX-LEROSEY, I., LEQUIN, D., BRUGIERES, L., RIBEIRO, A., DE PONTUAL, L., COMBARET, V., RAYNAL, V., PUISIEUX, A., SCHLEIERMACHER, G., PIERRON, G., VALTEAU-COUANET, D., FREBOURG, T., MICHON, J., LYONNET, S., AMIEL, J. & DELATTRE, O. 2008. Somatic and germline

activating mutations of the ALK kinase receptor in neuroblastoma. *Nature,* 455**,** 967-70.
JANSSEN, E. M., LEMMENS, E. E., WOLFE, T., CHRISTEN, U., VON HERRATH, M. G. & SCHOENBERGER, S. P. 2003. CD4+ T cells are required for secondary expansion and memory in CD8+ T lymphocytes. *Nature,* 421**,** 852-856.
JAVANMARDI, N., FRANSSON, S., DJOS, A., SJÖBERG, R.-M., NILSSON, S., TRUVÉ, K., KOGNER, P. & MARTINSSON, T. 2019. Low Frequency ALK Hotspots Mutations In Neuroblastoma Tumours Detected By Ultra-deep Sequencing: Implications For ALK Inhibitor Treatment. *Scientific Reports,* 9**,** 2199.
JAYARAMAN, J., MELLODY, M. P., HOU, A. J., DESAI, R. P., FUNG, A. W., PHAM, A. H. T., CHEN, Y. Y. & ZHAO, W. 2020. CAR-T design: Elements and their synergistic function. *EBioMedicine,* 58.
JENA, B., MAITI, S., HULS, H., SINGH, H., LEE, D. A., CHAMPLIN, R. E. & COOPER, L. J. N. 2013. Chimeric antigen receptor (CAR)-specific monoclonal antibody to detect CD19-specific T cells in clinical trials. *PloS one,* 8**,** e57838-e57838.
JOACHIMS, M. L., CHAIN, J. L., HOOKER, S. W., KNOTT-CRAIG, C. J. & THOMPSON, L. F. 2006. Human alpha beta and gamma delta thymocyte development: TCR gene rearrangements, intracellular TCR beta expression, and gamma delta developmental potential--differences between men and mice. *Journal of immunology (Baltimore, Md. : 1950),* 176**,** 1543-1552.
JONNALAGADDA, M., MARDIROS, A., URAK, R., WANG, X., HOFFMAN, L. J., BERNANKE, A., CHANG, W. C., BRETZLAFF, W., STARR, R., PRICEMAN, S., OSTBERG, J. R., FORMAN, S. J. & BROWN, C. E. 2015. Chimeric antigen receptors with mutated IgG4 Fc spacer avoid fc receptor binding and improve T cell persistence and antitumor efficacy. *Mol Ther,* 23**,** 757-68.
KAKARLA, S., CHOW, K. K. H., MATA, M., SHAFFER, D. R., SONG, X.-T., WU, M.-F., LIU, H., WANG, L. L., ROWLEY, D. R., PFIZENMAIER, K. & GOTTSCHALK, S. 2013. Antitumor Effects of Chimeric Receptor Engineered Human T Cells Directed to Tumor Stroma. *Molecular Therapy,* 21**,** 1611-1620.
KANNAN, A., HUANG, W., HUANG, F. & AUGUST, A. 2012. Signal transduction via the T cell antigen receptor in naïve and effector/memory T cells. *The international journal of biochemistry & cell biology,* 44**,** 2129-2134.
KASAKOVSKI, D., XU, L. & LI, Y. 2018. T cell senescence and CAR-T cell exhaustion in hematological malignancies. *Journal of Hematology & Oncology,* 11**,** 91.
KAWALEKAR, O. U., O'CONNOR, R. S., FRAIETTA, J. A., GUO, L., MCGETTIGAN, S. E., POSEY, A. D., JR., PATEL, P. R., GUEDAN, S., SCHOLLER, J., KEITH, B., SNYDER, N. W., BLAIR, I. A., MILONE, M. C. & JUNE, C. H. 2016. Distinct Signaling of Coreceptors Regulates Specific Metabolism Pathways and Impacts Memory Development in CAR T Cells. *Immunity,* 44**,** 380-90.
KENNEDY, L. B. & SALAMA, A. K. S. 2020. A review of cancer immunotherapy toxicity. *CA: A Cancer Journal for Clinicians,* 70**,** 86-104.
KLEBANOFF, C. A., GATTINONI, L. & RESTIFO, N. P. 2012. Sorting through subsets: which T-cell populations mediate highly effective adoptive immunotherapy? *Journal of immunotherapy (Hagerstown, Md. : 1997),* 35**,** 651-660.
KLOSS, C. C., CONDOMINES, M., CARTELLIERI, M., BACHMANN, M. & SADELAIN, M. 2013. Combinatorial antigen recognition with balanced signaling promotes selective tumor eradication by engineered T cells. *Nat Biotechnol,* 31**,** 71-5.
KLOSS, C. C., LEE, J., ZHANG, A., CHEN, F., MELENHORST, J. J., LACEY, S. F., MAUS, M. V., FRAIETTA, J. A., ZHAO, Y. & JUNE, C. H. 2018. Dominant-Negative TGF-β Receptor Enhances PSMA-Targeted Human CAR T Cell Proliferation And Augments Prostate Cancer Eradication. *Mol Ther,* 26**,** 1855-1866.

KRIJGSMAN, D., HOKLAND, M. & KUPPEN, P. J. K. 2018. The Role of Natural Killer T Cells in Cancer—A Phenotypical and Functional Approach. *Frontiers in Immunology,* 9**,** 367.

KÜNKELE, A., JOHNSON, A. J., ROLCZYNSKI, L. S., CHANG, C. A., HOGLUND, V., KELLY-SPRATT, K. S. & JENSEN, M. C. 2015. Functional Tuning of CARs Reveals Signaling Threshold above Which CD8+ CTL Antitumor Potency Is Attenuated due to Cell Fas-FasL-Dependent AICD. *Cancer Immunol Res,* 3**,** 368-79.

KUZNETSOVA, M., LOPATNIKOVA, J., SHEVCHENKO, J., SILKOV, A., MAKSYUTOV, A. & SENNIKOV, S. 2019. Cytotoxic Activity and Memory T Cell Subset Distribution of in vitro-Stimulated CD8+ T Cells Specific for HER2/neu Epitopes. *Frontiers in Immunology,* 10**,** 1017.

LABANIEH, L., MAJZNER, R. G. & MACKALL, C. L. 2018. Programming CAR-T cells to kill cancer. *Nature Biomedical Engineering,* 2**,** 377-391.

LAMANT, L., PULFORD, K., BISCHOF, D., MORRIS, S. W., MASON, D. Y., DELSOL, G. & MARIAME, B. 2000. Expression of the ALK tyrosine kinase gene in neuroblastoma. *Am J Pathol,* 156**,** 1711-21.

LANITIS, E., POUSSIN, M., KLATTENHOFF, A. W., SONG, D., SANDALTZOPOULOS, R., JUNE, C. H. & POWELL, D. J., JR. 2013. Chimeric antigen receptor T Cells with dissociated signaling domains exhibit focused antitumor activity with reduced potential for toxicity in vivo. *Cancer Immunol Res,* 1**,** 43-53.

LI, N., FU, H., HEWITT, S. M., DIMITROV, D. S. & HO, M. 2017. Therapeutically targeting glypican-2 via single-domain antibody-based chimeric antigen receptors and immunotoxins in neuroblastoma. *Proceedings of the National Academy of Sciences,* 114**,** E6623-E6631.

LIADI, I., SINGH, H., ROMAIN, G., REY-VILLAMIZAR, N., MEROUANE, A., ADOLACION, J. R. T., KEBRIAEI, P., HULS, H., QIU, P., ROYSAM, B., COOPER, L. J. N. & VARADARAJAN, N. 2015. Individual Motile CD4(+) T Cells Can Participate in Efficient Multikilling through Conjugation to Multiple Tumor Cells. *Cancer immunology research,* 3**,** 473-482.

LIM, W. A. & JUNE, C. H. 2017. The Principles of Engineering Immune Cells to Treat Cancer. *Cell,* 168**,** 724-740.

LIU, B., YAN, L. & ZHOU, M. 2019. Target selection of CAR T cell therapy in accordance with the TME for solid tumors. *American journal of cancer research,* 9**,** 228-241.

LONG, A. H., HASO, W. M., SHERN, J. F., WANHAINEN, K. M., MURGAI, M., INGARAMO, M., SMITH, J. P., WALKER, A. J., KOHLER, M. E., VENKATESHWARA, V. R., KAPLAN, R. N., PATTERSON, G. H., FRY, T. J., ORENTAS, R. J. & MACKALL, C. L. 2015. 4-1BB costimulation ameliorates T cell exhaustion induced by tonic signaling of chimeric antigen receptors. *Nature medicine,* 21**,** 581-590.

LONG, A. H., HIGHFILL, S. L., CUI, Y., SMITH, J. P., WALKER, A. J., RAMAKRISHNA, S., EL-ETRIBY, R., GALLI, S., TSOKOS, M. G., ORENTAS, R. J. & MACKALL, C. L. 2016. Reduction of MDSCs with All-trans Retinoic Acid Improves CAR Therapy Efficacy for Sarcomas. *Cancer Immunology Research,* 4**,** 869-880.

LORÉN, C. E., ENGLUND, C., GRABBE, C., HALLBERG, B., HUNTER, T. & PALMER, R. H. 2003. A crucial role for the Anaplastic lymphoma kinase receptor tyrosine kinase in gut development in Drosophila melanogaster. *EMBO reports,* 4**,** 781-786.

LOUIS, C. U., SAVOLDO, B., DOTTI, G., PULE, M., YVON, E., MYERS, G. D., ROSSIG, C., RUSSELL, H. V., DIOUF, O., LIU, E., LIU, H., WU, M. F., GEE, A. P., MEI, Z., ROONEY, C. M., HESLOP, H. E. & BRENNER, M. K. 2011.

Antitumor activity and long-term fate of chimeric antigen receptor-positive T cells in patients with neuroblastoma. *Blood,* 118**,** 6050-6.
LYNN, R. C., WEBER, E. W., SOTILLO, E., GENNERT, D., XU, P., GOOD, Z., ANBUNATHAN, H., LATTIN, J., JONES, R., TIEU, V., NAGARAJA, S., GRANJA, J., DE BOURCY, C. F. A., MAJZNER, R., SATPATHY, A. T., QUAKE, S. R., MONJE, M., CHANG, H. Y. & MACKALL, C. L. 2019. c-Jun overexpression in CAR T cells induces exhaustion resistance. *Nature,* 576**,** 293-300.
MAETZIG, T., GALLA, M., BAUM, C. & SCHAMBACH, A. 2011. Gammaretroviral vectors: biology, technology and application. *Viruses,* 3**,** 677-713.
MAHER, J., BRENTJENS, R. J., GUNSET, G., RIVIERE, I. & SADELAIN, M. 2002. Human T-lymphocyte cytotoxicity and proliferation directed by a single chimeric TCRzeta /CD28 receptor. *Nat Biotechnol,* 20**,** 70-5.
MAJZNER, R. G., RIETBERG, S. P., SOTILLO, E., DONG, R., VACHHARAJANI, V. T., LABANIEH, L., MYKLEBUST, J. H., KADAPAKKAM, M., WEBER, E. W., TOUSLEY, A. M., RICHARDS, R. M., HEITZENEDER, S., NGUYEN, S. M., WIEBKING, V., THERUVATH, J., LYNN, R. C., XU, P., DUNN, A. R., VALE, R. D. & MACKALL, C. L. 2020. Tuning the Antigen Density Requirement for CAR T-cell Activity. *Cancer Discov,* 10**,** 702-723.
MARTINEZ, M. & MOON, E. K. 2019. CAR T Cells for Solid Tumors: New Strategies for Finding, Infiltrating, and Surviving in the Tumor Microenvironment. *Frontiers in immunology,* 10**,** 128-128.
MATTHAY, K. K., MARIS, J. M., SCHLEIERMACHER, G., NAKAGAWARA, A., MACKALL, C. L., DILLER, L. & WEISS, W. A. 2016. Neuroblastoma. *Nature Reviews Disease Primers,* 2**,** 16078.
MENARES, E., GÁLVEZ-CANCINO, F., CÁCERES-MORGADO, P., GHORANI, E., LÓPEZ, E., DÍAZ, X., SAAVEDRA-ALMARZA, J., FIGUEROA, D. A., ROA, E., QUEZADA, S. A. & LLADSER, A. 2019. Tissue-resident memory CD8+ T cells amplify anti-tumor immunity by triggering antigen spreading through dendritic cells. *Nature Communications,* 10**,** 4401.
MICELI, M. C. & PARNES, J. R. 1991. The roles of CD4 and CD8 in T cell activation. *Semin Immunol,* 3**,** 133-41.
MOOG-LUTZ, C., DEGOUTIN, J., GOUZI, J. Y., FROBERT, Y., BRUNET-DE CARVALHO, N., BUREAU, J., CREMINON, C. & VIGNY, M. 2005. Activation and inhibition of anaplastic lymphoma kinase receptor tyrosine kinase by monoclonal antibodies and absence of agonist activity of pleiotrophin. *J Biol Chem,* 280**,** 26039-48.
MORGAN, R. A., YANG, J. C., KITANO, M., DUDLEY, M. E., LAURENCOT, C. M. & ROSENBERG, S. A. 2010. Case report of a serious adverse event following the administration of T cells transduced with a chimeric antigen receptor recognizing ERBB2. *Molecular therapy : the journal of the American Society of Gene Therapy,* 18**,** 843-851.
MORGENSTERN, D. A., BAGATELL, R., COHN, S. L., HOGARTY, M. D., MARIS, J. M., MORENO, L., PARK, J. R., PEARSON, A. D., SCHLEIERMACHER, G., VALTEAU-COUANET, D., LONDON, W. B. & IRWIN, M. S. 2019. The challenge of defining "ultra-high-risk" neuroblastoma. *Pediatr Blood Cancer,* 66**,** e27556.
MORITZ, D. & GRONER, B. 1995. A spacer region between the single chain antibody- and the CD3 zeta-chain domain of chimeric T cell receptor components is required for efficient ligand binding and signaling activity. *Gene Ther,* 2**,** 539-46.
MORRIS, S. W., KIRSTEIN, M. N., VALENTINE, M. B., DITTMER, K. G., SHAPIRO, D. N., SALTMAN, D. L. & LOOK, A. T. 1994. Fusion of a kinase gene, ALK, to a nucleolar protein gene, NPM, in non-Hodgkin's lymphoma. *Science,* 263**,** 1281-4.

MOSSE, Y. P., LAUDENSLAGER, M., LONGO, L., COLE, K. A., WOOD, A., ATTIYEH, E. F., LAQUAGLIA, M. J., SENNETT, R., LYNCH, J. E., PERRI, P., LAUREYS, G., SPELEMAN, F., KIM, C., HOU, C., HAKONARSON, H., TORKAMANI, A., SCHORK, N. J., BRODEUR, G. M., TONINI, G. P., RAPPAPORT, E., DEVOTO, M. & MARIS, J. M. 2008. Identification of ALK as a major familial neuroblastoma predisposition gene. *Nature,* 455**,** 930-5.

MOSSE, Y. P., WOOD, A. & MARIS, J. M. 2009. Inhibition of ALK signaling for cancer therapy. *Clin Cancer Res,* 15**,** 5609-14.

NEWICK, K., O'BRIEN, S., MOON, E. & ALBELDA, S. M. 2017. CAR T Cell Therapy for Solid Tumors. *Annu Rev Med,* 68**,** 139-152.

NIE, Y., LU, W., CHEN, D., TU, H., GUO, Z., ZHOU, X., LI, M., TU, S. & LI, Y. 2020. Mechanisms underlying CD19-positive ALL relapse after anti-CD19 CAR T cell therapy and associated strategies. *Biomarker Research,* 8**,** 18.

NIKOLICH-ZUGICH, J., SLIFKA, M. K. & MESSAOUDI, I. 2004. The many important facets of T-cell repertoire diversity. *Nat Rev Immunol,* 4**,** 123-32.

O'DONNELL, J. S., TENG, M. W. L. & SMYTH, M. J. 2019. Cancer immunoediting and resistance to T cell-based immunotherapy. *Nature Reviews Clinical Oncology,* 16**,** 151-167.

OREN, R., HOD-MARCO, M., HAUS-COHEN, M., THOMAS, S., BLAT, D., DUVSHANI, N., DENKBERG, G., ELBAZ, Y., BENCHETRIT, F., ESHHAR, Z., STAUSS, H. & REITER, Y. 2014. Functional comparison of engineered T cells carrying a native TCR versus TCR-like antibody-based chimeric antigen receptors indicates affinity/avidity thresholds. *J Immunol,* 193**,** 5733-43.

PALMER, RUTH H., VERNERSSON, E., GRABBE, C. & HALLBERG, B. 2009. Anaplastic lymphoma kinase: signalling in development and disease. *Biochemical Journal,* 420**,** 345-361.

PAPAIOANNOU, G. & MCHUGH, K. 2005. Neuroblastoma in childhood: review and radiological findings. *Cancer imaging : the official publication of the International Cancer Imaging Society,* 5**,** 116-127.

PARK, J. R., DIGIUSTO, D. L., SLOVAK, M., WRIGHT, C., NARANJO, A., WAGNER, J., MEECHOOVET, H. B., BAUTISTA, C., CHANG, W. C., OSTBERG, J. R. & JENSEN, M. C. 2007. Adoptive transfer of chimeric antigen receptor re-directed cytolytic T lymphocyte clones in patients with neuroblastoma. *Mol Ther,* 15**,** 825-33.

PARK, S., SHEVLIN, E., VEDVYAS, Y., ZAMAN, M., PARK, S., HSU, Y. S., MIN, I. M. & JIN, M. M. 2017. Micromolar affinity CAR T cells to ICAM-1 achieves rapid tumor elimination while avoiding systemic toxicity. *Sci Rep,* 7**,** 14366.

PASSONI, L., LONGO, L., COLLINI, P., COLUCCIA, A. M., BOZZI, F., PODDA, M., GREGORIO, A., GAMBINI, C., GARAVENTA, A., PISTOIA, V., DEL GROSSO, F., TONINI, G. P., CHENG, M., GAMBACORTI-PASSERINI, C., ANICHINI, A., FOSSATI-BELLANI, F., DI NICOLA, M. & LUKSCH, R. 2009. Mutation-independent anaplastic lymphoma kinase overexpression in poor prognosis neuroblastoma patients. *Cancer Res,* 69**,** 7338-46.

PENNOCK, N. D., WHITE, J. T., CROSS, E. W., CHENEY, E. E., TAMBURINI, B. A. & KEDL, R. M. 2013. T cell responses: naive to memory and everything in between. *Advances in physiology education,* 37**,** 273-283.

PERRET, R. & RONCHESE, F. 2008. Memory T cells in cancer immunotherapy: which CD8+ T-cell population provides the best protection against tumours? *Tissue Antigens,* 72**,** 187-194.

PETERS, P. J., BORST, J., OORSCHOT, V., FUKUDA, M., KRÄHENBÜHL, O., TSCHOPP, J., SLOT, J. W. & GEUZE, H. J. 1991. Cytotoxic T lymphocyte granules are secretory lysosomes, containing both perforin and granzymes. *Journal of Experimental Medicine,* 173**,** 1099-1109.

PETERSEN, C. T., HASSAN, M., MORRIS, A. B., JEFFERY, J., LEE, K., JAGIRDAR, N., STATON, A. D., RAIKAR, S. S., SPENCER, H. T., SULCHEK, T.,

FLOWERS, C. R. & WALLER, E. K. 2018. Improving T-cell expansion and function for adoptive T-cell therapy using ex vivo treatment with PI3Kδ inhibitors and VIP antagonists. *Blood advances,* 2**,** 210-223.
PHILIP, B., KOKALAKI, E., MEKKAOUI, L., THOMAS, S., STRAATHOF, K., FLUTTER, B., MARIN, V., MARAFIOTI, T., CHAKRAVERTY, R., LINCH, D., QUEZADA, S. A., PEGGS, K. S. & PULE, M. 2014. A highly compact epitope-based marker/suicide gene for easier and safer T-cell therapy. *Blood,* 124**,** 1277-1287.
PULE, M. A., SAVOLDO, B., MYERS, G. D., ROSSIG, C., RUSSELL, H. V., DOTTI, G., HULS, M. H., LIU, E., GEE, A. P., MEI, Z., YVON, E., WEISS, H. L., LIU, H., ROONEY, C. M., HESLOP, H. E. & BRENNER, M. K. 2008. Virus-specific T cells engineered to coexpress tumor-specific receptors: persistence and antitumor activity in individuals with neuroblastoma. *Nature medicine,* 14**,** 1264-1270.
RAFIQ, S., HACKETT, C. S. & BRENTJENS, R. J. 2020. Engineering strategies to overcome the current roadblocks in CAR T cell therapy. *Nature Reviews Clinical Oncology,* 17**,** 147-167.
RAMAKRISHNA, S., HIGHFILL, S. L., WALSH, Z., NGUYEN, S. M., LEI, H., SHERN, J. F., QIN, H., KRAFT, I. L., STETLER-STEVENSON, M., YUAN, C. M., HWANG, J. D., FENG, Y., ZHU, Z., DIMITROV, D., SHAH, N. N. & FRY, T. J. 2019. Modulation of Target Antigen Density Improves CAR T-cell Functionality and Persistence. *Clinical Cancer Research,* 25**,** 5329.
RESTIFO, N. P., DUDLEY, M. E. & ROSENBERG, S. A. 2012. Adoptive immunotherapy for cancer: harnessing the T cell response. *Nat Rev Immunol,* 12**,** 269-81.
RICHARDS, R. M., SOTILLO, E. & MAJZNER, R. G. 2018. CAR T Cell Therapy for Neuroblastoma. *Frontiers in immunology,* 9**,** 2380-2380.
RICHMAN, S. A., NUNEZ-CRUZ, S., MOGHIMI, B., LI, L. Z., GERSHENSON, Z. T., MOURELATOS, Z., BARRETT, D. M., GRUPP, S. A. & MILONE, M. C. 2018. High-Affinity GD2-Specific CAR T Cells Induce Fatal Encephalitis in a Preclinical Neuroblastoma Model. *Cancer Immunol Res,* 6**,** 36-46.
RIKER, A., CORMIER, J., PANELLI, M., KAMMULA, U., WANG, E., ABATI, A., FETSCH, P., LEE, K. H., STEINBERG, S., ROSENBERG, S. & MARINCOLA, F. 1999. Immune selection after antigen-specific immunotherapy of melanoma. *Surgery,* 126**,** 112-20.
ROHAAN, M. W., WILGENHOF, S. & HAANEN, J. B. A. G. 2019. Adoptive cellular therapies: the current landscape. *Virchows Archiv : an international journal of pathology,* 474**,** 449-461.
ROSENBERG, S. A. 2014. IL-2: the first effective immunotherapy for human cancer. *J Immunol,* 192**,** 5451-8.
ROSSIG, C., BOLLARD, C. M., NUCHTERN, J. G., MERCHANT, D. A. & BRENNER, M. K. 2001. Targeting of GD2-positive tumor cells by human T lymphocytes engineered to express chimeric T-cell receptor genes. *International Journal of Cancer,* 94**,** 228-236.
RUDNICK, S. I. & ADAMS, G. P. 2009. Affinity and avidity in antibody-based tumor targeting. *Cancer biotherapy & radiopharmaceuticals,* 24**,** 155-161.
SADELAIN, M., BRENTJENS, R. & RIVIÈRE, I. 2013. The basic principles of chimeric antigen receptor design. *Cancer discovery,* 3**,** 388-398.
SALZER, B., SCHUELLER, C. M., ZAJC, C. U., PETERS, T., SCHOEBER, M. A., KOVACIC, B., BURI, M. C., LOBNER, E., DUSHEK, O., HUPPA, J. B., OBINGER, C., PUTZ, E. M., HOLTER, W., TRAXLMAYR, M. W. & LEHNER, M. 2020. Engineering AvidCARs for combinatorial antigen recognition and reversible control of CAR function. *Nature Communications,* 11**,** 4166.
SCHÄFER, D., HENZE, J., PFEIFER, R., SCHLEICHER, A., BRAUNER, J., MOCKEL-TENBRINCK, N., BARTH, C., GUDERT, D., AL RAWASHDEH, W. E.,

JOHNSTON, I. C. D. & HARDT, O. 2020. A Novel Siglec-4 Derived Spacer Improves the Functionality of CAR T Cells Against Membrane-Proximal Epitopes. *Frontiers in Immunology,* 11.
SCHLEIERMACHER, G., JANOUEIX-LEROSEY, I. & DELATTRE, O. 2014. Recent insights into the biology of neuroblastoma. *International Journal of Cancer,* 135**,** 2249-2261.
SCHREIBER, R. D., OLD, L. J. & SMYTH, M. J. 2011. Cancer immunoediting: integrating immunity's roles in cancer suppression and promotion. *Science,* 331**,** 1565-70.
SCHWARTZBERG, P. L., FINKELSTEIN, L. D. & READINGER, J. A. 2005. TEC-family kinases: regulators of T-helper-cell differentiation. *Nature Reviews Immunology,* 5**,** 284-295.
SEEGER, R. C., BRODEUR, G. M., SATHER, H., DALTON, A., SIEGEL, S. E., WONG, K. Y. & HAMMOND, D. 1985. Association of multiple copies of the N-myc oncogene with rapid progression of neuroblastomas. *N Engl J Med,* 313**,** 1111-6.
SHEDLOCK, D. J. & SHEN, H. 2003. Requirement for CD4 T cell help in generating functional CD8 T cell memory. *Science,* 300**,** 337-9.
SMITH-GARVIN, J. E., KORETZKY, G. A. & JORDAN, M. S. 2009. T cell activation. *Annual review of immunology,* 27**,** 591-619.
SMITH, V. & FOSTER, J. 2018. High-Risk Neuroblastoma Treatment Review. *Children (Basel, Switzerland),* 5**,** 114.
SODA, M., CHOI, Y. L., ENOMOTO, M., TAKADA, S., YAMASHITA, Y., ISHIKAWA, S., FUJIWARA, S., WATANABE, H., KURASHINA, K., HATANAKA, H., BANDO, M., OHNO, S., ISHIKAWA, Y., ABURATANI, H., NIKI, T., SOHARA, Y., SUGIYAMA, Y. & MANO, H. 2007. Identification of the transforming EML4-ALK fusion gene in non-small-cell lung cancer. *Nature,* 448**,** 561-6.
SOKOL, E. & DESAI, A. V. 2019. The Evolution of Risk Classification for Neuroblastoma. *Children (Basel, Switzerland),* 6**,** 27.
SOMMERMEYER, D., HILL, T., SHAMAH, S. M., SALTER, A. I., CHEN, Y., MOHLER, K. M. & RIDDELL, S. R. 2017. Fully human CD19-specific chimeric antigen receptors for T-cell therapy. *Leukemia,* 31**,** 2191-2199.
SOMMERMEYER, D., HUDECEK, M., KOSASIH, P. L., GOGISHVILI, T., MALONEY, D. G., TURTLE, C. J. & RIDDELL, S. R. 2016. Chimeric antigen receptor-modified T cells derived from defined CD8+ and CD4+ subsets confer superior antitumor reactivity in vivo. *Leukemia,* 30**,** 492-500.
SOTILLO, E., BARRETT, D. M., BLACK, K. L., BAGASHEV, A., OLDRIDGE, D., WU, G., SUSSMAN, R., LANAUZE, C., RUELLA, M., GAZZARA, M. R., MARTINEZ, N. M., HARRINGTON, C. T., CHUNG, E. Y., PERAZZELLI, J., HOFMANN, T. J., MAUDE, S. L., RAMAN, P., BARRERA, A., GILL, S., LACEY, S. F., MELENHORST, J. J., ALLMAN, D., JACOBY, E., FRY, T., MACKALL, C., BARASH, Y., LYNCH, K. W., MARIS, J. M., GRUPP, S. A. & THOMAS-TIKHONENKO, A. 2015. Convergence of Acquired Mutations and Alternative Splicing of CD19 Enables Resistance to CART-19 Immunotherapy. *Cancer Discovery,* 5**,** 1282.
SPITS, H. 2002. Development of alphabeta T cells in the human thymus. *Nat Rev Immunol,* 2**,** 760-72.
SRIVASTAVA, S. & RIDDELL, S. R. 2015. Engineering CAR-T cells: Design concepts. *Trends in immunology,* 36**,** 494-502.
SRIVASTAVA, S. & RIDDELL, S. R. 2018. Chimeric Antigen Receptor T Cell Therapy: Challenges to Bench-to-Bedside Efficacy. *Journal of immunology (Baltimore, Md. : 1950),* 200**,** 459-468.
STONE, J. D., AGGEN, D. H., SCHIETINGER, A., SCHREIBER, H. & KRANZ, D. M. 2012. A sensitivity scale for targeting T cells with chimeric antigen receptors (CARs) and bispecific T-cell Engagers (BiTEs). *Oncoimmunology,* 1**,** 863-873.

STRAATHOF, K., FLUTTER, B., WALLACE, R., JAIN, N., LOKA, T., DEPANI, S., WRIGHT, G., THOMAS, S., CHEUNG, G. W.-K., GILEADI, T., STAFFORD, S., KOKALAKI, E., BARTON, J., MARRIOTT, C., RAMPLING, D., OGUNBIYI, O., AKARCA, A. U., MARAFIOTI, T., INGLOTT, S., GILMOUR, K., AL-HAJJ, M., DAY, W., MCHUGH, K., BIASSONI, L., SIZER, N., BARTON, C., EDWARDS, D., DRAGONI, I., SILVESTER, J., DYER, K., TRAUB, S., ELSON, L., BROOK, S., WESTWOOD, N., ROBSON, L., BEDI, A., HOWE, K., BARRY, A., DUNCAN, C., BARONE, G., PULE, M. & ANDERSON, J. 2020. Antitumor activity without on-target off-tumor toxicity of GD2–chimeric antigen receptor T cells in patients with neuroblastoma. *Science Translational Medicine,* 12**,** eabd6169.

SZYMCZAK-WORKMAN, A. L., VIGNALI, K. M. & VIGNALI, D. A. 2012. Design and construction of 2A peptide-linked multicistronic vectors. *Cold Spring Harb Protoc,* 2012**,** 199-204.

SZYMCZAK, A. L., WORKMAN, C. J., WANG, Y., VIGNALI, K. M., DILIOGLOU, S., VANIN, E. F. & VIGNALI, D. A. A. 2004. Correction of multi-gene deficiency in vivo using a single 'self-cleaving' 2A peptide–based retroviral vector. *Nature Biotechnology,* 22**,** 589-594.

TAKABA, H. & TAKAYANAGI, H. 2017. The Mechanisms of T Cell Selection in the Thymus. *Trends Immunol,* 38**,** 805-816.

TARTARI, C. J., GUNBY, R. H., COLUCCIA, A. M. L., SOTTOCORNOLA, R., CIMBRO, B., SCAPOZZA, L., DONELLA-DEANA, A., PINNA, L. A. & GAMBACORTI-PASSERINI, C. 2008. Characterization of Some Molecular Mechanisms Governing Autoactivation of the Catalytic Domain of the Anaplastic Lymphoma Kinase*. *Journal of Biological Chemistry,* 283**,** 3743-3750.

TEMIN, H. M. & MIZUTANI, S. 1970. Viral RNA-dependent DNA Polymerase: RNA-dependent DNA Polymerase in Virions of Rous Sarcoma Virus. *Nature,* 226**,** 1211-1213.

TRAN, E., CHINNASAMY, D., YU, Z., MORGAN, R. A., LEE, C.-C. R., RESTIFO, N. P. & ROSENBERG, S. A. 2013. Immune targeting of fibroblast activation protein triggers recognition of multipotent bone marrow stromal cells and cachexia. *Journal of Experimental Medicine,* 210**,** 1125-1135.

TRIGG, R. M., LEE, L. C., PROKOPH, N., JAHANGIRI, L., REYNOLDS, C. P., AMOS BURKE, G. A., PROBST, N. A., HAN, M., MATTHEWS, J. D., LIM, H. K., MANNERS, E., MARTINEZ, S., PASTOR, J., BLANCO-APARICIO, C., MERKEL, O., DE LOS FAYOS ALONSO, I. G., KODAJOVA, P., TANGERMANN, S., HÖGLER, S., LUO, J., KENNER, L. & TURNER, S. D. 2019. The targetable kinase PIM1 drives ALK inhibitor resistance in high-risk neuroblastoma independent of MYCN status. *Nature Communications,* 10**,** 5428.

TRIGG, R. M. & TURNER, S. D. 2018. ALK in Neuroblastoma: Biological and Therapeutic Implications. *Cancers (Basel),* 10.

TURATTI, F., FIGINI, M., BALLADORE, E., ALBERTI, P., CASALINI, P., MARKS, J. D., CANEVARI, S. & MEZZANZANICA, D. 2007. Redirected Activity of Human Antitumor Chimeric Immune Receptors is Governed by Antigen and Receptor Expression Levels and Affinity of Interaction. *Journal of Immunotherapy,* 30**,** 684-693.

TURTLE, C. J., HANAFI, L. A., BERGER, C., GOOLEY, T. A., CHERIAN, S., HUDECEK, M., SOMMERMEYER, D., MELVILLE, K., PENDER, B., BUDIARTO, T. M., ROBINSON, E., STEEVENS, N. N., CHANEY, C., SOMA, L., CHEN, X., YEUNG, C., WOOD, B., LI, D., CAO, J., HEIMFELD, S., JENSEN, M. C., RIDDELL, S. R. & MALONEY, D. G. 2016. CD19 CAR-T cells of defined CD4+:CD8+ composition in adult B cell ALL patients. *J Clin Invest,* 126**,** 2123-38.

VAN DER STEGEN, S. J. C., HAMIEH, M. & SADELAIN, M. 2015. The pharmacology of second-generation chimeric antigen receptors. *Nature reviews. Drug discovery,* 14**,** 499-509.
VARGAS, J. E., CHICAYBAM, L., STEIN, R. T., TANURI, A., DELGADO-CAÑEDO, A. & BONAMINO, M. H. 2016. Retroviral vectors and transposons for stable gene therapy: advances, current challenges and perspectives. *Journal of Translational Medicine,* 14**,** 288.
VERNERSSON, E., KHOO, N. K., HENRIKSSON, M. L., ROOS, G., PALMER, R. H. & HALLBERG, B. 2006. Characterization of the expression of the ALK receptor tyrosine kinase in mice. *Gene Expr Patterns,* 6**,** 448-61.
VESELY, M. D., KERSHAW, M. H., SCHREIBER, R. D. & SMYTH, M. J. 2011. Natural innate and adaptive immunity to cancer. *Annu Rev Immunol,* 29**,** 235-71.
VESELY, M. D. & SCHREIBER, R. D. 2013. Cancer immunoediting: antigens, mechanisms, and implications to cancer immunotherapy. *Annals of the New York Academy of Sciences,* 1284**,** 1-5.
VIGNALI, D. & KALLIKOURDIS, M. 2017. Improving homing in T cell therapy. *Cytokine Growth Factor Rev,* 36**,** 107-116.
WALKER, A. J., MAJZNER, R. G., ZHANG, L., WANHAINEN, K., LONG, A. H., NGUYEN, S. M., LOPOMO, P., VIGNY, M., FRY, T. J., ORENTAS, R. J. & MACKALL, C. L. 2017. Tumor Antigen and Receptor Densities Regulate Efficacy of a Chimeric Antigen Receptor Targeting Anaplastic Lymphoma Kinase. *Mol Ther,* 25**,** 2189-2201.
WANG, X., CHANG, W.-C., WONG, C. W., COLCHER, D., SHERMAN, M., OSTBERG, J. R., FORMAN, S. J., RIDDELL, S. R. & JENSEN, M. C. 2011. A transgene-encoded cell surface polypeptide for selection, in vivo tracking, and ablation of engineered cells. *Blood,* 118**,** 1255-1263.
WATANABE, K., KURAMITSU, S., POSEY, A. D. & JUNE, C. H. 2018. Expanding the Therapeutic Window for CAR T Cell Therapy in Solid Tumors: The Knowns and Unknowns of CAR T Cell Biology. *Frontiers in Immunology,* 9.
WATANABE, K., TERAKURA, S., MARTENS, A. C., VAN MEERTEN, T., UCHIYAMA, S., IMAI, M., SAKEMURA, R., GOTO, T., HANAJIRI, R., IMAHASHI, N., SHIMADA, K., TOMITA, A., KIYOI, H., NISHIDA, T., NAOE, T. & MURATA, M. 2015. Target antigen density governs the efficacy of anti-CD20-CD28-CD3 zeta chimeric antigen receptor-modified effector CD8+ T cells. *J Immunol,* 194**,** 911-20.
WATANABE, K., TERAKURA, S., UCHIYAMA, S., MARTENS, A. C., MEERTEN, T. V., KIYOI, H., NISHIDA, T., NAOE, T. & MURATA, M. 2014. Excessively High-Affinity Single-Chain Fragment Variable Region in a Chimeric Antigen Receptor Can Counteract T-Cell Proliferation. *Blood,* 124**,** 4799-4799.
WATANABE, N., BAJGAIN, P., SUKUMARAN, S., ANSARI, S., HESLOP, H. E., ROONEY, C. M., BRENNER, M. K., LEEN, A. M. & VERA, J. F. 2016. Fine-tuning the CAR spacer improves T-cell potency. *Oncoimmunology,* 5**,** e1253656-e1253656.
WEIJTENS, M. E. M., HART, E. H. & BOLHUIS, R. L. H. 2000. Functional balance between T cell chimeric receptor density and tumor associated antigen density: CTL mediated cytolysis and lymphokine production. *Gene Therapy,* 7**,** 35-42.
WHITTLE, S. B., SMITH, V., DOHERTY, E., ZHAO, S., MCCARTY, S. & ZAGE, P. E. 2017. Overview and recent advances in the treatment of neuroblastoma. *Expert Review of Anticancer Therapy,* 17**,** 369-386.
WILKIE, S., VAN SCHALKWYK, M. C., HOBBS, S., DAVIES, D. M., VAN DER STEGEN, S. J., PEREIRA, A. C., BURBRIDGE, S. E., BOX, C., ECCLES, S. A. & MAHER, J. 2012. Dual targeting of ErbB2 and MUC1 in breast cancer using chimeric antigen receptors engineered to provide complementary signaling. *J Clin Immunol,* 32**,** 1059-70.

WU, L. & VAN KAER, L. 2011. Natural killer T cells in health and disease. *Frontiers in bioscience (Scholar edition),* 3**,** 236-251.
WU, W., ZHOU, Q., MASUBUCHI, T., SHI, X., LI, H., XU, X., HUANG, M., MENG, L., HE, X., ZHU, H., GAO, S., ZHANG, N., JING, R., SUN, J., WANG, H., HUI, E., WONG, C. C. & XU, C. 2020. Multiple Signaling Roles of CD3ε and Its Application in CAR-T Cell Therapy. *Cell,* 182**,** 855-871.e23.
YANG, L., MA, X., LIU, Y.-C., ZHAO, W., YU, L., QIN, M., ZHU, G., WANG, K., SHI, X., ZHANG, Z., WANG, J., SUN, Y., DONG, L., TSAO, S.-T., ZHANG, R. & CHANG, L.-J. 2017. Chimeric Antigen Receptor 4SCAR-GD2-Modified T Cells Targeting High-Risk and Recurrent Neuroblastoma: A Phase II Multi-Center Trial in China. *Blood,* 130**,** 3335-3335.
YEKU, O. O. & BRENTJENS, R. J. 2016. Armored CAR T-cells: utilizing cytokines and pro-inflammatory ligands to enhance CAR T-cell anti-tumour efficacy. *Biochemical Society transactions,* 44**,** 412-418.
YING, Z., HUANG, X. F., XIANG, X., LIU, Y., KANG, X., SONG, Y., GUO, X., LIU, H., DING, N., ZHANG, T., DUAN, P., LIN, Y., ZHENG, W., WANG, X., LIN, N., TU, M., XIE, Y., ZHANG, C., LIU, W., DENG, L., GAO, S., PING, L., WANG, X., ZHOU, N., ZHANG, J., WANG, Y., LIN, S., MAMUTI, M., YU, X., FANG, L., WANG, S., SONG, H., WANG, G., JONES, L., ZHU, J. & CHEN, S. Y. 2019. A safe and potent anti-CD19 CAR T cell therapy. *Nat Med,* 25**,** 947-953.
YOSHIDA, T., MIHARA, K., TAKEI, Y., YANAGIHARA, K., KUBO, T., BHATTACHARYYA, J., IMAI, C., MINO, T., TAKIHARA, Y. & ICHINOHE, T. 2016. All-trans retinoic acid enhances cytotoxic effect of T cells with an anti-CD38 chimeric antigen receptor in acute myeloid leukemia. *Clinical & translational immunology,* 5**,** e116-e116.
YU, A. L., GILMAN, A. L., OZKAYNAK, M. F., LONDON, W. B., KREISSMAN, S. G., CHEN, H. X., SMITH, M., ANDERSON, B., VILLABLANCA, J. G., MATTHAY, K. K., SHIMADA, H., GRUPP, S. A., SEEGER, R., REYNOLDS, C. P., BUXTON, A., REISFELD, R. A., GILLIES, S. D., COHN, S. L., MARIS, J. M., SONDEL, P. M. & CHILDREN'S ONCOLOGY, G. 2010. Anti-GD2 antibody with GM-CSF, interleukin-2, and isotretinoin for neuroblastoma. *The New England journal of medicine,* 363**,** 1324-1334.
ZHANG, H., CHUA, K. S., GUIMOND, M., KAPOOR, V., BROWN, M. V., FLEISHER, T. A., LONG, L. M., BERNSTEIN, D., HILL, B. J., DOUEK, D. C., BERZOFSKY, J. A., CARTER, C. S., READ, E. J., HELMAN, L. J. & MACKALL, C. L. 2005. Lymphopenia and interleukin-2 therapy alter homeostasis of CD4+CD25+ regulatory T cells. *Nat Med,* 11**,** 1238-43.
ZHANG, H., PAO, L. I., ZHOU, A., BRACE, A. D., HALENBECK, R., HSU, A. W., BRAY, T. L., HESTIR, K., BOSCH, E., LEE, E., WANG, G., LIU, H., WONG, B. R., KAVANAUGH, W. M. & WILLIAMS, L. T. 2014. Deorphanization of the human leukocyte tyrosine kinase (LTK) receptor by a signaling screen of the extracellular proteome. *Proceedings of the National Academy of Sciences of the United States of America,* 111**,** 15741-15745.
ZHAO, Z., VERMA, V. & ZHANG, M. 2015. Anaplastic lymphoma kinase: Role in cancer and therapy perspective. *Cancer Biology & Therapy,* 16**,** 1691-1701.
ZHENG, Z., CHINNASAMY, N. & MORGAN, R. A. 2012. Protein L: a novel reagent for the detection of Chimeric Antigen Receptor (CAR) expression by flow cytometry. *Journal of Translational Medicine,* 10**,** 29.
ZHONG, S., MALECEK, K., JOHNSON, L. A., YU, Z., VEGA-SAENZ DE MIERA, E., DARVISHIAN, F., MCGARY, K., HUANG, K., BOYER, J., CORSE, E., SHAO, Y., ROSENBERG, S. A., RESTIFO, N. P., OSMAN, I. & KROGSGAARD, M. 2013. T-cell receptor affinity and avidity defines antitumor response and autoimmunity in T-cell immunotherapy. *Proceedings of the National Academy of Sciences,* 110**,** 6973-6978.

ZHU, S., LEE, J.-S., GUO, F., SHIN, J., PEREZ-ATAYDE, A. R., KUTOK, J. L., RODIG, S. J., NEUBERG, D. S., HELMAN, D., FENG, H., STEWART, R. A., WANG, W., GEORGE, R. E., KANKI, J. P. & LOOK, A. T. 2012. Activated ALK collaborates with MYCN in neuroblastoma pathogenesis. *Cancer cell,* 21**,** 362-373.

ZIMMERMANN, K., KUEHLE, J., DRAGON, A. C., GALLA, M., KLOTH, C., RUDEK, L. S., SANDALCIOGLU, I. E., NEYAZI, B., MORITZ, T., MEYER, J., ROSSIG, C., ALTVATER, B., EIZ-VESPER, B., MORGAN, M. A., ABKEN, H. & SCHAMBACH, A. 2020. Design and Characterization of an "All-in-One" Lentiviral Vector System Combining Constitutive Anti-G(D2) CAR Expression and Inducible Cytokines. *Cancers,* 12**,** 375.